Operating Reserve Assessment of Wind Integrated Power Systems

A Thesis Submitted to the College of

Graduate Studies and Research

In Partial Fulfillment of the Requirements

for the Degree of

Doctor of Philosophy

in the

Department of Electrical Engineering

University of Saskatchewan

Saskatoon

By

Bipul Karki

This thesis is dedicated to:

My dad, who has a dream and faith on me and I just cannot disappoint him;

My mom, who always filled enormous wisdom in me to look forward;

My Wife Prashamsha, who was always there supporting and encouraging me no matter what happens;

My little daughter Suhani, who filled my days with full of joys and sometimes wondered if her papa becomes a doctor who will become her papa then.

PERMISSION TO USE

I agree that the Library, University of Saskatchewan, may make this thesis freely available for inspection. I further agree that permission for copying of this thesis for scholarly purpose may be granted to the professor or professors who supervised the thesis work recorded herein or, in their absence, by the Head of the Department or the Dean of the College in which the thesis work was done. It is understood that due recognition will be given to me and to the University of Saskatchewan in any use of the material in this thesis. Copying or publication or any other use of this thesis for financial gain without approval by the University of Saskatchewan and my written permission is prohibited.

Request for permission to copy or to make any other use of the material in this thesis in whole or part should be addressed to:

Head of the Department of Electrical Engineering

57 Campus Drive

University of Saskatchewan

Saskatoon, Saskatchewan

Canada S7N 5A9

ACKNOWLEDGEMENTS

The author would like to thank his supervisor Professor Roy Billinton for all the help, encouragement, guidance and support during the course of his research works and while preparing this thesis. The author feels lack of words to express his gratitude for Professor Billinton, who at the height of his physical discomfort was always available for discussions and guidance. His humility, patience, professionalism and dedication to his job will always guide the author in his carrier path. The author feels very proud and lucky to have the opportunity to work under the supervision of Professor Roy Billinton.

The author would like to thank his co-supervisor Professor R. Karki, Professor R. Gokaraju and the advisory committee members Professor S.O. Faried, Professor D. Teng, Professor M. Boulfiza and Professor N. Nguyen for all the critics, supports and encouragements during the course of this research work. The author would like to thank Professor R. Johanson for working as graduate chair in his final thesis hearing. The author would also like to thank Professor Athula D. Rajapakse from the University of Manitoba for acting as the external examiner in his final thesis defense.

The author would like to thank his sister Binita, her husband Ishwor, brother Bishal, friends from Kathmandu University, Nepal and all well wishers and relatives for their supports and encouragements for his academic pursuit.

Financial assistance provided in part by the Natural Sciences and Engineering Research Council of Canada and in part by the University of Saskatchewan in the form of a Graduate Scholarship is gratefully acknowledged.

ABSTRACT

Wind power is variable, uncertain, intermittent and site specific. The operating capacity credit associated with a wind farm is therefore considerably different from that assigned to a conventional generating unit and as wind penetrations in conventional power systems increase, it is vital that wind power be fully integrated in power system planning and operating protocols.

The research described in this thesis is focused on the determination of the operating capacity benefits associated with adding wind power to a conventional power system. Probabilistic techniques are used to quantify the risk and operating capacity benefits under various risk criteria. A short term wind speed probability distribution and short term wind power probability distribution forecasting model is presented and a multi-state model of a wind farm is utilized to determine several operating performance indices. The concepts and developed model are illustrated by application to two published test systems. The increase in peak load carrying capability attributable to added wind power is examined under a range of system operating conditions that include the effects of seasonality, locality and wind parameter trends. The operating capacity credit associated with dependent and independent wind farms is also examined. The dependent and independent conditions provide boundary values that clearly indicate the effects of wind speed correlation. Well-being analyses which incorporate the accepted deterministic criterion in an evaluation of the system operating state probabilities is applied to the wind integrated test systems using a novel approach to calculate the operating state probabilities. Most modern power systems are interconnected to one or more other power systems and therefore have increased access and exposure to wind power. This thesis examines the risk benefits associated with wind integrated interconnected power systems under various conditions using the two test systems.

The research described in this thesis clearly illustrates that the operating capacity benefits associated with wind power can be quantified and used in making generating capacity scheduling decisions in a wind integrated power system.

TABLE OF CONTENTS

LIST OF TABLES

LIST OF FIGURES

LIST OF ABBREVIATIONS

ARMA	Auto-Regressive and Moving Average
CCOPT	Conditional Capacity Outage Probability Table
CEA	Canadian Electrical Association
COPT	Capacity Outage Probability Table
CWPD	Conditional Wind Power Distribution
CWS	Conditional Wind Speed
CWSD	Conditional Wind Speed Distribution
Dep.	Dependent
EENS	Expected Energy not Supplied
f	Failure
FOR	Forced Outage Rate
H	Health
HIWS	High initial wind speed
HL	Hierarchical Levels
HL-I	Hierarchical Level-I
HL-II	Hierarchical Level-II
HL-III	Hierarchical Level-III
hrs	Hours
HSP	Healthy State Probability
HSPC	Healthy State Probability Criterion/ Criteria
IEEE-RTS	IEEE Reliability Test System
IEEE-RTSM	Modified IEEE-Reliability Test System
Indep.	Independent
Inter.	Interconnected
IPLCC	Increase in Peak Load Carrying Capability
ISO	Independent System Operator
Isol.	Isolated
IUCR	Interconnected Unit Commitment Risk
LCC	Load Carrying Capability

LIWS	Low initial wind speed
LOLE	Loss of Load Expectation
M	Margin
MSP	Marginal State Probability
MW	Megawatt
NID	Normally Independently Distributed
NWP	Numerical Weather Prediction
OCC	Operating Capacity Credit
ORR	Outage Replacement Rate
P(h)	Probability of Healthy state
P(m)	Probability of Marginal state
P(r)	Probability of At risk state
PLCC	Peak Load Carrying Capability
PLCC benefit factor	Peak Load Carrying Capability benefit factor
P_r	Rated Power
R	At risk
RBTS	Roy Billinton Test System
REC	Renewable Energy Credit
RPS	Renewable Portfolio Standard
SC	Scheduled Capacity
Syst.	System
TSO	Transmission System Operators
UCR	Unit Commitment Risk
UCRC	Unit Commitment Risk Criterion/Criteria
V_{ci}	Cut-in Speed
V_{co}	Cut-out Speed
V_r	Rated Speed
WECS	Wind Energy Conversion System
WT	Wind Turbine
WTG	Wind Turbine Generator/ Generators
yr	Year

1. INTRODUCTION

1.1 Introduction

The basic function of an electric power system is to provide electrical energy to its customers as economically as possible and with an acceptable degree of continuity and quality [1]. Modern society depends highly on electrical energy and demands a very reliable and continuous supply of electricity. Maintaining a high degree of system reliability often requires a high investment and sound engineering choices from various alternate schemes in system planning and operation.

Power systems have gone through tremendous changes in the last decade. Power systems in many part of the world have emerged from public domains to private domains due to deregulation of the electricity market. The deregulation of the electricity market provides grid accessibility to all private energy investors based on the lowest bid at every power system network level, wherever feasible. This scenario creates considerable technical challenges to the operation of power systems. In a deregulated electricity market, Independent System Operators (ISOs) are responsible for power system reliability and stability. Another important change in power system operation is the rapid increase of wind energy applications throughout the world. Wind power generation is intermittent in nature and depends on site specific wind speeds. Uncertainty in power generation from the wind creates new challenges in system planning and operation. Economic considerations faced by system planners and operators requires them to apply sound engineering judgment to the capacity and operating reserve requirements for an acceptable level of reliability.

1.2 Power System Reliability

Power system reliability can be divided into the two basic aspects of system adequacy and system security [1]. System adequacy relates to the existence of sufficient facilities within the system to satisfy the consumer load demand and system operational constraints. These include the facilities necessary to generate sufficient energy and the associated transmission and distribution facilities required to transport the energy to the consumer load points [2]. System security relates to the ability of the system to respond to disturbances arising within the system, and is associated with the response of the system to whatever perturbations it is subject to [2]. An adequate system can become insecure if appropriate dispatch decisions are not made during system operation. Analyzing a complete power system including the generation, transmission and distribution facilities is very complex and is not a practical approach to reliability evaluation of large power systems. Power systems can, however, be divided into three hierarchical levels designated as hierarchical level 1(HL-I), hierarchical level 2 (HL-II) and hierarchical level 3 (HL-III) [3, 4]. HL-I considers the generation capacity, HL-II covers both generation and transmission and HL-III includes the generation, transmission and distribution facilities. This thesis is focused on power system security evaluation at the HL-I.

Power system security refers to the degree of risk associated with the ability of a power system to survive imminent disturbances (contingencies) without interruption to customer service. It relates to the robustness of the system to imminent disturbances and, hence, depends on the system operating conditions and the contingent probabilities of disturbances [5]. System security deals with the operational risks associated with the various causes of power imbalances in system operation, such as load forecast uncertainty, possible outages of generation plant or transmission lines etc [1]. A wide range of power system security analyses are performed to obtain relevant information on different system operating aspects in order to achieve overall economic and reliable system operation [5, 6].

1.3 Power System Operation

A major requirement in system security analysis is to estimate the system operating reserve required to meet sudden capacity deficiencies due to unit failures or load changes. Unit commitment analysis is performed to determine which generating units should operate and at what times in order to meet the expected load with a reasonable operating reserve. Deterministic methods such as the N-1 criterion are conventionally used in power utilities to maintain system security [7]. Under this criterion, a power system should be able to withstand the loss of the single largest element in the system. Conventionally, unit commitment at HL-I includes an operating reserve at least equal to the largest generating unit committed. At HL-II, the single largest element in the system is usually a generating unit or a major transmission line or transformer. At this level, the system should also be able to transmit the required energy without violating line overload and voltage limits due to any single contingency [8].

The deterministic approach to determining operating reserve based on the loss of the largest operating unit does not recognize the inherent probabilistic nature of system behavior and component failures and therefore does not incorporate the system operating risk. This is well known and has been discussed extensively in the literature [9-12]. The first major probabilistic technique for operating reserve assessment was published in 1963 by members of the Pennsylvania-New Jersey- Maryland power pool [13] and is known as the PJM method. In this approach, the unit commitment risk (UCR) is defined as the probability of just carrying or failing to carry the expected load during a specified time into the future designated as the lead time [13]. The assumption is made that any assistance to increase the reserve margin can only be obtained after a specified lead time. This is the time required to start and synchronize additional units. The lead time required to place a unit in service is dependent upon many factors, the most important of which is the unit type. Thermal units can take several hours depending on their prior operating history while hydro and gas turbine units require much shorter times. Operating reserve in an HL-I study is provided in the form of spinning reserve, hot reserve, and rapid start units or by interruptible loads. The basic PJM method does not consider the effect of rapid start units and therefore the method has been augmented to incorporate a wide range of additional factors such as load forecast uncertainty [14], rapid start units [15], interconnection studies[16-21], multistate

generating models [17, 22], interruptible loads [23-27], and system operating states in the form of well-being analysis[28, 29]. A composite generation and transmission system security approach using a security function is proposed in [30-32].

Power system operating states can be generally classified as Normal, Alert, Emergency, Extreme emergency and Restorative states [21] using deterministic criteria. A new operating state following a contingency can make the system acceptable or unacceptable. The information available to the decision maker is mostly probabilistic in nature, such as future load conditions, the next contingency, the neighboring system states etc. Many of the factors generally considered as deterministic suffer from various degrees of uncertainty, due to limitations in detail and data and hence are better modeled by probability distributions rather than with deterministic default values.

The five state representation noted above was modified to create a three state model which represents the system operating condition as being either Healthy, Marginal or At risk [28]. This hybrid method, known as system well-being analysis incorporates the deterministic criterion in a probabilistic framework and evaluates the system risk in terms of the ability of the system to meet a specified deterministic criterion such as N-1 for operating reserve assessment [18, 33-39]. The well-being model provides information to the system operator on the likelihood of the system entering into the troubled states (Emergency and Extreme emergency). Well-being analysis [28] provides an opportunity to enhance the unit commitment risk index (UCR) to recognize the different operating conditions noted above [21] . It also allows the accepted deterministic criteria utilized by utilities to be incorporated in a probabilistic framework.

The addition of wind power to a conventional generating system introduces a new dimension in the determination of operating reserve due to the variable and intermittent nature of the wind. The output of a wind turbine generator (WTG) depends on the available wind speed at the particular point in time. The wind is intermittent, variable and uncertain. A deterministic criterion, such as the loss of the largest unit, therefore, cannot be readily applied to incorporate wind energy generation in an existing power system. New techniques and models are required that can recognize the intermittent nature of wind power and incorporate this characteristic in an

evaluation of the system operating risk under a set of given conditions. This thesis is focused on the development of probabilistic techniques to quantify the operating capacity benefits of adding wind power to a conventional power system.

1.4 Wind energy sources in power systems

Wind power is one of the fastest growing energy sources in modern electric power systems and at present there is a total installed worldwide capacity of about 120,000 MW [40]. The installation worldwide of wind turbines (WT) has increased annually at a rate of almost 25% for the eight year period from 2000-2008 [40]. The rapid growth of wind energy application in power systems is primarily driven by governmental incentives put in place to address environmental concerns. Despite the intermittent nature of wind power, the energy content in the wind is enormous and free from pollution. Electricity production costs from other conventional sources will keep on rising due to ever increasing fuel costs whereas the cost of electricity production from wind is declining with the continuous development in wind technology [41]. Market mechanisms, such as the renewable energy credit (REC), are being experimented within many countries around the world to sustain the growth of renewable energy. Wind energy is expected to increase considerably in the next decade. Canada at present has about 1700 MW of installed wind power and has a target of 10,000 MW by the end of 2010 [42].

Wind power penetration is defined as the ratio of the total installed wind capacity to the total installed generating capacity in a power system. Despite the rapid growth, global wind power penetration is still not very significant. The Renewable Portfolio Standard (RPS) is a new policy currently being implemented to promote significant growth in wind power. Implementation of the RPS is a commitment to meet a certain power penetration target from renewable energy sources within a specified time in the future (such as 5 to 10 years). Many countries have signed and are in the process of implementing their RPS [40-42]. The wind penetration targets under the RPS range from 5% to 25%. Due to the RPS, wind penetration is likely to grow rapidly in the near future.

As noted earlier, the worldwide installation of wind turbines is increasing rapidly. The policy regarding generation and integration of the renewable energy sources including wind power is also changing so as to address the challenges and facilitate the opportunities generated by this new and emerging energy source. The world wide installation of wind power is still relatively insignificant (less than 1%), however, some country already have 20% of their installed capacity from wind turbines. There are instances when the instantaneous wind power penetration has increased to 100% in some parts of Denmark [43, 44]. It is again important to note that on Nov. 24, 2008 at 5 a.m. 43% of Spain's total electrical load (with 9,253 MW of wind power in operation - of the 21,264 MW total demands) was carried by the wind power [45-47].

References [41-43, 45, 47-50] are web pages that continually update policy, technology and opportunities with wind power. Due to the rapid growth of wind power these online sources of information and discussion forums [46] are valuable sources of general information.

Integrating wind energy sources in a power system creates increased difficulties in maintaining system reliability. Power system security is generally achieved by spinning reserve allocations, use of rapid start units, or making arrangements for interruptible load if the latter is justified by mutual economic benefits. Accurate analysis of operational reserve requirements is beneficial from both system reliability and economic points of view. Over scheduling and under scheduling are not desirable and are directly related to system reliability and economy.

The output power from a conventional unit can be controlled to provide a specified value. Wind power generation is stochastic in nature and thus variable. Efforts can be made to regulate wind power in a very limited range by varying the pitch angle of the rotor blades of a WTG, but its output capacity at a particular instant is basically dependent on the available wind speed at that moment. A WTG starts generating electricity at a minimum wind speed called the cut-in wind speed (V_{ci}). The power curve is a non-linear function of the wind speed between the cut-in and the rated (V_r) wind speed. A WTG generates its rated power when the wind speed is between the rated and the cut-out wind speed (V_{co}). A WTG is removed from service when the wind speed exceeds the cut-out speed [51]. Wind power generation mostly lies within the non-linear portion of the curve, and constant power output is not usually obtained. A small change in the

wind speed in the non-linear region results in a relatively large change in the power output. A typical WTG power curve is shown in Fig. 1.1.

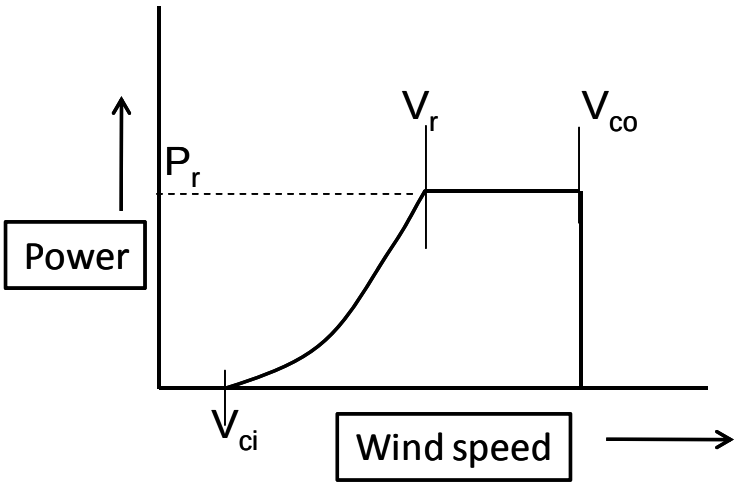

Fig. 1.1: A generic wind power curve

Probabilistic techniques that recognize the random variation in the available wind power are required to determine the appropriate operating reserve to maintain system security when there is a significant level of wind penetration in a power system. These techniques can be utilized to evaluate the system operating risk in order to determine the required operating reserve. Unlike conventional units, the rated capacity of a WTG is not indicative of the actual power output since this value is dictated by the available wind speed. The risk associated with depending on a WTG in system operation is always greater than that with a conventional unit. A deterministic criterion for spinning reserve allocation, therefore, could be highly inconsistent when considering wind power in security assessment.

Wind energy is normally dispatched whenever there is sufficient wind and used to replace conventional units. When there is a significantly high penetration of wind power, utilizing wind power whenever available may require conventional units to be shut down. Wind energy therefore, cannot be simply regarded as energy that can be fed into the system whenever the wind is available and procedures to perform realistic evaluations of system security

considering wind power are therefore necessary. The commitment of wind power in conjunction with other conventional units to meet the short term load is an important task in the operation of a system with high wind power penetration.

1.5 Research framework

Wind is normally considered as an energy source and not as a power source because of its stochastic nature. The operating conditions in a power system always require a power balance to be maintained. Without a realistic evaluation of the capacity contribution provided by wind power, balancing a power system becomes extremely difficult as the wind power penetration increases.

The addition of wind power in systems with different types and sizes of conventional units can have significantly different impacts on system security. Two test systems were therefore used to study the impacts. The Roy Billinton Test system (RBTS) [52] is a relatively small system intended for educational purposes. It has 11 generating units, two generator buses, four load buses and nine transmission lines. A total installed generating capacity of 240 MW is intended to serve a peak load of 185 MW. The IEEE-Reliability Test System (IEEE-RTS) [53] is a more complex system with a generating capacity of 3405 MW and a peak load of 2850 MW. It has a total of 32 generating units with 10 generator buses, 17 load buses, 33 transmission lines and 5 transformers. The operating risk is highly dependent on the time into the future that the scheduled generation is committed to meet the forecasted load. Hydro, thermal and rapid start units are examples of different conventional units that have very different lead times and operating characteristics.

Reliability of a power system can be evaluated by either analytical or simulation methods. In a large complex system, an analytical method often requires approximations in the developed model and it may be difficult to obtain a suitable model. Monte-Carlo simulation method can be used to model the system by creating an experiment of the system behavior. It is a time consuming process and can require a large number of simulations to predict the required results. System operators have to decide quickly and therefore simulation based models may not

be appropriate for making operating decisions. The research in this thesis is focused on the development of an appropriate analytical procedure to evaluate the operating risk in a wind integrated power system and the models required to support the procedure.

A basic schematic diagram for a Wind Energy Conversion System (WECS) is shown in Fig. 1.2 and involves a wind speed model and a WTG power curve in the form shown in Fig. 1.1.

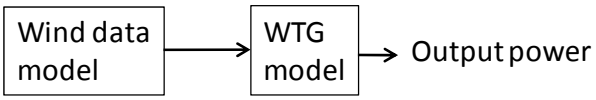

Fig. 1.2: A WECS schematic diagram

The wind speed is a simulated parameter specific to the wind site under consideration. In the research described in the thesis the simulated wind speeds are generated using time series Auto Regressive Moving Average (ARMA) models developed using historical wind speeds. The parameters and the order of the ARMA are unique to each wind site. Reference [54] describes a procedure for developing an ARMA model. References [55-64] utilize the method presented in [54] to evaluate the planning benefits of adding wind power to a system.

The wind turbine power curves have different characteristics depending on the make and model of the WTG [51, 65]. A generic model of a WTG is used in the research described in this thesis. This model is described in detail in [51]. It can be replaced in a specific application by a more applicable model if the wind turbine manufacturer or the operating utility has one available. A detailed description of the WECS model used in this research is presented in Chapter 3.

1.6 Research objectives and plan

The basic objectives of the research described in this thesis are to develop a method to evaluate the operating risk in a power system with high wind power penetration, and to use the developed method to conduct a wide range of studies in order to evaluate the impact of different

system conditions on the system security. In order to achieve these objectives the research was conducted in the following steps.

I. The development of a security model of a power system with wind penetration.

The overall framework is shown in Fig. 1.3. The model consists of the following elements; wind data modeling, WTG modeling, conventional generation modeling, integration of wind and conventional generation models, and combining the overall generation model with the forecasted load model to obtain the operating risk indices.

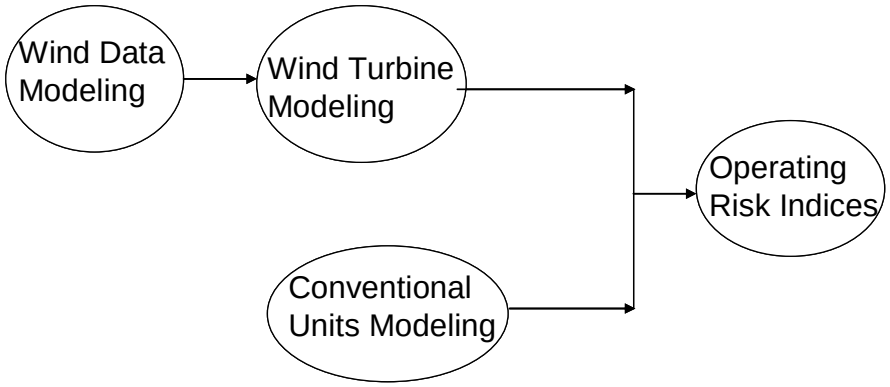

Fig. 1.3: Modeling elements in evaluating the operating risk

II. Application to operating risk assessment

As noted earlier, the objective was to use an analytical method rather than a simulation approach. The models developed for wind energy conversion and the conventional units were used to estimate the operating risk in the RBTS and IEEE-RTS. In order to achieve the stated objectives, the peak load carrying capabilities of the test systems under different levels of wind power penetration and different risk criteria were evaluated. The impacts on the system operating performance due to seasonal wind variation were examined and the effects of wind site geographic location assessed.

III. System well-being analysis

The basic method developed to evaluate the operating risk in a power system with high wind power penetration was extended using the well-being framework.

IV. Operating risk determination in interconnected systems

The single system analyses described above were extended to include interconnected system studies using the two test systems.

1.7 Summary of the Thesis

The thesis is divided into eight chapters. Chapter 2 describes the basic probabilistic technique used to evaluate the Unit Commitment Risk (UCR) in a power system. The UCR of the RBTS and the IEEE-RTS are evaluated for different scheduled capacities and different lead times. Operating performance indices such as the Load Carrying Capability (LCC) and the Peak Load Carrying Capability (PLCC) are determined under different conditions. The variability in the performance indices and in the required spinning reserve is examined for various unit commitment risk criteria, scheduled capacities and lead times.

Power system security evaluation is based on the identification of the system operating state at a point in time. The initial conditions are therefore known at time zero. Chapter 3 introduces the concept of short term wind speed modeling and the development of a conditional wind power distribution. The developed model is an extension of the ARMA model described earlier.

Chapter 4 presents the procedure used to integrate wind power in a conventional power system in order to estimate the operating capacity benefit of added wind power. The wind power capacity model developed in Chapter 3 is applied to evaluate the UCR for the RBTS and the IEEE-RTS under two different initial wind speed conditions. Various operating performance indices are determined for different initial wind speeds, UCRC, lead time and scheduled capacities.

The operating capacity benefits of added wind power are quantified by creating indices designated as the Increase in Peak Load Carrying Capability (IPLCC) and PLCC benefit factors. The effects on the IPLCC of using derated state unit representations for the conventional generating units in IEEE-RTS are illustrated.

Chapter 5 illustrates the IPLCC of a wind integrated power system considering seasonality, locality and wind trend effects. The operating capacity credit associated with wind power addition of dependent and independent wind farms using Regina wind site data are examined for two different wind speed cases and different lead times using the IEEE-RTS.

Chapter 6 extends the concepts applied in the earlier chapters to evaluate the well-being indices in wind integrated power system. An alternate approximate method to conducting system well-being analysis is presented to speed up the calculation process. The RBTS, IEEE-RTS and a modified IEEE-RTS are studied with and without added wind power.

Chapter 7 presents a UCR analysis of two interconnected wind integrated power systems. The focus of the research in this chapter is on the UCR benefits associated with wind power in an interconnected framework. The RBTS and IEEE-RTS is used in these studies.

Chapter 8 presents a summary and the conclusions of this research work.

2. OPERATING RESERVE ASSESSMENT OF CONVENTIONAL POWER SYSTEMS

2.1 Introduction

Adequate operating reserve is a basic requirement in providing reliable electric power supply and is an important factor in generating unit scheduling and dispatch. The operating reserve contains two basic components, the first of which is the actual commitment of units in order to meet the forecast load requirement and satisfy the system reliability criterion. The second aspect is the allocation of load on the committed units in order to provide adequate response to the constant changes in system load. The required operating reserve has traditionally been related to the loss of the largest generating unit and divided into spinning reserve and rapid response components. Unit commitment decisions are usually based on generating unit merit orders or bid processes and are made in advance and subsequently modified as additional system load information becomes available. Conventional generating capacity such as hydro, fossil, nuclear and gas turbines are considered to be dispatchable and can be scheduled for service under predictable constraints. There is a wide range of literature dealing with conventional generating unit commitment [8, 15, 16, 18, 20, 22, 25, 27-29, 33-36, 38, 66-87]. The vast majority of these papers deal with economic aspects of unit commitment and the risks associated with unit commitment decisions are not explicitly considered. The deterministic approach to allocating operating reserve based on the loss of the largest operating unit does not recognize the inherent probabilistic nature of system behavior and component failures and therefore cannot

provide a constant system operating risk. This is well known and has been discussed extensively in the literature [9-12]. As noted in Chapter 1, the first major probabilistic technique for operating reserve assessment was published in 1963 by members of the Pennsylvania-New Jersey- Maryland power pool [13] and is known as the PJM method. In this approach, the Unit Commitment Risk (UCR) is defined as the probability of just carrying or failing to carry the expected load during a specified time into the future designated as the lead time. The lead time required to place a unit in service is dependent upon many factors, the most important of which is the unit type. Thermal units can take several hours depending on their prior operating history while hydro and gas turbine units require much shorter times. As noted in Chapter 1, the PJM method has been augmented to incorporate a wide range of additional factors. The analyses in this thesis are done on a total system basis in which transmission constraints are not considered. Radial transmission associated with generating facilities or assistance from neighboring systems can be incorporated in the developed capacity models [1] . The operating reserve requirement for a given UCR usually increases for increased system lead times [15].

Unit commitment decisions are normally evaluated several times in a day. The PJM interconnection [13] noted that based on three unit commitment decisions per day, a UCR of 0.001 would lead to an average of approximately one violation /year of the UCR definition. It should be noted that actual generating unit loading levels due to dispatch changes occur almost continually throughout a day.

2.1.1 Pennsylvania-New Jersey-Maryland (PJM) Interconnected System Method

The most common model for a conventional generating unit is a two –state representation in which the unit is either in the up or down state. If the failure and repair times are exponentially distributed, the probability of finding a unit on outage at time t given that the unit is available at time t= 0 is given by (2.1).

$$P(down) = \frac{\lambda}{\lambda+\mu} - \frac{\lambda}{\lambda+\mu} e^{-(\lambda+\mu)t} \tag{2.1}$$

where λ and μ are the failure and repair rates respectively.

Repair of a failed unit is not generally possible in a short lead time and (2.1) becomes

$$P(down) = 1 - e^{-\lambda t} \tag{2.2}$$

If the lead time is very short i.e. 4 to 6 hours, then $\lambda t << 1$ and (2.2) becomes

$$P(down) \approx \lambda t \tag{2.3}$$

The probability of the unit failing during the interval t in (2.3) is known as the Outage Replacement Rate (ORR) [1] and is applied in the basic PJM method [13]. The risk associated with just carrying or failing to carry a specified load level can be obtained from the cumulative probabilities associated with the various capacity outage levels in the Capacity Outage Probability Table (COPT) created for the scheduled units. The generating units can be represented by two state or multi-state models and a detailed algorithm for developing a COPT is presented in [1].

The basic generating unit statistic in generating capacity adequacy evaluation is the unit unavailability or Forced Outage Rate. This is the probability of finding the unit on outage at some distant time in the future. In an operating reserve study, the time in the future is relatively short and repair given a failure is not generally possible. The ORR for a generating unit is considerably smaller than the FOR value.

A COPT is an array of system capacity levels and their associated probabilities. Generating unit failures are assumed to be independent events in combining the individual generating unit failure probabilities. A COPT usually contains four items: the capacity on outage designated as Capacity Out, the available capacity designated as Capacity In, the probability of each individual capacity state and the cumulative probability of the each capacity state. A COPT can be built recursively using the algorithm [1] presented in (2.4).

The cumulative probability of a particular capacity outage state X MW after a unit of capacity C MW and forced outage rate U is added is given by

$$P(X) = (1-U)\, P'(X) + (U)\, P'\,(X-C) \tag{2.4}$$

where P'(X) and P(X) denote the cumulative probabilities of the capacity outage state of X MW before and after the unit is added. The above expression is initialized by setting P'(X) =1.0 for X≤0 and P'(X) =0 otherwise.

Equation (2.4) can be extended to include multi-state generating unit representations.

$$P(X) = \sum_{i=1}^{n} p_i\, P'(X-C_i) \tag{2.5}$$

where n= number of unit states

C_i = capacity outage state of i for the unit being added

p_i = probability of existence of the unit state i

Equation (2.5) becomes (2.4) when n is 2.

The PJM method is focused directly on operating reserve assessment and is relatively easy to apply. A more general approach designated as the Security Function Method is proposed in [30-32].

2.1.2 Security Function Method

The security function is mathematically described as

$$S(t)=\sum_{i} P_i(t)^* Q_i(t) \tag{2.6}$$

where $P_i(t)$ = probability of the system being in state i at a time t in the future

$Q_i(t)$ = probability that state i constitutes a breach of security at time t in the future.

In the security function approach, a breach of security is defined as inadequate spinning generation capacity, unacceptable low voltage somewhere in the system, transmission line or

equipment overload, loss of system stability or intolerable operating conditions. In its complete form, the evaluated security index is a global system risk covering generation and transmission limit violations. A complete global security index involves exhaustive calculation of all the different system operating states. The time required to formulate the initial states of the system and to compute the required index could be quite lengthy in a large system where the system operator requires fast responses to system dynamic changes. It is important to note that the security function and the PJM approach are basically identical when the focus is confined to evaluating the system operating risk due to generating unit commitment. In this case if the load in the given time interval is greater than the generation then $Q_i(t)$ in (2.6) is unity.

Equation (2.4) can then be written as

$$S(t)=\sum_i P_i(t) \qquad (2.7)$$

The research described in this thesis is focused on extending the basic PJM technique to determine the unit commitment risk in systems including wind turbine generating units.

2.2 Test Systems

The approach presented in this thesis is illustrated by application to two well known test systems. The first test system is the Roy Billinton Test System (RBTS) [52, 88]. This is a small test system developed at the University of Saskatchewan by the Power System Research Group and intended for educational and research purposes. The system contains 11 generating units and has a total installed capacity of 240 MW and a load of 185 MW. The individual unit capacities and failure rates, and the priority loading order of the generating units as used in this thesis are given in Appendix A1. The second test system used in this work is the IEEE Reliability Test System (IEEE-RTS) [53]. The IEEE-RTS is a relatively large system with an installed capacity of 3405 MW in 32 generating units and has a load of 2850MW. The unit priority loading order and the generating unit data are given in Appendix A2. The installed generating capacity in the IEEE-RTS is approximately the same as that in the SaskPower system in Saskatchewan, Canada.

The basic concepts of UCR are first illustrated in this chapter by application to the RBTS followed by application to a larger system in the form of the IEEE-RTS.

2.3 Unit Commitment Evaluation

The literature contains many publications on the various ways to select generating units for commitment. One of the most popular methods is based on the economic priority loading order in which lower cost units are scheduled first. The units are selected on this basis and a priority list is developed. The loading orders, for the RBTS and the IEEE-RTS are given in Appendices A1 and A2 respectively.

The Unit Commitment Risk (UCR) is obtained directly from the developed Capacity Outage Probability Table (COPT). As noted earlier, a COPT contains the different discrete capacity levels, created from the various combinations of operating unit capacities and their associated cumulative probabilities. The cumulative probability associated with each capacity level is used to calculate the UCR. The UCR moves in discrete steps as the generating unit capacities are discrete values.

A typical example of calculating the UCR level is presented in Table 2.1 for the RBTS. It shows the COPT for the RBTS when 7 generating units (scheduled capacity 190 MW) are committed using a lead time of 4 hours. The UCR is the probability of just carrying or failing to carry a particular load. Table 2.1 shows that the UCR for carrying a load from 160 MW to 169.9 MW using a load level precision of 0.1 MW is 0.00685. If the Unit Commitment Risk Criterion (UCRC) is 0.01then this committed capacity can carry a maximum load of 169.9 MW as any load greater than this level would exceed the specified UCRC. The Peak Load Carrying Capability (PLCC) is defined as the maximum load that the operating units can collectively carry without violating the specified reliability criterion designated as the UCRC. The UCRC is a management decision. If a UCRC of 0.001 is selected then the system can carry a peak load of 149.9 MW. A pictorial view of the UCR variation with load as shown in Table 2.1 is presented in Fig. 2.1. This figure illustrates the basic profile of the UCR as a function of the system load. The exact values of the UCR are contained in the COPT shown in Table 2.1.

Table 2.1: COPT for the RBTS for 7 scheduled units

Capacity Out MW	Capacity In MW	Probability	Cumulative Probability
0	190	0.98692170	1
10	180	0.00180590	0.01307835
20	170	0.00442389	0.01127246
30	160	0.00000809	0.00684857
40	150	0.00678259	0.00684047
50	140	0.00001241	0.00005788
60	130	0.00003038	0.00004547
70	120	0.00000006	0.00001509
80	110	0.00001493	0.00001503
90	100	0.00000003	0.00000010
100	90	0.00000007	0.00000008
110	80	0.00000000	0.00000001
120	70	0.00000001	0.00000001

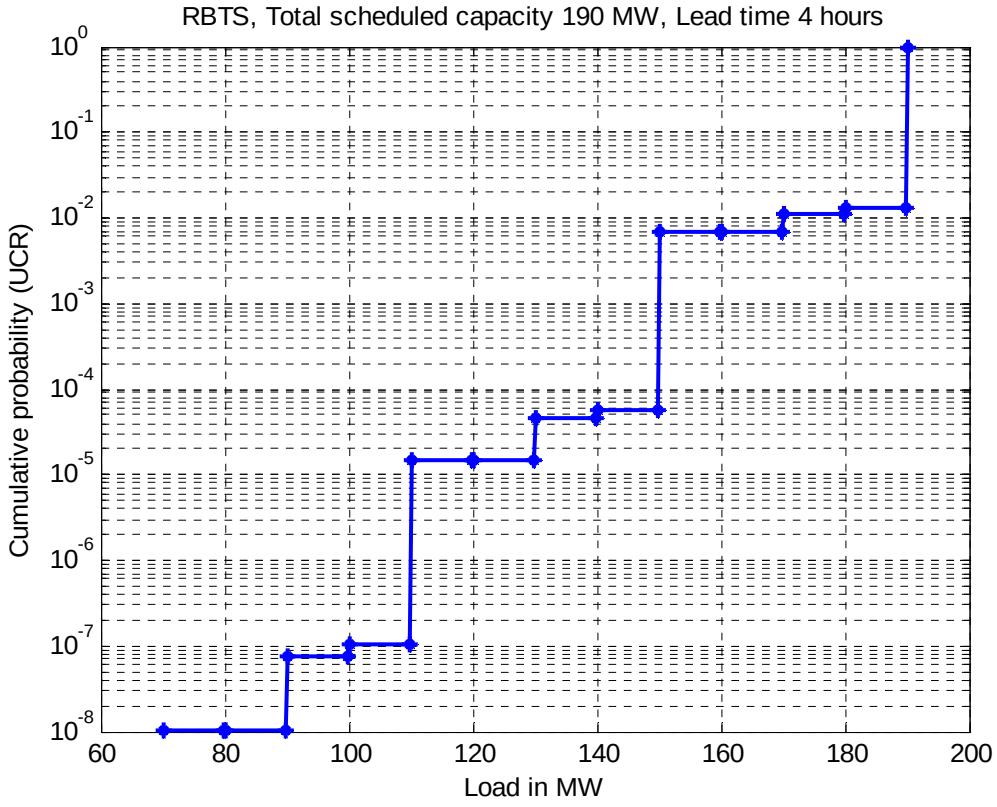

Fig. 2.1: UCR variation with load for the RBTS

2.4 Risk Analysis of the RBTS for Various Lead Times at Different Load Levels

The following section present a series of studies to illustrate the variation in the UCR with load and scheduled capacity for various lead times using the RBTS and the IEEE-RTS. The UCR as a function of load for the RBTS with lead times of 1 and 4 hours is presented in Fig. 2.2. Different commitment levels involving 5, 6, 7 and 8 generating units with capacities of 160 MW, 180MW, 190MW and 210 MW respectively based on the RBTS merit order are used to illustrate the UCR variation with load at different operating capacity levels.

In the case of 5 committed units, the UCR for a load of 119.9 MW and 120 MW for a lead time of 1 hour are 0.00000188 and 0.00171. These UCR values change to 0.0000299 and 0.00684 respectively for the same load levels if the lead time is 4 hours. At a lead time of 4 hours, the system is able to carry loads of 119.9 MW, 139.9 MW and 149.9 MW at a UCRC of 0.001 for committed generation of 5, 6 and 7 units respectively. These load levels can also be carried at a UCRC of 0.0001.

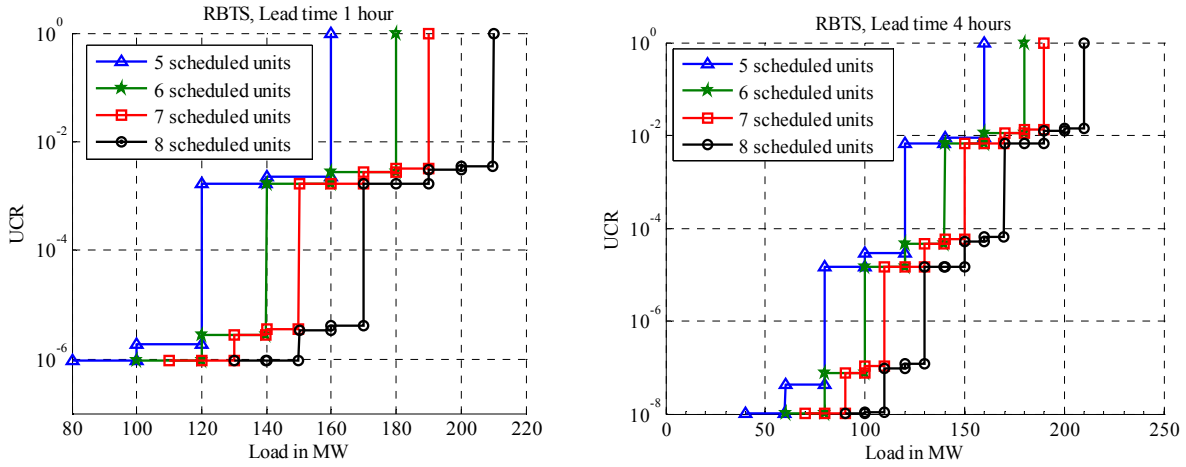

(a): Lead time 1 hour (b): Lead time 4 hours

Fig. 2.2: UCR as a function of load for the RBTS

Definite patterns of large discrete UCR steps at each committed generation level occur as a function of load level for both lead times in Fig. 2.2. The load levels at which these changes in UCR occur are the same load points for a given scheduled capacity and are not influenced by the lead times. Table 2.2 presents a summary of the load levels at which the large steps in the UCR

as shown in Fig. 2.2 are obtained. The lead time was varied from 1 to 4 hours. For simplicity only three instances of significant risk steps and their corresponding load levels are presented. It can be seen that for a scheduled capacity of 190 MW, the first significant risk step occurs when the load changes from 189.9 MW to 190 MW. The second large UCR step is obtained when the load changes from 149.9 to 150 MW and the third major change is obtained when the load increases from 109.9 MW to 110 MW. Similar major UCR steps obtained for other scheduled capacity levels are shown in Table 2.2. The load levels for these major risk changes are different for each scheduled capacity but they all show that the large risk steps occur when the system has spinning capacity equal to an integer multiple of 40 MW. This is due to the fact that the largest operating unit is 40 MW in the RBTS priority loading order.

Table 2.2: Summary of the significant risk jump states of the RBTS

No of units in operation	Total Capacity in MW	Load level at which the first major change in risk level is observed (MW)		Load level at which the second major change in risk level is observed (MW)		Load level at which the third major change in risk level is observed (MW)		Spinning capacity (MW) = Generation-Load
		From	To	From	To	From	To	
5	160	159.9	160	119.9	120	79.9	80	n*40
6	180	179.9	180	139.9	140	99.9	100	n*40
7	190	189.9	190	149.9	150	109.9	110	n*40
8	210	209.9	210	169.9	170	129.9	130	n*40

where n = 0, 1, 2, 3, 4,… etc

The variations in the UCR for 7 scheduled units (190 MW) at a load of 130 MW at different lead times are presented in Table 2.3. It shows that the UCR increases as the lead time increases even if the system load and generation remains fixed.

Table 2.3: UCR variation with lead time for a fixed load and scheduled capacity

Load (MW)	Lead time (hours)	UCR
130	1	2.850841E-06
130	2	1.139121E-05
130	3	2.560290E-05
130	4	4.546775E-05

2.5 Load Carrying Capability of the RBTS under Different Lead Times

Comparisons of the scheduled capacities, total number of scheduled units and total spinning capacities for lead times of 1 and 4 hours under various UCRC are presented in Fig. 2.3, 2.4 and 2.5.

The total scheduled capacities, total committed units and spinning capacities are the same for UCRC of 0.001, 0.0001 and 0.00001 at most of the load points at a lead time of 1 hour. Changes are seen only at a load below 80 MW.

The total scheduled capacities, number of scheduled units and spinning capacities for a lead time of 4 hours are the same for the UCRC of 0.001 and 0.0001 as shown in Fig. 2.3(b), 2.4(b) and 2.5(b). These parameters, however, have higher values for a UCRC of 0.00001 and the system needs assistance to carry its peak load under this criterion.

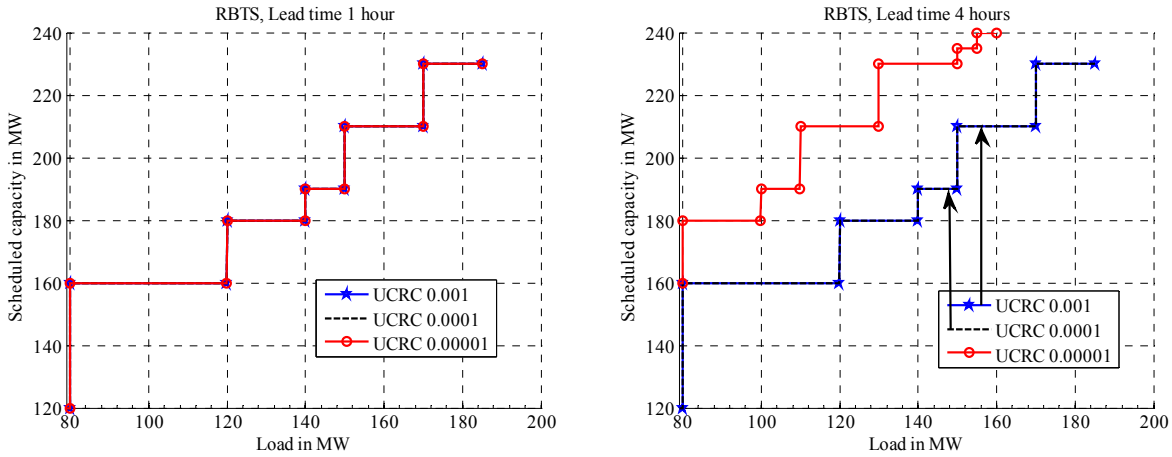

(a): Lead time 1 hour (b): Lead time 4 hours

Fig. 2.3: Generation scheduled for the RBTS as a function of load

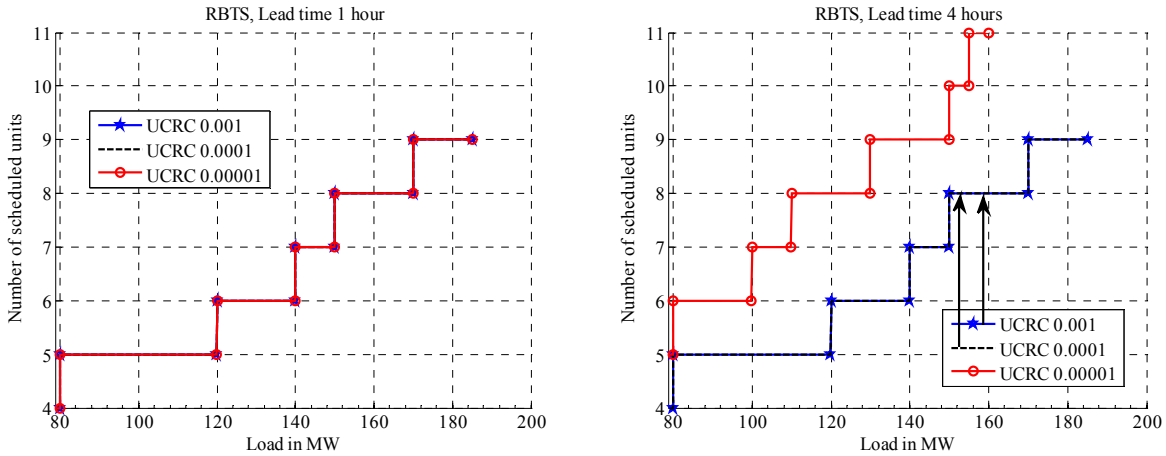

(a): Lead time 1 hour (b): Lead time 4 hours

Fig. 2.4: No. of scheduled units for the RBTS as a function of load

Fig. 2.5 (a) shows that the system needs a minimum spinning capacity of 40.1 MW to maintain UCRC of 0.001, 0.0001 and 0.00001 for a lead time of 1 hour. Fig. 2.5(b) shows a minimum spinning capacity of 80.1 MW is required to maintain a UCRC of 0.00001. The profiles are the same at UCRC of 0.001 and 0.0001 and the minimum spinning capacity is still 40.1 MW.

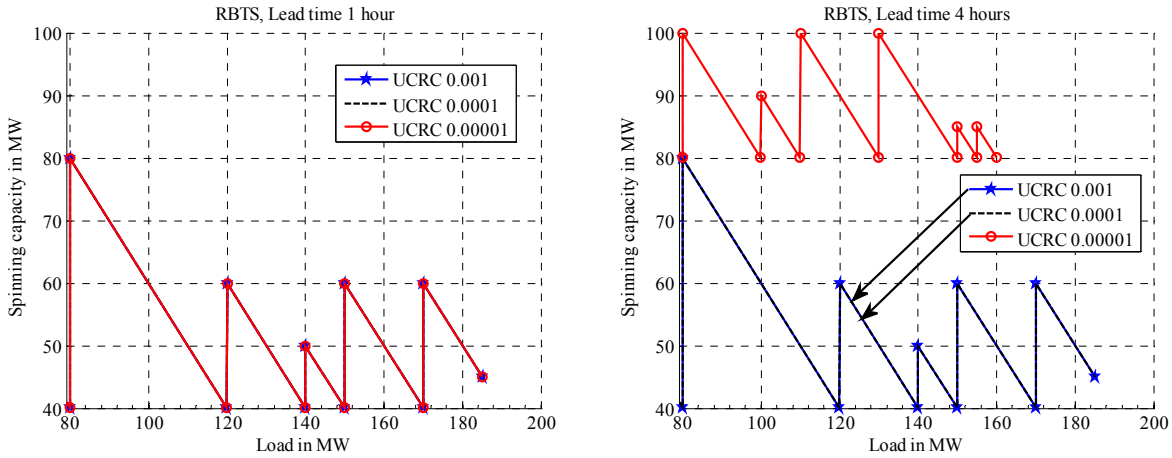

(a): Lead time 1 hour (b): Lead time 4 hours

Fig. 2.5: Spinning capacity for the RBTS

A comparison of the effects of different lead times on the number of scheduled units, scheduled capacities and the spinning capacity is presented in Figs. 2.6, 2.7 and 2.8 respectively. The number of scheduled units, the scheduled capacities and the system spinning reserve requirements are the same for the conditions shown in the figure box and are different for a UCRC of 0.00001 at a lead time of 4 hour. The RBTS cannot support its peak load (185 MW) under this condition and assistance from other sources is required. A minimum spinning capacity of 40.1 MW is needed to maintain the UCRC for the conditions in the figure box. A minimum spinning capacity of 80.1 MW is required at a UCRC of 0.00001 and a 4 hour lead time.

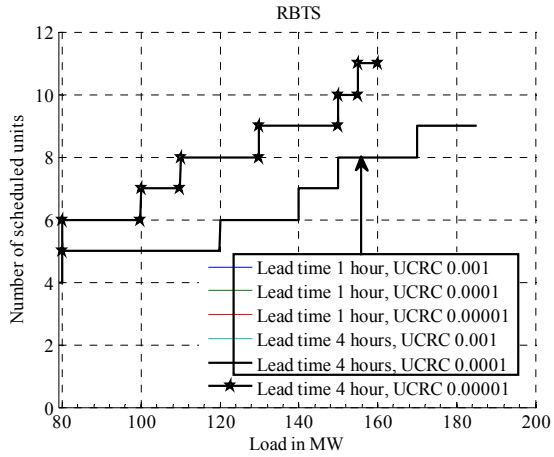

Fig. 2.6: No. of scheduled units for the RBTS as a function of load with different lead times

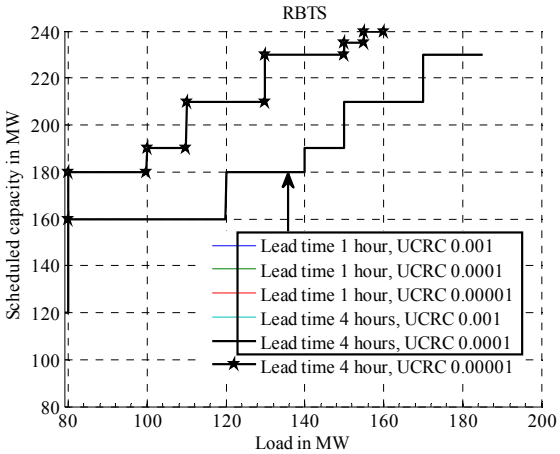

Fig. 2.7: Scheduled capacities for the RBTS as a function of load with different lead times

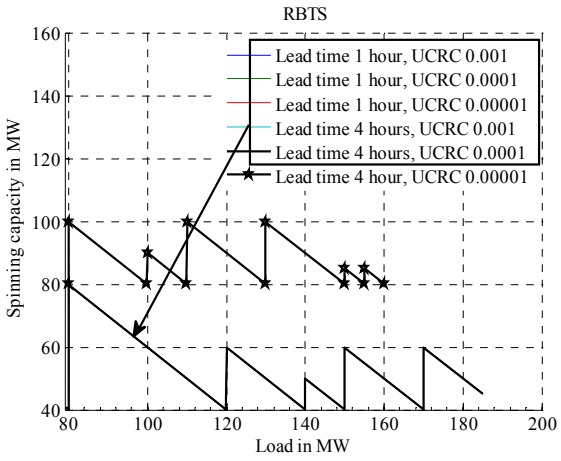

Fig. 2.8: Spinning capacity for the RBTS as a function of load with different lead times

2.6 Risk Analysis of the IEEE-RTS for Various Lead Times at Different Load Levels

Fig. 2.9 presents a comparison of the system risk for lead times of 1 and 4 hours for the IEEE-RTS. The UCR for a load of 2005.9 MW for 13 committed units (2406 MW) at a lead time of 1 hour is 0.0000229. The corresponding risk increases to 0.00183 for load of 2006 MW. The system is able to carry a maximum load of 2250.9 MW at a UCRC of 0.001 and this is the PLCC value at this UCRC. Fig. 2.9(b) shows that the same number of committed units at an UCRC of 0.001 can carry a peak load of 2005.9 MW and the UCR is 0.000364 for a lead time of 4 hours. The risk jumps to 0.00738 for a load of 2006 MW.

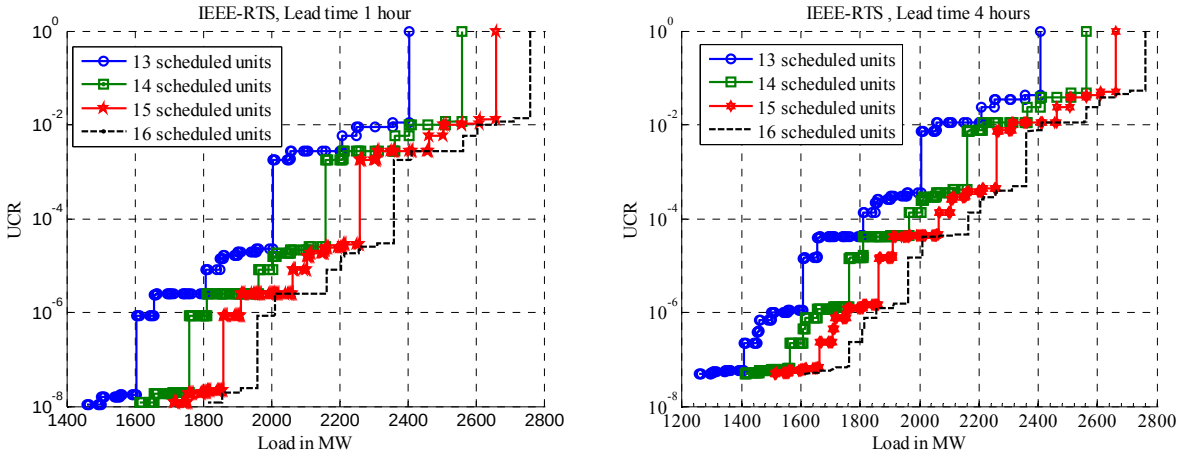

(a): Lead time 1 hour (b): Lead time 4 hours

Fig. 2.9: UCR as a function of load for the IEEE-RTS

The risk profiles shown in Fig. 2.9 and in those Fig. 2.2 for the RBTS are similar in form and clearly show how the peak load carrying capability of the scheduled generating units decreases with increase in the system lead time. The system is able to carry a load of 2260.9 MW and 2360.9 MW for an UCRC of 0.001 when the number of committed units are 15 (2661 MW) and 16 (2761 MW) respectively for a lead time of 4 hour.

Fig. 2.9 shows a definite pattern of large discrete UCR steps as the load changes for both lead times and committed generation level. For example, the jump in the risk level is relatively large for 13 scheduled units when the loads change from 2205.9 to 2206, 1605.9 to 1606 etc for both lead times of 1 and 4 hours. These large steps in UCR occur at the load levels where the difference in the generation and the load is an integer multiple of the capacity of the largest operating unit in the system. These significant UCR steps occur for each scheduled capacity and particular load levels. The loads levels at which the significant UCR jumps occur are independent of the system lead time. A summary of the load levels at which these large steps in the UCR are obtained for lead times of 1 to 4 hours are presented in Table 2.4. As in the RBTS analysis, only three significant risk steps and the corresponding load levels are presented.

Table 2.4: Summary of the significant risk steps for the IEEE-RTS

No of units in operation	Total Capacity in operation (MW)	Load level at which 1st major change in risk level is observed (MW)		Load level at which 2nd major change in risk level is observed (MW)		Load level at which 3rd major change in risk level is observed (MW)		Spinning capacity (MW) =Generation-Load
		From	To	From	To	From	To	
13	2406	2405.9	2406	2005.9	2006	1505.9	1506	n*400
14	2561	2560.9	2561	2160.9	2161	1760.9	1761	n*400
15	2661	2660.9	2661	2260.9	2261	1860.9	1861	n*400
16	2761	2760.9	2761	2360.9	2361	1960.9	1961	n*400

where n = 0, 1, 2, 3, 4… etc

The variation in the UCR for 13 scheduled units at a load of 2200 MW at different lead times are shown in Table 2.5. The UCR increases as the lead time increases even if the system

load and generation remains fixed due to the fact that the failure probability of the operating units increases with the lead time.

Table 2.5: UCR variation with lead time for a fixed load and scheduled capacity

Load (MW)	Lead time (hours)	UCR
2200	1	2.710256E-03
2200	2	5.460466E-03
2200	3	8.249808E-03
2200	4	1.107747E-02

2.7 Load Carrying Capability of the IEEE-RTS under Different Lead Times

A Load Carrying Capability (LCC) profile was created for the IEEE-RTS under various UCRC and lead times. A LCC profile is a sensitivity analysis that indicates the load levels that the system can carry under various conditions. The required number of generating units, scheduled generating capacities and the spinning reserves in the system were evaluated for every 0.1 MW increase in load level from 40 % to 100 % of the peak load at the different UCRC. An analysis of the total scheduled capacities, number of scheduled units and the spinning capacities for lead times of 1 and 4 hours at different UCRC are illustrated in Fig. 2.10, 2.11 and 2.12 respectively.

For a lead time of 1 hour, the system is capable of carrying its peak load at all the three UCRC considered. The total scheduled capacities are the same for the UCRC of 0.001 and 0.0001 for a lead time of 1 hour as shown in Fig. 2.10(a). Fig. 2.10(b) shows that the system has a capacity deficiency for a lead time of 4 hours at the UCRC of 0.0001 and 0.00001 for higher loads. The system can only carry loads of 2805 and 2600 MW respectively, at these UCRC with the existing capacity of 3405 MW.

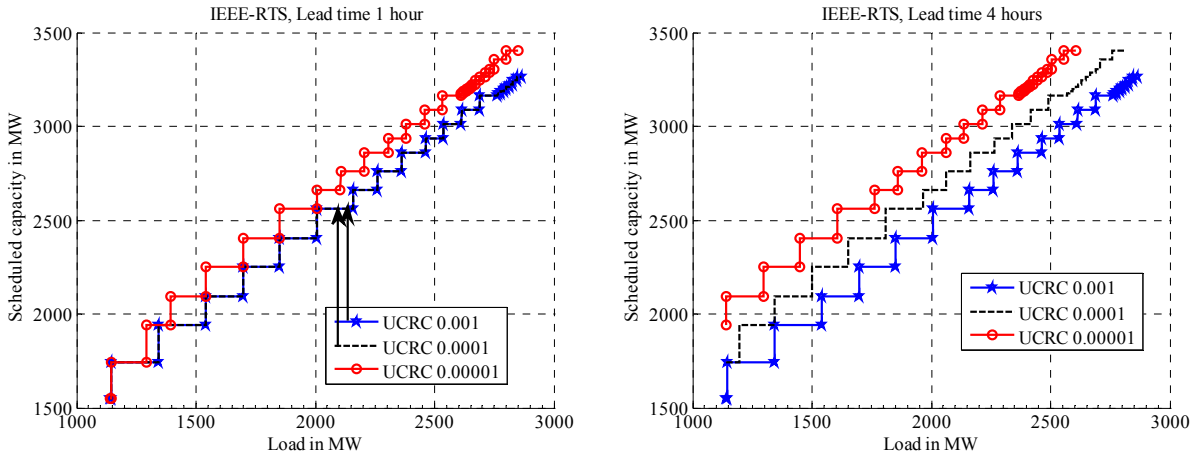

(a): Lead time 1 hour (b): Lead time 4 hours

Fig. 2.10: Generation scheduled for the IEEE-RTS as a function of load

A comparison of the total number of scheduled units required to meet the load for the two lead times of 1 and 4 hours is presented in Fig. 2.11. At a lead time of 4 hours, the total required capacity at loads higher than 2805 MW and 2600 MW exceeds the system capacity for UCRC of 0.0001 and 0.00001. Capacity assistance therefore is required to maintain the designated system reliability. It can be seen from Fig. 2.11 that a large number of units are scheduled to provide a relatively small increase in load level due to the small generating capacities of the committed units., The number of units scheduled to meet the same load level for a lead time of 1 hour are less than the number of units scheduled for a lead time of 4 hours.

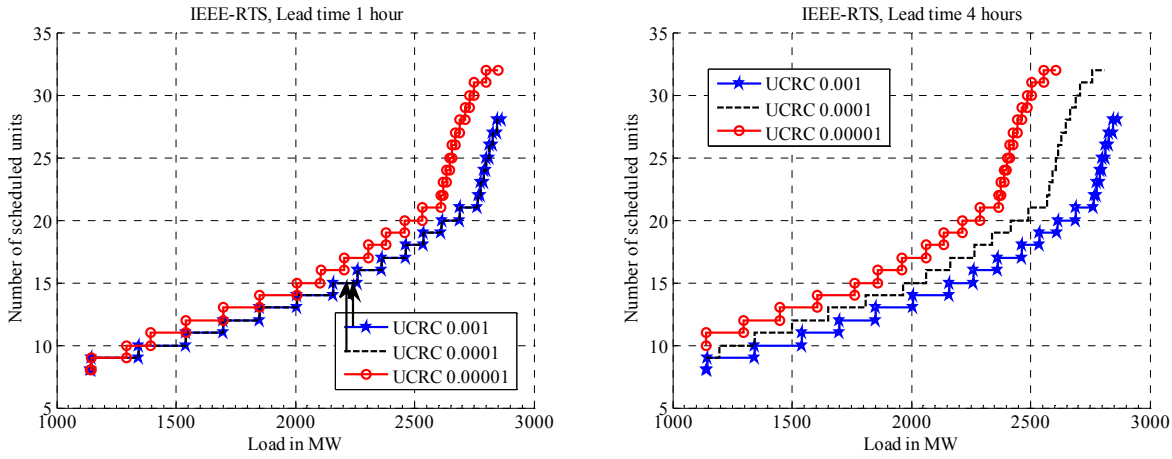

(a): Lead time 1 hour (b): Lead time 4 hours

Fig. 2.11: No. of scheduled units for the IEEE-RTS as a function of load

Fig. 2.12 shows that for each UCRC, the spinning reserve required to maintain the UCRC varies as additional units are committed to meet the increasing load demand. A new unit is scheduled when the operating capacity can no longer meet the load demand at that UCRC. The spinning reserve varies from a maximum to a minimum value as the load increases. As shown in Fig. 2.12, the maximum spinning reserve depends on the size of the incoming unit but there is always a fixed minimum spinning capacity required to meet the load at a designated UCRC. The minimum spinning capacity generally tends to saturate to a fixed value at higher load levels for each UCRC. The minimum spinning capacity for higher load increases with lower UCRC and higher lead times as shown in Fig. 2.12.

A large number of small units in the system can have a favorable impact on system economic operation as these units can significantly reduce the difference in the maximum and minimum amount of system spinning reserve required to maintain the reliability criteria as seen in Fig. 2.12. At higher loads, the variation in spinning reserve for all UCRC when the small capacity units are committed is 12 MW.

A minimum spinning reserve of 400.1 MW, 597.1 MW and 800 MW is required under the UCRC of 0.001, 0.0001 and 0.00001 for a lead time of 4 hours for load levels greater than 1343.9 MW. The spinning reserves at a UCRC of 0.0001 and light loading conditions are lower. The system lacks sufficient generating capacity for UCRC of 0.0001 and 0.00001 at higher loads. The system requires a minimum of 400.1 MW spinning capacity to maintain the UCRC of 0.001 and 0.0001 for a lead time of 1 hour.

The minimum spinning capacities to satisfy UCRC of 0.0001 and 0.00001 at a lead time of 1 hour are lower than those required for a lead time of 4 hours. This indicates that lower spinning capacity can provide the same reliability if additional system assistance can be quickly provided.

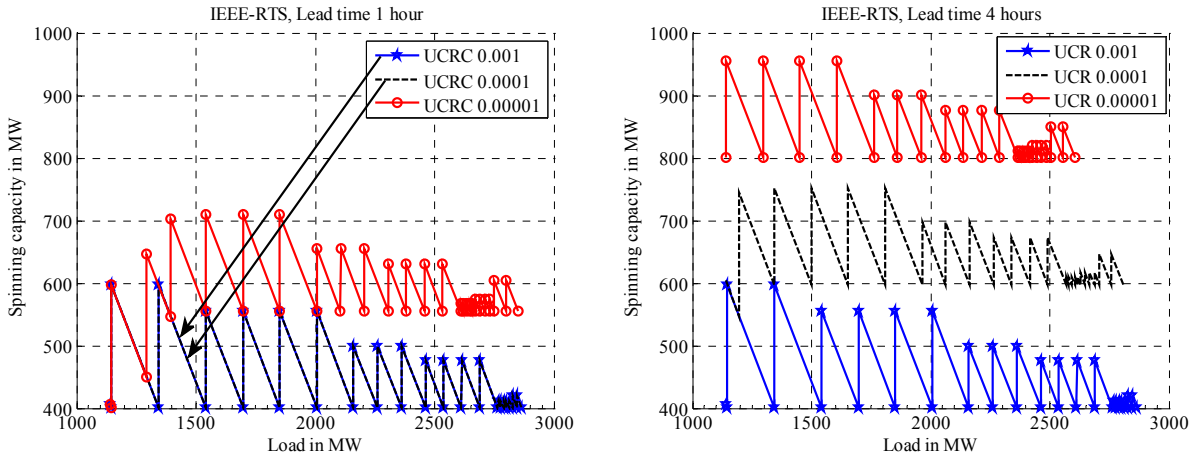

(a): Lead time 1 hour (b): Lead time 4 hours

Fig. 2.12: Spinning capacity for the IEEE-RTS as a function of load

2.8 Comparison of Scheduled Capacity for a Fixed Risk at Variable Lead Times

A comparative study is shown in Fig. 2.13 for the total scheduled capacity of the IEEE-RTS for a lead time of 1 and 4 hours at various UCRC. Fig. 2.13(a), 2.13(b) and 2.13(c) show the variation in the scheduled capacity for UCRC of 0.001, 0.0001 and 0.00001 respectively. These figures show that the scheduled capacities are greater for a lead time of 4 hours than for 1 hour for all the cases except at an UCRC of 0.001. At an UCRC of 0.001 the scheduled capacity does not change even when the lead time changes from 1 hour to 4 hour as shown in Fig. 2.13(a) as the reliability criterion (UCRC) is relatively high. The system cannot support the system peak load of 2850 MW for a lead time of 4 hours for UCRC of 0.0001 and 0.00001 without additional online capacity support as shown in Fig. 2.13(c).

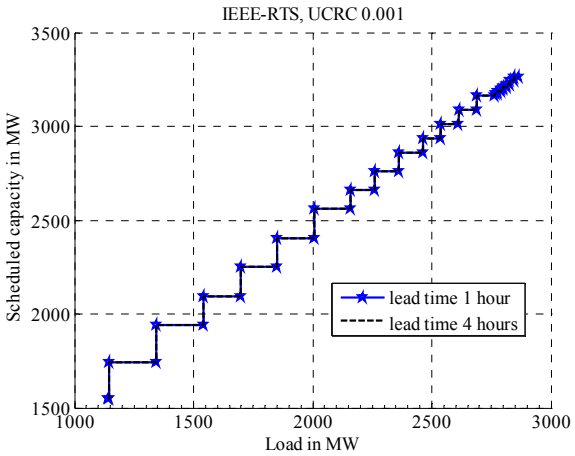

(a): UCRC 0.001

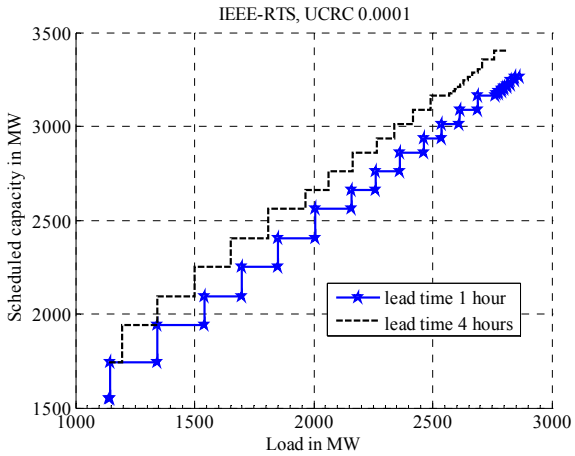

(b): UCRC 0.0001

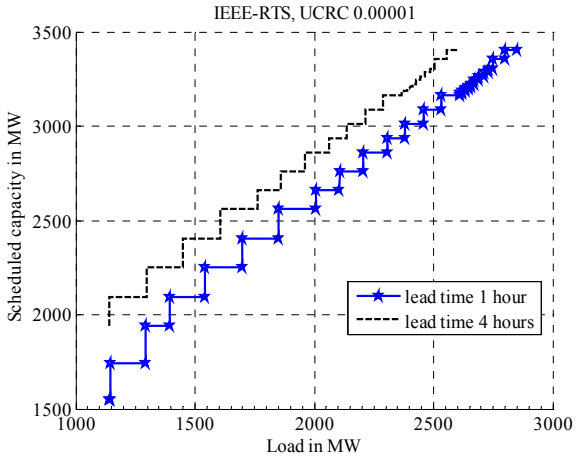

(c): UCRC 0.00001

Fig. 2.13: Scheduled capacity for the IEEE-RTS as a function of load for different lead times

2.9 Comparison of the Total Spinning Capacity for a Fixed UCR and Variable Lead times

A comparison of the spinning capacity at different UCRC is presented in Fig. 2.14. The spinning capacities required for both lead times are the same for a UCRC of 0.001 as shown in Fig. 2.14(a). Therefore a change in lead time may or may not increase the need for additional spinning capacity to meet the load level especially when the UCRC is relatively high. The system needs assistance from other systems to carry its peak load (2850MW) at a UCRC of 0.0001 and 0.00001 as shown in Fig. 2.14(b) and Fig. 2.14(c). Fig. 2.14 indicates that for each

case, there is a fixed minimum spinning reserve requirement to meet a specific UCRC at high loads. A summary of the minimum spinning capacity required to carry high loads for different conditions are presented in Table 2.6. It is clearly seen that higher reliability demands more spinning capacity in the system. The spinning capacity can be decreased by decreasing the lead time or by increasing the UCRC.

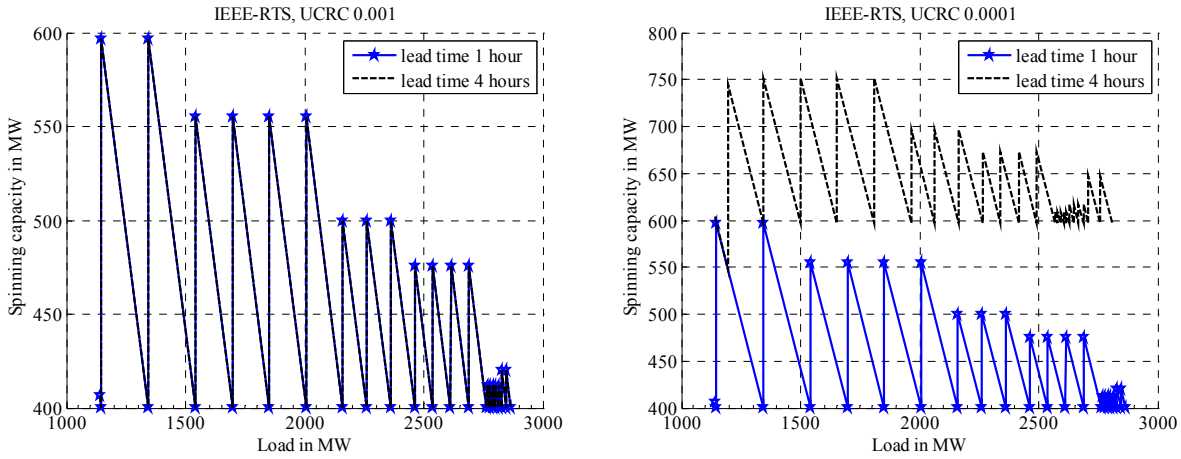

(a): UCRC 0.001

(b): UCRC 0.0001

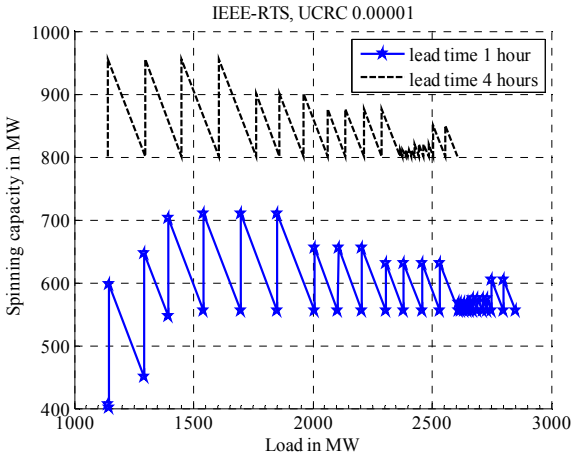

(c): UCRC 0.00001

Fig. 2.14: Spinning capacities for the IEEE-RTS as a function of load for different lead times

Table 2.6: Minimum spinning capacity requirement for high load levels

UCRC	Minimum Spinning Capacity required for higher loads in (MW)			
	Lead time 1 hour	Lead time 2 hours	Lead time 3 hours	Lead time 4 hours
0.001	400.1	400.1	400.1	400.1
0.0001	400.1	500.1	555.1	597.1
0.00001	555.1	702.1	750.1	800.1

2.10 Conclusion

This chapter describes the procedure used to evaluate the Unit Commitment Risk (UCR) in a power system. Two test systems are used to illustrate evaluation of the scheduled capacity, number of scheduled generating units and the spinning reserve requirement to maintain a specified Unit Commitment Risk Criterion (UCRC). The analyses were carried out for two different lead times.

The UCR at a given load and a specified number of scheduled units increases with the lead time as the failure probability of the operating units increase with time. A small decrease in the UCR occurs if the system is able to sustain the outage of a relatively small unit but a relatively larger UCR decrease occurs at certain load points irrespective of the lead time. These large UCR decreases are obtained in the RBTS and the IEEE-RTS whenever the difference between the total committed capacity and the load are integer multiples of 40 and 400 MW respectively. In both test systems, significant risk decreases are obtained when the difference between the total committed generation and the load level are integer multiples of the largest operating unit in the system.

If the existing generating capacity is insufficient to carry the system peak load and maintain the reliability criterion (UCRC) then assistance is required from other sources. The analyses carried out illustrate that the lead time has a high impact on the system operating conditions. At short lead times the operating conditions for various UCRC may not change due to the relatively small outage replacement rate. The operating conditions, however, will be generally different for higher lead times. Each power system is different in size, unit types, unit capacities and failure rates. Each system therefore has its own unique operating reserve

requirements including the system lead time even for the same UCRC. The operating reserve requirements should, therefore, be evaluated for each individual system.

The operating reserve in a power system at a given load level is determined by the specified UCRC. If a low value of UCRC is chosen, than the spinning reserve required to maintain the reliability criterion will be generally high. The operating reserve requirement for a given UCRC generally increases with increased system lead times.

This chapter illustrates the concept of Unit Commitment Risk (UCR) and it's response to a number of basic elements in the calculation process by application to the RBTS and the IEEE-RTS. The following chapters in the thesis illustrate the research conducted to integrate wind power in the assessment of operating risk and to determine the contribution that wind power can add to the spinning reserve under a constant risk criterion.

3. WIND POWER MODELING

3.1 Introduction

Appropriate wind speed and wind power modeling is of primary importance in evaluating the impacts of integrating wind power in a power system. The initial state of the system (at time zero) is assumed to be known in a power system operating study. It is also important to know the wind power in the next few hours based on the known value of the wind speed at the present time. The wind, however, is variable, intermittent and uncertain and unlike conventional generating units, wind power is not generally dispatchable. It is essential to develop procedures to estimate short term (4-6 hours) wind power production given that other generating units can be placed in service after that time. This time period is described as the lead time in Chapter 1. This chapter presents the approach used in this research to model short term wind power production over the next few hours in the form of probability distributions.

Short term wind speed prediction is generally categorized in three basic approaches designated as Persistence, Numerical Weather Prediction (NWP) and Time series models. Each model has its own advantages and disadvantages and outweighs other models in some aspects. All wind speed models contain some error in their forecasted values, which depend on many factors such as the forecast time horizon, local site orography, seasonality, diurnal wind pattern, height above the ground etc.

3.1.1 Persistence Prediction

A persistence prediction is a simple forecasting technique, which assumes that the forecast value is the same as the initial value at zero hour for the entire forecast horizon. The

inherent assumption in a persistence model is that the current value will not change in the near future. The performance of all other prediction systems are compared with the persistence model [89, 90] as it contains information on the actual metrological condition at the wind site at the time when the prediction horizon starts. A Persistence model generally gives better predictions of wind speed than a NWP model for a time frame of less than six hours [89-91].

3.1.2 Numerical Weather Prediction Models

Numerical Weather Prediction (NWP) systems simulate the future movements of the atmosphere by numerically integrating the non-linear equations of motion from the current atmospheric state. This approach maps the world continuously on a discrete three dimensional grid and requires a large amount of online data to be collected for every meteorological change and is used by national weather services. These weather services use a global model with horizontal resolutions of 100 *100 km^2 down to 50*50 km^2 to capture the development of worldwide weather systems. A local model is derived from these global models, which have horizontal resolutions of 10*10 km^2 to 7*7 km^2.

Data collection for a NWP model is a complex task which requires continuous measurement of atmospheric states on a regular basis by using a large number of synoptic stations, buoys, radiosondes, ships, satellites and planes all over the world. Global meteorological data are made available to the weather services for use in their individual NWP model, after processing by the World Meteorological Organization (WMO) [92, 93].

Extended resolution of NWP system data may not be very useful for application at a specific wind site as it does not account for the orography of the location. Corrections are also required to create a wind power production model that recognizes the thermal stratification of the location and height at the wind turbine hub. The surface wind becomes more turbulent during the day than at night due to the solar radiation. The accuracy level of a wind speed prediction over the course of a day is also reported to vary due to thermal stratification at the local site [92].

Two types of forecasting models have been developed which use NWP model output. One approach known as the physical approach [94-99] uses the actual conditions at the wind site and the physical variables of the wind conditions before predicting the power using the WTG power curve. This approach considers the actual physical parameters of the terrain while estimating the power generated from the wind at the hub height. The Wind Power Prediction Tool (WPPT) [100] is based on the physical approach [101-103] and it is used to continuously derive a relationship between the online measured wind speed and the predicted wind power output with some local refinement. This system has been used in Denmark since 1997 by the Danish power production utilities Elsam and Eltra. The physical approach generally requires a relatively long time to estimate the forecast wind power at a particular site.

Another approach known as the statistical approach [89, 104-114] analyzes the connection between weather forecasts and power production from time series of the past and describes this connection in a way that enables it to be used in the future [115]. These are generally black box approaches such as artificial neural networks (ANN) [106, 114, 116-121] and fuzzy logic [122] . An ANN based system called Wind Power Management System (WPMS) [123] are used by several German transmission system operators (TSO). These models are trained with the historical wind data of a representative site and are used to predict the future wind power for an entire region by scaling up using a multiplying factor. This second approach does not consider the physical conditions at the local wind site. A range of wind power forecasting techniques using different methods are presented in [89, 92, 115, 124].

3.2 Short-Term Wind Speed Probability Distributions Using Time Series Auto-regressive Moving Average (ARMA) models

The time frame is of primary concern in wind power forecasting. Highly advanced techniques involving numerical weather prediction (NWP) models are necessary for long forecast horizons. Persistence and time series ARMA methods can be applied for short forecast horizons. Persistence models are reported to have shown better performance than NWP based models for lead times of 4–6 hour [91, 125]. Time series ARMA models are also used for forecasting future wind speed [108, 109, 126, 127] and outperform the NWP-based models for

forecast horizons less than 4–6 hour [126]. Wind speed prediction using ARMA models has been used extensively in generating capacity adequacy evaluation as this is an independent technique that involves historical data at the wind site under consideration. Persistence and time series ARMA models do not involve NWP model input [109]. Reference [128] discusses a wide range of methods suitable for different forecast time horizons. This includes time series techniques such as ARMA models.

The approach [129] used in this thesis is based on a time series model that does not require NWP data. The time series used is an auto-regressive moving average (ARMA) model developed specifically for the wind site(s) in question. A method for developing a suitable ARMA model is described in [54]. It can be used in a unique way to determine the variability in the wind speed over the next few hours given that the wind speed at time zero is known. The ARMA model can be used to generate sufficient data to express the variability in the form of a probability distribution that depends on the initial wind speed and can be updated at successive points in time. The procedure used to obtain the probability distributions of the future wind speed for a known value of initial wind speed at the zero hour is described in the following.

1) A time series ARMA model for the wind site of interest was developed [130] using the approach reported in [54].

2) The hourly wind speed for the particular hours of concern was simulated using the ARMA model, for a large number (8000) of simulation years. The simulated mean and standard deviation of the wind speed for each hour closely match the actual mean and standard deviation of the wind speed at each hour.

3) Regression analyses were conducted between two simulated hour speeds. For example if the wind speed probability distribution at hour X for a known value of wind speed at the zero hour is needed then a regression of the wind speed at hour zero and hour X is required.

4) The distribution of the wind speed at the specified hour X around the regression line for a known value of initial wind speed at the zero hour indicates the variability of the wind speed in the hour X.

5) The probability distributions of the wind speed were passed through the WTG power curve, to obtain the wind power probability distribution associated with each hour. The approach does not attempt to forecast the future wind speed at each lead time. It creates a probability distribution of the variability in wind speeds at each lead time given that the wind speed at time zero is known.

The purposed model does not try to bring the uncertainty associated with the future wind speed into a certainty domain as used in other methods but rather brings the uncertainty into a probability domain. The recognized uncertainty in the future wind speed is utilized to obtain a UCR value in the wind power integrated power system.

This chapter is focused on describing the proposed Conditional Wind Speed Distributin (CWSD) model. The application of the developed model is presented in the subsequent chapters. A case study is presented using wind data from a site at Swift Current in Saskatchewan, Canada. The annual ARMA (4, 3) model [130] for the site is

$$y_t = 1.1772\, y_{t-1} + 0.1001\, y_{t-2} - 0.3572\, y_{t-3} + 0.0379\, y_{t-4} + \alpha_t - 0.5030\alpha_{t-1} - 0.2924\alpha_{t-2} + 0.1317\alpha_{t-3}$$

$$\alpha_t \in \mathrm{NID}(0, 0.524760^2) \qquad (3.1)$$

where NID is Normally Independently Distributed. The simulated wind speed SW_t can be calculated from (3.2) using the wind speed time series model.

$$SW_t = \mu_t + \sigma_t * y_t \qquad (3.2)$$

where μ_t is the mean observed wind speed at hour t; σ_t is the standard deviation of the observed wind speed at hour t; $\{\alpha_t\}$ is a normal white noise process with zero mean and the variance

0.524760. Hourly wind speeds for hours 4–7 (January 1, 4 a.m. to 7 a.m.) and 5039–5042 (August 15, 2 p.m. to 5 p.m.) for the Swift Current location were simulated using (3.2). Each hour is simulated 8000 times. A comparison of the actual mean and standard deviation with the simulated values are shown in Table 3.1. The simulated mean wind speed and standard deviation closely match the actual values. There is a strong correlation between the initial wind speed at time zero and the wind speed at the next hour. Table 3.2 shows that the correlation decreases as the forecast time horizon increases.

Table 3.1: Actual /simulated wind speed for Swift Current

		Hour 4	Hour 5	Hour 6	Hour 7
Mean wind speed (km/hr)	Actual	21.87	21.73	22.07	23.20
	Simulated	21.97	21.91	22.28	23.37
Standard deviation of wind speed (km/hr)	Actual	10.9	14.34	12.44	12.11
	Simulated	11.15	14.78	12.86	12.58
		Hour 5039	Hour 5040	Hour 5041	Hour 5042
Mean wind speed (km/hr)	Actual	13.20	13.33	16.00	14.40
	Simulated	13.16	13.25	15.97	14.35
Standard deviation of wind speed (km/hr)	Actual	5.86	6.72	6.37	5.83
	Simulated	5.95	6.87	6.46	5.94

The probability distribution of the wind speeds at each future hour in the lead time period are designated as Conditional Wind Speed Distributions (CWSD) and capture the uncertainty associated with the wind speed at these hours for a known initial wind speed. These distributions can be transformed using the WTG power curve into multi-derated state capacity models. The variability of the wind speed at hour 5 and 6 relative to hour 4 is shown in Fig. 3.1(a) and 3.1(b). Both the figures show that the number of observations in the sample space decreases as the initial speed in the independent axis moves to a very low or a very high value.

Table 3.2: Correlation between the simulated hourly wind speeds for the Swift Current site

	Hour 4	Hour 5	Hour 6	Hour 7
	Correlation Coefficients			
Hour 4	1	0.8346	0.7516	0.6855
Hour 5		1	0.8350	0.7536
Hour 6			1	0.8340
Hour 7				1
	Hour 5039	Hour 5040	Hour 5041	Hour 5042
	Correlation Coefficients			
Hour 5039	1	0.8255	0.7451	0.6705
Hour 5040		1	0.8301	0.7433
Hour 5041			1	0.8272
Hour 5042				1

The conditional distribution of the predicted wind speed is not a smooth curve and the shapes vary when the initial wind speed at the X-axis changes. The distribution is generally symmetrically distributed around the mean value and gradually loses this shape as the wind speed moves towards its extreme values.

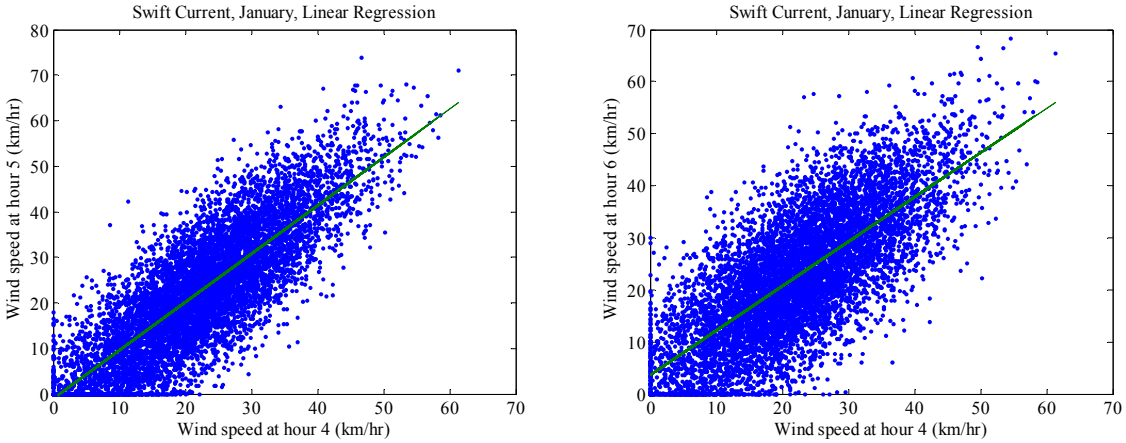

(a): Wind speed variability at hour 5 (b): Wind speed variability at hour 6

Fig.3.1: Wind speed variability at hour 5 and 6 relative to hour 4

The linear regression line in the proposed CWSD forecast indicates a strong link between the proposed model and the Persistence model which dominates short term wind power forecasting [90, 91, 101, 102, 124, 125, 131].

Each hour has a distinct mean and standard deviation and every wind site has a unique ARMA model, and therefore the CWSD depends on the initial wind condition, the hour of the year concerned and the specific site of interest. The CWSD at hour 5 and 5040 for initial wind speeds of 19.5-20.5 km/hr and 25.5-26.5 km/hr at hour 4(January 1st) and 5039 (August 15th) are presented in Fig. 3.2(a) and 3.2(b) respectively. Table 3.1 shows that a wind speed of 25.5-26.5 km/hr is well above the mean wind speed in the month of August. It was noted that for the given hour, if the initial wind speed is high then the wind speed in the next hour does not abruptly drop to a very low value and that the chances of having a high wind speed in the next hour will still be relatively high.

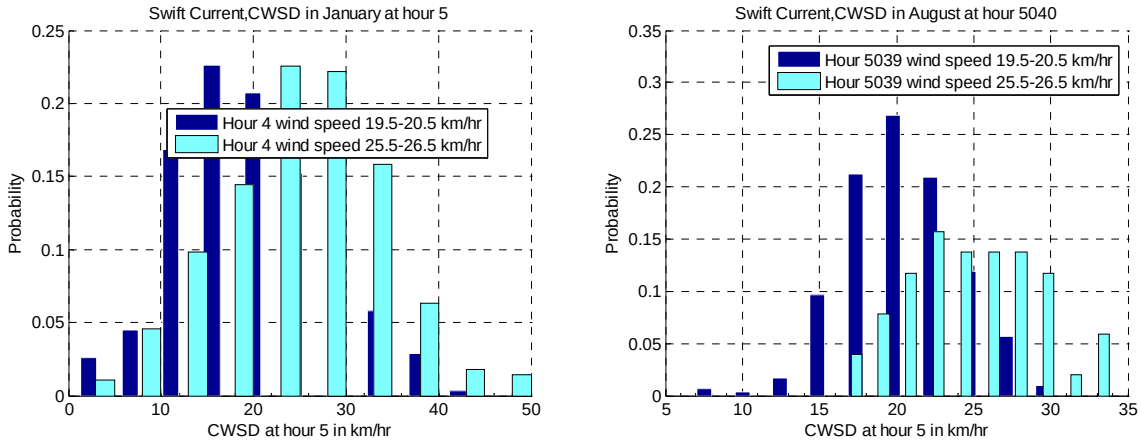

(a): CWSD at hour 5 (b): CWSD at hour 5040

Fig.3.2: Conditional Wind Speed Distributions at hour 5 and 5040

3.3 Conditional Wind Power Distribution

A WTG starts generating when the wind speed exceeds the cut-in V_{ci} speed. At rated wind speed V_r the turbine output remains constant and if the wind speed increases to a value greater than or equal to the cut-out speed V_{co}, the WTG is shut down. The output power from a WTG is not linear between the cut-in and rated wind speed [44]. Although the basic characteristic remains the same, different designs can be used to create different cut-in, cut-out and rated wind speeds and the associated power output values.

The V_{ci}, V_r, V_{co} values for the Vestas WTG installed in the Centennial Wind Farm in Swift Current, Saskatchewan are 15, 50 and 90 km/hr respectively. These WTG are designed to operate in the non-linear portion of the power curve. The rated power capacity (P_r) of each WTG is 1.8 MW. These data are used in the operating reserve assessment studies described in this thesis.

The conditional wind speed (CWS) data at each designated hour is passed through the wind power curve to generate the CWPD. The applied model for the wind power curve used in this research is described in detail in [51]. This is a generic model that has been used in a wide range of studies. As noted in Chapter 1, the generic model could be easily replaced in a specific application by a more applicable model if the wind turbine manufacturer or the operating utility has one available. Equation (3.3) was used to generate the CWPD. The parameters A, B and C are dependent on the WTG characteristics and are determined using (3.4), (3.5) and (3.6).

$$P = \begin{cases} 0 & 0 \le CWS < V_{ci} \\ \left\{A + B \times (CWS) + C \times (CWS)^2\right\} \times P_r & V_{ci} \le CWS < V_r \\ P_r & V_r \le CWS < V_{co} \\ 0 & CWS \ge V_{co} \end{cases} \tag{3.3}$$

where CWS is the Conditional Wind Speed and the parameters A, B and C are given by (3.4) , (3.5) and (3.6) respectively [51].

$$A = \frac{1}{(V_{ci} - V_r)^2}\left\{V_{ci}(V_{ci} + V_r) - 4V_{ci} \times V_r\left(\frac{V_{ci} + V_r}{2V_r}\right)^3\right\} \tag{3.4}$$

$$B = \frac{1}{(V_{ci} - V_r)^2}\left\{4(V_{ci} + V_r) \times \left(\frac{V_{ci} + V_r}{2V_r}\right)^3 - 3(V_{ci} + V_r)\right\} \tag{3.5}$$

$$C = \frac{1}{(V_{ci} - V_r)^2}\left\{2 - 4\left(\frac{V_{ci} + V_r}{2V_r}\right)^3\right\} \tag{3.6}$$

The CWPD obtained from the CWSD in Fig. 3.2(a) is shown in Fig. 3.3(a) and that from Fig. 3.2(b) is shown in Fig. 3.3(b). The CWPD at a particular hour and for a particular future hour during the lead time is entirely dependent on the related CWSD.

The CWPD are widely dissimilar for the Swift Current wind site for the two seasons for the same initial wind speeds. This is due to the large differences in the historical mean and variability of the wind speed in January and August as shown by the standard deviations in Table 3.1.

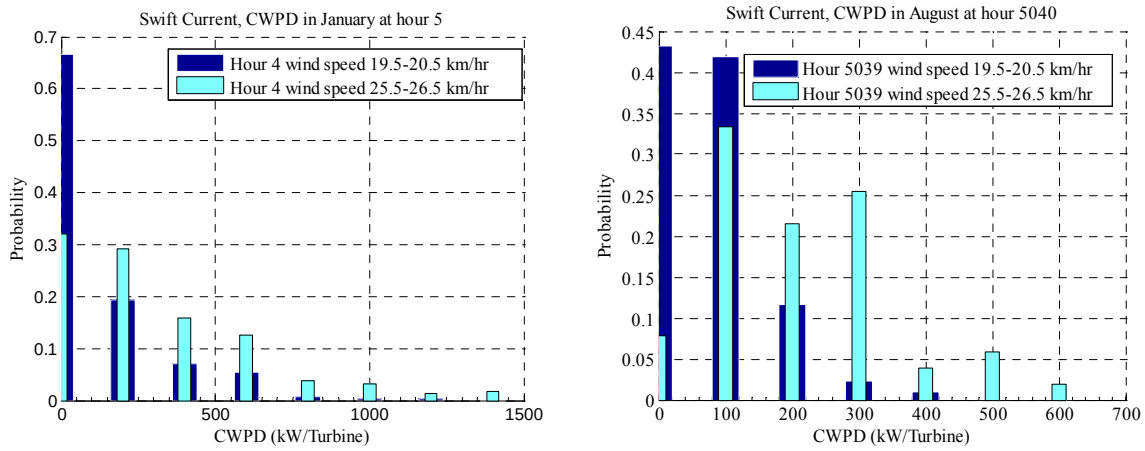

(a): CWPD at hour 5 (b): CWPD at hour 5040

Fig.3.3: Conditional Wind Power Distributions at hours 5 and 5040

A maximum power of 1288 kW was obtained at hour 5 for a single wind turbine generator operating at an initial wind speed of 19.5 to 20.5 km/hour at hour 4 in January. The same initial wind speed at hour 5039 in August has a maximum power state of 408 kW at hour 5040. These maximum power states have very low probabilities and make relatively small contributions to the system reliability. It is important to note that both initial wind speed conditions in the month of August (August 15th at hour 5040) result in considerably less maximum power than occurs in January under similar conditions.

Fig. 3.4(a) and 3.4(b) show the CWPD for a lead time of 2 hours in the month of January and August. The reference time zero values are still hours 4 and 5039 in January and August respectively as in Fig. 3.3. It is important to note that the CWPD obtained for a lead time of 1 hour shown in Fig. 3.3(a) and 3.3(b)) are not the same as the CWPD obtained for the lead time of 2 hours.

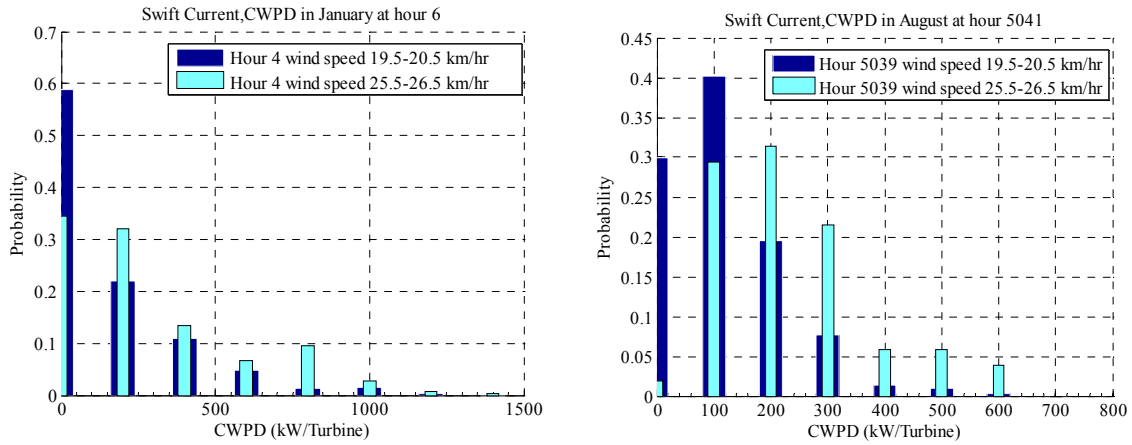

(a): CDFW at hour 6 (b): CDFW at hour 5041

Fig. 3.4: Conditional Wind Power Distribution at hour 6 and 5041

3.4 Conclusion

The approach used to forecast short term future wind speed probability distributions is presented in this chapter. The proposed technique is based on the ARMA model and depends on the historical value of the wind at a particular site. The approach does not try to bring the uncertainty associated with the stochastic nature of the wind into a certainty domain. It recognizes that the uncertainty in the future wind speed can be directly applied in UCR analysis of wind integrated power system operation. The developed model is unique as it is based on the local wind conditions and predicts the future wind speed in the form of a Conditional Wind Speed Distribution (CWSD). The model also recognizes the dependence of short term future wind speed on the present wind speed.

A persistence model is a very simple model of wind speed forecasting that assumes that the future *w*ind speed will be the same as the wind speed at present time. The model has shown to be more accurate than highly sophisticated models for short forecast horizons. Highly advanced techniques such as Numerical Weather Predication (NWP) models or Statistical models require input data from the state of the present atmosphere. It takes a considerably long time for weather services to generate the weather map of the atmosphere and by the time the local weather conditions are predicted the state of the atmosphere would have already changed which can result in new set of forecasts. Highly sophisticated models are not suitable for short term wind speed forecasting and are good only for long time horizons. The short term wind power output could be obtained directly from the initial wind speed and the power curve using only Persistence model. This however will not recognize the residual uncertainty in the future wind power. The studies shown in this chapter illustrate that there is considerable uncertainty in the wind power output in the next hour given the wind speed at the initial point in time. The proposed model acknowledges the strength of the Persistence approach and extends this using a forecast in the form of a probability distribution that essentially captures all possible wind speeds in the next hour.

4. OPERATING RESERVE ASSESSMENT OF WIND INTEGRATED POWER SYSTEMS

4.1 Introduction

Accurate prediction of future wind speed is not an easy task and the error increases with the forecast time horizon. Many countries and provinces have made commitments to generate a certain percentage of their electricity demand from renewable energy sources including wind, and the world wide installation of wind turbines is forecast to increase considerably. In such a scenario, suitable methods to access the risks associated with integrating wind power in conventional power systems and the operating capacity credit associated with wind power become increasingly important. The concept of determining the capacity credit associated with wind power has received considerable attention around the world. The bulk of the work in this area is in the domain of adequacy assessment, which relates to the existence of sufficient facilities to supply the aggregate electrical demand and energy requirements of the system customers at all times, taking into account scheduled and reasonably expected unscheduled outages of the system elements [132]. It is generally agreed that the most comprehensive way to evaluate wind capacity credit is to determine the increase in peak load carrying capability (IPLCC) at the criterion risk level that can be attributed to the specified wind facilities [133]. This can be done using analytical methods, Monte Carlo simulation [130], or alternative techniques such as population-based intelligent search methods [118].

Adequacy assessment is an integral element in generation, transmission and distribution planning. There has, however, been relatively little work done on assessing the capacity credit associated with wind power in the operating domain. These studies fall in the general category of security assessment, which involves the ability of the system to withstand sudden disturbances such as electric short circuits or the unanticipated loss of system elements [5, 132]. Security

assessment covers an extremely wide range of activities such as dynamic, steady state, voltage and overload evaluations, and there are many publications on these subjects. This includes the general areas of dynamic and transient stability [5] and on-line risk based security assessment [134].

Considering wind capacity credit in the operating domain involves the unit commitment and dispatch framework within which the electric power utility operates. There is a wide range of literature dealing with unit commitment [135, 136] which consider operational, power flow and environmental constraints, together with network contingencies [80, 81]. The vast majority of these papers deal with economic aspects of unit commitment and the risks associated with unit commitment decisions are not considered. Some of the more recently published material such as [121, 137, 138] consider wind power in unit commitment decisions but do not consider risk assessment and focus on the economic benefits of adding wind. Reference [82] incorporates reliability considerations in a unit commitment framework by developing LOLE and EENS indices that provide useful information on long-term operating decisions. Reference [139] recognizes the variability associated with wind power and introduces a procedure to commit and dispatch non-wind generation units economically with sufficient ramping capability to accommodate the volatility of wind power generation, and indicate that the procedure can be used in day ahead and long term operational planning.

Wind power behaves quite differently than conventional power generation. If wind and other renewable power sources are to be integrated rather than simply added in conventional power systems then procedures need to be developed to analyze their risk contributions that incorporate their unique characteristics. A wind turbine generator (WTG) is fundamentally different from conventional generating units in many aspects. The main difference is that the power output of each WTG in a given wind farm is dependent in the instantaneous wind speed at the turbine blades. The wind power at each WTG in the wind farm will change as the overall wind speed changes and can drop to zero when the wind speed drops below the WTG cut-in speed. Determination of the UCR in systems with significant wind power generation therefore has to be considered in a different manner than has previously been used in systems composed of conventional units [135, 136].

This chapter presents an approach to evaluate the contribution that wind power can make to the load carrying capability of a power generating system in an operating scenario. The basic concepts of unit commitment risk analysis are extended to include the inherent variability associated with wind power using the short term probability distributions of the wind speed and wind power output model described in Chapter 3. As discussed in Chapter 3, short term wind speed probability distributions based on the initial known wind speeds are generated and used to produce conditional wind power probability distributions. These distributions are used to create derated state models that can be combined with the conventional generating capacity models in a COPT to determine the UCR associated with different loading conditions and lead times.

The focus in this chapter is to further extend the PJM method discussed in Chapter 1 and 2 by incorporating wind generating capacity in the assessment of unit commitment risk and to assess the contribution made by wind generation to the system operating reserve. The analysis is done on a total system basis in which transmission constraints are not considered, however, assistance from neighboring systems can be incorporated in the developed capacity models [1]. The actual capacity credit associated with any generation plant is dependent on the topology of the system and any security constraints that may apply to the injection of energy into the system at the connection point. This is particularly true in regard to wind energy which is highly volatile.

This chapter describes the operating capacity contributions attributable to wind power in four subsections. Section 4.2 illustrates the concepts of wind power modeling and the capacity contributions of wind power to the RBTS [52]. Similar studies using the IEEE-RTS [53] are presented in Section 4.3. The unit commitment schedules used in the thesis are based on the priority loading order. The Outage Replacement Rate (ORR) of a wind turbine during a short interval of few hours is virtually insignificant compared to the variability associated with the wind speed during the same time interval. Wind turbines also have small individual power capacity ratings compared to conventional generating units. The failure rates of the WTG are therefore not included in this thesis. Section 4.4 illustrates the effects of using multi-state models to represent the large conventional generating units. Section 4.5 shows the effect of added wind power in both test systems using a PLCC benefit factor.

4.2 Operating Reserve Assessment with the RBTS

4.2.1 Unit Commitment Risk Analysis with Wind Power

As noted in Chapter 2, the UCR is the probability that the scheduled operating capacity will just carry or fail to carry the system load for a designated time period in the future. The generating reserve requirement for a constant UCR usually increases for increased system lead times [15]. If the lead time is fixed, the scheduled capacity can be considered to carry a maximum load designated as the Peak Load Carrying Capability (PLCC) for a given UCRC. The PLCC decreases as the required lead time increases.

The following analysis uses the wind regime at the Swift Current site in the month of January from hour 4 to 7. A total of 26 WTG are assumed to be installed in the wind farm. The total installed capacity is 46.8 MW. The RBTS with the addition of 46.8 MW of WTG is designated as the RBTSW. Wind speeds of 25.5-26.5 km/hr and 35.5-36.5 km/hr at the zero hour (hour 4 in this case) are considered as Low Wind speed and High Wind speed respectively for discussion purposes. A wind speed interval of 1 km/hr (e.g.25.5-26.5 km/hr) was utilized at the zero hour in order to capture a large data sample of the predicted wind speed in the next hours. A description of the developed short term wind speed probability distributions and the ARMA model for the Swift Current wind site is presented in Chapter 3.

Operating schedules including 5, 6, 7 and 8 units from the RBTS merit order were used to examine the variations in the UCR with the load for different lead times at both Low Wind speed and High Wind speeds. Failures of WTG during the various lead times are not included in the analysis as these possible events have virtually no impact on the results. The output of a wind farm is dominated by the possible variability in the wind speed at the site. Fig. 4.1 presents the UCR profiles for four generating unit schedules with a lead time of 4 hours.

The uncertainty increases with the lead time and therefore hour 7 contains many possible power states depending on the initial magnitude of the wind speed at hour 4 (zero hour). The large number of possible power state probabilities has an observable impact on the UCR profile,

shown in Fig. 4.1. This figure can be compared with Fig. 2.2(b), which shows the UCR for the RBTS with no added wind.

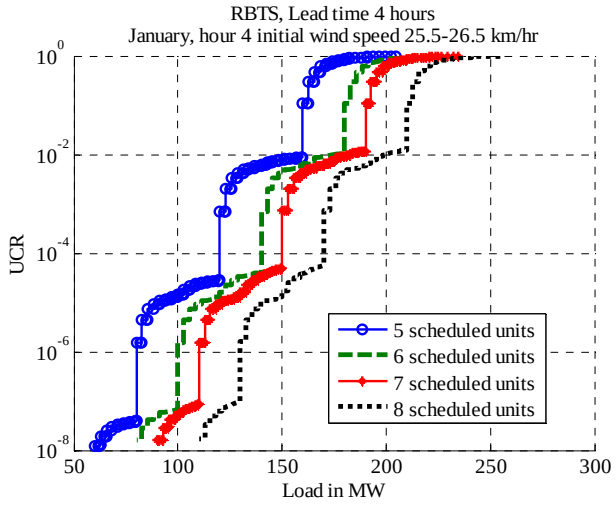

Fig.4.1: RBTSW UCR with various scheduled capacities

Table 4.1 presents a summary of the observed changes in UCR when 7 units are scheduled to carry a load of 130 MW with and without WTG. The UCR increases as the lead time increases and decreases when the initial wind speed increases. The decrease in the system lead time and increase in the initial wind speed have a favorable impact on the system UCR. Therefore, for a given load level and defined UCRC, there is always the possibility of carrying additional load if the system lead time is decreased or the initial wind speed increases at some point in time.

Table 4.1. UCR variation with lead time and initial wind speed for the RBTS

Lead time (Hours)	UCR		
	No WTG	WTG-Low Wind	WTG-High Wind
1	2.8508E-06	9.3948E-07	9.3860E-07
2	1.1391E-05	4.2248E-06	1.6086E-06
3	2.5603E-05	9.5137E-06	4.9454E-06
4	4.5468E-05	1.6168E-05	8.5617E-06

The UCR changes are basically discrete due to the discrete representation of the conventional units. It is therefore not automatic that a small decrease in the risk level will result

in an increase in the load carrying capability. In certain cases, there has to be a significant decrease in the risk level in order to produce a higher load carrying capability.

4.2.2 Load Carrying Capability

System Load Carrying Capability (LCC) studies of the RBTSW were carried out for a gradual increase of the load in small steps from 40 % to 100 % of the 185 MW peak value. Load levels higher than 80% of the peak load are termed as high loads. The scheduled capacity increases for higher lead times as the UCRC is decreased. UCR values of 0.001, 0.0001 and 0.00001 are considered as High, Medium and Low Risk criteria respectively for discussion purposes. Fig. 4.2 shows that for a lead time of 4 hours, the capacity required to carry a given load at the Low Risk (0.00001) criterion is considerably higher than that required under the High (0.001) and Medium Risk (0.0001) criteria. A comparison of Fig. 4.2 with Fig. 2.3(b) shows that there is very little difference in the LCC profile due to adding the designated wind power.

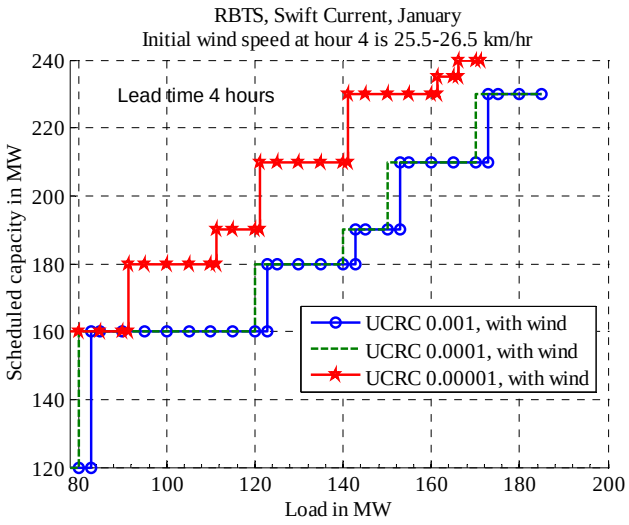

Fig. 4.2: RBTSW LCC profile

Fig. 4.3 shows the variations in the system spinning reserve as a function of the system load. A comparison of Fig. 4.3 with Fig. 2.5(b) shows the effects on the spinning reserve profile of adding the designated wind power. The minimum and maximum spinning capacity

requirement to satisfy a given UCRC decreases with the wind power additions, and there is some separation in the spinning capacity profiles for the High and Medium UCRC.

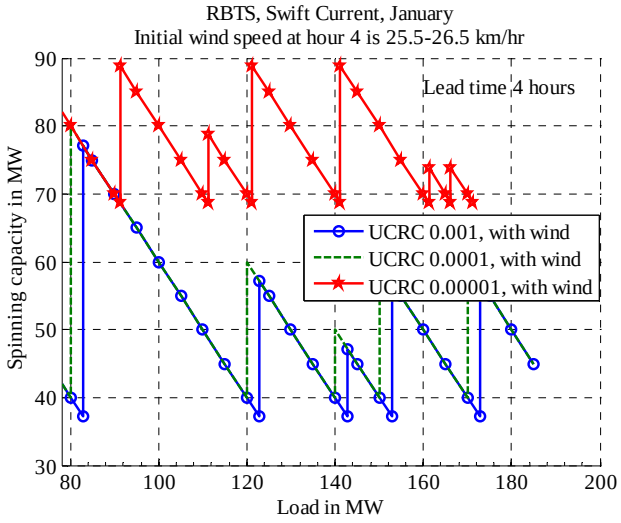

Fig.4.3: RBTSW spinning capacity profile

Table 4.2 contains a summary of the minimum spinning reserve required to maintain each UCRC under Low and High wind conditions for 1,2,3 and 4 hour lead times. The minimum spinning capacity required to maintain a given UCRC for a short lead time such as 1 hour, however, may remain constant as shown in Table 4.2. This is not the case as the lead time increases. In this case, the minimum spinning capacity increases as the UCRC decreases.

Table 4.2. Summary of the minimum spinning reserve from the conventional units at higher loads under various conditions for the RBTSW

UCRC	Minimum Spinning Capacity for a Lead time of 1 hour (MW)			Minimum Spinning Capacity for a Lead time of 2 hours (MW)		
	No WTG	Low Wind	High Wind	No WTG	Low Wind	High Wind
High	40.1	34.37	22.06	40.1	37.08	22.98
Medium	40.1	34.37	22.06	40.1	34.37	31.49
Low	40.1	34.37	22.06	60.1	51.23	40.00
UCRC	Minimum Spinning Capacity for a Lead time of 3 hours (MW)			Minimum Spinning Capacity for a Lead time of 4 hours (MW)		
	No WTG	Low Wind	High Wind	No WTG	Low Wind	High Wind
High	40.1	37.67	31.49	40.1	37.19	35.75
Medium	40.1	40.00	40.00	40.1	40.00	40.00
Low	60.1	60.00	51.49	80.1	68.78	58.73

4.2.3 Peak Load Carrying Capability

The PLCC of the RBTS without wind power remains constant at 80 MW, 120 MW, 140 MW, 150 MW and 170 MW for scheduled capacities of 120 MW, 160MW, 180 MW, 190 MW and 210 MW (4, 5,6,7 and 8 scheduled units) respectively for lead times of 1-4 hours under the High Risk and Medium Risk criteria. Fig. 4.4 shows that this is not case for the Low Risk criterion. The PLCC generally decreases with increasing lead times. Fig. 4.4 shows that the PLCC for 6, 7 and 8 committed units are constant for some lead time periods.

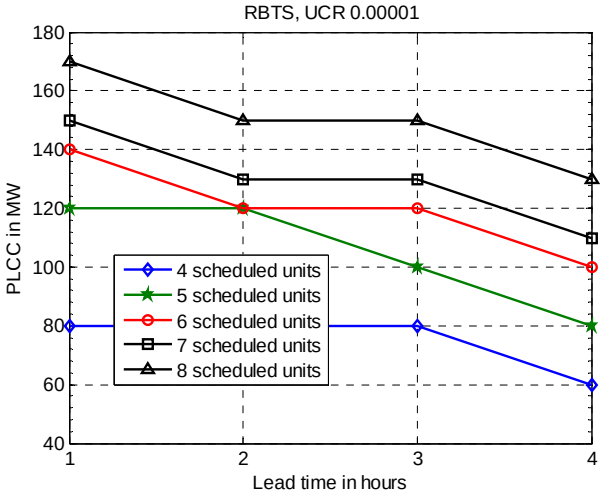

Fig. 4.4: RBTS PLCC variation with lead time

The PLCC of the RBTS and RBTSW with a scheduled capacity of 190 MW for lead times of 1, 2, 3 and 4 hours are shown in Fig. 4.5 and 4.6. Low and High initial wind speed conditions are applied in Fig. 4.5 and 4.6 respectively. The figures show that the system with the wind power addition generally has a higher PLCC than the system without the wind capacity. The system PLCC decreases as the UCRC is decreased i.e. a higher reliability standard is imposed. The increased initial wind speed has a favorable impact on the system PLCC. The PLCC under the High Risk criterion changes from 155.6 MW to 167.9 MW at a lead time of 1 hour when the initial wind speed changes from its Low value to a High value. Similar improvements in the PLCC at other lead times are also present in these two figures. Fig. 4.5 and 4.6 also illustrate how the addition of wind power tends to create a smoother decrease in the PLCC with lead time due to the large number of possible power output levels from the WTG.

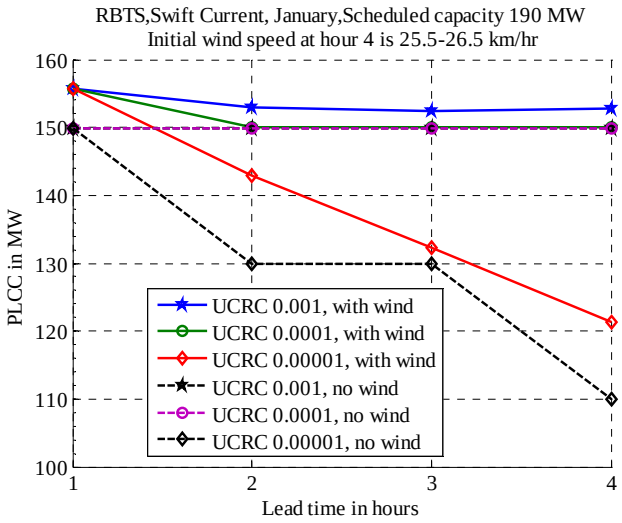

Fig. 4.5: RBTS and RBTSW PLCC under Low initial wind speed conditions

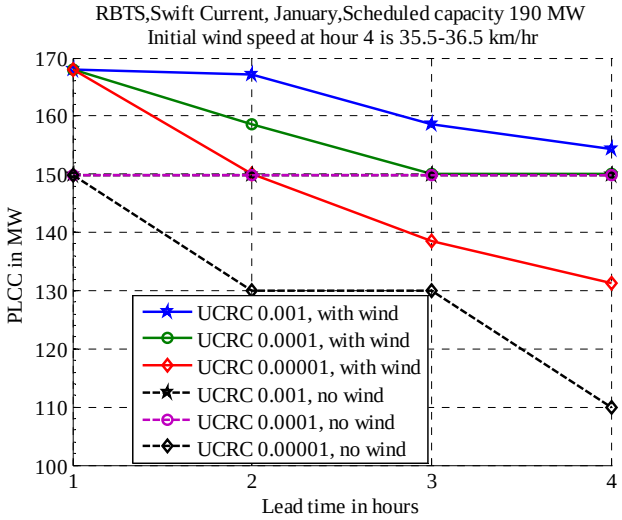

Fig. 4.6: RBTS and RBTSW PLCC under High initial wind speed conditions

4.2.4 Increase in Peak Load Carrying Capability

The capacity benefit of adding wind power can be quantified using an index designated as the Increase in Peak Load Carrying Capability (IPLCC). The IPLCC is defined as the difference between the PLCC of the wind integrated power system and the basic power system without wind power. The IPLCC for the two systems under different UCRC and initial wind speed conditions are shown in Fig. 4.7 and 4.8.

These figures show that the increase in wind speed from the Low to the High level generally creates an increase in the IPLCC for all three UCRC. The IPLCC benefits are higher for the High Risk criterion than for the Medium Risk criterion in all the cases. The IPLCC generally decreases with lead time for these two risk criteria. This is not the case for the Low Risk criterion where the IPLCC shows considerable variability with lead time. It should be appreciated that the IPLCC is the difference in PLCC. An increase in IPLCC could be due to a decrease in the PLCC at a given lead time in the basic system with no wind power addition as illustrated in Fig. 4.4.

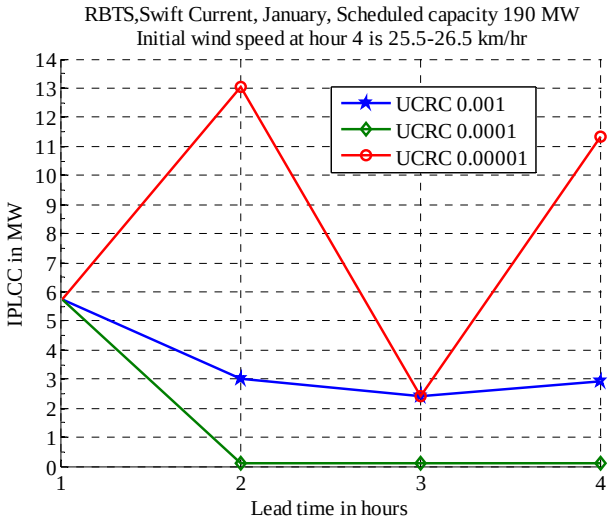

Fig. 4.7: RBTSW IPLCC under Low initial wind speed conditions

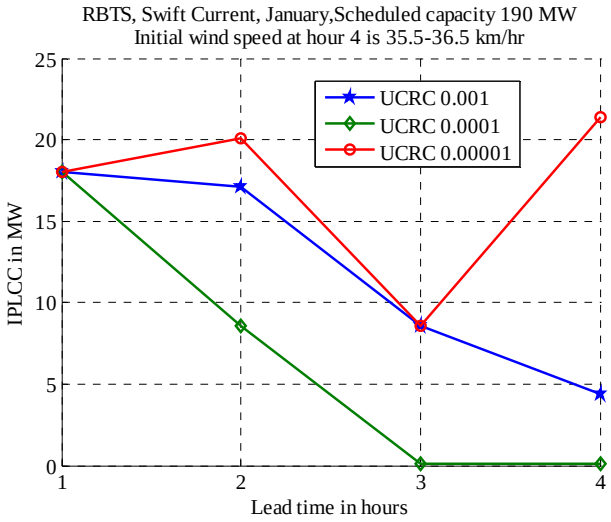

Fig. 4.8: RBTSW IPLCC under High initial wind speed conditions

Table 4.3 shows some exceptions for the scheduled capacities of 120 MW and 160 MW at the Low Risk criterion for a lead time of 2 hours at which there are no PLCC gains due to increased initial wind speed. This does not mean there is no benefit with higher wind speeds. The UCR decreases at those conditions as shown in Table 5 but not by a sufficient margin to carry extra load. It should be noted that the scheduled capacity of 120 MW and 160 MW includes a commitment decision involving two 40 MW thermal units.

Table 4.3. UCR variation with a Low UCRC for a lead time of 2 hours

	scheduled capacity 120 MW		scheduled capacity 160 MW	
	Actual UCR	PLCC (MW)	Actual UCR	PLCC (MW)
No. WTG	3.187419E-06	79.9	7.494280E-06	119.9
Low Wind	2.920853E-06	79.9	7.019798E-06	119.9
High Wind	1.752789E-06	79.9	4.855548E-06	119.9

The actual UCR decreases due to changes in the conditions for both scheduled capacities shown in Table 4.3 are relatively small. At these peak loads (79.9 MW and 119.9 MW), both the scheduled capacities have just enough spinning reserve to cope with the loss of a single largest unit in the system, which in this case is 40 MW. Any further increase in PLCC demands a significant increase in the generation capacity to maintain the UCRC. This is illustrated in Figs. 2.3(b) and 4.1. The maximum IPLCC due to adding wind power is also dependent on the system operating point in the UCR-Load profile.

4.3 Operating Reserve Assessment with the IEEE-RTS

The IEEE-RTS [53] consists of 32 generating units with a total installed capacity of 3405 MW. The unit details and the merit loading order are presented in Appendix A2. The wind regime at the Swift Current site is used in this analysis and 370 WTG are assumed to be installed in a single wind farm. The total installed capacity is 666.0 MW. The initial condition (zero hour) is hour 4 (January 1, 4 am) and the lead-time is 4 hours. The wind speed at the zero hour is assumed to be 25.5-26.5 km/hr. A wind speed interval of 1 km/hr is used in the analysis.

Operating schedules involving 13, 14, 15 and 16 units from the IEEE-RTS merit order are used to examine the UCR. The UCR profiles for the four operating schedules are shown in Fig. 4.9. The IEEE-RTS with the addition of 666.0 MW of WTG is designated as the IEEE-RTSW. The uncertainty in wind power output increases with the lead-time and therefore the CWPD contains many derated states. This has an observable impact on the UCR profile for the IEEE-RTSW as shown in Fig. 4.9. The discrete steps in Fig. 2.9(b) for the IEEE-RTS are dampened by the addition of the WTG in Fig. 4.9. Fig. 4.10 shows the LCC profile of the IEEE-RTSW. The scheduled capacity as a function of the system load is shown for the three UCRC. The figure clearly shows that for a lead-time of 4 hours, the capacity required to carry a given load at the Low Risk criterion is considerably higher than that required under the High and Medium Risk criteria. The LCC are generally higher than that shown in Fig. 2.4(b). Fig. 4.11 shows the variations in the system spinning reserve as a function of the system load. In this Fig., as in Fig. 2.6(b), the spinning reserve increases as new units are committed to meet the increasing load, following which the spinning reserve decreases as the load increases.

Fig. 4.12 shows the PLCC of the IEEE-RTSW as a function of the lead-time for the three UCRC and a scheduled capacity of 2561 MW. The IPLCC due to the added wind capacity is shown in Fig. 4.13. The PLCC profiles in Fig. 4.12 show a general decrease in PLCC as a function of the lead-time. This is not the case in Fig. 4.13 as the IPLCC is the difference between the PLCC values for the two systems. A significant increase in IPLCC for a given lead-time could occur due to a large decrease in PLCC for that lead-time in the basic IEEE-RTS. This is a function of many variables, including the conventional unit capacity levels, the wind regime, and the UCRC adopted. Fig. 4.13 clearly shows that wind capacity can contribute to the operating reserve and that this contribution can be quantified [140].

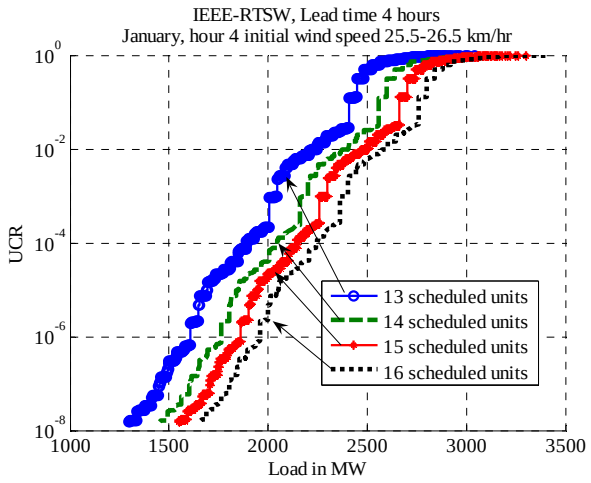

Fig. 4.9: IEEE-RTSW for a lead-time of 4 hours

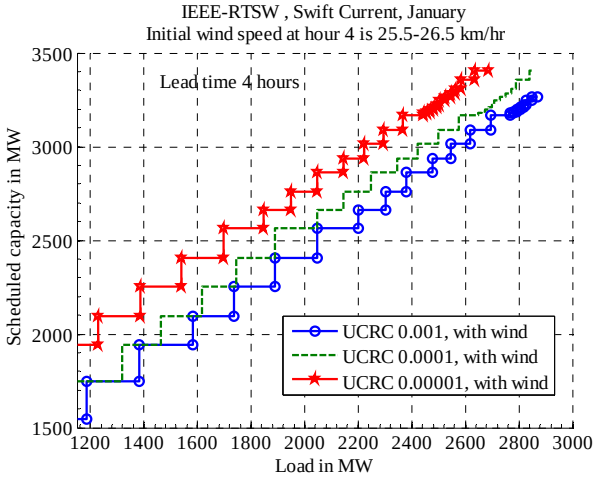

Fig. 4.10: IEEE-RTSW LCC profile

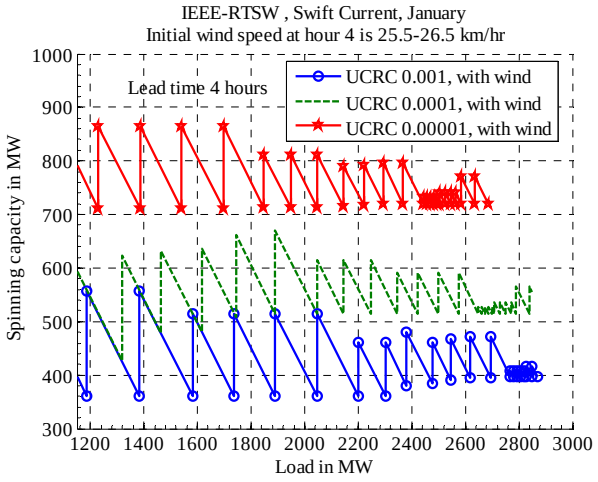

Fig. 4.11: IEEE-RTS spinning capacity

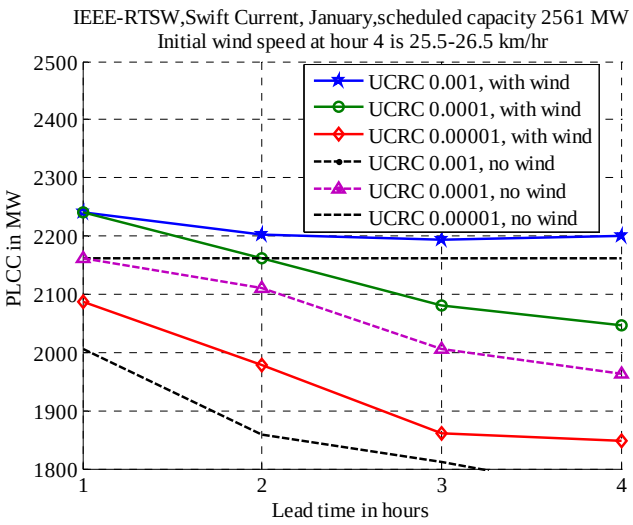

Fig. 4.12: IEEE-RTS and IEEE-RTSW PLCC

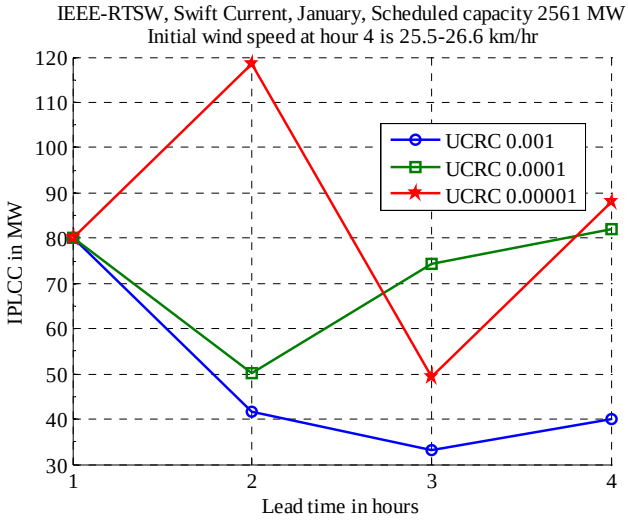

Fig. 4.13: IEEE-RTSW IPLCC

4.4 Utilization of Multi-State Generating Unit Models in Unit Commitment Risk

Large conventional generating units often operate at derated capacity levels because of variations in ambient conditions or failure of one or more of their operating components. The incorporation of these conditions in system reliability assessment involves a detailed investigation of unit performance and the determination of the transition rates between different derated capacity states. The utilization of two state models for large conventional generating units in system studies can lead to pessimistic appraisals of the system operating indices [22].

The recognition and incorporation of suitable derated state models provide more accurate estimates of the system reliability. Considerable work has been done in this area and the use of multi-state models for large units is a conventional practice in generating capacity adequacy assessment [1] [2]. Relatively little work has been done, however, in the incorporation of multi-state generating unit models [1, 15, 16, 22] in operating reserve assessment due to the difficulties in obtaining suitable transition rate data. This section is focused on operating reserve assessment in wind integrated electric power systems containing large conventional generating units.

The section illustrates the impacts of using multi-state models to represent large conventional generating units in operating reserve assessment using the IEEE-RTS [53]. This section presents a study to assess the Peak Load Carrying Capability (PLCC) of a power system containing multi-state conventional generating units and WTG. The operating capacity contributions of the WTG are considered using the IPLCC.

4.4.1 Derated State Modeling of the IEEE-RTS

Generating system security evaluation using probabilistic techniques involves recognition of the transition rates between the various generating unit operating states. The IEEE-RTS described in [53] includes the transition rates required to create two state generating unit models but does not include the required data for derated state modeling.

As noted earlier, the basic generating unit statistic in generating capacity adequacy assessment is the unit unavailability or Forced Outage Rate (FOR). This is determined using the unit failure and repair rates and the FOR is the probability of finding the unit on outage at some distant time in the future. In an operating reserve study, the time in the future is relatively short and repair is not considered to be possible. The basic generating unit statistic in this case is the Outage Replacement Rate (ORR) and is determined using the unit failure rate and the system lead time [1]. The generating unit is presumed to be in the operating state at time zero and the ORR is the probability of the unit failing during the lead time.

Appendix A.2 presents some relevant data for the IEEE-RTS [53] including the unit priority loading order for unit commitment purposes, the generating unit capabilities, and the failure rates for a two state unit representation. The IEEE-RTS as shown in Appendix A.2 contains 400 MW, 350 MW and 197 MW units. In order to illustrate the effects of large unit derated state modeling in unit commitment analysis, these units were modeled using representative data obtained from the Canadian Electrical Association (CEA). Reference [141] describes a detailed study conducted using data provided by the CEA. The transition rate data in [141] were used to create two state, three state and eleven state models for the 400 MW, 350 MW and 197 MW units. The data for a 400 MW nuclear unit is shown in Table 4.4 and Figs. 4.14 and 4.15. Similar data for the 350 MW and 197 MW units are shown in the Table 4.5 and 4.6 respectively. The remaining units in the IEEE-RTS are represented by two state models using the data shown in Appendix A.2. The modified system obtained by replacing the transition rates for the 400 MW, 350 MW and 197 MW units by CEA data is designated as the modified IEEE-RTS (IEEE-RTSM). The capacities of the single derated states in the three state models of the 400 MW, 350 MW and 197 MW units obtained using the minimum variance technique [141] are 80.19%, 70.13% and 60.07% respectively

Table 4.4. Transition rates for the 400 MW nuclear unit based on CEA data

Eleven state model (Transition from 400 MW to the given derated capacity)	
Derated Capacity (MW)	Transition Rate (f/yr)
0	3.04
40	0.2
80	0
120	0.01
160	0.12
200	0.37
240	0.21
280	0.23
320	0.46
360	5.82

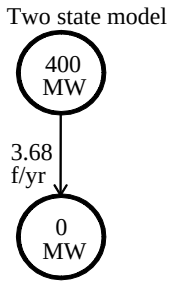

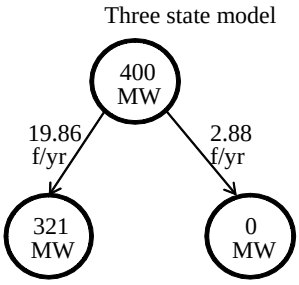

Fig.4.14: Two state model Fig.4.15: Three state model

Table 4.5. Transition rates for the 350 MW coal/steam unit based on CEA data

Two state model (Transition from 350 MW to the given derated capacity)		Three state model (Transition from 350 MW to the given derated capacity)		Eleven state model (Transition from 350 MW to the given derated capacity)	
Derated Capacity (MW)	Transition Rate (f/yr)	Derated Capacity (MW)	Transition Rate (f/yr)	Derated Capacity (MW)	Transition Rate (f/yr)
0	17.15	0	14.19	0	14.82
		245	97.2	35	0.69
				70	0.29
				105	0.71
				140	1.73
				175	6.88
				210	5.75
				245	9.16
				280	28.01
				315	32.15

Table 4.6. Transition rates for the 197 MW oil/steam unit based on CEA data

Two state model (Transition from 197 MW to the given derated capacity)		Three state model (Transition from 197 MW to the given derated capacity)		Eleven state model (Transition from 197 MW to the given derated capacity)	
Derated Capacity (MW)	Transition Rate (f/yr)	Derated Capacity (MW)	Transition Rate (f/yr)	Derated Capacity (MW)	Transition Rate (f/yr)
0	58.66	0	50.62	0	61.46
		119	115.95	20	9.54
				39	0.82
				59	2.65
				79	2.71
				99	13.09
				118	13.54
				138	12.24
				158	23.18
				177	23.39

4.4.2 Unit Commitment Risk Analysis

Fig. 4.16 shows the UCR-load profile of the IEEE-RTSM obtained using two-state generating unit models with a lead time of 2 hours when 13, 14, 15 and 16 units with capacity values of 2406, 2561, 2661 and 2761 MW respectively are committed. Fig. 4.16 shows the

discrete nature of the UCR profile due to the two-state generating unit representation. There are significant UCR decreases at each 197 and 400 MW reserve level for all the scheduled capacities due to the fact that the 197 MW oil/steam units have relatively high failure rates, as shown in the Table 4.6. The 400 MW units are the largest generating units in the system and have a distinct impact on the UCR-load profile shown in Fig. 4.16. The UCR-load profile for the IEEE-RTSM using two state, three state and eleven state models for the designated units for a scheduled capacity of 2561 MW and a lead time of 2 hours is shown in Fig.4.17. The discrete nature of the UCR-load profile is modified considerably by using multi-state models for the large generating units.

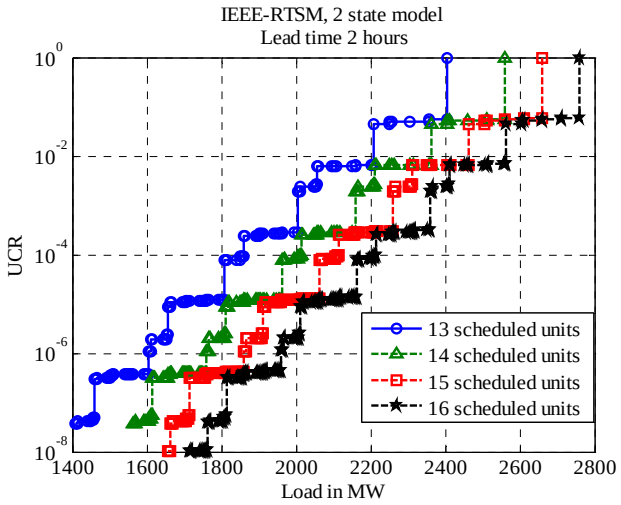

Fig. 4.16: IEEE-RTSM UCR-Load profile obtained using two-state generating unit models

The PLCC for the two state, three state and eleven state models are the same for a UCRC of 0.001. The PLCC for the two state case is higher than that for the eleven state case but lower than that for the three state case at a UCRC of 0.0001. The PLCC for the two state case at a UCRC of 0.00001 is lower than that for both the eleven state and three state cases. The decreases in PLCC for the eleven state case are generally higher than those for the two state and three state cases with lower UCRC.

Fig.4.17 indicates that the PLCC of the system is highly dependent on the UCRC and influenced by recognizing the possible generating unit derated states. The application of derated state models could indicate higher or lower PLCC values than those obtained using two state

models and produce smoother and more accurate UCR-load profiles compared to those for two state models, which create large discrete steps in the UCR levels. Detailed multi-state models provide a more accurate representation of the performance of a generating unit and therefore more accurate assessment of the UCR. They also require considerable data collected over a suitable period of time under consistent and carefully prepared protocols [141].

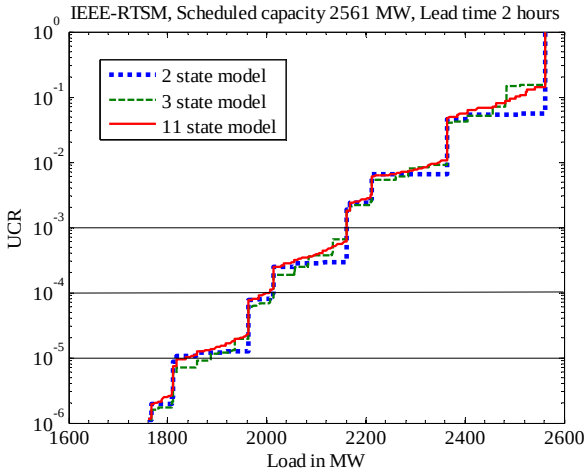

Fig. 4.17: IEEE-RTSM UCR-load profile obtained using multi-state generating unit models

4.4.3 PLCC Variations Due to the Changes in System State Modeling

The PLCC variations at different UCRC for the applied two state and eleven state models in the IEEE-RTSM are shown in Figs. 4.18 and 4.19 and the corresponding UCR are presented in Fig.4.20 and 4.21 respectively for the scheduled capacity of 2561 MW. As noted earlier, the UCR is defined as the probability of just carrying or failing to carry the load for a specified time. The actual UCR therefore is usually slightly smaller than the UCRC. The system can sustain a constant peak load for a lead time up to 3 hours if operated with a high risk (UCRC 0.001) criterion using two state models as shown in Fig.4.18. Fig. 4.20 shows the UCR variation for the PLCC shown in Fig. 4.18.

Fig. 4.19 shows that the PLCC decreases with the lead time when the eleven state models are used in the IEEE-RTSM at all the UCRC due to the large number of derated unit output levels.

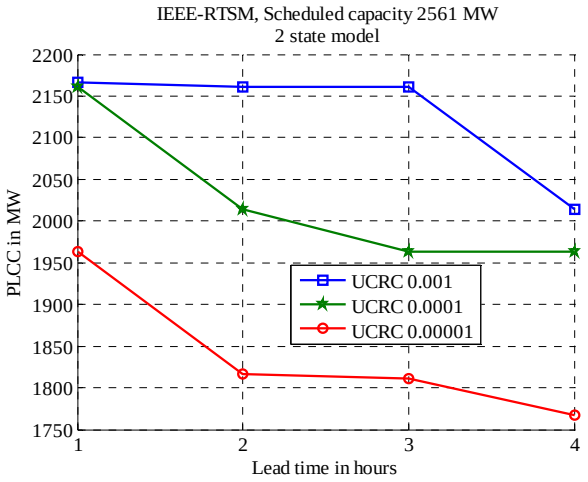

Fig. 4.18: PLCC variation using two state models

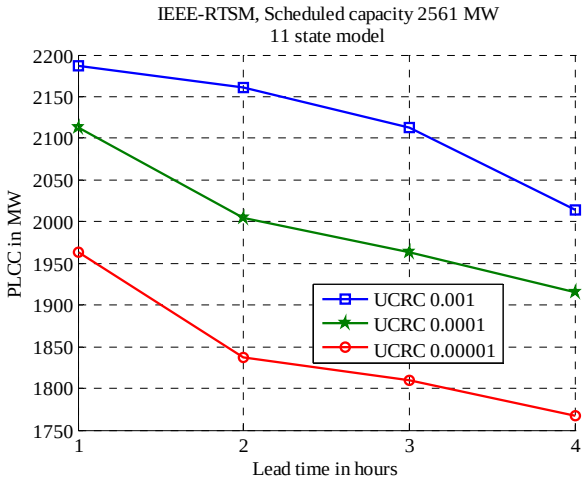

Fig. 4.19: PLCC variation using eleven state models

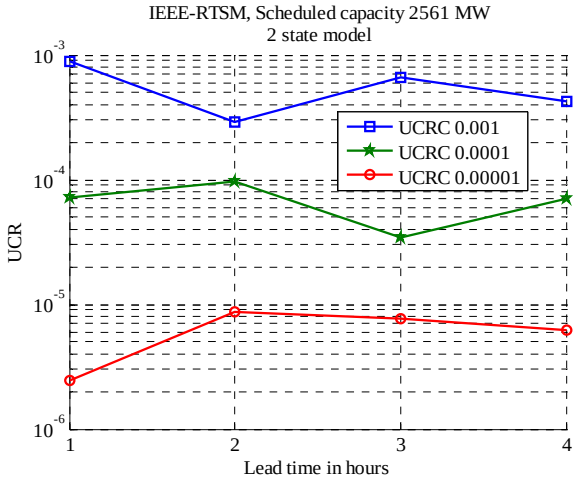

Fig. 4.20: UCR changes for the PLCC in Fig. 4.18

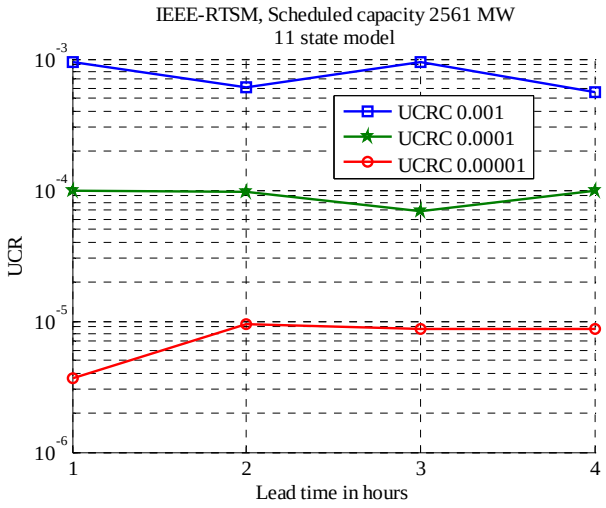

Fig. 4.21: UCR changes for the PLCC in Fig. 4.19

4.4.4 Unit Commitment Risk of the Wind Integrated IEEE-RTSM

The wind farm data used in Section 4.3 to study the IEEE-RTSW was applied to the IEEE-RTSM. The UCR of the IEEE-RTSM for a 2 hour lead time for the given initial wind speed of 25.5-26.5 km/hr at hour 4 is shown in Figs. 4.22 and 4.23 for the two state and eleven state cases respectively. The scheduled conventional capacity is 2561 MW in both cases. The UCR-load profile with the additional wind capacity moves to the right in both figures indicating the extra load carrying capability for a given UCRC. Fig.4.23 shows that the eleven state case provides a much smoother graph from which to estimate the increased load carrying capability than the two state case profile shown in Fig.4.22. It should be noted that at certain load points, the decreases in UCR due to adding wind power are substantial and therefore at these values the increases in load carrying capability are very high. The actual system operating point in the UCR-load profile is a determining factor for the system increased load carrying benefits due to adding wind power.

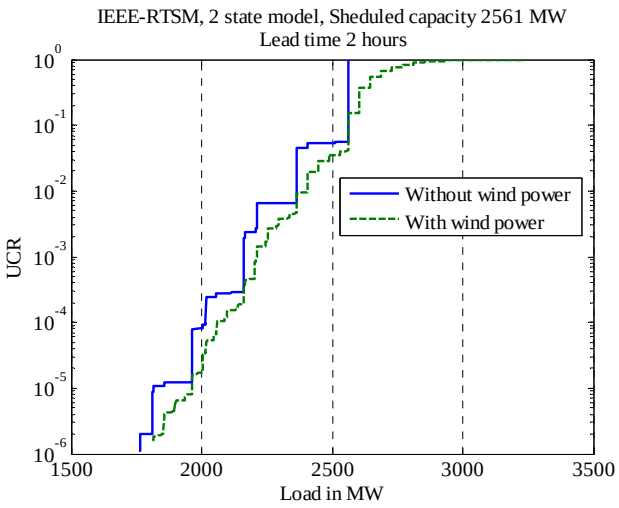

Fig. 4.22: UCR-load profile for the two state case

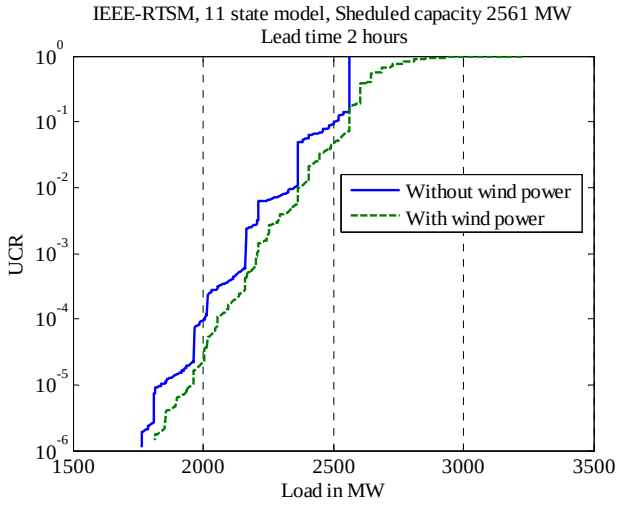

Fig.4.23: UCR-load profile for the eleven state case

4.4.5 PLCC of the Wind Integrated IEEE-RTSM

The PLCC of the IEEE-RTSM using two state, three state and eleven state models for the designated units with and without wind power are presented in Figs. 4.24, 4.25 and 4.26 for UCRC of 0.001, 0.0001 and 0.00001 respectively. As expected, the PLCC of the system is highly dependent on the selected UCRC. The PLCC profiles of the higher state cases tend to be more linear than those of the two state case over the range of lead times.

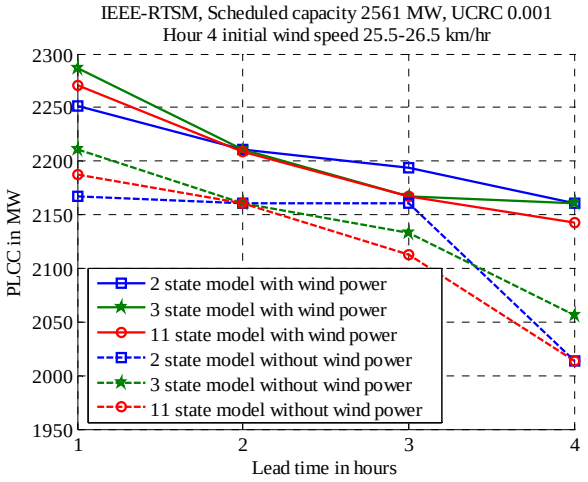

Fig.4.24: PLCC at a UCRC of 0.001

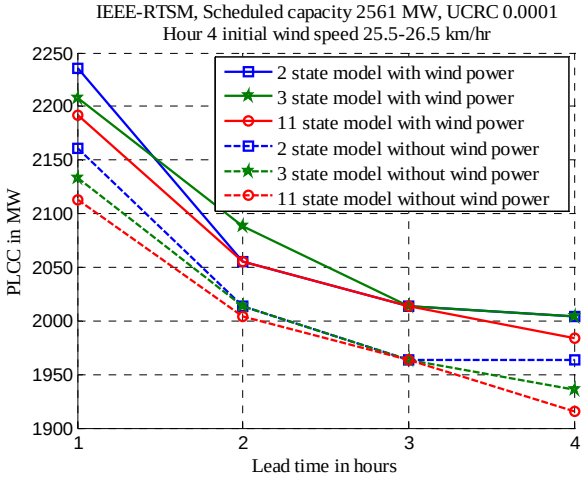

Fig. 4.25: PLCC at a UCRC of 0.0001

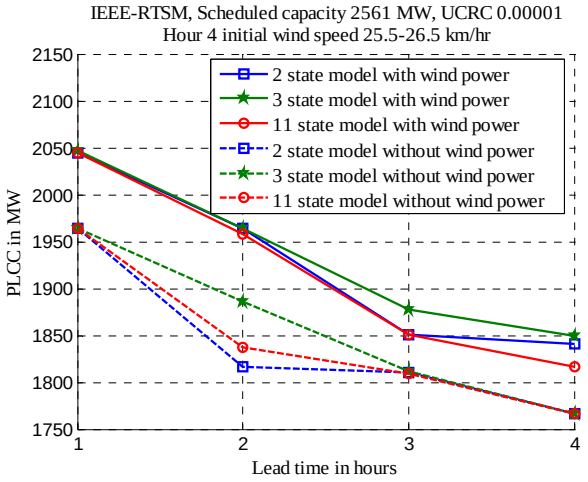

Fig. 4.26: PLCC at a UCRC of 0.00001

4.4.6 Increase in Peak Load Carrying Capability (IPLCC)

The IPLCC is the difference between the PLCC of the wind integrated system and the system without wind power. The IPLCC at UCRC of 0.001, 0.0001 and 0.00001 are presented in Figs. 4.27, 4.28 and 4.29 respectively. The IPLCC profiles at the UCRC of 0.001 are the same for the three state and eleven state cases as shown in Fig. 4.27. The three state case has the highest IPLCC for a UCRC of 0.0001 at a lead time of 2 hours, however, it has the lowest IPLCC for the UCRC of 0.00001 for the same lead time.

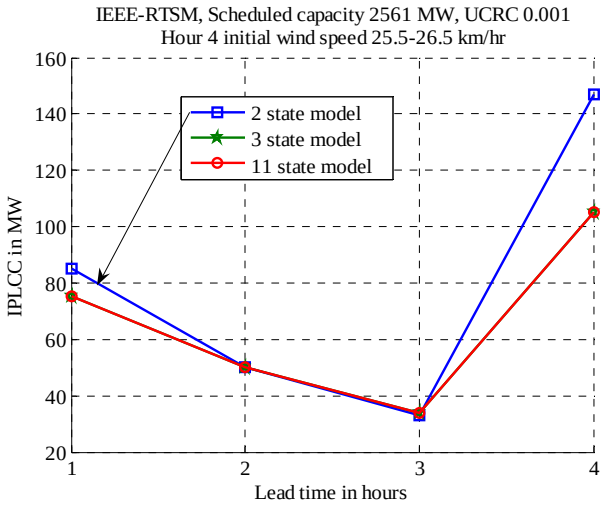

Fig 4.27: IPLCC at a UCRC of 0.001

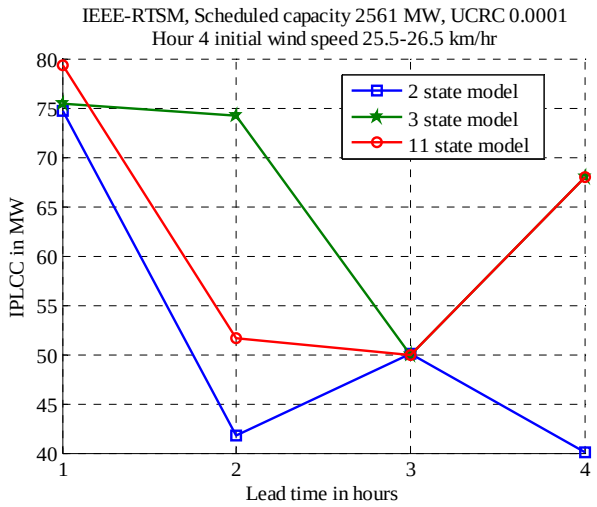

Fig.4.28: IPLCC at a UCRC of 0.0001

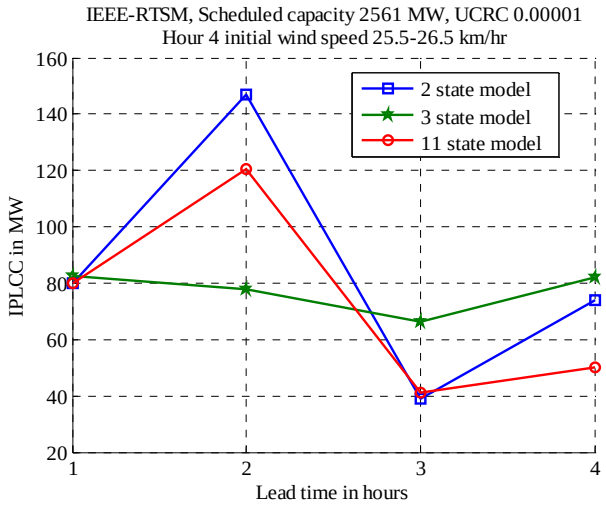

Fig.4.29: IPLCC at a UCRC of 0.00001

4.5 Load Carrying Capability of Wind Integrated Power Systems

The benefits of added wind power in an operating situation can be quite different at different scheduled capacity levels. The benefits can also be significantly different in different power systems. This section illustrates the capacity benefit of added wind power at different scheduled capacities in the two test systems at different UCRC and lead times. The capacity benefits in the two systems under changing initial wind speed conditions are also examined.

As in the previous studies, 370 and 26 1.8 MW WTG are added to the IEEE-RTS and RBTS respectively. The IEEE-RTS and the RBTS with the addition of wind power are designated as IEEE-RTSW and RBTSW.

The analysis utilizes the wind regime at the Swift Current site in the month of January from hour 4 to 7. Wind speeds of 25.5-26.5 km/hr and 35.5-36.5 km/hr at the zero hour (hour 4 in this case) are considered as Low wind speed and High wind speed respectively for discussion purposes.

4.5.1 Increase in Peak Load Carrying Capability for the IEEE-RTSW

The IPLCC variations with lead time for different scheduled capacities under different UCRC are shown in Fig. 4.30 – 4.33 for different initial wind speeds for the IEEE-RTSW. Fig. 4.30 and 4.31 show that for an UCRC of 0.001, the IPLCC are basically the same for all the scheduled capacity levels. This is not the case for the UCRC of 0.0001 and the IPLCC can change for different scheduled capacity additions. Figs. 4.30 and 4.31 clearly show the impact of the High initial wind speed on the IPLCC at this risk level. The effect can also be seen in Figs. 4.32 and 4.33.

The IPLCC, however, do not follow a linear trend for the UCRC of 0.0001 as shown in Figs.4.32 and 4.33. This is due to the fact that the PLCC of the conventional units remain constant for the UCRC of 0.001 but show a decrease in some cases for the UCRC of 0.0001. This phenomenon is illustrated in Fig. 4.5, 4.6 and 4.7. The sudden decreases in the PLCC of the conventional units over the lead time create irregular changes in the IPLCC profiles.

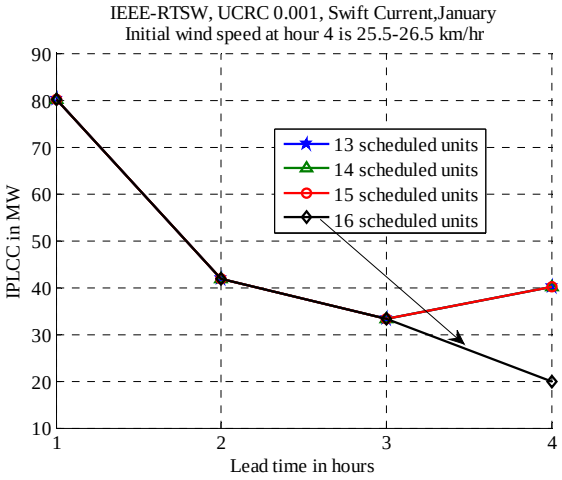

Fig. 4.30: IPLCC of the IEEE-RTSW at a Low initial wind speed and a 0.001 UCRC

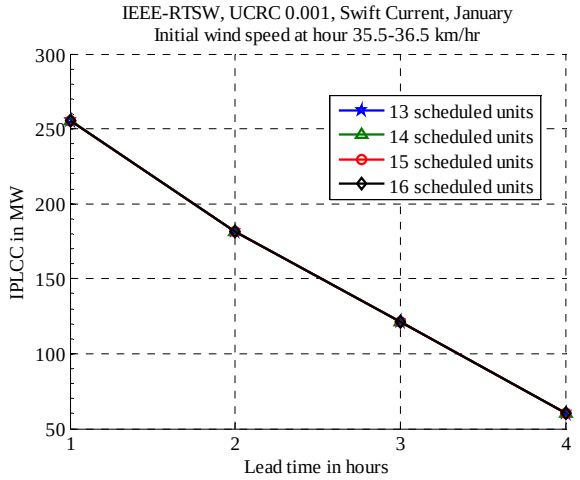

Fig. 4.31: IPLCC of the IEEE-RTSW at a High initial wind speed and a 0.001 UCRC

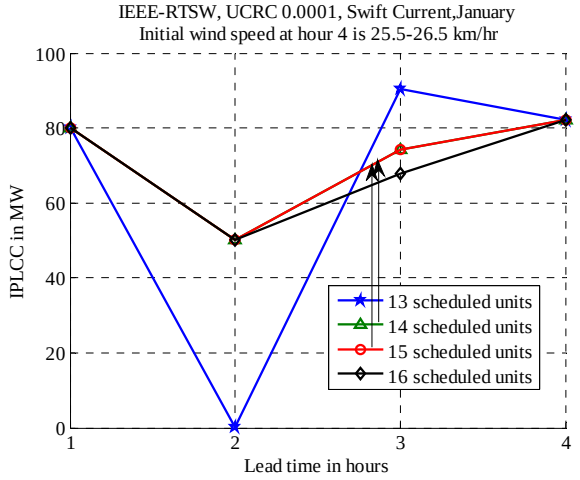

Fig. 4.32: IPLCC of the IEEE-RTSW at a Low initial wind speed and a 0.0001 UCRC

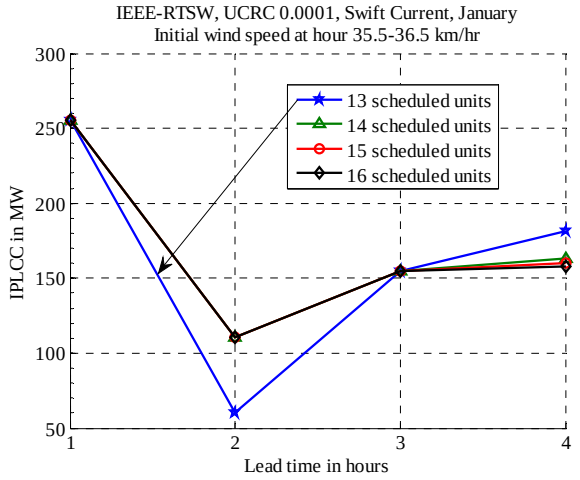

Fig. 4.33: IPLCC of the IEEE-RTSW at a High initial wind speed and a 0.0001 UCRC

4.5.2 PLCC benefit factor for the IEEE-RTSW

The ratio of the PLCC of the wind integrated power system to the PLCC of the basic system without wind is designated as the PLCC benefit factor. Figs. 4.34 and 4.35 show the PLCC benefit factor for a UCRC of 0.001 for the Low and High initial wind speeds respectively. Both figures show that the PLCC benefit factors generally decrease as the lead time increases. The figures illustrate that the PLCC benefit factors are higher for lower scheduled capacities due to the higher ratio of wind power to total capacity at these unit commitment levels. Fig. 4.35 shows that the PLCC benefit factors are higher for the High initial wind speed condition than when the initial wind speed is Low. Similar observations can be made for a UCRC of 0.0001 when the initial wind speed changes from the Low to the High value, as shown in Fig.4.36 and 4.37. The PLCC benefit factors, however, overlap in some cases because of the decrease in the PLCC of the conventional units at these lead times [142].

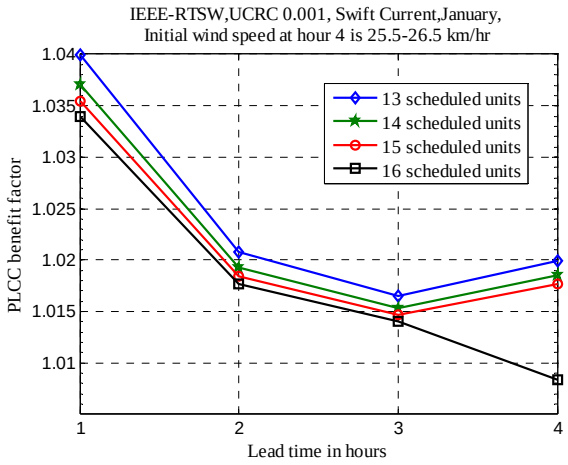

Fig. 4.34: PLCC benefit factor for the IEEE-RTSW at a Low wind speed and a 0.001 UCRC

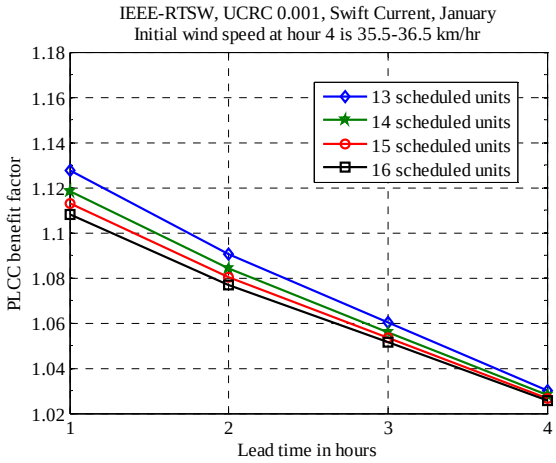

Fig. 4.35: PLCC benefit factor for the IEEE-RTSW at a High wind speed and 0.001 UCRC

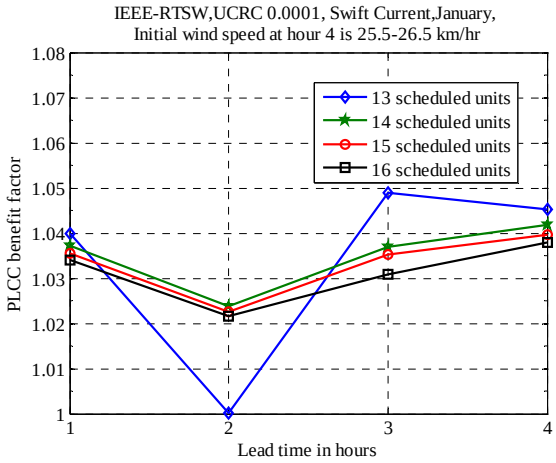

Fig. 4.36: PLCC benefit factor for the IEEE-RTSW at a Low wind speed and a 0.0001 UCRC

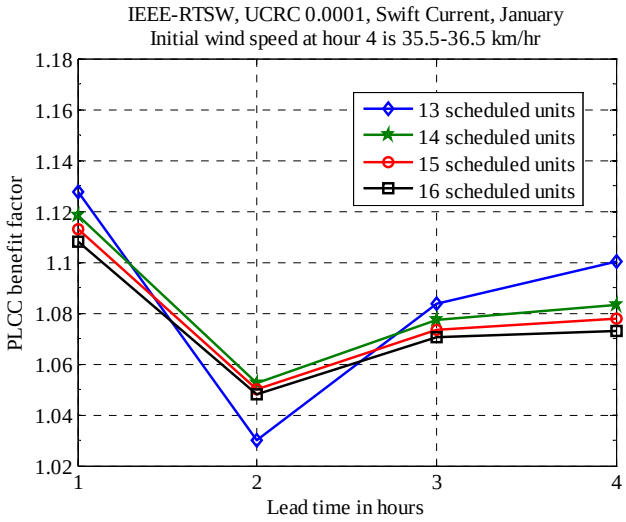

Fig. 4.37: PLCC benefit factor for the IEEE-RTSW at a High wind speed and a 0.0001 UCRC

4.5.3 Increase in Peak Load Carrying Capability for the RBTSW

The IPLCC for the RBTSW are shown in Fig. 4.38 and 4.39 for Low and High initial wind speeds respectively for an UCRC of 0.001. These figures show that the change in wind speed from Low to High creates a significant increase in the IPLCC. The scheduled capacity of 120 MW with 4 units shows a higher IPLCC than all other higher scheduled capacities in both figures.

Fig. 4.40 and 4.41 show the IPLCC for an UCRC of 0.0001 at Low and High initial wind speeds respectively. Fig.4.40 shows that the IPLCC is effectively zero for all the scheduled capacities from a lead time of 2 to 4 hours when the initial wind speeds are Low. The IPLCC is the PLCC difference between the wind integrated power system and the conventional power system without wind power. At this UCRC, the PLCC of the RBTS remains constant for a lead time up to 4 hours and the wind farm does not generate enough power to contribute to the PLCC. Even though the IPLCC are zero, the system UCR decreases due to the addition of wind power. Fig. 4.41 indicates that the IPLCC benefit improves with increase in the wind speed to the High wind speed condition.

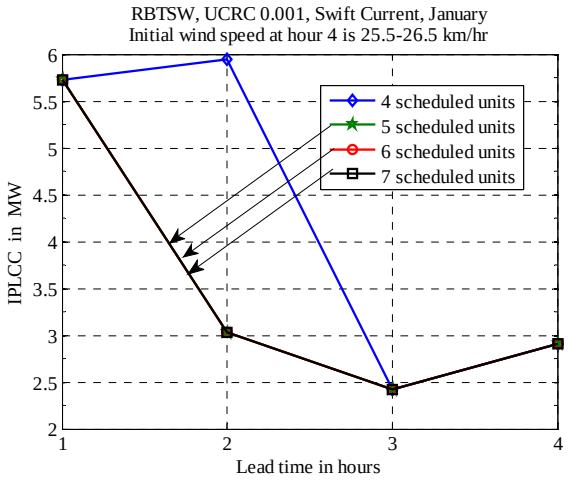

Fig. 4.38: IPLCC for the RBTSW at a Low initial wind speed conditions and a 0.001 UCRC

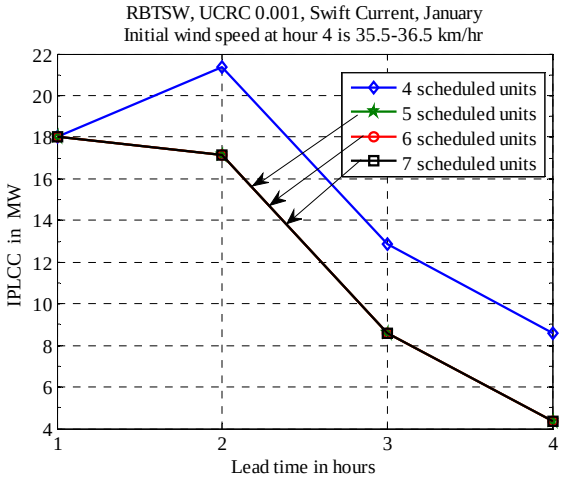

Fig. 4.39: IPLCC for the RBTSW at a High initial wind speed conditions and a 0.001 UCRC

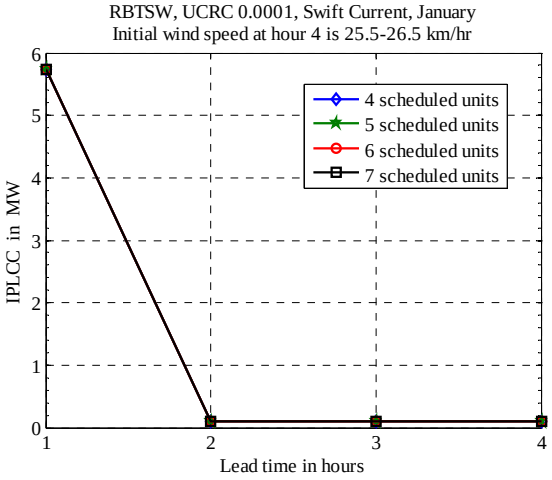

Fig. 4.40: IPLCC for the RBTSW at a Low initial wind speed conditions and a 0.0001 UCRC

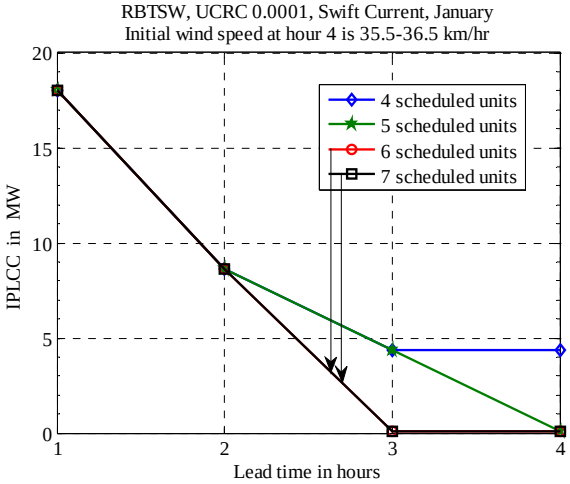

Fig. 4.41: IPLCC for the RBTSW at a High initial wind speed conditions and a 0.0001 UCRC

4.5.4 PLCC benefit factors for the RBTSW

Figs. 4.42 and 4.43 show the PLCC benefit factors for a UCRC of 0.001 for Low and High initial wind speed conditions respectively. The PLCC benefit factors are considerably higher for the High initial wind speed and generally decrease with the lead time. Both figures show that the PLCC benefit factors are higher for lower scheduled capacities due to the higher share of wind power. The PLCC benefit factors for a UCRC of 0.0001 are shown in Figs. 4.44 and 4.45 for Low and High initial wind speeds respectively. As expected, the PLCC benefit factors are higher when the initial wind speeds are higher.

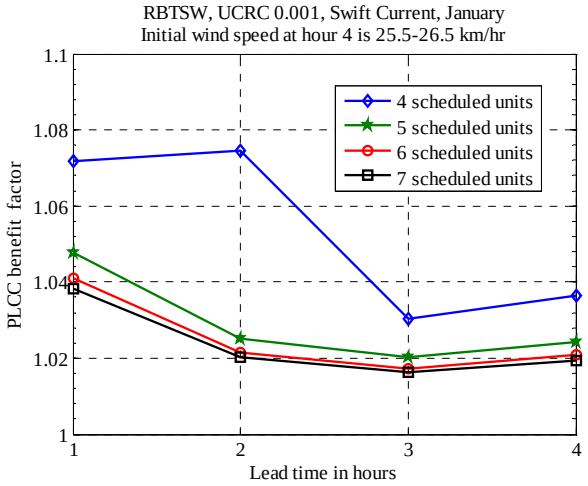

Fig. 4.42: PLCC benefit factors for the RBTSW at a Low initial wind speed and a 0.001 UCRC

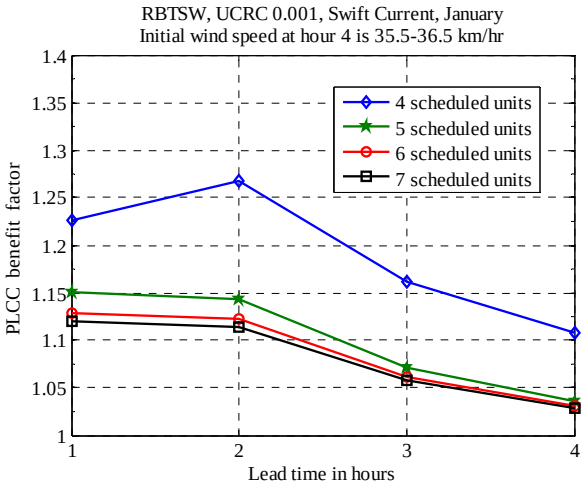

Fig. 4.43: PLCC benefit factors for the RBTSW at a High initial wind speed and a 0.001 UCRC

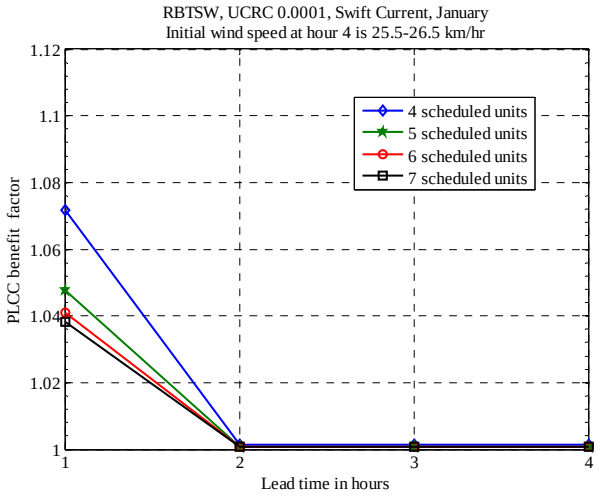

Fig. 4.44: PLCC benefit factor for the RBTSW at a Low initial wind speed and a 0.0001 UCRC

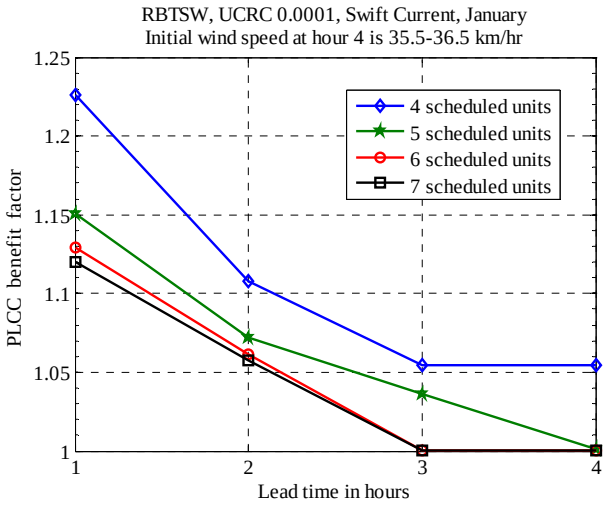

Fig. 4.45: PLCC benefit factor for the RBTSW at a High initial wind speed and a 0.0001 UCRC

4.6 Conclusions

This chapter illustrates the use of a probabilistic method to examine the benefits of adding wind power to a conventional power system. Short term wind speed probability distributions based on the initial known wind speeds are generated to produce conditional wind power probability distributions. The conditional wind power probability distributions are then used to create derated state models that can be combined with the conventional generating capacity models to determine the Unit Commitment Risk associated with different loading conditions and lead times. The novel contribution in this thesis is the recognition that wind

power output during a specified lead time can be modeled in the form of a multi-state generating unit and added to quickly create a total generating unit COPT that can be updated on an hourly or period basis. The process is not stationary and therefore regular updating of the COPT on a period basis is essential to accommodate the new wind condition as time moves on. This situation is a typical in power system operation where the system has to be continuously monitored and updated as the system states such as the load changes or some form of contingency such as generation outages, line outages, transmission line congestions etc. occurs. This procedure provides a consistent approach to calculating the operating risk in a wind integrated generating system.

The approach presented in this chapter uses auto-regressive moving average time series models and regression analysis to create the short term probability distributions of future wind speeds at a given wind site. Each model is unique to the site and the local wind conditions. The focus is on the inherent variability associated with the wind power output rather than on an exact future wind speed forecast. The system operating performance is examined in terms of the load carrying capability, peak load carrying capability and the increase in peak load carrying capability associated with wind power generation. The concepts and the implications of using different Unit Commitment Risk criteria and lead times are examined are illustrated using a small test system and a relatively larger test system in the form of the RBTS and the IEEE-RTS respectively.

In a general sense, the addition of wind power to a conventional generating system is always beneficial in terms of decreasing the Unit Commitment Risk and increasing the Peak Load Carrying Capability. The load carrying capability benefit is a complex phenomenon and depends on the initial wind speed, the time of the day and year, the site wind regime, the wind capacity and the size and types of the conventional units etc. Each power system has unique characteristics in terms of its unit sizes, lead-times and failure rates, and has different operating strategies. A general conclusion regarding wind power benefits is hard to achieve and each system should be evaluated individually in order to quantify the actual benefits.

The most important factors in assessing the operating benefits associated with a specific wind site are the initial wind speed and the site wind regime. The initial wind speed can be continuously monitored and updated to produce revised risk assessments for the required lead time. The Increase in Peak Load Carrying Capability attributable to the wind generating capacity will therefore vary with time. In systems with high wind power penetration this may result in requiring frequent unit commitment decisions in order to maintain an acceptable Unit Commitment Risk.

The studies show that wind capacity can make a recognizable contribution to the system operating reserve and that this contribution can be quantified. This is an important conclusion in view of the increasing addition of wind generating capacity to electric power systems throughout the world

The effect of incorporating derated states in a Unit Commitment Risk and Peak Load Carrying Capability analysis of a wind integrated power system is also examined using the IEEE-RTS.

The PLCC of the system is highly dependent on the UCRC and influenced by recognizing the possible generating unit derated states. The application of derated state generating unit models can show higher or lower PLCC values than those obtained using two state models but produces smoother and more representative UCR-load profiles compared to those for two state models, which create large discrete steps in the UCR levels. Detailed multi-state models provide a more accurate representation of the performance of a generating unit and therefore more accurate assessment of the UCR. They also require considerable data collected over a suitable period of time under consistent and carefully prepared protocols.

5. FACTORS AFFECTING THE IPLCC DUE TO WIND POWER

5.1 Introduction

Recent initiatives to exploit increasing amounts of wind energy for electricity production create further challenges when using the deterministic N-1 criterion, as wind power is uncertain, intermittent and variable. Conventional generating units are relatively large and using these units as ready reserve can result in excessive utility costs. Procedures to determine the capacity benefits of added wind power in a planning sense are described in [143]. There is, however, little published work on assessing the operating capacity benefit of added wind power [121, 137, 138].

A new approach to risk assessment due to the addition of wind power and the effects on unit commitment decisions is presented in [129, 140, 142, 144] and is described in Chapter 2, 3 and 4. The earlier chapters, however, do not examine the effect of different hourly wind speed distributions on the operating capacity and risk benefits of added wind power. The daily pattern of historical wind speed can create different impacts on the UCR and PLCC. The effects of hourly changes in wind speeds on the estimation of these benefits are illustrated by evaluating the operating situations at two different times of the day in two different seasons of the year in this chapter.

The actual wind speed profile is unique to the wind site due to the site topography and other physical factors. The benefits of integrating wind power can therefore be quite different at different wind sites. The effect of seasonal and topographical changes in wind profiles on the PLCC is examined by developing wind models for different seasons and wind sites and integrating them in conventional generation models.

The capacity credit that can be assigned to a particular wind power site is dependent on the wind regime at that site. This chapter examines the concept of the capacity credit associated with one or more wind farms using the IEEE-RTS. The studies are focused on wind power capacity credit in a system operating context in the IEEE-RTS due to the addition of one or more wind farms. The basic UCR probability index is used to assess the IPLCC attributable to an added wind facility and the assigned capacity credit. The analyses consider multiple wind sites with dependent and independent wind regimes.

5.2 Effect of Hourly Wind Trends on the Peak Load Carrying Capability of a Wind Integrated Power System

The effects of the hourly variability of wind speed on the PLCC benefits are demonstrated using the RBTS [52]. A total of 26 WTG were assumed to be installed in a wind farm with the installed generating capacity of 46.8 MW. The cut-in, cut-out and rated wind speeds are same as those used in Chapter 4.

The time series ARMA model describing the wind regime of the Swift-Current wind site is given in (3.1). The procedure used to develop CWSD and CWPD are also described in Chapter 3. In this section, the focus is to quantify and demonstrate the effects of hourly wind trends on the PLCC and IPLCC. The effect of hourly wind trends on the benefits of added wind power is demonstrated using two different times in two different seasons of a year.

5.2.1 Conditional Wind Speed Distributions

Table 5.1 shows the historical hourly mean and standard deviation of the wind speed at different times of the year for the period 1984 to 2003. Hours 4 to 7 and 15 to 18 fall on January 1st and are 4 a.m. to 7 a.m. and 3 p.m. to 6 p.m. respectively. Similarly the hours 5049 to 5052 and 5059 to 5062 fall on August 15th and are 12 a.m. to August 16th, 3 a.m. and August 16th, 10 a.m. to 1 p.m. respectively. The wind speeds at these hours were purposely chosen for their different historical mean wind speed trends. The historical trends in the mean hourly wind speed over a particular lead time period contain important information on the need to obtain specific CWSD for each hour in the period. Table 5.1 shows that the historical mean wind speeds during

hours 4-7 are close to those in hours 15-18. The historical mean wind speed during hours 5049-5052 and hours 5059-5062 are quite different. It can be seen that the mean wind speed has an increasing trend during hours 5049 - 5052 and a decrease trend during hours 5059-5062. The standard deviations also increase in hours 5049-5052 and decrease in hours 5059-5062.

Table 5.1: Actual mean wind speed parameters at the Swift Current wind site at different hours

	Hour 4	Hour 5	Hour 6	Hour 7
Mean wind speed (km/hr)	21.87	21.73	22.07	23.2
Standard deviation of wind speed(km/hr)	10.9	14.34	12.44	12.11
	Hour 15	Hour 16	Hour 17	Hour 18
Mean wind speed (km/hr)	22.2	23.6	23.67	25.27
Standard deviation of wind speed(km/hr)	11.97	14.22	10.61	11.45
	Hour 5049	Hour 5050	Hour 5051	Hour 5052
Mean wind speed (km/hr)	16.6	20.93	22.87	24.4
Standard deviation of wind speed(km/hr)	8.55	9.69	12.13	13.44
	Hour 5059	Hour 5060	Hour 5061	Hour 5062
Mean wind speed (km/hr)	20.4	18	13.8	14.27
Standard deviation of wind speed(km/hr)	9.99	8.28	7.8	5.51

The CWSD at hours 5 and 16, for an initial wind speed of 25.5-26.5 km/hr at hour 4 and 15 respectively are shown in Fig. 5.1. Similarly, the CWSD at hours 5050 and 5060 for the same initial wind speed at hour 5049 and 5059 respectively are presented in Fig. 5.2. The CWSD observed at hours 5 and 16 in Fig. 5.1 are similar, compared to the distributions obtained for hours 5050 and 5060 in Fig. 5.2, which are quite different. This is due to the fact that the historical wind speeds at hour 5 and 16 as shown in Table 5.1 are very similar and the historical average wind speeds at hour 5050 and 5060 are quite different. The higher mean wind speed and standard deviation at hour 5050 increases the probability of having higher wind speed than that at hour 5060 as shown in Fig. 5.2.

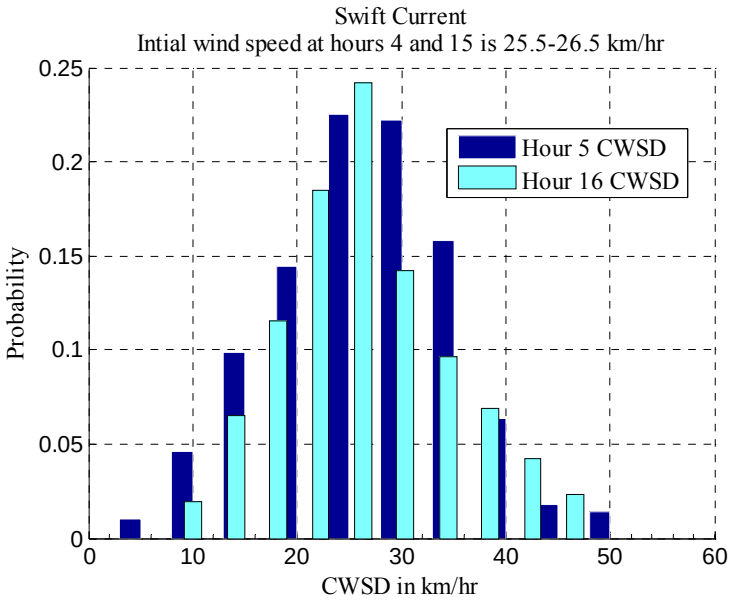

Fig. 5.1: The CWSD at hours 5 and 16

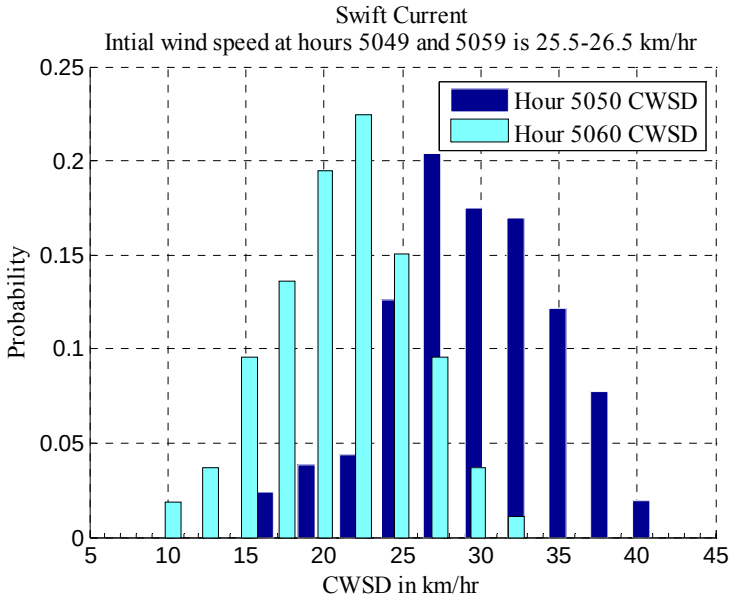

Fig. 5.2: The CWSD at hours 5050 and 5060

5.2.2 Conditional Wind Power Distributions

The CWPD obtained from the CWSD in Fig. 5.1 are shown in Fig. 5.3 and those from Fig. 5.2 are shown in Fig. 5.4. The CWPD at a particular hour and for a particular future hour during the lead time is entirely dependent on the related CWSD. The CWPD for hour 5 and 16

shown in Fig 5.3 are quite similar. The distributions shown in Fig. 5.4 are very different at hours 5050 and 5060. The probability of having zero power output at hour 5060 is higher than at hour 5050 and the probabilities of having higher power states are smaller. This situation decreases the PLCC of the system at hour 5060 and is discussed in Section 5.2.5.

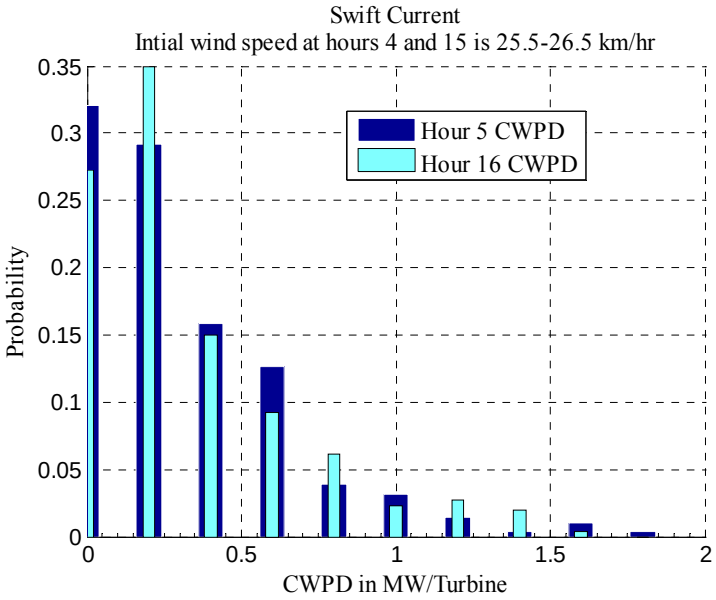

Fig. 5.3: The CWPD at hours 5 and 16

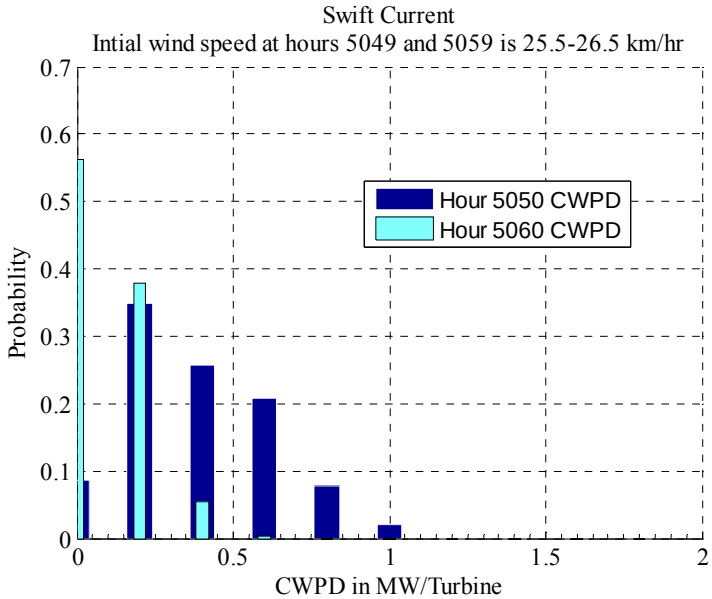

Fig. 5.4: The CWPD at hours 5050 and 5060

5.2.3 Peak Load Carrying Capability Comparisons in January

The PLCC of the RBTS with and without wind power for different UCRC and lead times during the hours 4 to 7 are presented in Fig. 5.5. Fig. 5.6 shows the PLCC during hours 15 to 18. The scheduled conventional capacity in both figures is 190 MW. These figures show that the PLCC profiles for the wind integrated power system are very similar for the two time periods. This is illustrated in Fig. 5.7. As shown in Table 5.1, the historical hourly wind speed parameters at these different times of the same day are very similar. The CWPD in Fig. 5.3 shows similar wind power probability distributions for the given initial wind speed condition, which results in similar PLCC.

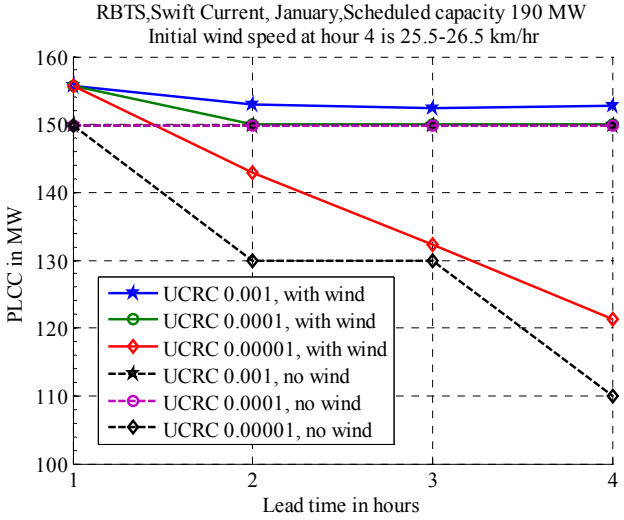

Fig. 5.5: The PLCC during hours 4-7

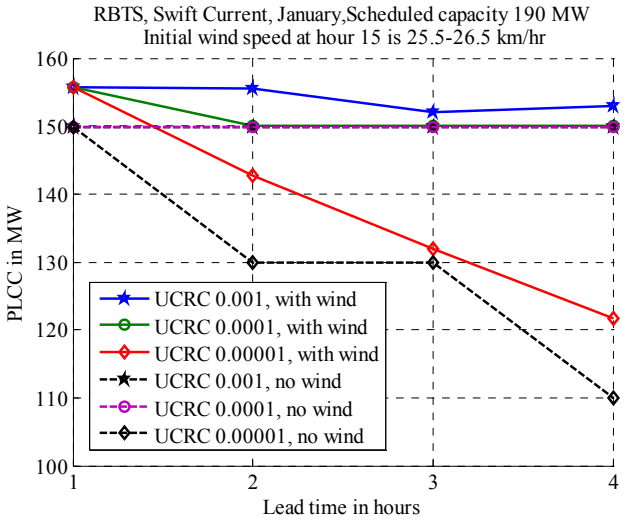

Fig. 5.6: The PLCC during hours 15-18

5.2.4 IPLCC Comparison in January

The IPLCC for the two cases shown in Fig. 5.5 and 5.6 are very similar and are both shown in Fig.5.7 for the hours 4-7 and 15 -18 at the same scheduled capacity and initial wind speed. The IPLCC are very close for the lower UCRC (high reliability) and a small difference in IPLCC is seen when the reliability criterion is relaxed (UCRC 0.001). The CWSD of each hour is related to its historical wind speed parameters through the developed ARMA model, the trend in parameters, and the initial wind speed. The CWSD for different hours of the same day can be quite different. The hours 4-7 and 15-18 have similar historical mean wind speeds and trends and therefore generate similar CWSD and hence have similar IPLCC. It may therefore not be necessary to generate new CWSD for each individual hour of the day and CWSD can be developed for blocks of time.

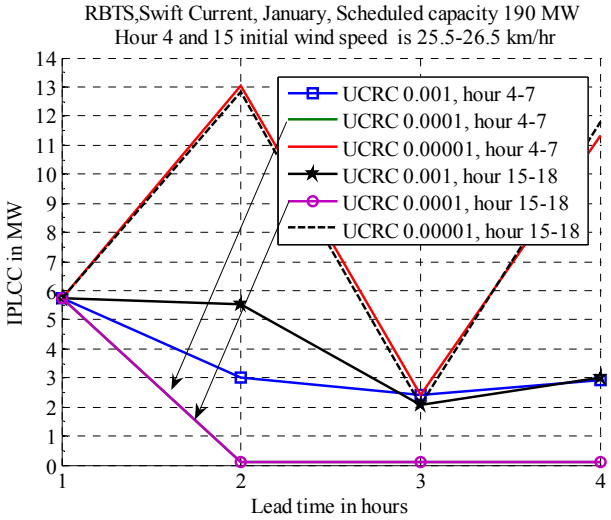

Fig. 5.7: The IPLCC during hours 4-7 and 15-18

5.2.5 Peak Load Carrying Capability Comparisons in August

The PLCC of the wind integrated RBTS in the month of August at hours 5049-5052 and hours 5059-5062 for different UCRC and lead times for a scheduled capacity of 190 MW are shown in Fig. 5.8 and 5.9.

Fig. 5.8 shows that the PLCC of the wind integrated RBTS during hours 5049-5052 remains relatively constant with lead time for UCRC of 0.001 and 0.0001. Fig. 5.9 shows that for

the same initial wind speed, the PLCC during hours 5059-5062 decreases as the lead time increases. An examination of Table 5.1 shows that historically the hours 5049-5052 have an increasing wind speed trend whereas hours 5059-5062 have a decreasing wind speed trend. The increasing trend during hours 5049-5052 reduces the risk associated with increasing lead time and higher PLCC are obtained for all the UCRC. The opposite effect arises during hours 5059-5062 where the wind speed has a historically decreasing trend. This observation is supported by the CWPD shown in Fig. 5.4.

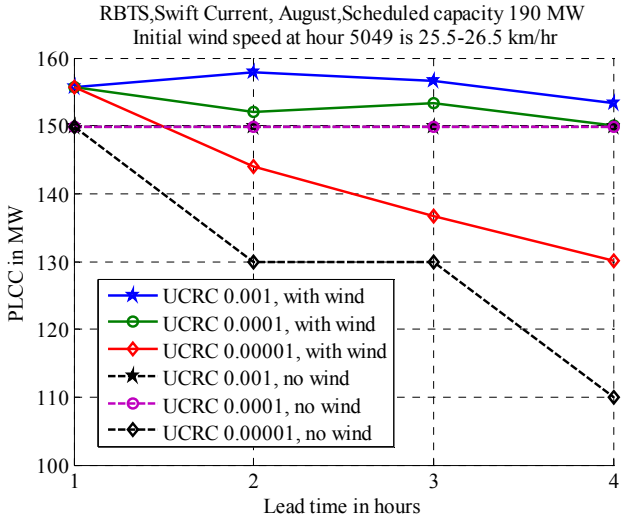

Fig.5.8: The PLCC during hours 5049-5052

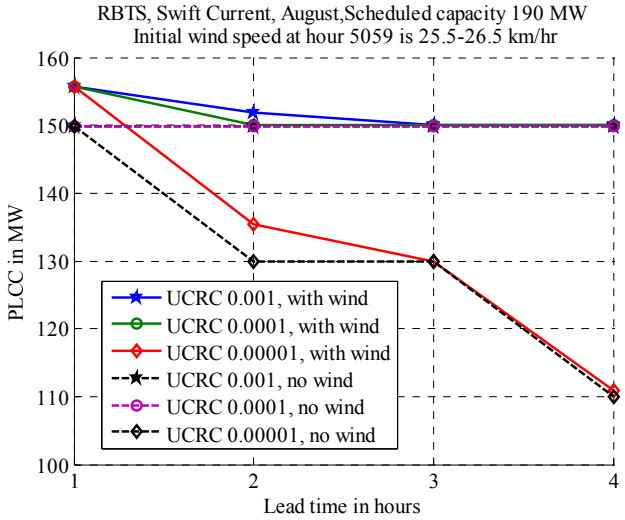

Fig. 5.9: The PLCC during hours 5059-5062

5.2.6 IPLCC Comparison in August

The IPLCC for the PLCC profiles presented in Fig. 5.8 and 5.9 are presented in Fig. 5.10 and 5.11 respectively. The IPLCC during hours 5049-5052 are higher than those in hours 5059-5062. The IPLCC decreases rapidly with lead time in hours 5059-5062, as these hours have decreasing mean wind speeds as shown in Table 5.1. There are higher IPLCC for hours 5049-5052, even at a lead time of 3 hours for UCRC of 0.001 and 0.0001, than for hours 5059-5062. The mean wind speeds for the two times of day have different trends, and therefore the IPLCC are different. Fig. 5.10 and 5.11 show that the PLCC of the basic RBTS decreases unevenly as the lead time increases due to the discrete large unit capacities. This results in a large variation in the IPLCC at the UCRC of 0.00001. The utilization of multi-state models for the conventional units produces much smoother PLCC profiles [144].

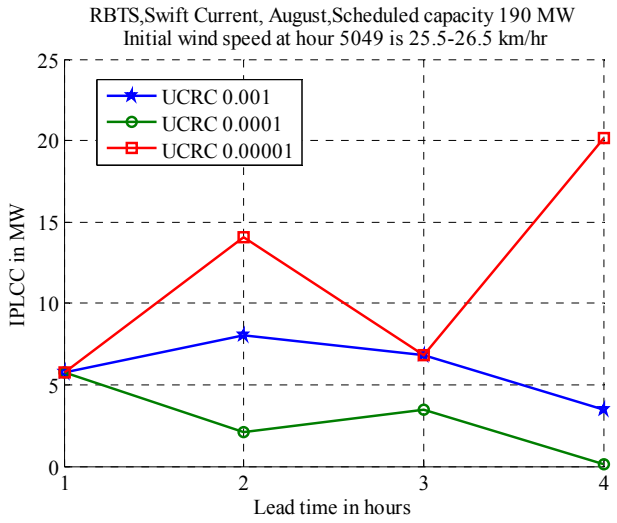

Fig. 5.10: The IPLCC during hours 5049-5052

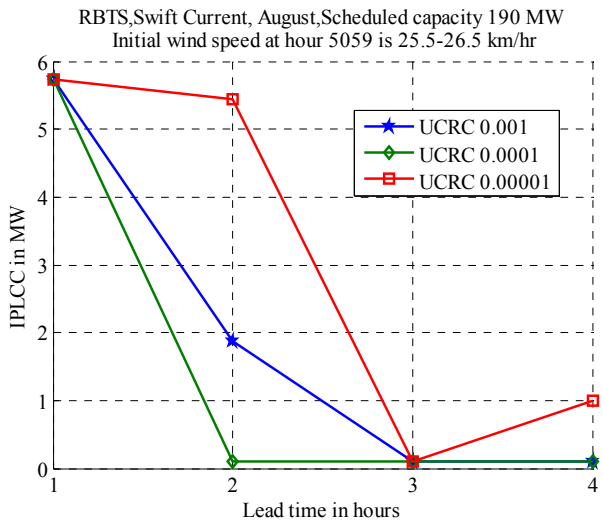

Fig. 5.11: The IPLCC during hours 5059-5062

The risk associated with system lead time can be offset by a favourable future mean wind speed trend. The historical mean wind speed trend during the hours of concern is therefore an important indicator of the operating capacity benefit of the added wind power [145]. The actual UCR decreases [129] with added wind power even if the PLCC remains the same.

5.3 Effects of Seasonality and Locality on the Operating Capacity Benefit of Wind Power

The effects of seasonality and locality on the operating capacity benefit of wind power are demonstrated using the RBTS. The wind turbine parameters are the same as those described in Section 5.2. Two wind sites located at Swift Current and Regina are used in the analysis. A total of 26 WTG are assumed to be installed on each wind site and the system is designated as the RBTSW. Comparisons are made for two seasons, winter and summer in the month of January and August for both wind sites. The initial wind speed at hour 4 (January 1st, 4 a.m.) and 5039 (August 15th, 2 p.m.) for both seasons are assumed to be at 25.5-26.6 km/hr for comparison purposes. The time series ARMA model for the Swift Current wind site is given in (3.1). The ARMA (4, 3) model for the Regina wind site [61] is shown below.

Regina model:

$$y_t = 0.9336\, y_{t-1} + 0.4506\, y_{t-2} - 0.5545\, y_{t-3} + 0.1110\, y_{t-4} + \alpha_t - 0.2033\alpha_{t-1} - 0.4684\alpha_{t-2} + 0.2301\alpha_{t-3}$$

$$\alpha_t \in \mathrm{NID}(0, 0.409423^2) \qquad (5.1)$$

The simulated wind speed SW_t can be calculated from (5.2) using the wind speed time series model.

$$SW_t = \mu_t + \sigma_t * y_t \qquad (5.2)$$

where μ_t is the mean observed wind speed at hour t; σ_t is the standard deviation of the observed wind speed at hour t; $\{\alpha_t\}$ is a normal white noise process with zero mean and a variance of 0.409423.

The regression analysis between hour 4 and 5 for the Regina wind site is shown in Fig. 5.12 and for the Swift Current wind site in Fig. 3.1. The observations are very similar at these two different wind sites for the given hours.

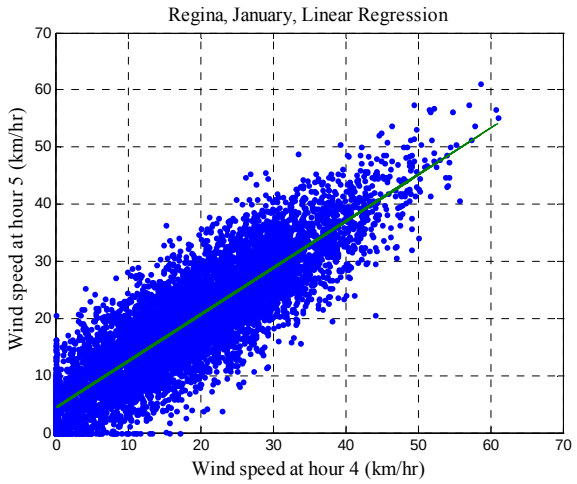

Fig. 5.12: Wind speed variability at hour 5 relative to hour 4 at the Regina wind site

5.3.1 Conditional Wind Speed Distributions

The historical hourly mean and standard deviation of wind speed for hour 4-7 for both wind sites are presented in Table 5.2.

Table 5.2: Actual mean wind speed values at the Regina and Swift Current wind sites for hour 4-7

		Hour 4	Hour 5	Hour 6	Hour 7
		Wind speed in km/hr			
Mean wind speed	Regina	18.0	18.2	18.6	19.2
	Swift-Current	21.87	21.73	22.07	23.20
Standard deviation of wind speed	Regina	14.0	12.9	12.1	12.8
	Swift-Current	10.90	14.34	12.44	12.11

This table shows that the Regina wind site has lower average wind speed during these hours than the Swift Current wind site. The standard deviations, however, are greater in hour 4 and 7. The CWSD generated at hour 6 for both wind sites for an initial wind speed of 25.5-26.5 km/hr at hour 4 are shown in Fig. 5.13. The Swift Current wind site shows higher probabilities of having higher wind speed at hour 6 than the Regina wind site.

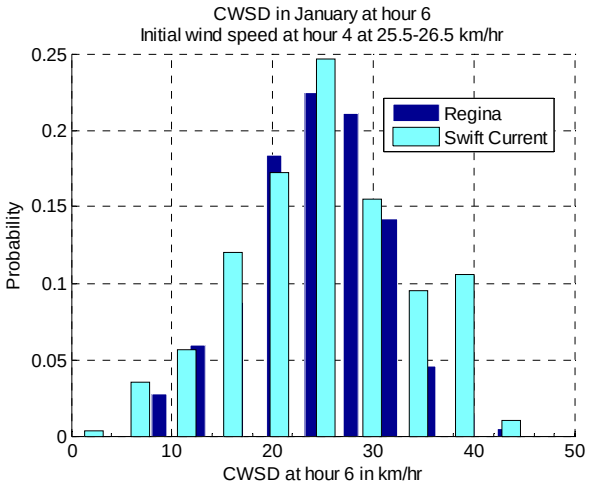

Fig. 5.13: CWSD at hour 6

Table 5.3 shows the historical hourly mean and standard deviation of wind speed for hours 5039-5042 for both wind sites. The average wind speeds at Regina and Swift Current for

the month of August are similar but the Regina wind site shows higher dispersion than the Swift Current site in the given hours.

Table 5.3. Actual wind speed data for the Regina and Swift Current wind sites for hour 5039-5042

		Hour 5039	Hour 5040	Hour 5041	Hour 5042
		Wind speed in km/hr			
Mean wind speed	Regina	14.1	13.9	15.6	14.2
	Swift-Current	13.2	13.33	16	14.4
Standard deviation of wind speed	Regina	8.9	9.9	11.4	10
	Swift-Current	5.86	6.72	6.37	5.83

As shown in Table 5.3, the Regina wind speed has a higher standard deviation than the Swift Current site at hour 5041. Although the mean wind speeds at both the wind sites are very close, this higher dispersion produces higher wind speeds at Regina than at Swift Current as shown in Fig. 5.14.

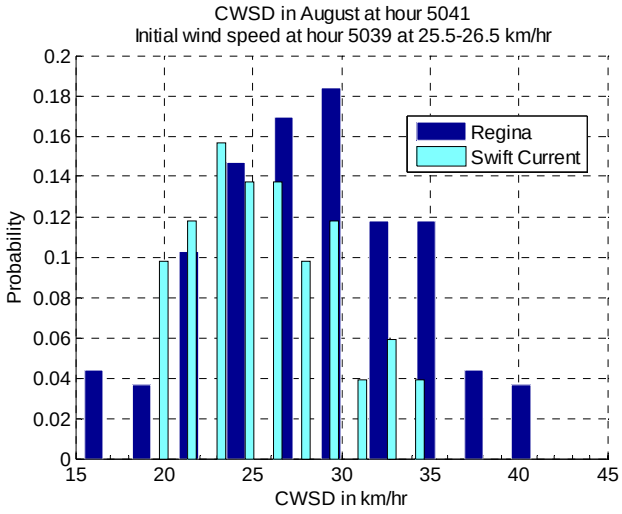

Fig. 5.14: CWSD at hour 5041

The wind speed values at the high end of the CWSD are important for wind power production as the power output from a WTG is directly proportional to the cube of the wind velocity between the cut-in and rated value. As indicated in Fig.5.12, if the initial hour (time

zero) wind speed is high, there will be higher likelihood that the next hour's wind speed will also be relatively high. This is consistent with the fact that the persistence model of wind forecasting is considered to generally give better estimates of possible wind speed over the next 4 to 6 hours than other more advanced techniques [125].

5.3.2 Conditional Wind Power Distributions

Wind turbine generators are generally designed to operate in the non-linear portion of the power curve and the rated wind speed is obtained only for few hours in a year. This is reflected in the parameters of the WTG installed in the Centennial Wind Farm located near Swift Current, Canada.

The conditional wind speed (CWS) pertaining to an initial wind speed condition is passed through the wind power curve given in [51] to generate the CWPD. The CWPD are not the same for each hour. Fig. 5.15 show the CWPD for Swift Current and Regina in January at hour 6 when the initial wind speed at hour 4 is assumed to be 25.5-26.5 km/hr. The Swift Current wind site shows higher probabilities at the higher wind power states than the Regina wind site due to its higher mean value of wind speed at these hours as shown in Table 5.2.

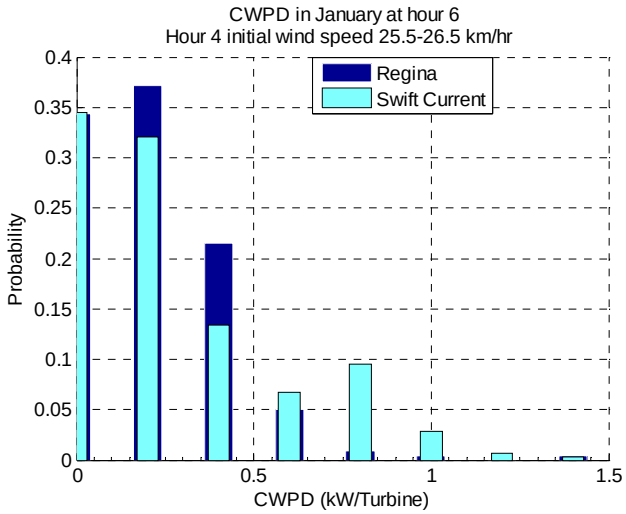

Fig.5.15: CWPD at hour 6

Fig. 5.16 shows the CWSD for both the Regina and Swift Current wind sites for hour 5041 with a given wind speed of 25.5-26.5 km/hr at hour 5039. In this figure, the Regina wind site has a better CWPD from a system reliability point of view as the lower power states have lower probabilities than those for the Swift Current site. The Regina CWPD shown in Fig. 5.16 has higher power states than the Swift Current due to the higher historical dispersion of wind at hour 5041 at this wind site.

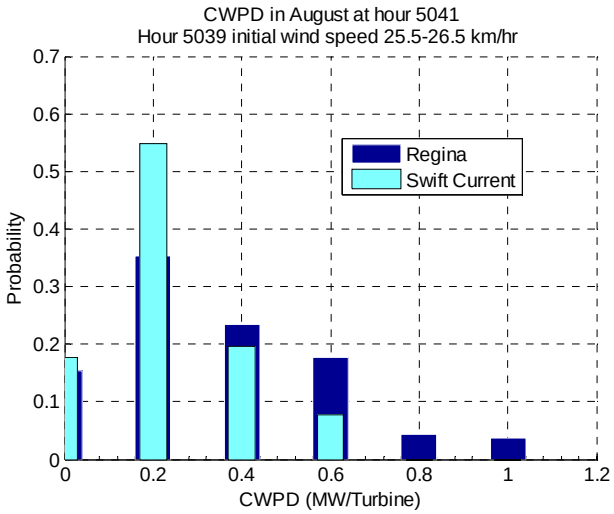

Fig. 5.16: CWPD at hour 5041

5.3.3 Unit Commitment Risk of the RBTSW

Fig.5.17 shows the UCR-load profile for the RBTSW using Regina and Swift Current wind data and the RBTS for a lead time of 3 hours. This figure shows that there is very little difference in the UCR for the two wind sites under these conditions. Further discussion in this regard is given in Section 5.3.4.

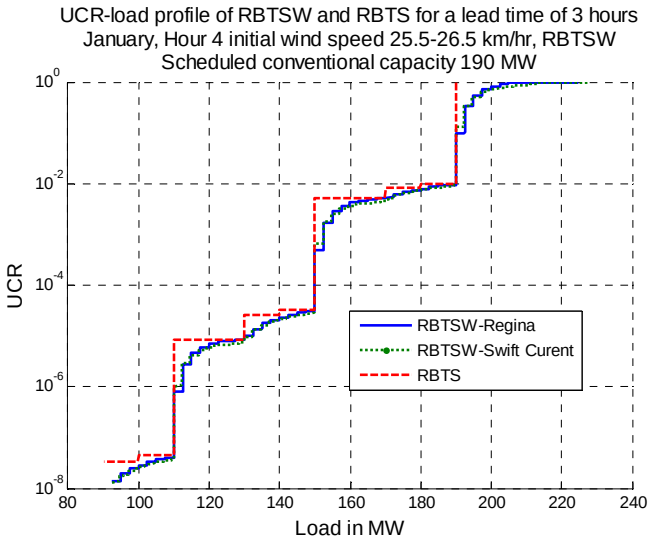

Fig. 5.17: UCR-load profile for the RBTSW and the RBTS

5.3.4 Peak Load Carrying Capability in January

Fig. 5.18 and 5.19 shows the PLCC at different lead times for the RBTS and RBTSW in the month of January. The PLCC are evaluated for UCRC of 0.001, 0.0001 and 0.00001. It can be seen from Fig. 5.18 and 5.19 that the PLCC are quite sensitive to the selected UCRC. The PLCC of the conventional generating units may or may not decrease in a small interval of time because of the large discrete capacities of the conventional units. As noted earlier in Chapter 4, the PLCC of the RBTS remains constant for the entire 4 hour lead time for the UCRC of 0.001 and 0.0001. The conventional units are represented by two state models and the WTG are represented by a relatively large number of derated states created due to the uncertainty associated with wind power. Both figures indicate that the PLCC of the RBTSW is generally greater than that for the RBTS and is dependent on the selected UCRC. The PLCC of the RBTSW therefore shows a relatively constant decrease over the lead time. The PLCC of the RBTSW are not the same for the two wind sites.

Similar analyses were carried out for the two sites in the month of August at hour 5039. The initial wind conditions and number of WTG are considered to be the same. The changes in the PLCC for the two wind sites are shown in Fig. 5.20 and 5.21. As expected, the PLCC of the RBTSW at these two site locations for the lead times are again different.

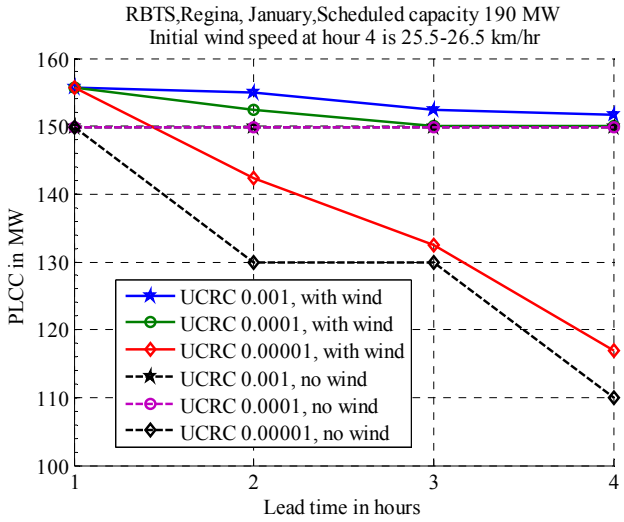

Fig. 5.18: PLCC for Regina in January for the given condition

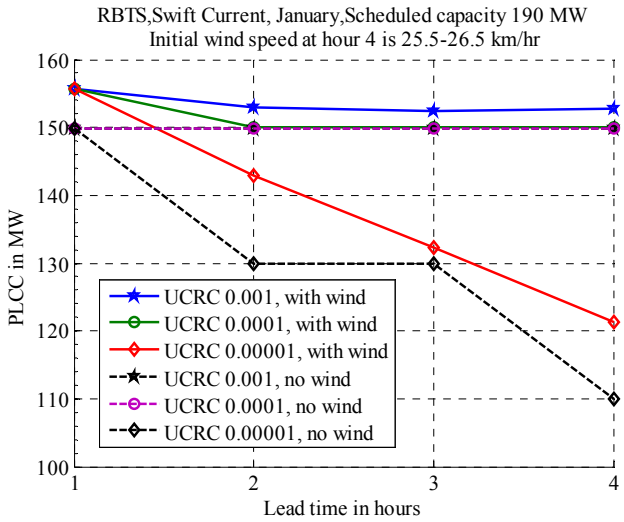

Fig. 5.19: PLCC for Swift Current in January for the given condition

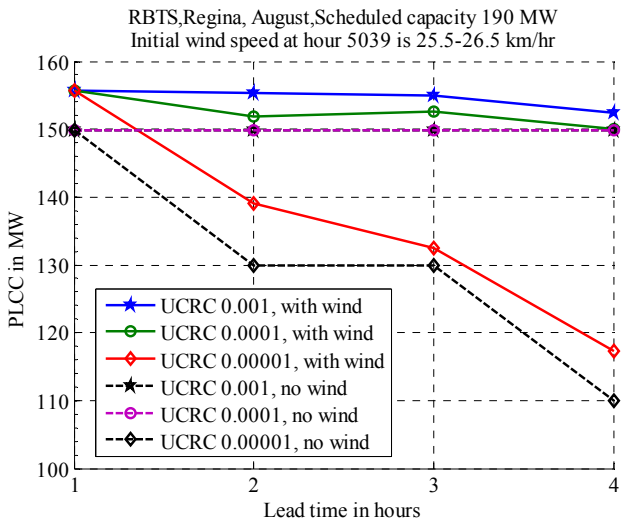

Fig. 5.20: PLCC for Regina in August for the given condition

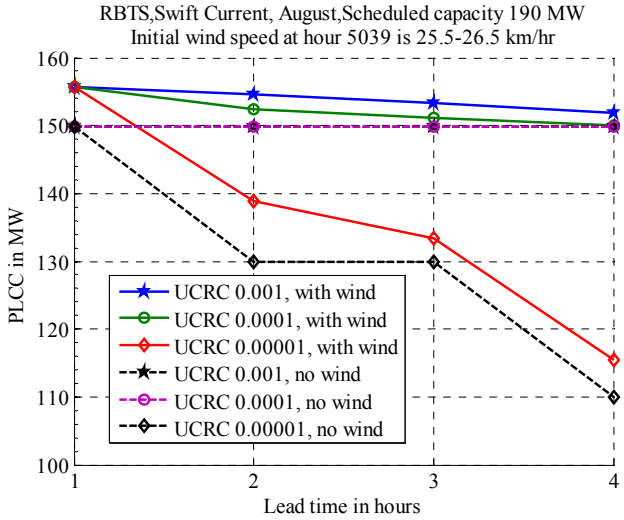

Fig. 5.21: PLCC for Swift Current in August for the given condition

The PLCC of a wind integrated power system is dependent on the initial wind speed and higher PLCC can be generally expected for higher initial wind speeds. Depending on the operating point in the UCR-load profile, the PLCC may not increase for higher wind speeds but in these conditions the UCR will decrease. It can be concluded that the addition of wind power is always beneficial in terms of Unit Commitment Risk (UCR) or an increased PLCC or both [129].

Table 5.4 shows the PLCC and the UCR at a lead time of 3 hours and a UCRC of 0.00001 for both wind sites at different scheduled conventional capacity. It can be seen that

there is a trade-off between the PLCC and the actual system risk. If the PLCC is higher with the wind power addition at one location, the actual system risk is also higher. Table 5.4 shows that the system is carrying higher peak load using the Swift Current wind regime at higher risk (but below the designated UCRC of 0.00001) than when using the Regina data for given scheduled capacities of 120 MW, 180 MW and 190 MW.

Table 5.4. PLCC and the actual RBTSW risk for Regina and Swift current for a lead time of 3 hours and a UCRC of 0.00001 at hour 5041

	PLCC in MW		UCR	
Scheduled Capacity in MW	Regina	Swift Current	Regina	Swift Current
120	79.9	81.2	6.69E-06	7.17E-06
160	105.0	103.4	9.30E-06	8.60E-06
180	122.5	123.4	8.02E-06	8.79E-06
190	132.5	133.4	8.04E-06	8.81E-06

5.3.5 Increase in Peak Load Carrying Capability

The IPLCC of the RBTSW with Regina and Swift Current wind sites for the month of January at initial hour 4 are shown in Fig. 5.22 and 5.23 for the same initial conditions. The IPLCC for the Regina wind site are generally better than those for the Swift Current site. The CWPD shown in Fig. 5.15 indicate that the Regina wind site does not promise a higher power output but has higher probabilities of having relatively low power states than for Swift Current. Swift Current has higher power states but their probabilities are relatively small and they do not contribute appreciably to the system reliability. The overall result is a generally slight improvement in the IPLCC profiles for Regina. The IPLCC observed at the UCRC of 0.00001 shows a highly irregular pattern because of the sudden decrease in the PLCC of the RBTS over the lead time at this UCRC as shown in Figs. 5.18 through 5.21.

The IPLCC for Regina and Swift Current for the month of August at initial hour 5039 are shown in Fig. 5. 24 and 5.25 respectively.

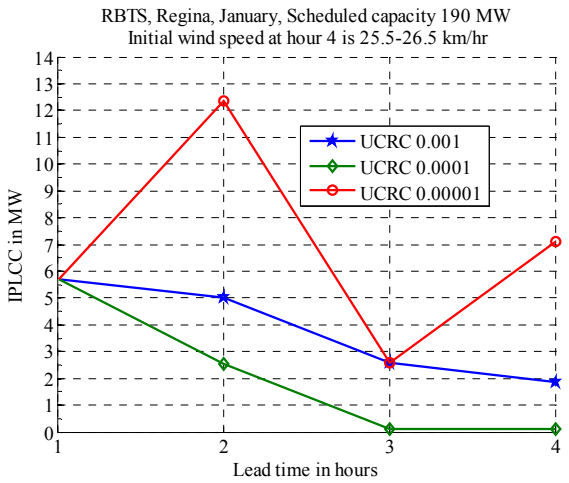

Fig. 5.22: IPLCC for Regina in January for the given conditions

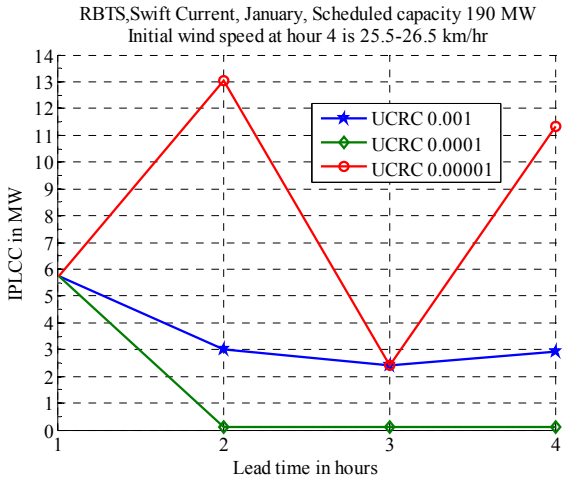

Fig. 5.23: IPLCC for Swift Current in January for the given conditions

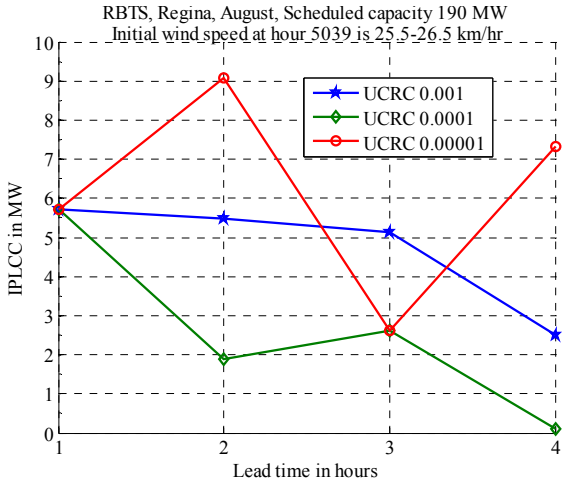

Fig. 5.24: IPLCC for Regina in August for the given conditions

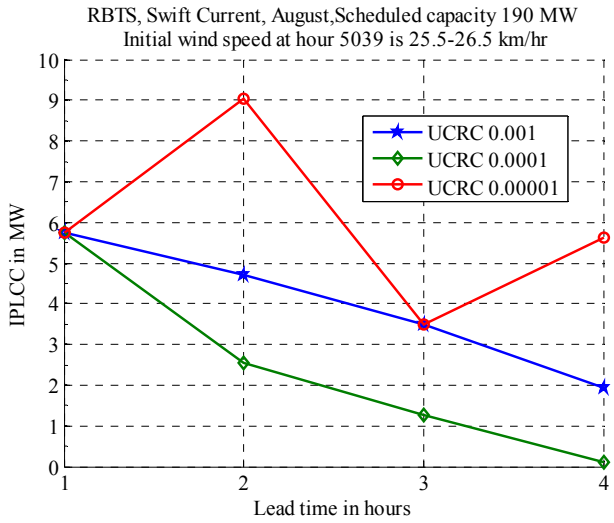

Fig. 5.25: IPLCC for Swift Current in August for the given conditions

The IPLCC for both wind sites are significantly different for the two seasons. A comparison of the Regina wind site and the Swift Current wind site results shows that the variations are more prominent due to seasonal changes than for the wind site changes. The IPLCC is the difference between the PLCC of the wind integrated power system and that of the basic system without wind power and it should not be evaluated and interpreted independently as this can lead to erroneous conclusions. This is demonstrated in [146]. The IPLCC could be higher (generally seen at the UCRC of 0.00001 than at the UCRC of 0.001 and 0.0001) but the overall PLCC could be actually lower. As noted earlier, the system operating risk criterion applied to the UCR-load profile is an important factor in determining the operating capacity benefit of adding wind power. The IPLCC together with the corresponding PLCC and the actual system risk therefore, should be analyzed together to properly understand the operating capacity contribution of wind power at a particular site.

5.4 Wind Power Operating Capacity Credit Assessment

It is generally agreed, that the most comprehensive risk based approach to establishing a generating unit capacity credit is to determine the increase in peak load carrying capability (IPLCC) that can be attributed to the generating facility at the criterion reliability level. This is

not a new concept and is designated as the generating unit effective load carrying capability (ELCC) in [147]. The criterion level IPLCC concept is used in this section to determine Operating Capacity Credit (OCC) values for the IEEE-RTS [53]. An OCC is defined as the ratio of the IPLCC to the total installed wind farm rated capacity and is expressed as a percentage. The results are system and data specific. They do, however, clearly indicate the capacity contributions that wind energy conversion systems (WECS) can make in a modern electric power system. This appreciation will become increasingly important as wind power penetration levels increase.

This section is focused on the determination and appreciation of the capacity credit associated with the addition of wind driven generating capacity to a system composed of conventional units in a system operating context. This is illustrated using data for a site located at Regina in Saskatchewan, Canada, which has a wind speed mean and standard deviation of 19.52 km/h and 10.99 km/h respectively. The ARMA model for the Regina wind site is given in (5.1). Five 100 MW WECS were added sequentially to the IEEE-RTS using the Regina wind regime data. As noted earlier, different WTG manufacturer make different WTG with different basic cut-in, cut-out, rated speed and rated power outputs. The cut-in, cut-out and rated wind speeds are assumed to be 14.4, 36 and 80 km/hour respectively in the studies in this section. Each WTG is rated at 1.0 MW.

5.4.1 Effects on the System Reliability Indices due to the Addition of Wind Power

The added wind capacity is considered to be either completely dependent or fully independent. The site wind regimes for each wind farm addition are completely correlated when the site wind regimes are dependent and there is zero correlation when the site wind regimes are independent. These conditions may not exist in an actual system and there will be some degree of cross-correlation between the site wind regimes. The dependent and independent conditions provide boundary values that clearly indicate the effects of site wind speed correlation. Incorporation of wind speed correlation in generating capacity adequacy evaluation using a sequential Monte Carlo simulation approach is illustrated in [130]. The system reliability

benefits associated with wind capacity additions are the highest when the site wind regimes are independent, and decrease as the degree of site wind regime correlation increases.

Fig. 5.26 shows a typical example of the CWPD for Regina in January at hour 5 when the initial wind speed at hour 4 is assumed to be 25.5-26.5 and 35.5-36.5 km/hr. It can be observed that for the same hour, if the initial wind speed increases, the chances of getting higher power output in the next hour also increases and the probability of getting no power in the next hour decreases.

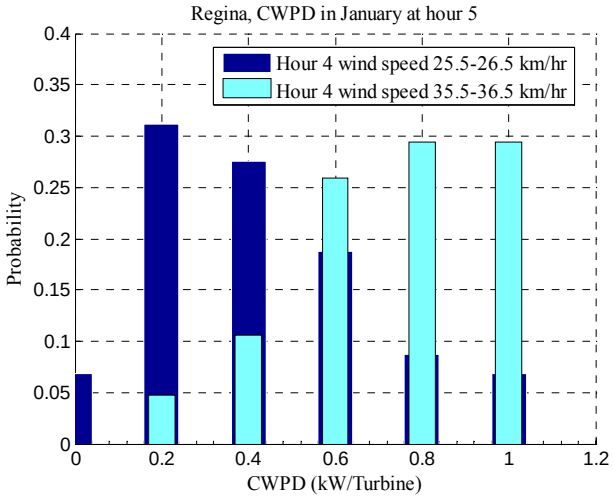

Fig. 5.26: The CWPD at hour 5

5.4.2 Unit Commitment Risk (UCR)

The UCR-load profile for an initial wind speed of 25.5-26.5 km/hr at hour 4 is shown in Fig. 5.27. The total installed wind capacity added to the IEEE-RTS is 100 MW. Due to the derated state effects of the WTG output, the UCR-load profiles are smoother than those in Fig. 2.9 (b).

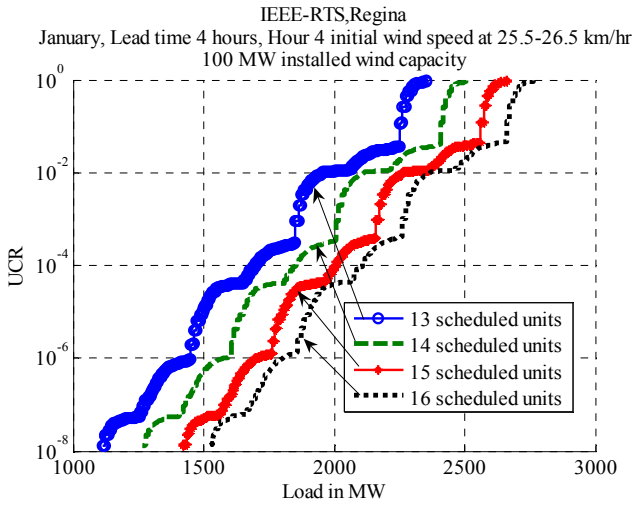

Fig. 5.27: The UCR-Load profile for the IEEE-RTS with 100 MW of wind capacity

5.4.3 Increase in Peak Load Carrying Capability (IPLCC) for Independent Wind Farms

Two different wind speed cases with dependent and independent wind farms are used to examine the IPLCC in this study. The wind speed data are obtained using (5.2) and the initial wind speeds at hour 4 in the month of January are 25.5-26.5 and 35.5-36.5 km/hr and are designated as low and high wind speeds respectively for discussion purposes. A UCRC of 0.001 is adopted in the analysis. In the independent wind farm case, the individual wind farms are added separately and independently to the conventional unit COPT to create the wind integrated system model. In the dependent wind farm case, the aggregate wind capacity model is added to conventional unit COPT.

The IPLCC due to independent wind farm additions are shown in Fig. 5.28 for the low initial wind speed. The IPLCC increases with the addition of each WECS. As the system lead time increases, the uncertainty associated with the wind speed increases and the IPLCC gradually decrease.

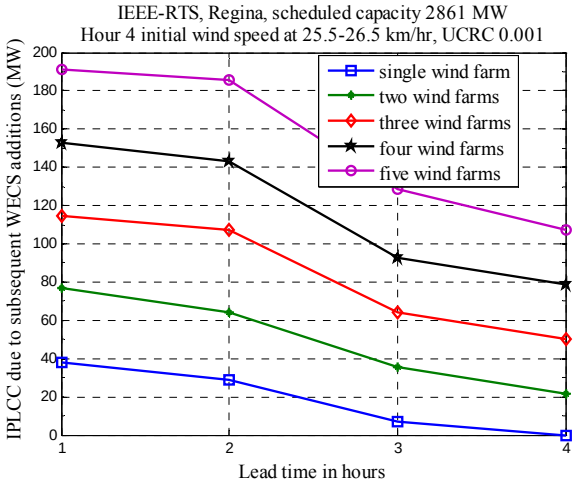

Fig. 5.28: The IPLCC as a function of the lead time for independent 100 MW wind farm additions

The IPLCC attributed to each WECS addition are shown in Fig. 5.29. This figure shows that the IPLCC are almost equal for a lead time of 1 hour but as the uncertainty increases in the subsequent hours, the IPLCC become variable. The IPLCC due to the first wind farm is the lowest and generally increases with increase in the number of wind farms.

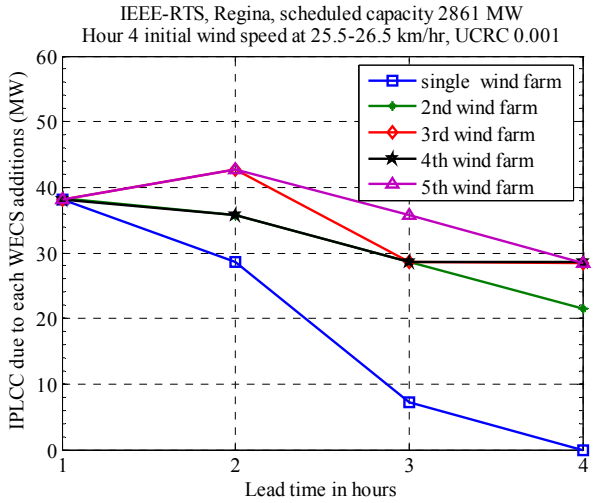

Fig. 5.29: The IPLCC as a function of the lead time for each individual independent wind farm addition

5.4.4 Increase in Peak Load Carrying Capability (IPLCC) for Dependent Wind Farms

The IPLCC due to dependent wind farm additions are shown in Fig. 5.30. As noted earlier, this situation could occur when multiple wind farms are located in close proximity to each other or when a single wind farm is expanded by adding more wind capacity. The IPLCC increases as the wind farm grows and decreases with increase in the system lead time. The IPLCC drops sharply in the dependent wind farm case and shows minimal benefits compared to those shown in Fig. 5.28 when the lead times are relatively high.

The IPLCC attributed to each 100 MW WECS is shown in Fig. 5.31. The IPLCC values are not constant in the dependent wind farm case. The PLCC of the 400 MW wind farm and 500 MW wind farm for a lead time of 3 hours are basically the same and the additional 100 MW capacity (from 400 MW to 500 MW) appears to have no effect on the PLCC. The PLCC in both cases remains constant at 2510.9 MW. The UCR and the PLCC are interrelated and do not have a linear relationship due to the discrete capacities of the generating units. The UCR at a lead time of 3 hour for the 400 MW wind farm is 9.968042E-04 and decreases to 9.645883E-04 when a 500 MW wind farm is considered. The PLCC is a function of the UCR-Load profile. In this particular case, the PLCC remains the same while the UCR decreases. This situation is discussed in [129].

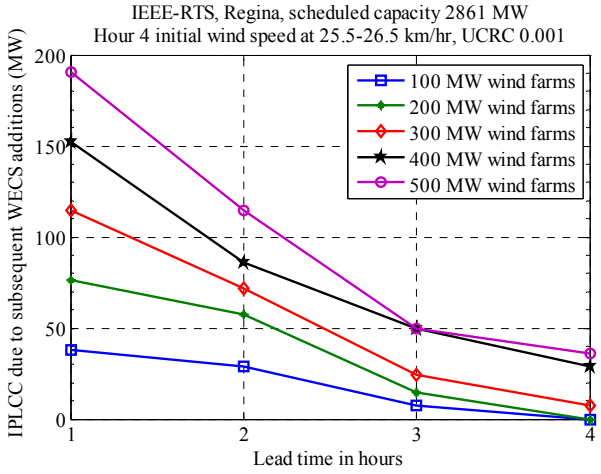

Fig. 5.30: The IPLCC as a function of the lead time for dependent wind farm additions

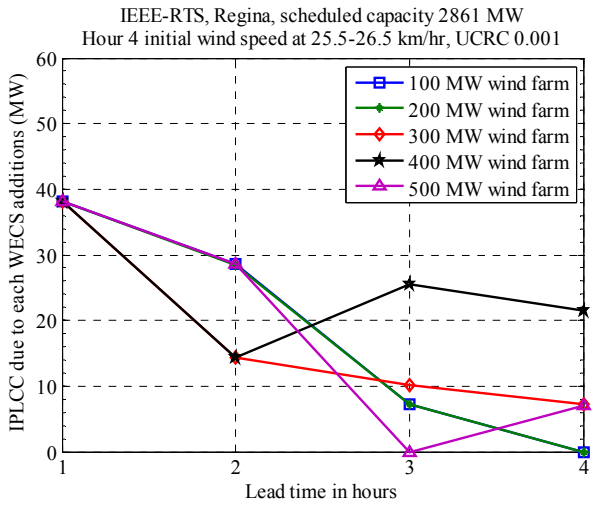

Fig. 5.31: The IPLCC as a function of the lead time for each individual dependent wind farm addition

5.4.5 Operating Capacity Credit (OCC)

Fig. 5.32 shows the Operating Capacity Credit for equal capacity wind systems composed of five independent and dependent 100 MW WECS. The figure shows that the aggregate or cumulative OCC is considerably larger in the independent wind farm case for lead times of two hours or more.

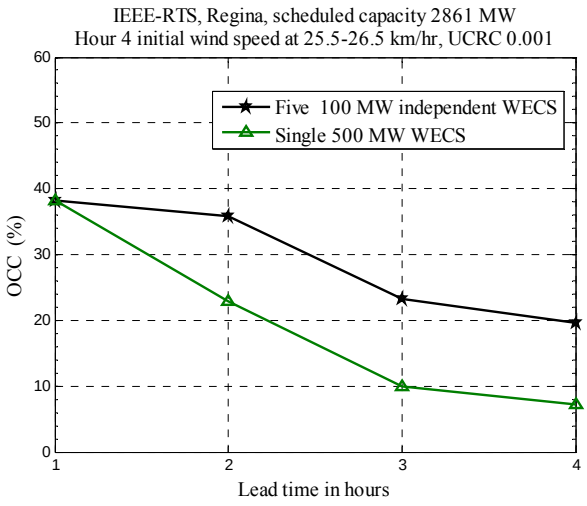

Fig. 5.32: The aggregate OCC for independent and dependent wind farms with low initial wind speed

Table 5.5 shows the OCC for each individual 100 MW wind farm and for the aggregate wind capacity at a lead time of 2 hours as the number of added wind farm increases for independent and dependent wind regimes.

Table 5.5. Incremental and aggregate OCC at low initial wind speed

Indv.Wind Capacity (MW)	Wind Regimes		Agg.Wind Capacity (MW)	Wind Regimes	
	Dep. OCC(%)	Indep. OCC(%)		Dep. OCC(%)	Indep. OCC(%)
0	0	0	0	0	0
1*100	28.7	28.7	100	28.7	28.7
2*100	28.5	35.7	200	28.6	32.2
3*100	14.3	42.8	300	23.8	35.7
4*100	14.3	35.8	400	21.5	35.8
5*100	28.6	42.8	500	22.9	37.2

The aggregate OCC for the five independent wind farms and the 500 MW dependent wind farm are compared in Fig. 5.33 for the high initial wind speed case. The aggregate OCC of the independent wind farms are considerably higher than the dependent wind farm values. The performance in both cases due to higher initial wind speed condition is better than that shown in Fig. 5.32 for the low initial wind speed.

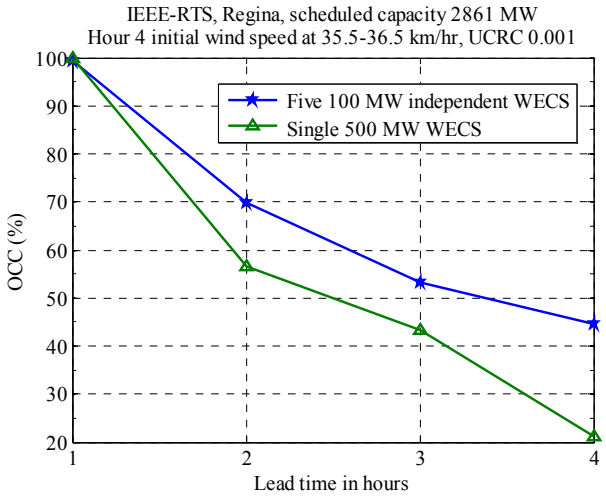

Fig. 5.33: The aggregate OCC for independent and dependent wind farms with high initial wind speed.

Table 5.6 shows the incremental and aggregate OCC values for each capacity addition under the independent and dependent wind conditions for a lead time of 2 hours at the high initial wind speed. The incremental and aggregate OCC associated with each capacity addition are higher in the independent cases than in the dependent cases.

Table 5.6. Incremental and aggregate OCC at high initial wind speed

Indv.Wind Capacity (MW)	Wind Regimes		Agg. Wind Capacity (MW)	Wind Regimes	
	Dep. OCC(%)	Indep. OCC(%)		Dep. OCC(%)	Indep. OCC(%)
0	0	0	0	0	0
1*100	64.5	64.5	100	64.5	64.5
2*100	64.4	67.8	200	64.5	66.2
3*100	60.9	69.9	300	63.3	67.4
4*100	46.6	73.2	400	59.1	68.9
5*100	46.6	73.3	500	56.6	69.7

5.5 Conclusion

This chapter illustrates the effect of the daily variation in mean wind speed parameter trends on the Peak Load Carrying Capability of a wind integrated power system. Two typical sets of hourly wind speeds, one in January and another in August are analyzed. The wind speed parameter trends in January are similar although they are at different times of the same day. The results indicate that the Increase in Peak Load Carrying Capabilities are very similar. It can therefore be concluded that if the hourly mean wind speed parameter trend at different times of the day are similar, they will produce similar results for the same initial wind speed and therefore it may not be necessary to develop Conditional Wind Speed Distributions for each individual hour in the day.

Similar analyses were carried out for the month of August where the mean wind speed trends are quite different. One set of hours has a historically increasing mean wind speed trend and the other set has a decreasing mean wind speed trend. The PLCC benefits are higher for the hours which show an increasing trend and result in an increased IPLCC. The historical mean wind speed trend is an important indicator and should be considered in the IPLCC evaluation. This can be of practical significance at some wind sites where for a certain period of time the

wind shows an increasing mean wind speed trend while at other times it is either decreasing or relatively constant.

The effects of seasonality and wind site variations on the Peak Load Carrying Capability of a wind integrated power system are demonstrated in this chapter. Wind speed data for two sites located at Regina and Swift Current in Saskatchewan, Canada for the month of January and August are used in the described studies. The initial conditions of the system states are assumed to be known in a power system security study and therefore a specific initial wind speed is assumed in all the study cases to compare the operating capacity benefits in different scenarios.

Two cases were investigated for the two sites, one with different historical means but similar standard deviations and the other with similar historical means but different standard deviations. The study results show that the IPLCC is influenced significantly by the changes in the season rather than the change in the wind sites. The benefits are highly dependent on the initial wind speed and the historical wind speed profile.

This chapter illustrates operating capacity credits associated with adding independent and dependent wind farms to a system composed of conventional generating units. The concepts are presented using the IEEE-Reliability Test System. The numerical results are therefore a function of the test system and the input data used in the studies. Similar studies can be conducted for other systems. The studies described show a number of conditions and trends that are applicable to a wide range of systems.

The capacity credits attributable to wind power are evaluated using the concept of increased peak load carrying capability at the criterion risk level. The OCC is a function of the initial wind speed and the lead time associated with the additional available system capacity.

The studies presented clearly illustrate the considerable difference in operating capacity credits attributable to wind power additions associated with dependent and independent wind regimes. The dependent and independent conditions provide boundary values that clearly indicate the effects of site wind speed correlation. This is an important factor in all wind

integrated power systems and will become increasingly important in the future as wind power penetration levels increase.

6. WELL-BEING ANALYSIS OF WIND INTEGRATED POWER SYSTEMS

6.1 Introduction

The operating reserve in a power system continuously varies due to changes in the system load level and in the scheduled generating capacity. The system load depends on many factors such as system load types, consumer behavior, environmental factors etc. The system scheduled capacity must always be greater than the load and be capable of responding to unexpected outages of generating capacity or a sudden increase in the load level. The operating generating capacity in excess of the load determines the operating states of a power system.

The power system operating states can be represented by a five state model involving Normal, Marginal, Emergency, Extreme emergency and Restorative states as shown in [39]. This is illustrated in Fig. 6.1. In the Normal operating state, the system is considered to have adequate generation to meet the load and has enough spinning reserve to satisfy an accepted operating philosophy such as the N-1 criterion. In the Marginal state, the system can still work normally but can not satisfy the accepted criterion. In an Emergency condition, the generating capacity is equal to the load and if appropriate action is not taken, the system will move to the Extreme Emergency state, where some portion of the load must be curtailed to restore the system.

Detailed definitions of the system operating states as described in [39] are presented in Appendix A3.

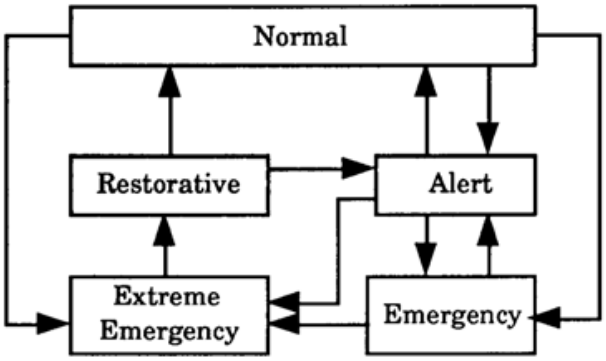

Fig.6.1: Power system operating states

The deterministic approach embedded in the five operating state model shown in Fig. 6.1 does not recognize the probabilistic nature of system failures. A survey noted in [7] indicates that Canadian utilities do not actively utilize the probabilistic technique suggested in [13] for operating reserve assessment. The reason behind this is considered to be the difficulty in interpreting the risk index and the lack of system operating information in the use of a single risk value. The shortcomings of the probability model [13], which assumes a two operating state model describing comfort and risk is modified in [29] to contain three states designated as Healthy, Marginal and At risk operating states as shown in Fig.6.2.

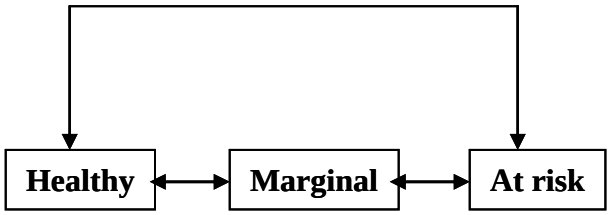

Fig. 6.2: Modified power system operating states

In this modified approach, a system is said to be in the Healthy state if it has enough operating reserve to satisfy the deterministic criterion. In the Marginal state the system does not have enough operating reserve to satisfy the deterministic criterion and in the At risk state the system load is equal to or greater than the operating capacity. The proposed model is more informative than the basic two state model [13] as it provides a warning to the system operator before the system enters into the At risk (Emergency and Extreme Emergency) state. This

approach is known as system well-being analysis. Well-being analysis [34, 37, 38] provides an opportunity to augment the single risk index (UCR) with additional indices that recognize the different operating conditions noted in [39]. The well-being approach brings acceptable deterministic criteria utilized by electrical power utilities into a probabilistic framework. The sum of the Healthy State Probability (HSP), the Marginal State Probability (MSP) and the Unit Commitment Risk (UCR) at a given load level is unity.

System operating performance indices such as the PLCC and IPLCC can be evaluated using a single or a dual risk criterion. The single risk criterion could be the HSP or the UCR. In a single risk criterion, the system must maintain a HSP greater than the specified Healthy State Probability Criterion (HSPC) or a UCR lower than the specified UCRC. In a dual risk criterion, the system must maintain both designated HSPC and UCRC. This chapter is focused on the evaluation of the well-being states of the wind integrated RBTS, IEEE-RTS and modified IEEE-RTS designated as the RBTSW, IEEE-RTSW and IEEE-RTSMW respectively. A single UCRC of 0.001 and a dual risk criterion with HSPC of 0.9 and UCRC of 0.001 are adopted in the initial analyses. Other constraints and assumptions used in this chapter are introduced in appropriate places.

6.2 Methodology

Different methodologies that can be used to determine the well-being state probabilities at HL-I are presented below.

6.2.1 Contingency Enumeration method

The Contingency Enumeration approach [38] utilizes a generation model in the form of an array that lists all the different possible combinations of the existing generating unit outages, their probabilities and the capacity of the largest unit associated with each contingency state. Each contingency in the generation model is compared with the corresponding system load to determine the amount of capacity reserve available at each condition. When the available reserve is equal to or more than the capacity of the largest unit, that particular contingency state is

considered to be Healthy. When the available reserve is less than the capacity of the largest unit but greater than zero, the contingency state is said to be Marginal and when it is less than or equal to zero, the contingency state is said to be At risk. The HSP is the sum of the individual state probabilities for which the contingency states are Healthy. Similarly, the Marginal State Probability (MSP) is the sum of all the individual probabilities for which the contingency states are Marginal. The probability of risk is the sum of all the At risk state probabilities. A sample calculation of system well-being using contingency enumeration is presented in Table 6.1. This table shows the calculations involved for the RBTS when 120 MW of capacity are committed from the merit order shown in Appendix A1. The load is considered to be 50 MW and the system lead time is 4 hours.

Table 6.1: Contingency enumeration for a load of 50 MW and generation of 120 MW at a lead time of 4 hours

Unit no. Out	Capacity In (CIn) (MW)	Reserve = C-Load (MW)	Capacity of the Largest Operating Unit (CLOU) (MW)	System Operating State	Probability
0	120	70	40	H	0.99371265
1	80	30	40	M	0.00136312
2	100	50	40	H	0.00109019
3	100	50	40	H	0.00109019
4	80	30	40	M	0.00272998
1,2	60	10	40	M	0.00000150
1,3	60	10	40	M	0.00000150
1,4	40	-10	20	R	0.00000374
2,3	80	30	40	M	0.00000120
2,4	60	10	40	M	0.00000300
3,4	60	10	40	M	0.00000300
1,2,3	40	-10	40	R	1.64E-09
1,2,4	20	-30	20	R	4.11E-09
1,3,4	20	-30	20	R	4.11E-09
2,3,4	40	-10	40	R	3.29E-09
1,2,3,4	0	-50	0	R	4.51E-12

Let, P(h)= Probability of Health

P(m)= Probability of Margin

P(r) = Probability of At risk

From Table 6.1,

$$P(h) = \left[P(0) + P(2) + P(3)\right] \text{ unit out} \quad (6.1)$$

where, P(x) = Probability of having unit x out of service in Table 6.1.

$$\text{Or, } P(h) = \sum P(120) + P(100) \text{ MW In} \quad (6.2)$$

P(120) MW In is obtained from Col.2 of Table 6.1.

$$P(m) = \left[P(1) + P(4) + P(1,2) + P(1,3) + P(2,3) + P(2,4) + P(3,4)\right] \text{ unit out} \quad (6.3)$$

$$\text{Or, } P(m) = \sum P(80) + P(60) \text{ MW In} \quad (6.4)$$

$$P(r) = \left[P(1,4) + P(1,2,3) + P(1,2,4) + P(1,3,4) + P(2,3,4) + P(1,2,3,4)\right] \text{ unit out} \quad (6.5)$$

$$\text{Or, } P(r) = \sum P(40) + P(20) + P(0) \text{ MW In} \quad (6.6)$$

P(h)= 0.99589303

P(m)= 0.00410330

P(r)= 0.00000375

As noted earlier, P(h)+P(m)+ P(r) =1

The capacity model in Table 6.1 is developed using basic two state models for the generating units. Table 6.2 illustrates the basic procedure utilizing a derated state unit. Assume that unit number 4 in the priority listing is represented by a three state model. The three states are 40, 20 and 0 MW with transition rates of 2 and 4 failures per year respectively [2]. The lead time is considered to be 4 hours. The contingency enumeration table is shown in Table 6.2.

Table 6.2: Contingency enumeration for a load of 50 MW and generation of 120 MW at a lead time of 4 hours considering a derated state unit

Unit no. Out	Capacity In (CIn) (MW)	Reserve = C-Load (MW)	Capacity of the Largest Operating Unit (CLOU) (MW)	System Operating State	Probability
0	120	70	40	H	9.937126E-01
1	80	30	40	M	1.363117E-03
2	100	50	40	H	1.090194E-03
3	100	50	40	H	1.090194E-03
4 partial out	100	50	40	H	9.099932E-04
4 full out	80	30	40	M	1.819986E-03
1,2	60	10	40	M	1.495466E-06
1,3	60	10	40	M	1.495466E-06
1,4(4 partial out)	60	10	20	M	1.248276E-06
1,4(4 full out)	40	-10	20	R	2.496552E-06
2,3	80	30	40	M	1.196044E-06
2,4(4 partial out)	80	30	40	M	9.983466E-07
2,4 (4 full out)	60	10	40	M	1.996693E-06
3,4(4 partial out)	80	30	40	M	9.983466E-07
3,4 (4 full out)	60	10	40	M	1.996693E-06
1,2,3	40	-10	40	R	1.636169E-09
1,2,4 (4 partial out)	40	-10	40	R	1.365722E-09
1,2,4 (4 full out)	20	-30	20	R	2.731444E-09
1,3,4 (4 partial out)	40	-10	20	R	1.369474E-09
1,3,4 (4 full out)	20	-30	20	R	2.738948E-09
2,3,4(4 partial out)	60	10	40	M	1.095278E-09
2,3,4 (4 full out)	40	-10	40	R	2.190557E-09
1,2,3,4 (4 partial out)	20	-30	0	R	1.502439E-12
1,2,3,4 (4 full out)	0	-50	0	R	3.004879E-12

From Table 6.2

$$P(h) = \left[P(0) + P(2) + P(3) + P(4/po)\right] \text{ unit out} \quad (6.7)$$

$$\text{Or, } P(h) = \sum P(120) + P(100) \text{ MW In} \quad (6.8)$$

$$P(m) = \left[\begin{array}{l} P(1) + P(4/fo) + P(1,2) + P(1,3) + P(2,3) + P(2,4/fo) + \\ P(2,4/po) + P(3,4/\ fo) + P(3,4/po) + P(2,3,4/po) \end{array}\right] \text{ unit out} \quad (6.9)$$

$$\text{Or, } P(m) = \sum P(80) + P(60) \text{ MW In} \quad (6.10)$$

$$P(r)=\left[P(1,4)+P(1,2,3)+P(1,2,4)+P(1,3,4)+P(2,3,4)+P(1,2,3,4)\right] \text{ unit out} \quad (6.11)$$

$$\text{Or, } P(r)=\sum P(40)+P(20)+P(0) \text{ MW In} \quad (6.12)$$

P(h)= 0.99680302

P(m)= 3.194529E-03

P(r)= 2.508589E-06

where po = partial outage

fo= full outage

6.2.2 Conditional COPT method

In this method [55], the At risk (UCR) probability is evaluated directly using the COPT. The probability of Health is evaluated by developing several COPT using the conditional probabilities of the available states. The probability of Margin is calculated by subtracting the sum of the probabilities of Health and At risk from unity. This method gives similar results to the Contingency Enumeration approach but is considerably faster. The probabilities of high order contingencies are generally ignored in the Conditional COPT approach where truncation of the COPT is done by omitting outage levels that result in a cumulative probability less than a practical value. This method involves building several COPT to estimate the HSP and could require considerable time to arrive at a solution in a large power system.

6.2.3 Approximate method

The above procedures for finding the system well-being state probabilities can involve long computation times [38, 55]. The initial condition of the wind speed changes with time and therefore, a fast computing method is required to determine the well-being state probabilities in a wind integrated power system. This problem can be solved by using an approximate method to estimate the Healthy state probability for any loading condition for a given schedule capacity.

The ORR of a generating unit is generally very small for a lead time of a few hours and the system well-being state probabilities can be evaluated directly using a COPT with reasonable accuracy. This approach is designated as the Approximate method. The procedure to estimate the well-being states is described in the following section. Studies have shown that the Approximate method produces exactly the same result in almost all cases as that produced by the Contingency Enumeration approach. Different case studies comparing the Approximate method and the Contingency Enumeration approach are presented in Appendix A4.

An exception is observed when the system load is at a very low load level and is equal to the largest operating unit for a system with a relatively low scheduled capacity. This particular situation, however, is not generally observed in power system operation. This particular situation is described in the Appendix A5.

6.3 Procedure for Evaluating System Well-being State Probabilities Using the Approximate Method

The operating state probabilities can be found using the following steps.

1. Generate the COPT of the scheduled units for the given lead time. This should include the different Capacity In states, the cumulative probability (CP) and the individual probability (IP) associated with each Capacity In state.

2. Subtract the capacity of the largest operating generating unit (CLOU) from the Capacity In states of the COPT. The resulting capacity states represent the system Healthy load level for each Capacity In state.

3. In order to find the HSP for a given system load, add the IP of the Capacity In states corresponding to the Healthy load levels that are greater than or equal to the given system load level.

4. The system At risk probability (UCR) is obtained directly from the cumulative probability of just carrying or failing to carry the given load.

5. The system MSP is obtained by subtracting the sum of the probabilities of Healthy state and the UCR from unity.

6.3.1 Sample Calculation

Table 6.3 shows the Approximate method table for the four scheduled units described in Table 6.1 and a system load of 50 MW.

Table 6.3: Approximate method table for a scheduled capacity of 120 MW at a lead time of 4 hours

Capacity In (CIn) (MW)	CIn–CLOU (MW) (Healthy loads)	Individual Probability (IP)	Cumulative probability (CP)
120	80	9.937126E-01	1
100	60	2.180390E-03	6.287422E-03
80	40	4.094293E-03	4.107032E-03
60	20	8.981014E-06	1.273899E-05
40	0	3.749755E-06	3.757976E-06
20	-20	8.216847E-09	8.221354E-09
0	-40	4.507322E-12	4.507322E-12

In Table 6.3, the CIn, the CP and the IP are obtained from the COPT for the four generating units. Col.2 shows each of the corresponding Healthy load levels attributable to the Capacity In states in col.1. The load is 50 MW and the HSP can be obtained by adding the IP of the 120MW and 100 MW Capacity In states (step number 3). The HSP remains the same for any load level greater than 40 MW and less than or equal to 60 MW.

$$P(h) = \sum P(120) + P(100) \text{ MW In} \qquad (6.13)$$

Or, P (h) = 0.99589299

Equation (6.2) of the Contingency Enumeration and (6.13) of Approximate method are the same. The probability of the At risk state can be obtained directly from column 4 of Table 6.3.

P(r) = 3.757976E-06 =0.00000375

The MSP is given by (6.14)

P (m) = 1-P (h)-P(r) (6.14)

Or, P (m) = 0.00410325

The Approximate method table can be used to calculate the HSP for any loading condition for the given scheduled capacity. Table 6.4 shows the Approximate method table for the 40 MW unit derated state case described in Table 6.2.

Table 6.4. The Approximate method table for the derated state unit case in Table 6.2

Capacity In (CIn) (MW)	CIn –CLOU (MW) (Healthy loads)	Individual Probability (IP)	Cumulative probability (CP)
120	80	9.9371260E-01	1
100	60	3.0903830E-03	6.2874220E-03
80	40	3.1862970E-03	3.1970390E-03
60	20	8.2336920E-06	1.0742300E-05
40	0	2.5031220E-06	2.5086050E-06
20	-20	5.4794000E-09	5.4824050E-09
0	-40	3.0048810E-12	3.0048810E-12

Probability of Health, P(h)= $\sum P(120) + P(100)$ MW In (6.14)

Or, P(h)= 9.9680298E-01=0.99680298

Equation (6.8) and (6.14) are exactly the same and both methods produce the same result.

P(r) = 2.5086050E-06

P(m)= 1-P(h)-P(r) = 3.1945084E-03

6.4 Well-being Analysis of the Wind Integrated RBTS

The application of the Approximate method to find the well-being state probabilities of a test system is demonstrated using the RBTS. The wind speed parameters and the WTG

characteristics are those as described in Section 4.1. The wind integrated RBTS is designated as the RBTSW.

6.4.1 Risk Analysis

The system operating state profile for the RBTS and the RBTSW for a scheduled capacity of 190 MW and a lead time of 4 hours are shown in Figs. 6.3 and 6.4 respectively. Fig 6.3 shows the system state probabilities at various load levels for a scheduled capacity of 190 MW. The load is increased in small steps and the corresponding Healthy, Marginal and, At risk state probabilities are determined using the Approximate approach presented in Section 6.3. The generating unit capacities are discrete in nature and therefore all the available system states in the developed COPT exhibit a discrete profile. The HSP gradually decreases as the load is increased and falls to zero when the system scheduled capacity becomes insufficient to maintain the N-1 criterion. As the load continues to increase, the UCR increases and the MSP decreases. When the load equals the scheduled generation the UCR becomes unity and the MSP falls to zero.

Fig.6.4 shows the system well-being state profile when the 46.8 MW of wind power is added to the existing scheduled capacity. An initial wind speed of 35.5-36.5 km/hr is assumed at hour 4 for the Swift Current wind site. Fig.6.4 shows that the discrete nature of the Healthy and Marginal state probabilities is also muted by adding the multi-state WTG representation to the system COPT.

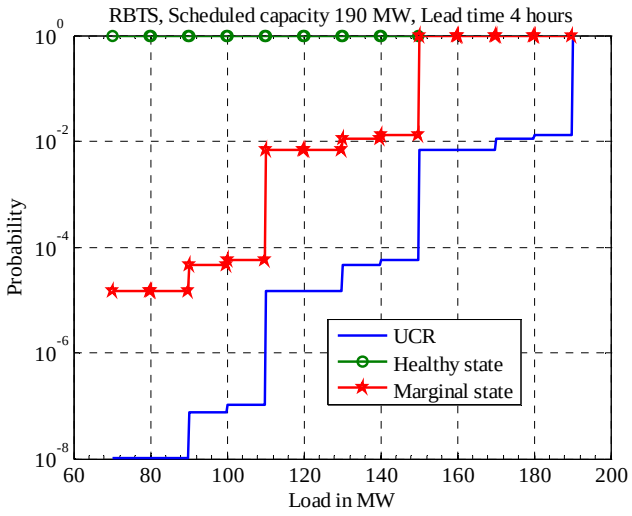

Fig. 6.3: Well-being states of RBTS

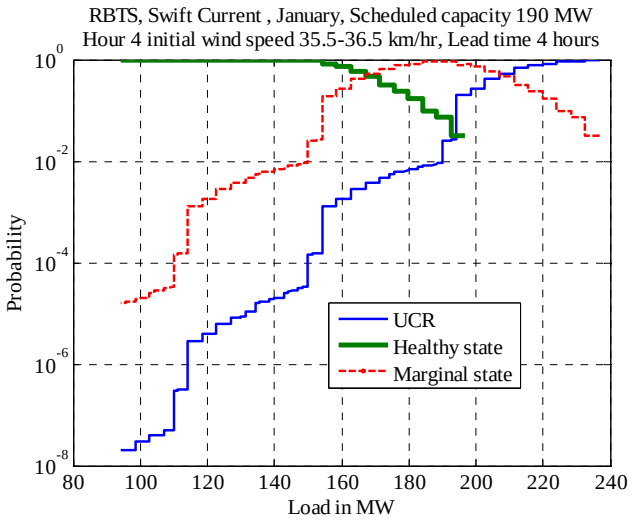

Fig. 6.4: Well-being states of the RBTSW

The system must carry sufficient spinning reserve to cope with the loss of the largest operating unit in the Healthy state. The maximum load (Peak Load) the system can carry in this condition is 150 MW at a scheduled conventional capacity of 190 MW. The HSP is higher than 0.9 and the UCR is less than 0.001 for lead times of 1, 2, 3 and 4 hours at this load level. A decrease in the HSPC does not permit extra load to be carried in this particular case as any load greater than 150 MW would result in a zero HSP and the MSP increases rapidly as the load increases.

6.4.2 Peak Load Carrying Capability (PLCC) of the RBTSW

The PLCC of the RBTSW has been evaluated using both the single and dual risk criterion for a scheduled capacity of 190 MW. The single criterion uses an UCRC of 0.001 while the dual criterion uses a UCRC of 0.001 and a HSPC of 0.9. The PLCC of the RBTSW is calculated for both the low (25.5-26.5 km/hr) and high (35.5-36.5 km/hr) initial wind speeds.

The PLCC of the RBTSW for low and high initial wind speed cases for both reliability criteria are shown in Fig 6.5 and 6.6 for different lead times. Both figures indicate that the PLCC at the single criterion is higher than with the dual criterion. The PLCC is higher for the high

initial wind speed than for the low initial wind speed with both risk criteria. The critical or limiting factor in the dual criterion is obviously the HSPC in these two cases.

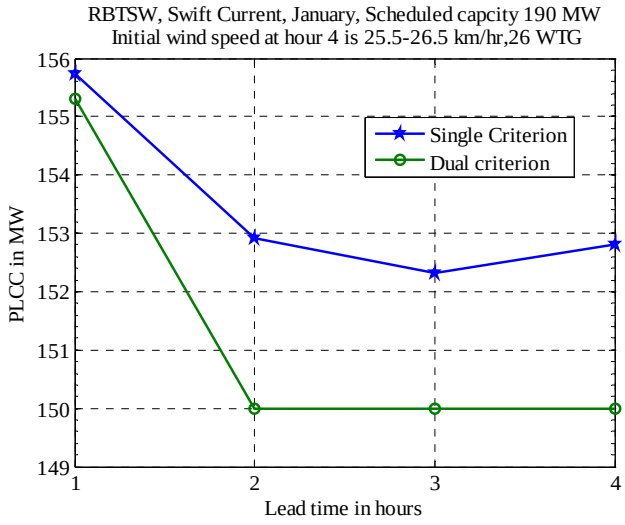

Fig.6.5: PLCC due to low initial wind speed for the RBTSW

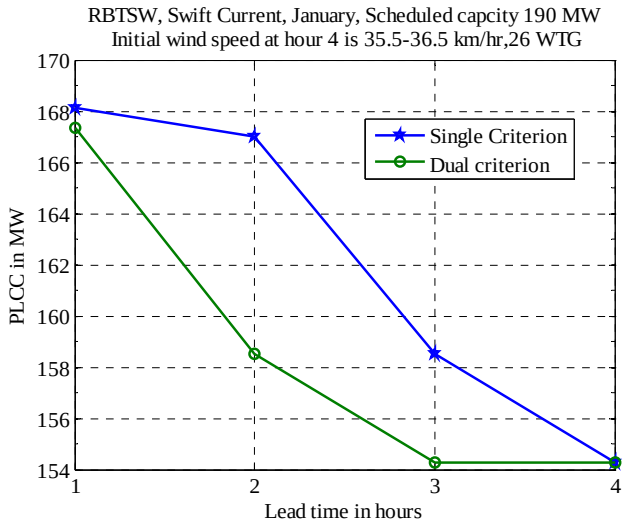

Fig. 6.6: PLCC due to high initial wind speed for the RBTSW

The IPLCC for both the low and high initial wind speed conditions are shown in Figs. 6.7 and 6.8. The IPLCC benefits are essentially zero if the dual criterion is applied in the low wind speed condition, however, the single risk criterion shows some capacity benefit. The IPLCC benefits are greater in the high wind speed condition shown in Fig.6.8 than that shown in Fig. 6.7

for the low wind speed condition. The capacity benefit generally decreases as the lead time increases.

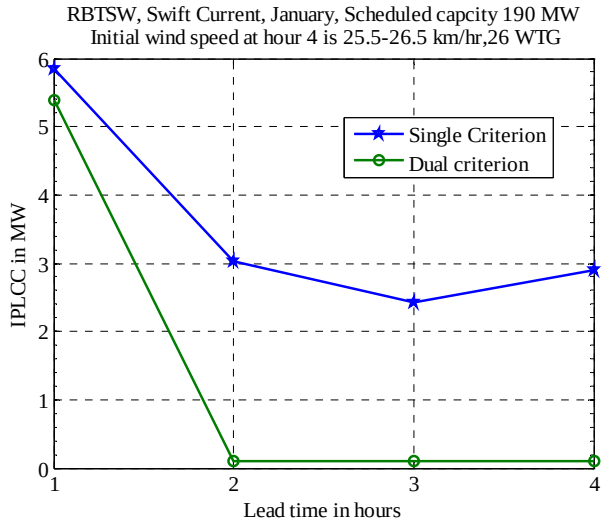

Fig. 6.7: IPLCC due to low initial wind speed for the RBTSW

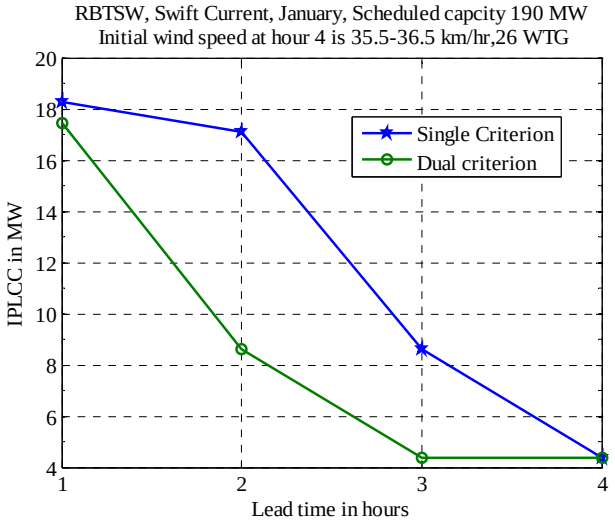

Fig. 6.8: IPLCC due to high initial wind speed for the RBTSW

In order to assess the impact of the risk criteria on the IPLCC, the number of WTG was increased from 26 to 65 with installed capacities of 46.8 MW and 117 MW respectively using the low wind speed condition. The results shown in Fig.6.9 indicate that the IPLCC is highly dependent on the applied reliability criterion as it can be seen that the IPLCC under the dual

criterion are the same for high lead times irrespective of the installed wind farm size. The IPLCC, however, is higher for the larger number of WTG case under the single risk criterion.

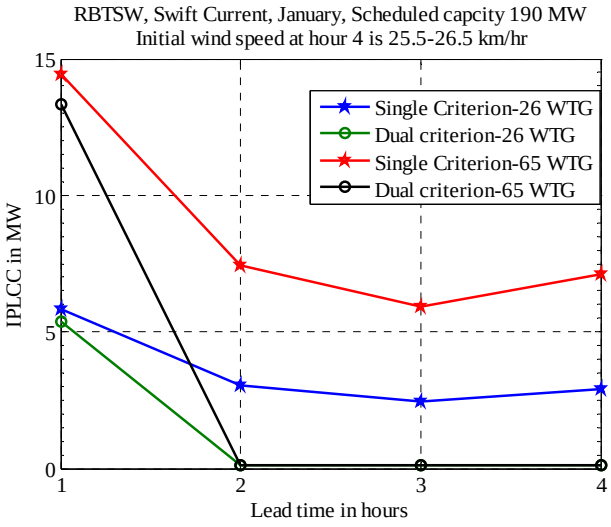

Fig. 6.9: IPLCC with different WTG capacity

Table 6.5 and 6.6 respectively show the system operating state probabilities when 26 WTG and 65 WTG are added to the RBTS at hour 4 with an initial wind speed of 25.5-26.5 km/hr, for different lead times. Table 6.5 shows that the application of the single risk criterion results in a higher PLCC than for the dual risk criterion, but at the expense of the HSP. The HSP are considerably lower and MSP are higher under the single criterion than with the dual criterion. Similar observations are shown in Table 6.6 for the larger wind farm. A comparison between Table 6.5 and 6.6 shows that even though the PLCC for lead times of 2, 3 and 4 hours under the dual risk criterion are the same in both cases, the system HSP are higher when the wind farm capacity is increased. The MSP and the UCR as expected are lower when more WTG are added. At these lead times, the additional WTG are not sufficient to create a change in the PLCC for the given initial wind speed condition but do create a change in the system state probabilities.

Table 6.5. Well-being state probabilities for 190 MW scheduled capacity, 26 WTG

	Single criterion (UCRC 0.001)			
Lead time (hr)	Peak Load (MW)	UCR	HSP	MSP
1	155.74	0.00090582	0.47028197	0.52881221
2	152.92	0.00040908	0.878429999	0.12116092
3	152.33	0.00064001	0.87223428	0.12712571
4	152.81	0.0007202	0.890570105	0.10870973
	Dual criterion (UCRC 0.001 and HSPC 0.9)			
Lead time (hr)	Peak Load (MW)	UCR	HSP	MSP
1	155.30	0.00012392	0.92652554	0.07335054
2	149.99	0.00001252	0.994054946	0.00593254
3	149.99	0.00002853	0.990968249	0.00900322
4	149.99	0.00004907	0.988236449	0.01171448

Table 6.6. 65 WTG, Well-being state probabilities for 190 MW scheduled capacity, 65 WTG

	Single criterion (UCRC 0.001)			
Lead time (hr)	Peak Load (MW)	UCR	HSP	MSP
1	164.34	0.00090582	0.47028197	0.52881221
2	157.31	0.00040594	0.87959813	0.11999593
3	155.81	0.00063327	0.874081457	0.12528528
4	157.01	0.00070576	0.893399933	0.10589430
	Dual criterion (UCRC 0.001 and HSPC 0.9)			
Lead time (hr)	Peak Load (MW)	UCR	HSP	MSP
1	163.24	0.00012392	0.92652554	0.07335054
2	149.99	0.00000811	0.995715292	0.00427659
3	149.99	0.00001988	0.993307522	0.00667259
4	149.99	0.00002971	0.992080294	0.00788999

6.5 PLCC of the IEEE-RTSW

The PLCC of the IEEE-RTSW is shown in Figs. 6.10 and 6.11 for the low and high initial wind speed conditions respectively. A total of 2861 MW from 17 conventional units in the merit order are assumed to be operating. The wind farm is considered to have a total of 370 WTG with a total installed capacity of 666 MW and the Swift Current wind site is considered for the initial hours described in Section 6.4. As with the RBTSW, Figs. 6.10 and 6.11 show that the application of the single risk criterion creates a higher PLCC than the dual risk criterion. The PLCC values are higher when the initial wind speed is high in both figures.

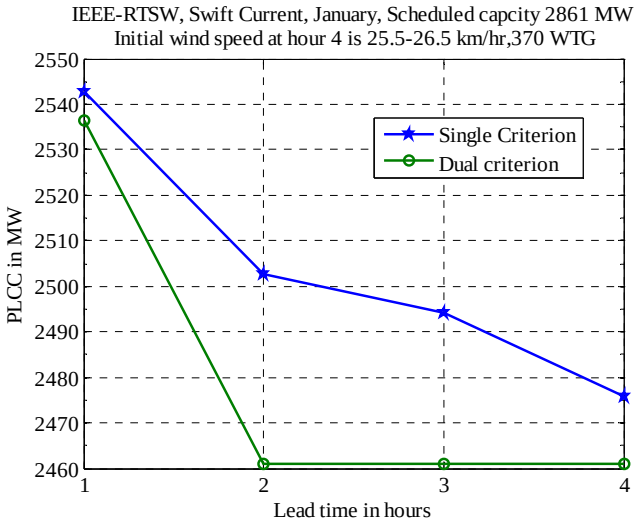

Fig. 6.10: PLCC due to low initial wind speed for the IEEE-RTSW

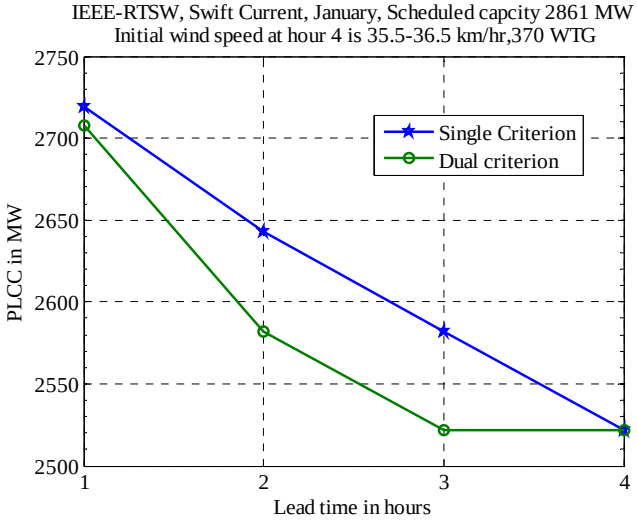

Fig. 6.11: PLCC due to high initial wind speed for the IEEE-RTSW

The IPLCC for the wind integrated IEEE-RTS is presented in Figs. 6.12 and 6.13 for the low and high initial wind speed respectively. The IPLCC are greater under the single risk criterion than with the dual risk criterion in both cases. There is no increase in the PLCC due to added wind power for the low wind speed case at high lead times when the dual risk criterion is adopted. The situation is improved when the initial wind speed changes to a high value, as shown in Fig. 6.13.

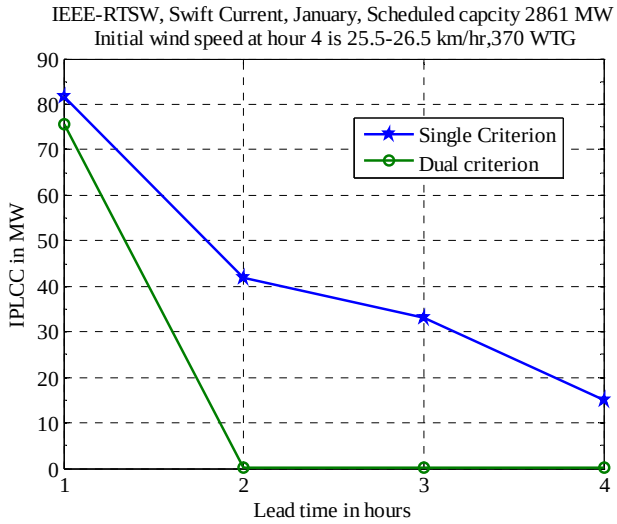

Fig. 6.12: IPLCC due to low initial wind speed for the IEEE-RTSW

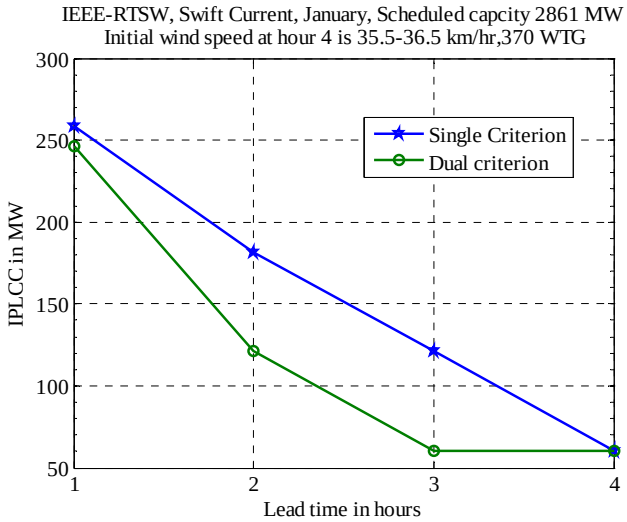

Fig. 6.13: IPLCC due to high initial wind speed for the IEEE-RTSW

6.6 Sensitivity Analysis for the RBTSW

The PLCC performance of the RBTSW under various risk criteria are presented in Figs. 6.14 and 6.15 for the low and high initial wind speed conditions. The probability of the Healthy state is varied from 0.6 to 0.9 keeping the UCRC fixed at 0.001. The figures show that the PLCC of the system decreases as the operating reserve policy is changed from a single to a dual criterion. A UCRC value of 0.001 is adopted for the single risk criterion. The PLCC generally

decreases as the HSPC increases. The system needs a reserve in excess of 40 MW to make any change in the system HSP and the PLCC may remain unchanged when the HSPC is changed by only a small amount. The higher initial wind speed increases the PLCC of the system for all the risk criteria as shown in Fig. 6.15.

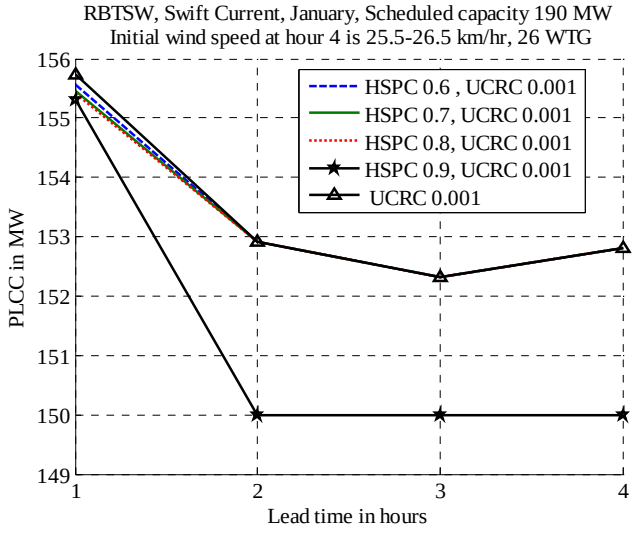

Fig.6.14: PLCC due to low initial wind speed for single and variable dual risk criteria for the RBTSW

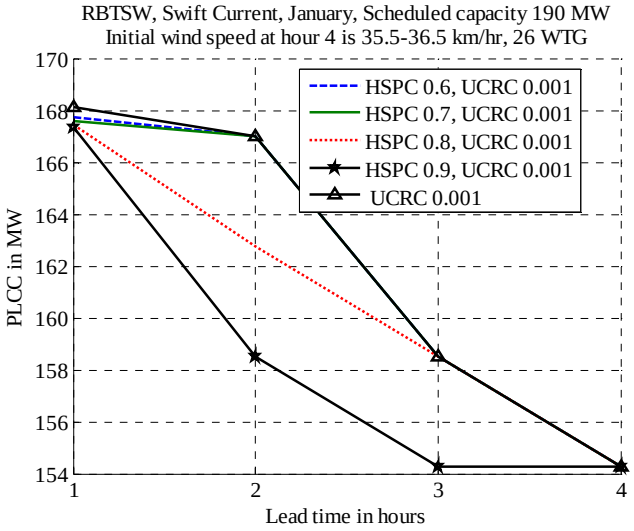

Fig.6.15: PLCC due to high initial wind speed for single and variable dual risk criteria for the RBTSW

The sensitivity of the PLCC to the HSPC is presented in Figs.6.16 and 6.17 for the low and high initial wind speed conditions respectively. The HSPC is changed from 0.6 to 0.9. The PLCC generally decreases with increase in the HSPC and sometimes shows an irregular pattern. Fig. 6.17 shows that the PLCC are higher for the high initial wind speed than the low initial wind speed case shown in Fig. 6.16 for all the given HSPC.

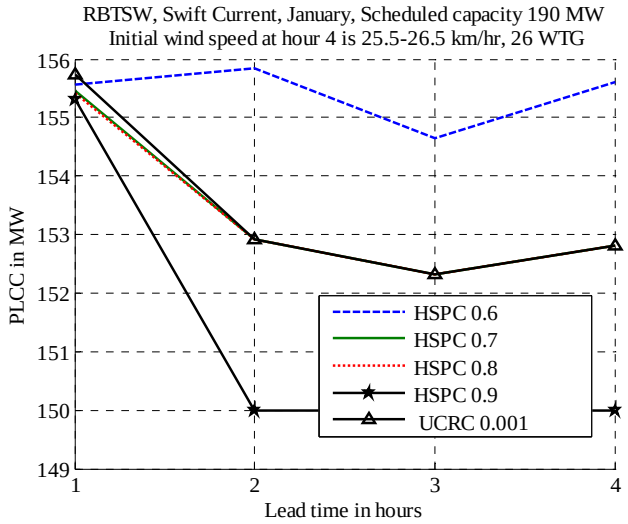

Fig. 6.16: PLCC due to low initial wind speed and single risk criteria for the RBTSW

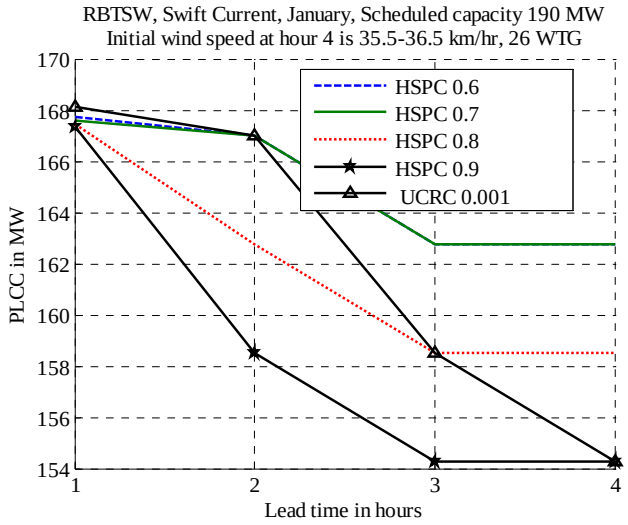

Fig.6.17: PLCC due to high initial wind speed and single risk criteria for the RBTSW

As noted earlier, the IPLCC is the difference in the PLCC of the wind integrated power system to the basic power system without the wind power. The HSP for the RBTS drops to 0 when the load exceeds 150 MW for the 190 MW scheduled capacity. The HSP at the UCRC of 0.001 for the RBTS is greater than 0.9 for lead times of 1- 4 hours.

The IPLCC profiles in Figs. 6.18 and 6.19 are based on a dual criterion that includes a UCRC of 0.001. The UCRC of 0.001 results in a HSP greater than 0.9 in the basic RBTS. The dual risk criterion with a HSPC of 0.9 and a UCRC of 0.001 produces the lowest IPLCC benefits for the dual risk criteria noted in these figures. The HSPC becomes the limiting factor in the RBTSW studies shown in Figs. 16.8 and 6.19. These figures also include the IPLCC profiles for a single UCRC of 0.001. The IPLCC are higher when the initial wind speed is high in Fig. 6.19.

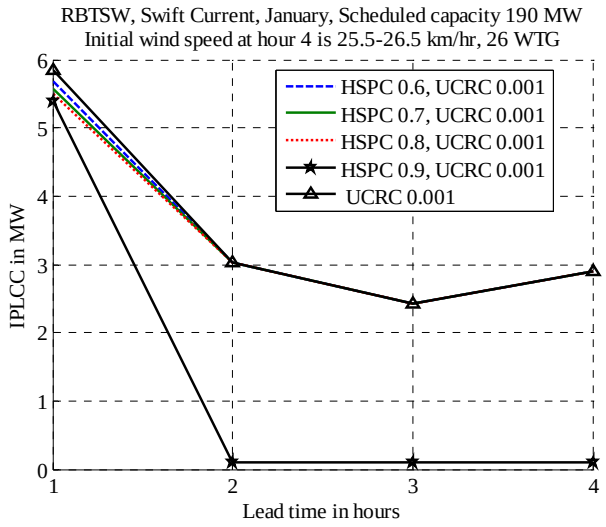

Fig.6.18: IPLCC due to low initial wind speed for the single and variable dual risk criteria for the RBTSW

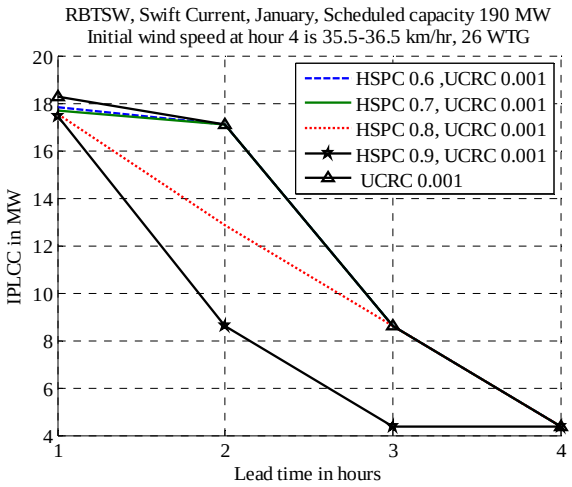

Fig.6.19: IPLCC due to high initial wind speed for the single and variable dual risk criteria for the RBTSW

The IPLCC based on the HSPC shown in Figs.6.20 and 6.21 is based on the PLCC of the conventional units for an UCRC of 0.001. Fig. 6.20 shows that a HSPC of 0.6 gives a higher IPLCC than the UCRC of 0.001. It is worth noting that the dual criterion with a HSPC of 0.6 and a UCRC of 0.001 in Fig. 6.18 produces less IPLCC than a single UCRC of 0.001. A single HSPC of 0.6 does not maintain a minimum UCRC of 0.001 at the low initial wind speed condition shown in Fig. 6.20. The situation changes in Fig. 6.21 where the HSPC of 0.6 and 0.7 produce a higher IPLCC than the single UCRC of 0.001 at higher lead times. The IPLCC benefits obtained at different wind speeds are more sensitive to the HSPC than to the UCRC.

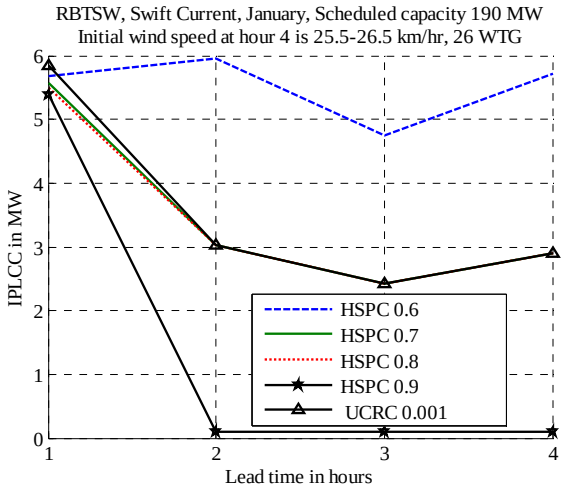

Fig.6.20: IPLCC due to low initial wind speed and a single risk criterion for the RBTSW

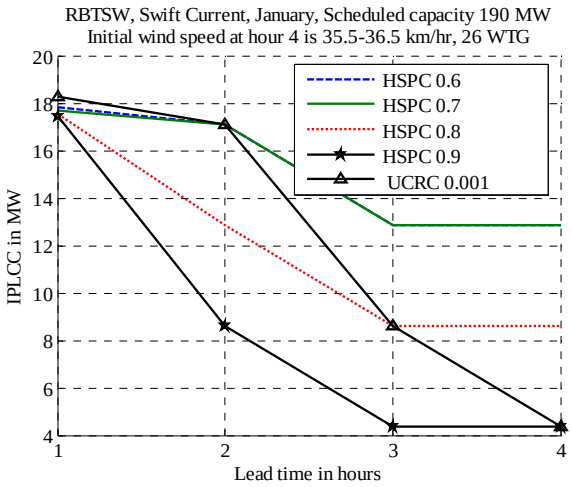

Fig.6.21: IPLCC due to high initial wind speed and a single risk criterion for the RBTSW

6.7 Sensitivity Analysis for the IEEE-RTSW

The PLCC of the IEEE-RTSW for a scheduled conventional capacity of 2861 MW (17 scheduled units) at different risk criteria and at low and high initial wind speeds are presented in Figs. 6.22 and 6.23. In both figures, the dual risk criteria generate lower PLCC than the single criterion. The PLCC decreases as the HSPC is increased. As in Figs. 6.18 and 6.19, Figs. 6.22 and 6.23 include the IPLCC profile for a single UCRC of 0.001.

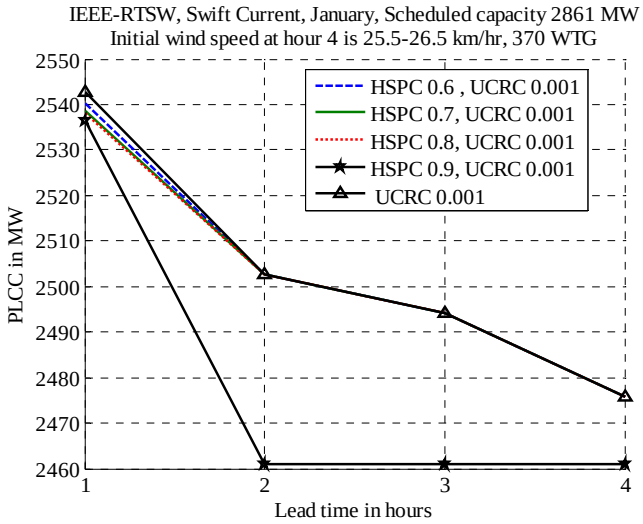

Fig. 6.22: PLCC due to low initial wind speed for the single and variable dual risk criteria for the IEEE-RTSW

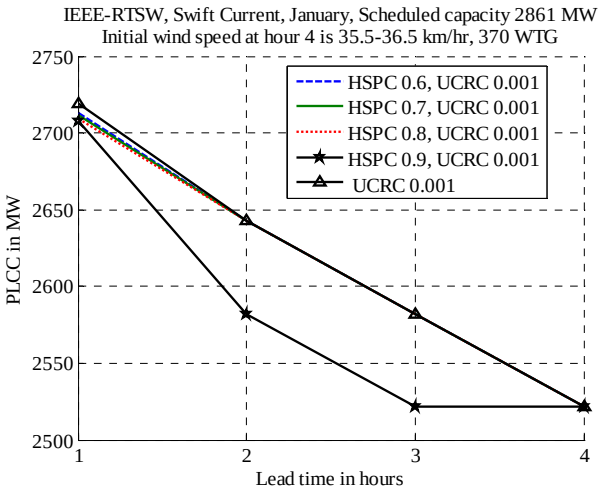

Fig. 6.23: PLCC due to high initial wind speed for the single and variable dual risk criteria for the IEEE-RTSW

The effects on the PLCC for the IEEE-RTSW of using a single HSPC under the low and high initial wind speed conditions are presented in Figs. 6.24 and 6.25. These figures also show the effects of using a single UCRC of 0.001. Lower Health criteria result in significantly higher PLCC than at the UCRC of 0.001. It can be concluded that lower HSPC do not maintain the UCRC of 0.001 and higher HSPC such as 0.9 are required to maintain a minimum UCR of 0.001 for this system under the given conditions. A HSPC may or may not uphold a designated UCRC depending upon the initial wind speed. The PLCC decreases as the HSPC increases.

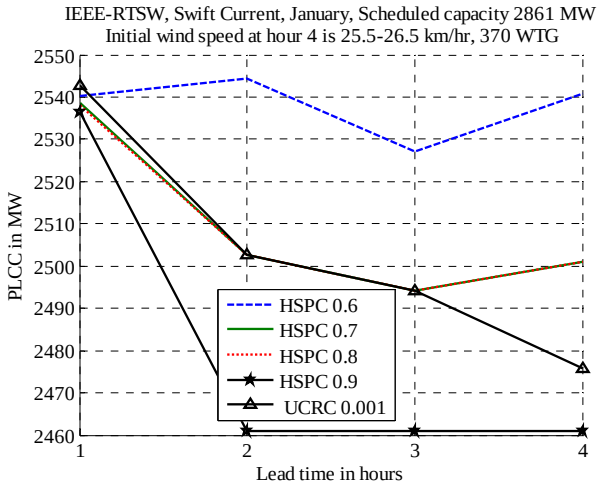

Fig.6.24: PLCC due to low initial wind speed and a single risk criterion for the IEEE-RTSW

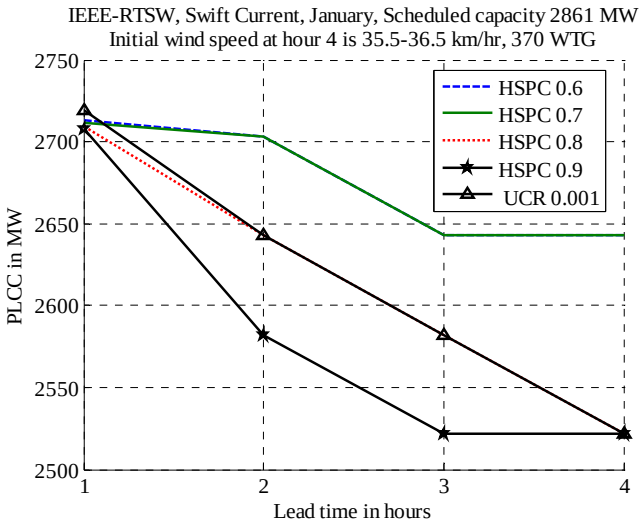

Fig. 6.25: PLCC due to high initial wind speed and a single risk criterion for the IEEE-RTSW

The IPLCC benefits under different risk criteria are compared in Figs. 6.26 and 6.27. Both figures show that the dual risk criteria estimate lower IPLCC than a single UCR criterion. Fig. 6.26 shows that the a dual risk criterion with a HSPC of 0.9 and a UCRC of 0.001 strictly constraints IPLCC at high lead times when the initial wind speed is relatively low. This situation improves when the initial wind speed is relatively high as shown in Fig. 6.27.

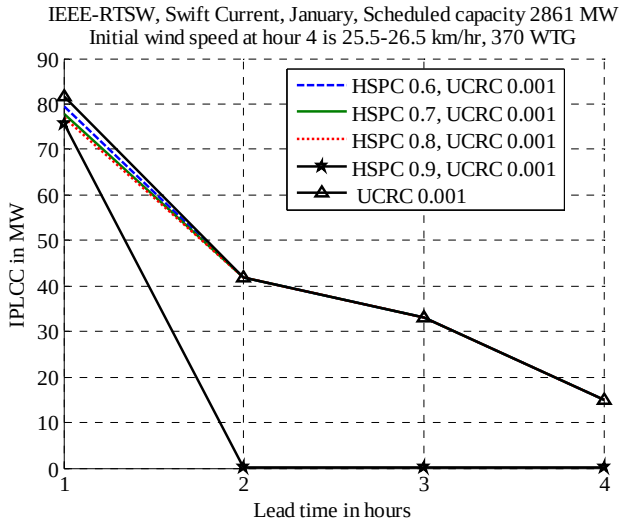

Fig. 6.26: IPLCC due to low initial wind speed for the single and variable dual risk criteria for the IEEE-RTSW

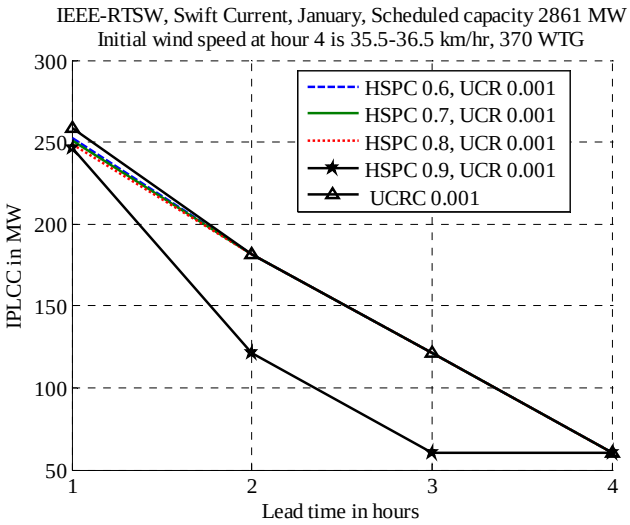

Fig. 6.27: IPLCC due to high initial wind speed for the single and variable dual risk criteria for the IEEE-RTSW

A comparison of the IPLCC when the system HSPC changes from 0.6 to 0.9 with the IPLCC at a UCRC of 0.001 for low and high initial wind speed condition is shown in Figs. 6.28 and 6.29. The IPLCC for relatively low Health criteria such as 0.6 are higher than for a UCRC of 0.001. The observations are similar to that obtained in Figs. 6.20 and 6.21. The IPLCC decreases as the HSPC increases.

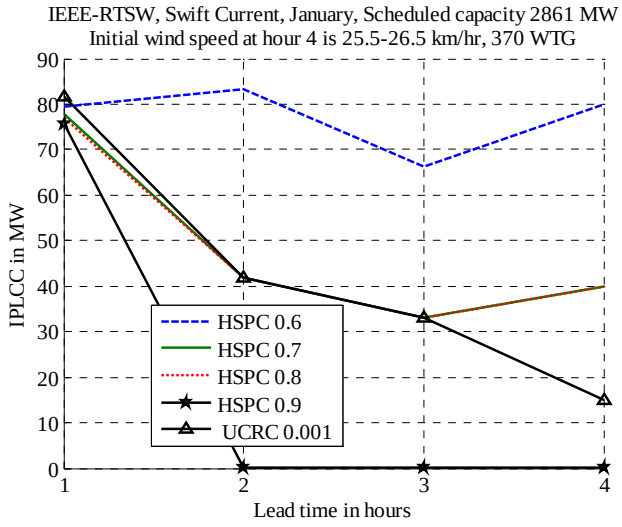

Fig. 6.28: IPLCC due to low initial wind speed and a single risk criterion for the IEEE-RTSW

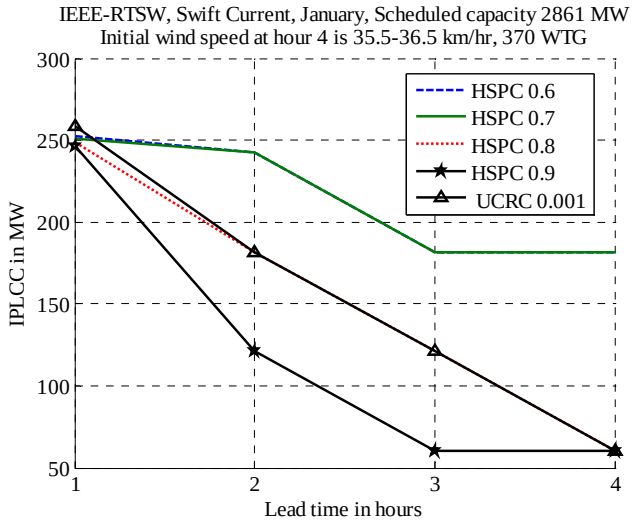

Fig. 6.29: IPLCC due to high initial wind speed and a single risk criterion for the IEEE-RTSW

6.8 Selecting a Unit Commitment Risk Criterion (UCRC)

Power systems differ in size, available generation, operating policy and are generally guided by their own operating philosophies and constraints. The previous studies show that different risk criteria will assign different IPLCC to wind power for a given system lead time. A risk criterion based only on the UCR generally creates very uneven steps in the IPLCC over the lead time and may not provide an acceptable HSP. As illustrated earlier in this chapter, a single risk criterion based only on a low HSPC can give a very optimistic projection of the IPLCC at the expense of very high UCR. The problem was addressed by adopting a dual risk criterion which assigns a HSPC and a UCRC. The required system reserve margins generally increase by adopting a dual risk criterion but this criterion may be too strict to indicate any capacity benefit of the added wind power. Selecting an operating risk criterion is a complex problem. The relationship between the UCRC and the HSPC are examined in this section using three different test systems. The wind speed parameters used in this study are the same as those used in Chapter 4.

6.8.1 RBTS Analysis

The changes in system HSP with change in the UCRC from 0.001 to 0.0001 and from 0.0001 to 0.00001 are presented in Figs.6.34 and 6.35 for the RBTSW with low and high initial wind speed conditions. The system HSP increases significantly when the UCRC is changed from 0.001 to 0.0001 in both the cases but shows relatively less improvement in the HSP when the UCRC changes from 0.0001 to 0.00001.

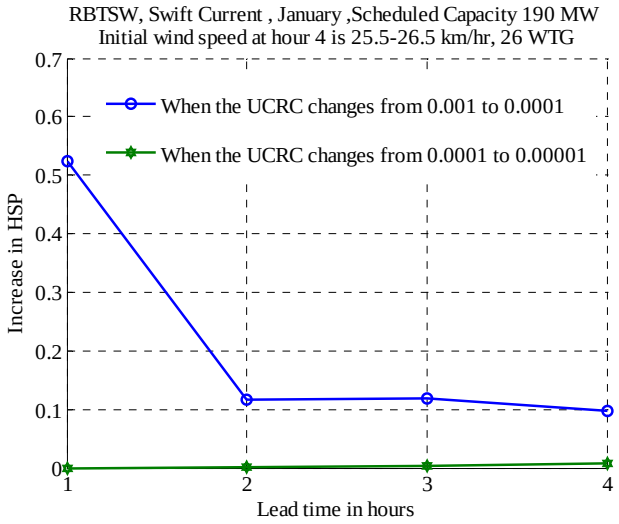

Fig. 6.30: System Health probability improvement at low initial wind speed for the RBTSW

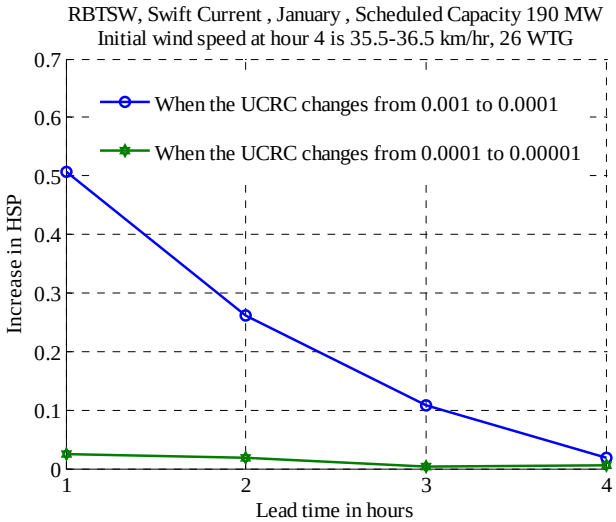

Fig. 6.31: System Health probability improvement at high initial wind speed for the RBTSW

6.8.2 IEEE-RTS Analysis

The changes in the system Health probability with change in the UCRC from 0.001 to 0.0001 and from 0.0001 to 0.00001 are presented in Figs. 6.32 and 6.33 for the IEEE-RTSW with low and high initial wind speed conditions. The system HSP increases significantly when the UCRC changes from 0.001 to 0.0001 in both cases but shows relatively less improvement in the HSP when the UCRC changes from 0.0001 to 0.00001.

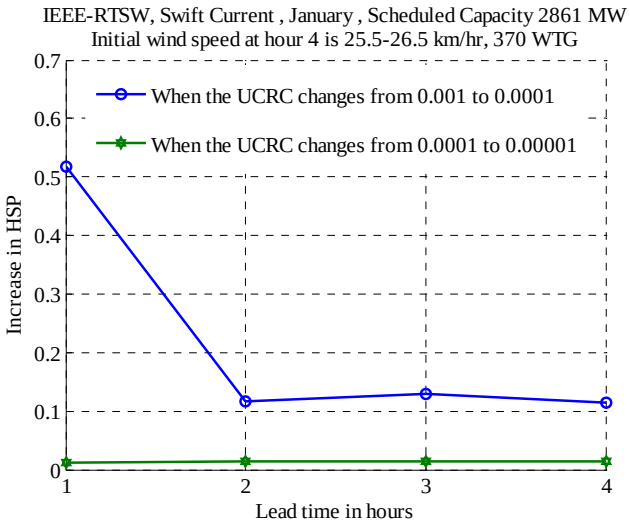

Fig. 6.32: System Health probability improvement at low initial wind speed for the IEEE-RTSW

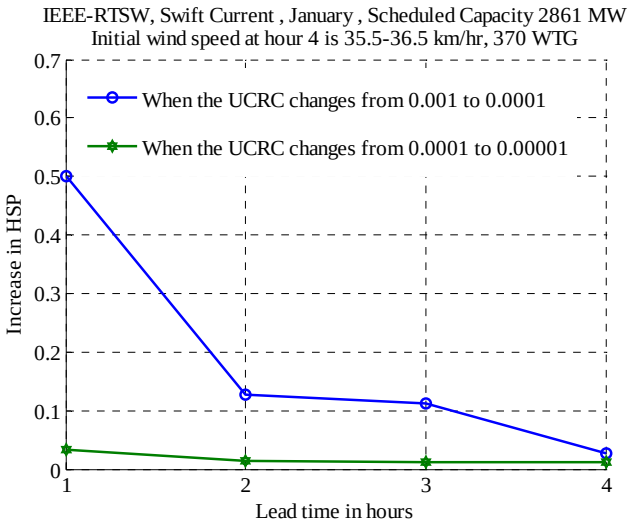

Fig. 6.33: System Health probability improvement at high initial wind speed for the IEEE-RTSW

6.8.3 Modified IEEE-RTS Analysis

The modified IEEE-RTS (IEEE-RTSM) presented in Chapter 4 was created by modifying the 400 MW, 199 MW and 350 MW thermal units in the original IEEE-RTS using the data from the Canadian Electrical Association [141].

Figs. 6.30 and 6.31 show the increases in the HSP when the UCRC changes from 0.001 to 0.0001 and from 0.0001 to 0.00001 under low and high initial wind speed conditions. Both figures show that the gain in the system HSP is relatively high when the UCRC changes from 0.001 to 0.0001. The gain in the HSP is relatively small when the UCRC changes from 0.0001 to 0.00001.

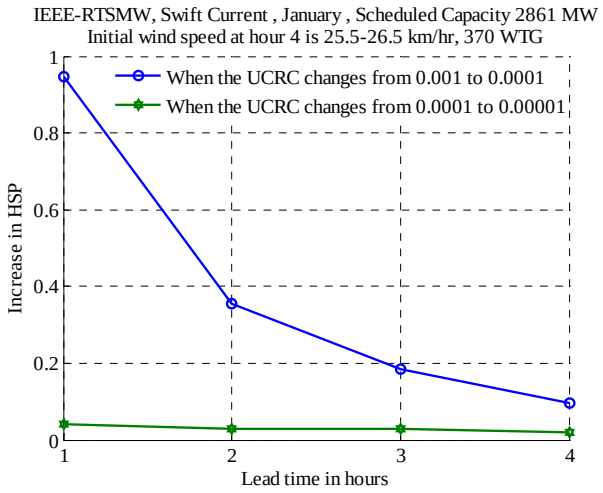

Fig. 6.34: System Health probability improvement at low initial wind speed for the IEEE-RTSMW

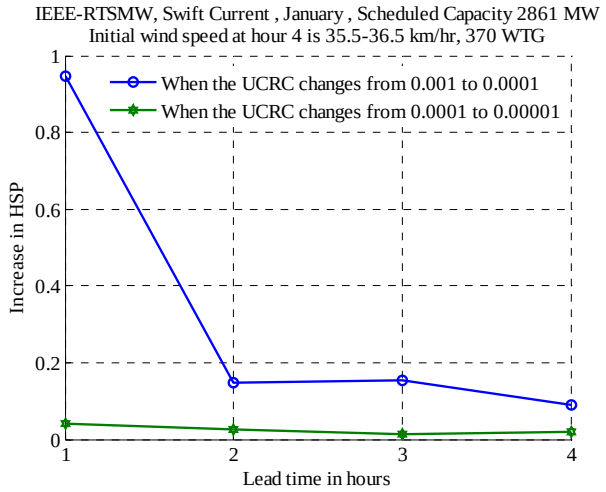

Fig. 6.35: System Health probability improvement at high initial wind speed for the IEEE-RTSMW

As shown in Chapter 4, the PLCC of systems with a UCRC of 0.00001 will be considerably lower than with UCRC of 0.0001 and 0.001. The study results for the RBTSW, IEEE-RTSW and the IEEE-RTSMW show that there are significant changes in the system HSP when the UCRC is changed from 0.001 to 0.0001. The improvements in the HSP are much smaller when the UCRC is changed from 0.0001 to 0.00001. Tables 6.7 and 6.8 illustrate the relative change in the HSP and PLCC for UCRC of 0.001, 0.0001 and 0.00001 under low and high initial wind speed conditions respectively using the IEEE-RTSM.

Table 6.7.Swift Current, IEEE-RTSM, Hour 4 initial wind speed 25.5-26.5 km/hr, 370 WTG, 2864 MW scheduled conventional capacity

	UCRC 0.001			UCRC 0.0001			UCRC 0.00001		
Lead time	PLCC (MW)	UCR	HSP	PLCC (MW)	UCR	HSP	PLCC (MW)	UCR	HSP
1 hr.	2569.4	9.99E-04	0	2487.6	9.95E-05	0.9458	2344.1	9.70E-06	0.9874
2 hrs.	2508.6	9.25E-04	0.6116	2355.6	8.00E-05	0.9661	2252.6	9.99E-06	0.9944
3 hrs.	2466.9	9.90E-04	0.7806	2310.3	9.99E-05	0.9655	2150.1	9.56E-06	0.9954
4 hrs.	2435.9	9.99E-04	0.8810	2276.9	9.99E-05	0.9767	2116.9	9.38E-06	0.9962

Table 6.8. Swift Current, IEEE-RTSM, Hour 4 initial wind speed 35.5-36.5 km/hr, 370 WTG, 2864 MW scheduled conventional capacity

	UCRC 0.001			UCRC 0.0001			UCRC 0.00001		
Lead time	PLCC (MW)	UCR	HSP	PLCC (MW)	UCR	HSP	PLCC (MW)	UCR	HSP
1 hr.	2745.2	9.98E-04	0	2661.4	9.99E-05	0.9468	2518.3	9.69E-06	0.9875
2 hrs.	2632.1	6.83E-04	0.8197	2495.6	9.13E-05	0.9682	2372.1	9.94E-06	0.9953
3 hrs.	2551.1	9.99E-04	0.8267	2385.1	9.02E-05	0.9813	2248.6	9.91E-06	0.9961
4 hrs.	2510.9	9.46E-04	0.8855	2329.2	9.98E-05	0.9754	2177.5	9.88E-06	0.9965

Tables 6.7 and 6.8 show that the HSP could be quite low for a UCRC of 0.001. The PLCC of the system decreases over the lead time and the corresponding HSP generally increases due to increased spinning reserve in the system. The HSP changes significantly when the UCRC is changed from 0.001 to 0.0001. The change in the HSP is relatively small when the UCRC changes from 0.0001 to 0.00001. The PLCC decreases considerably as the UCRC decreases. The results shown in Table 6.7 and 6.8 are for a representative case using the IEEE-RTSM and similar results can be obtained for the RBTS and the IEEE-RTS. The general observations made from the study results in Tables 6.7 and 6.8 based on the IEEE-RTSM will be similar for both the RBTS and the IEEE-RTS. The actual PLCC and the HSP values, however, will depend on the scheduled capacity, the UCRC adopted and the lead times.

6.9 Conclusion

An Approximate method for evaluating the well-being state probabilities is presented in this chapter and the results are compared with those from an established method. It is observed that the Approximate method provides reasonably accurate results in significantly less time. The method is applied in the system studies described in this chapter.

The Unit Commitment Risk, as suggested in the PJM method, is a single value risk index and does not directly indicate the system spinning reserve margins. It does not directly consider the generally adopted deterministic criterion used in system operation which assumes that a system should have at least enough spinning reserve to cope with the loss of the largest operating unit. Well-being analysis incorporates this deterministic criterion in a probabilistic domain and can be used to evaluate the system operating state risks. Well-being analysis of wind integrated RBTS and IEEE-RTS are presented in this chapter. The PLCC and IPLCC are determined and illustrated for two different initial wind speed conditions. The analyses are conducted using two different risk criteria designated as single risk and dual risk criteria. The UCRC and HSPC were applied individually as a single criterion and combined to form a dual risk criterion. A single risk criterion in a general sense usually provides higher PLCC than the application of a similar dual criterion. The dual criterion approach , however, takes full advantage of the ability to incorporate an accepted deterministic criterion such as N-1 in the PLCC and IPLCC evaluation process.

The studies presented clearly illustrate the effects of having higher initial wind speeds on the PLCC and IPLCC of wind integrated power systems. The studies also show that having additional wind capacity by increasing the number of WTG does not create a significant increase in the IPLCC due to the added wind power at the low initial wind speed using a dual risk criterion.

The PLCC and the IPLCC due to added generating capacity are very dependent on the magnitude of the acceptable UCR and HSP. This is illustrated in the studies shown in this chapter using single risk and dual risk criterion.

A sensitivity study of the HSP arising from different UCRC values was conducted for the RBTS, IEEE-RTS and IEEE-RTSM. The studies show that in all of these test systems, the HSP does not improve significantly when the UCRC is decreased from 0.0001 to 0.00001 and the decrease in PLCC is relatively high. The increase in the HSP when the UCRC is decreased from 0.001 to 0.0001 is considerable, especially when the lead times are short. It is therefore, suggested that a UCR value should be used that gives the maximum benefit in terms of the system HSP without severely compromising the PLCC. This is a general comment based on the

studies conducted in the three test systems and should be investigated by further work in this area using the concepts introduced in this research. The actual selection of numerical risk indices is, however, in the end a management decision.

7. INTERCONNECTED SYSTEM RISK ANALYSIS

7.1 Introduction

Most electric power systems operate as interconnected systems, as interconnections can increase both the system adequacy and the security [16, 17, 148-151]. System interconnections also permit the participating companies to export/ import electrical energy for mutual benefit. The load patterns in one system can be quite different than those in another system due to geographical location and consumer life style. Interconnection allows one system to assist another system and each area can operate with less spinning reserve than would be required for isolated operation [16]. The actual assistance received through an interconnection is limited by the tie-line capacity and is governed by the agreement between the participating organizations [17, 69, 72]. In an interconnected system study, the system which exports power to another system is designated as the assisting system and the system which receives power as the assisted system.

The above noted literature is focused on the benefits of interconnection in conventional power system structures where there is no wind power. The integration of large scale wind power in power systems is taking place rapidly throughout the world due to environmental issues. As discussed earlier, the wind is uncertain, intermittent, variable and site specific and these conditions need to be incorporated in interconnected system reliability studies of wind integrated systems.

This chapter describes a series of studies conducted using a probabilistic technique to evaluate the risk benefits in wind integrated interconnected power systems. The studies use the

wind speed data for the Swift Current wind site, consider two different initial wind speeds and apply the concepts illustrated in the previous chapters (Chapter 3 and 4) to the RBTS and the IEEE-RTS to assess the risk benefits associated with interconnection. The initial wind speeds of 25.5-26.5 km/hr and 35.5-36.5 km/hr in the month of January at hour 4 are considered as low and high initial wind speeds respectively. The WTG characteristics are the same as those described in Chapter 4. Wind capacities of 46.8 MW and 666 MW are added in the RBTS and IEEE-RTS studies respectively.

7.2 The Assistance Model

The capacity assistance available in one system to assist an interconnected system can be described by a capacity assistance model in the form of a multi-state capacity table that describes the capacity available to the assisted system. The capacity assistance model concept [1] is illustrated in the following discussion using two RBTS designated as System A and System B. System A is considered to be the assisting system and System B is the assisted system. The scheduled capacity in System A is assumed to be 190 MW and a system lead time of 4 hours is used. The Capacity Outage Probability Table (COPT) for System A using the algorithm presented in [1] is shown in Table 7.1.

Table 7.1: COPT of 7 scheduled units in the RBTS merit order for a lead time of 4 hours

Capacity In (MW)	Cumulative Probability (CP)	Individual Probability (IP)
190	1	9.869217E-01
180	1.307835E-02	1.805895E-03
170.0	1.127246E-02	4.423891E-03
160.0	6.848565E-03	8.094590E-06
150.0	6.840471E-03	6.782592E-03
140.0	5.787871E-05	1.241096E-05
130.0	4.546775E-05	3.037826E-05
120.0	1.508950E-05	5.558650E-08
110.0	1.503391E-05	1.492934E-05
100.0	1.045660E-07	2.731810E-08
90.0	7.724794E-08	6.675059E-08
80.0	1.049735E-08	1.221423E-10
70.0	1.037521E-08	1.031035E-08

System A is assumed to have a load of 150 MW. At this level, the maximum available assistance to System B is 40 MW. The probability of having this level of assistance is 9.869217E-01 in Table 7.1. The probability of having no assistance from System A is the cumulative probability associated with the 150 MW Capacity In level in Table 7.1. The other levels of assistance are shown in Table 7.2. The assistance model represents an additional 40 MW multi-state generating unit that is available to the assisted system.

Table 7.2: Assistance model of System A to B

Capacity In (MW)	Individual probability (IP)
0	6.840471E-03
10	8.094590E-06
20	4.423891E-03
30	1.805895E-03
40	9.869217E-01
	Sum= 1.0

The capacity assistance model shown in Table 7.2 is then convolved with the COPT of the assisted system (System B) and a new COPT is generated. The new COPT is used to determine the UCR values at different load levels in System B.

7.3 Application to Two Interconnected RBTS

The assistance model concept described in the previous section is utilized to evaluate the UCR in a single RBTS and two interconnected RBTS under a series of different conditions. In these studies, System A is considered to be assisting System B and the main focus is on the reliability benefits to System B. Similar studies could be conducted on System A. The load in System A is considered to be 120 MW and System A is operating at a UCRC of 0.001. The scheduled capacity in System A under this criterion and load level is 180 MW. The interconnected UCR (IUCR) in System B when it is connected with System A is shown in col.5 of Table 7.3. The UCR values are significantly lower when System B is operating in an interconnected mode than when it is operating in an isolated mode for the same load level due to the potential assistance available to System B from System A.

Table 7.3: System B risk in isolated and interconnected modes

		Isolated System B (Scheduled capacity 190 MW) Conventional units only		Interconnected System B Conventional units only
Lead time (col.1)	UCRC (col.2)	PLCC in MW (col.3)	UCR (col.4)	IUCR (col.5)
1 hour	0.001	149.9	3.631173E-06	1.778725E-09
	0.0001	149.9	3.631173E-06	1.778725E-09
	0.00001	149.9	3.631173E-06	1.778725E-09
2 hours	0.001	149.9	1.450633E-05	1.432078E-08
	0.0001	149.9	1.450633E-05	1.432078E-08
	0.00001	129.9	3.762750E-06	9.443481E-11
3 hours	0.001	149.9	3.259799E-05	4.863762E-08
	0.0001	149.9	3.259799E-05	4.863762E-08
	0.00001	129.9	8.477038E-06	4.774917E-10
4 hours	0.001	149.9	5.787871E-05	1.160072E-07
	0.0001	149.9	5.787871E-05	1.160072E-07
	0.00001	109.9	1.045660E-07	7.651729E-11

A series of studies involving the addition of wind power to Systems A and B is illustrated in the following sections. In these studies Systems A and B are the RBTS with no wind power. Systems AW and BW are the RBTS with 46.8 MW of added wind power.

Case 1: System A interconnected with System BW

Table 7.4 shows a case study when System A does not have wind power and System B has wind power. For clarity in analysis, Table 7.3 (col.1 through col.5) is also embedded in Table 7.4. In addition, Col.5 shows the IUCR of System B when both systems have only conventional generating units. The UCR of isolated System BW when carrying the PLCC shown in col. 3 at a low initial wind speed is shown in col.6. The IUCR when System BW at low initial wind speed is interconnected with System A is shown in col.7. The UCR decreases due to interconnection. The risk decreases are virtually nil for a short lead time such as 1 hour. The UCR of isolated

System BW for the load levels shown in col.3 are shown in col.8 for high initial wind speed and the IUCR are shown in col.9. A comparison of the IUCR shown in col.5,7 and 9 shows that the IUCR decreases by virtue of System BW having wind. The decrease in IUCR, however, depends on the lead time. Generally, the decreases in IUCR are small when the lead times are short.

Table 7.4: Risk in Systems B and BW due to interconnection with System A

		Isol. Syst. B (SC 190 MW) Conventional units only		Inter. Syst. B Convent-ional units only	Isol. Syst. BW (LIWS)	Syst. BW Inter. with Syst. A (LIWS)	Isol. Syst. BW. (HIWS)	Syst. BW Inter. with Syst. A (HIWS)
Lead time (col.1)	UCRC (col.2)	PLCC in MW (col.3)	UCR (col.4)	IUCR (col.5)	UCR (col.6)	IUCR (col.7)	UCR (col.8)	IUCR (col.9)
1 hour	0.001	149.9	3.631173 E-06	1.778725 E-09	3.631173 E-06	1.778725 E-09	2.850841 E-06	1.774053 E-09
	0.0001	149.9	3.631173 E-06	1.778725 E-09	3.631173 E-06	1.778725 E-09	2.850841 E-06	1.774053 E-09
	0.00001	149.9	3.631173 E-06	1.778725 E-09	3.631173 E-06	1.778725 E-09	2.850841 E-06	1.774053 E-09
2 hours	0.001	149.9	1.450633 E-05	1.432078 E-08	1.251897 E-05	1.269910 E-08	6.866449 E-06	5.892030 E-09
	0.0001	149.9	1.450633 E-05	1.432078 E-08	1.251897 E-05	1.269910 E-08	6.866449 E-06	5.892030 E-09
	0.00001	129.9	3.762750 E-06	9.443481 E-11	3.338431 E-06	8.124052 E-11	1.546063 E-06	3.727469 E-11
3 hours	0.001	149.9	3.259799 E-05	4.863762 E-08	2.852775 E-05	4.280775 E-08	1.909278 E-05	2.677887 E-08
	0.0001	149.9	3.259799 E-05	4.863762 E-08	2.852775 E-05	4.280775 E-08	1.909278 E-05	2.677887 E-08
	0.00001	129.9	8.477038 E-06	4.774917 E-10	7.463373 E-06	4.120843 E-10	4.664613 E-06	2.523406 E-10
4 hours	0.001	149.9	5.787871 E-05	1.160072 E-07	4.906892 E-05	1.011602 E-07	3.341906 E-05	6.206519 E-08
	0.0001	149.9	5.787871 E-05	1.160072 E-07	4.906892 E-05	1.011602 E-07	3.341906 E-05	6.206519 E-08
	0.00001	109.9	1.045660 E-07	7.651729 E-11	8.534808 E-08	6.633014 E-11	5.244497 E-08	4.051047 E-11

The following abbreviations are used in Table 7.4 and in subsequent tables in this section.

Syst. - System
Isol. –Isolated
Inter. - Interconnected
SC- Scheduled Capacity
LIWS- Low initial wind speed
HIWS- High initial wind speed

Case 2: System AW interconnected with System B

Table 7.5 shows the risk values in System A when it has added wind power. Many electric power utilities and particularly those with relatively small wind power penetrations consider WTG as energy sources rather than power sources. This situation is expected to change as wind power penetration increases. It is therefore important to consider the implications in interconnected system risk analysis of including wind power in the assistance provided from an interconnected system. Two conditions are investigated, one when System AW does not consider its wind power as having any capacity value and another when System AW considers the wind of capacity value. When System AW does not consider its wind as a power source, it needs to commit 180 MW of conventional generation to meet the load of 120 MW at a UCRC of 0.001 as discussed earlier. When System AW considers its wind to have capacity value, it will commit only 160 MW of conventional generating capacity to meet a load of 120 MW at a UCRC of 0.001. The UCR values shown in col.7 and 8 are therefore greater than those shown in col.5 and 6 respectively.

Table 7.5: Risk in isolated System A for no wind, low wind and high wind conditions

				System AW does not consider its wind power of any capacity value (Scheduled capacity 180 MW)		System AW considers its wind power of capacity value (Scheduled capacity 160 MW)	
			Isol. Syst. A (SC180 MW) Conventional units only	Isol. Syst.AW (LIWS)	Isol. Syst.AW (HIWS)	Isol. Syst.AW (LIWS)	Isol. Syst.AW (HIWS)
Lead time (col.1)	UCRC (col.2)	Load level in MW (col.3)	UCR (col.4)	UCR (col.5)	UCR (col.6)	UCR (col.7)	UCR (col.8)
1 hour	0.001	120	2.850841E-06	9.386043E-07	9.386043E-07	1.875049E-06	1.875049E-06
2 hours	0.001	120	1.139121E-05	4.220779E-06	1.606584E-06	4.036834E-04	3.283679E-05
3 hours	0.001	120	2.560290E-05	9.498497E-06	4.936275E-06	6.278863E-04	9.624571E-05
4 hours	0.001	120	4.546775E-05	1.613804E-05	8.539943E-06	6.989043E-04	1.334178E-04

The assistance model added to System B is not the same for the two conditions noted in Table 7.5. These two conditions create different risk levels in System B and are shown in Table 7.6. The IUCR of System B when System AW does not consider its wind of any capacity value are shown in col. 6 and 7 respectively for the low and high initial wind speed conditions. The IUCR when System AW does consider wind of capacity value are shown in col. 8 and 9. The IUCR in System B are higher when System AW considers its wind of capacity value than when System AW does not consider its wind of capacity value as shown in Table 7.5. The increase in IUCR is due to the lower assistance available to System B as System AW only schedules 160 MW of capacity to serve the 120 MW load.

Table 7.6: Risk in System B risk when System AW is interconnected with System B

		Both system have conventional units only			System AW does not consider its wind power of any capacity value		System AW considers its wind power of capacity value	
		Isol. Syst. B (SC 190 MW) Conventional units only		Inter. Syst.B Convent-ional units only	Syst. B Inter. with Syst. AW (LIWS)	Syst. B Inter. with Syst. AW (HIWS)	Syst. B Inter. with Syst. AW (LIWS)	Syst. B Inter. with Syst. AW (HIWS)
Lead time (col.1)	UCRC (col.2)	PLCC in MW (col.3)	UCR (col.4)	IUCR (col.5)	IUCR (col. 6)	IUCR (col.7)	IUCR (col.8)	IUCR (col.9)
1 hour	0.001	149.9	3.631173 E-06	1.778725 E-09	1.778726 E-09	1.774787 E-09	8.362206 E-09	6.600618 E-09
	0.0001	149.9	3.631173 E-06	1.778725 E-09	1.778726 E-09	1.774787 E-09	8.362206 E-09	6.600618 E-09
	0.00001	149.9	3.631173 E-06	1.778725 E-09	1.778726 E-09	1.774787 E-09	8.362206 E-09	6.600618 E-09
2 hours	0.001	149.9	1.450633 E-05	1.432078 E-08	1.270587 E-08	5.914478 E-09	5.738717 E-08	3.023576 E-08
	0.0001	149.9	1.450633 E-05	1.432078 E-08	1.270587 E-08	5.914478 E-09	5.738717 E-08	3.023576 E-08
	0.00001	129.9	3.762750 E-06	9.443481 E-11	8.263613 E-11	4.398453 E-11	1.258222 E-08	5.839393 E-09
3 hours	0.001	149.9	3.259799 E-05	4.863762 E-08	4.284155 E-08	2.687274 E-08	1.957746 E-07	1.282023 E-07
	0.0001	149.9	3.259799 E-05	4.863762 E-08	4.284155 E-08	2.687274 E-08	1.957746 E-07	1.282023 E-07
	0.00001	129.9	8.477038 E-06	4.774917 E-10	4.206513 E-10	2.793125 E-10	4.220767 E-08	2.642115 E-08
4 hours	0.001	149.9	5.787871 E-05	1.160072 E-07	1.012790 E-07	6.236744 E-08	4.488843 E-07	2.986091 E-07
	0.0001	149.9	5.787871 E-05	1.160072 E-07	1.012790 E-07	6.236744 E-08	4.488843 E-07	2.986091 E-07
	0.00001	109.9	1.045660 E-07	7.651729 E-11	6.658901 E-11	4.115006 E-11	6.550198 E-10	4.012802 E-10

Case 3: System AW interconnected with System BW

In this case, both Systems AW and BW have 46.8 MW of installed wind capacity. The assistance model again depends on whether System AW considers the available wind power to have any capacity value or not. It was noted earlier in connection with Table 7.5 that the assistance model changes as the scheduled capacity changes in System AW for each case. System AW schedules 180 MW when it does not consider the available wind power to have capacity value and schedules 160 MW if it considers the available wind power to have capacity value. Based on the scheduled capacities shown in Table 7.5, the IUCR for System BW is shown in Table 7.7. Col.6 and 7 show the IUCR in System BW when System AW does not consider its wind power to have capacity value and col.8 and 9 when System AW considers its wind power to have capacity value. The IUCR in System BW are higher when the assisting system considers wind power has capacity value than when it does not. The IUCR are lower when the initial wind speed increases to a high value in both situations. The IUCR shown in Table 7.7 are lower than those shown in Table 7.6 as both systems have wind power in the latter case.

Case 4: Minimum Assistance Model with System AW and System B

The system load varies continuously with time. The load in System AW is assumed to be 120 MW in the previous studies in this chapter. The capacity assistance model for a given level of scheduled capacity depends on the load level in the assisting system and will also vary with time. It is possible to establish a minimum assistance model that can be used for a range of load levels in the assisting system for a given level of scheduled capacity. The minimum assistance level is determined by the UCRC in the assisting system. The maximum load that System A with a scheduled capacity of 180 MW can carry at a UCRC of 0.001 and a lead time of 1-4 hours is 139.9 MW. The minimum capacity assistance model for this scheduled capacity level is determined based on the 139.9 MW value. The actual available assistance will increase as the load decreases. Two conditions are investigated, one when System AW considers its wind to have capacity value and another when System AW does not consider its wind to have capacity value. The UCR when AW does not consider wind has capacity value is shown in col. 5 and 6 in Table 7.8. The UCR are lower when the initial wind speed is high. When System AW considers

Table 7.7: Risk in System BW when System AW and BW are interconnected

		Both system have conventional units only			System AW does not consider its wind power of any capacity value		System AW considers its wind power of capacity value	
		Isol. Syst. B (SC 190 MW) Conventional units only		Inter. Syst. B convent-ional units only	Syst. BW Inter. with Syst. AW (LIWS)	Syst. BW Inter. with Syst. AW (HIWS)	Syst. BW Inter. with Syst. AW (LIWS)	Syst. BW Inter. with Syst. AW (HIWS)
Lead time (col.1)	UCRC (col.2)	PLCC in MW (col.3)	UCR (col.4)	IUCR (col.5)	IUCR (col. 6)	IUCR (col.7)	IUCR (col.8)	IUCR (col.9)
1 hour	0.001	149.9	3.631173 E-06	1.778725 E-09	1.774786 E-09	6.896488 E-12	6.600613 E-09	1.771298 E-09
	0.0001	149.9	3.631173 E-06	1.778725 E-09	1.774786 E-09	6.896488 E-12	6.600613 E-09	1.771298 E-09
	0.00001	149.9	3.631173 E-06	1.778725 E-09	1.774786 E-09	6.896488 E-12	6.600613 E-09	1.771298 E-09
2 hours	0.001	149.9	1.450633 E-05	1.432078 E-08	8.488970 E-09	3.894899 E-10	3.987169 E-08	6.112267 E-09
	0.0001	149.9	1.450633 E-05	1.432078 E-08	8.488970 E-09	3.894899 E-10	3.987169 E-08	6.112267 E-09
	0.00001	129.9	3.762750 E-06	9.443481 E-11	5.707472 E-11	6.935429 E-12	8.398725 E-09	3.674156 E-10
3 hours	0.001	149.9	3.259799 E-05	4.863762 E-08	3.176621 E-08	5.431910 E-09	1.475862 E-07	4.212511 E-08
	0.0001	149.9	3.259799 E-05	4.863762 E-08	3.176621 E-08	5.431910 E-09	1.475862 E-07	4.212511 E-08
	0.00001	129.9	8.477038 E-06	4.774917 E-10	3.145806 E-10	7.946215 E-11	3.127174 E-08	5.245649 E-09
4 hours	0.001	149.9	5.787871 E-05	1.160072 E-07	6.962026 E-08	1.599859 E-08	3.125059 E-07	1.100557 E-07
	0.0001	149.9	5.787871 E-05	1.160072 E-07	6.962026 E-08	1.599859 E-08	3.125059 E-07	1.100557 E-07
	0.00001	109.9	1.045660 E-07	7.651729 E-11	4.560790 E-11	1.062418 E-11	4.254604 E-10	1.186220 E-10

wind power of capacity value the scheduled capacities are recalculated and adjusted. Col.7 shows that the scheduled capacity remains constant at 180 MW for all the four lead times in the low initial wind speed case. The scheduled capacity, however, is only 160 MW for lead times of

1 and 2 hours and increases to 180 MW for lead times of 3 and 4 hours as shown in col. 8 for the high initial wind speed case.

Table 7.8: UCR in System A at the criterion load level

				System AW does not consider its wind power of any capacity value (Scheduled capacity 180 MW)		System AW considers its wind power of capacity value	
			Isol. Syst. A (SC180 MW) conventional units only	Isol. Syst. AW (LIWS)	Isol. Syst. AW (HIWS)	Isol. Syst. AW (LIWS)	Isol. Syst. AW (HIWS)
Lead time (col.1)	UCRC (col.2)	Load level (col.3)	UCR (col.4)	UCR (col.5)	UCR (col.6)	UCR (col.7)	UCR (col.8)
1 hour	0.001	139.9	2.850841E-06	2.850841E-06	9.386043E-07	2.850841E-06 (Scheduled 180 MW)	1.875049E-06 (Scheduled 160 MW)
2 hours	0.001	139.9	1.139121E-05	8.664116E-06	3.805266E-06	8.664116E-06 (Scheduled 180 MW)	4.542430E-04 (Scheduled 160 MW)
3 hours	0.001	139.9	2.560290E-05	2.056237E-05	1.157126E-05	2.056237E-05 (Scheduled 180 MW)	1.157126E-05 (Scheduled 180 MW)
4 hours	0.001	139.9	4.546775E-05	3.273020E-05	2.044205E-05	3.273020E-05 (Scheduled 180 MW)	2.044205E-05 (Scheduled 180 MW)

Table 7.9 shows the IUCR of System B when System AW carries a load of 139.9 MW. Two cases are investigated; one in which System AW does not recognize its wind capacity and the other when System AW considers wind power to have capacity value. The IUCR shown in col.6 and 8 in Table 7.9 are identical, as the scheduled capacities in System AW are the same in both the conditions as shown in col.5 and 7 of Table 7.8. Table 7.9 shows that the IUCR are different in col.7 and 9 for the high initial wind speed case with lead times of 1 and 2 hours, as

the scheduled capacity and therefore the assistance models are different in these two cases. The IUCR are equal for lead times of 3 and 4 hours in col. 7 and 9 as the scheduled capacities in System A are the same in these cases.

Table 7.9: Minimum assistance from System AW

		Both systems have conventional units only			System AW does not consider its wind power of any capacity value		System AW considers its wind power of capacity value	
		Isol. Syst. B (SC 190 MW) conventional units only		Inter. Syst. B Conventi-onal units only	Syst. B Inter. with Syst. AW (LIWS)	Syst. B Inter. with Syst. AW (HIWS)	Syst. B Inter. with Syst. AW (LIWS)	Syst. B Inter. with Syst. AW (HIWS)
Lead time (col.1)	UCRC (col.2)	PLCC in MW (col.3)	UCR (col.4)	IUCR (col.5)	IUCR (col. 6)	IUCR (col.7)	IUCR (col.8)	IUCR (col.9)
1 hour	0.001	149.9	3.631173 E-06	1.778725 E-09	7.135813 E-09	1.778726 E-09	7.135813 E-09	8.362213E-09
	0.0001	149.9	3.631173 E-06	1.778725 E-09	7.135813 E-09	1.778726 E-09	7.135813 E-09	8.362213E-09
	0.00001	149.9	3.631173 E-06	1.778725 E-09	7.135813 E-09	1.778726 E-09	7.135813 E-09	8.362213E-09
2 hours	0.001	149.9	1.450633 E-05	1.432078 E-08	4.191645 E-08	1.628935 E-08	4.191645 E-08	5.384206E-07
	0.0001	149.9	1.450633 E-05	1.432078 E-08	4.191645 E-08	1.628935 E-08	4.191645 E-08	5.384206E-07
	0.00001	129.9	3.762750 E-06	9.443481 E-11	9.302982 E-09	1.915420 E-09	9.302982 E-09	1.221234E-08
3 hours	0.001	149.9	3.259799 E-05	4.863762 E-08	1.501197 E-07	7.829914 E-08	1.501197 E-07	7.829914E-08
	0.0001	149.9	3.259799 E-05	4.863762 E-08	1.501197 E-07	7.829914 E-08	1.501197 E-07	7.829914E-08
	0.00001	129.9	8.477038 E-06	4.774917 E-10	3.414186 E-08	1.281457 E-08	3.414186 E-08	1.281457E-08
4 hours	0.001	149.9	5.787871 E-05	1.160072 E-07	3.157706 E-07	1.848950 E-07	3.157706 E-07	1.848950E-07
	0.0001	149.9	5.787871 E-05	1.160072 E-07	3.157706 E-07	1.848950 E-07	3.157706 E-07	1.848950E-07
	0.00001	109.9	1.045660 E-07	7.651729 E-11	4.039457 E-10	2.060122 E-10	4.039457 E-10	2.060122E-10

7.4 Application to Two Interconnected IEEE-RTS

The approach described earlier was examined further using two IEEE-RTS. The assisting system is designated as System X and the assisted system is designated as System Y. The fundamental approach is the same as that described in Section 7.3, however, due to the relatively large size of the IEEE-RTS, the complete assistance model is not easily applicable. The large number of derated states in the assistance model from System X leads to large computation times. The situation worsens if the System X has wind power in it as many derated states are created in the assistance model. The assistance model, for example, with wind power at the initial wind speed of 25.5-26.5 km/hr includes more than 400 derated states. The assistance model (and the number of derated states) even if the load and the scheduled capacity in System X remains the same, will be different at different lead times due to the uncertainties associated with wind speed at each lead time and will require a large computation time. The assistance model of System X, therefore has been reduced to a smaller number using the table rounding approach [1].

The general expression in the table rounding approach is

$$P(Cj) = \frac{Ck - Ci}{Ck - Cj} * P(Ci) \tag{7.1}$$

$$P(Ck) = \frac{Ci - Cj}{Ck - Cj} * P(Ci) \tag{7.2}$$

Equation (7.1) and (7.2) are used for all states i falling between the required rounding states j and k. P represents the individual state probability and C represents the capacity of a state.
A series of studies similar to those in Section 7.3 was conducted using System X and Y.

Case 1: System X Interconnected with System YW

The load in System X is considered to be 2359 MW and the system is operating at an UCRC of 0.001 with a scheduled capacity of 2761 MW. The PLCC of isolated System Y (with

conventional units only) change with the adopted UCRC. The PLCC of System Y corresponding to different UCRC and lead times are presented in col.3 of Table 7.10. Col.1, 2, 3 and 4 respectively show the lead time, adopted UCRC, the PLCC at the adopted UCRC for the given lead times and the UCR for carrying the load shown in col.3. Col.5 shows the IUCR for the load in col.3 when System Y is connected with System X. The data shown in col.1-5 are when both Systems X and Y have only conventional generating units. The IUCR is considerably lower in the interconnected mode than the isolated case.

The UCR of isolated System Y for carrying the PLCC shown in col. 3 at the low initial wind speed is shown in col.6. The IUCR when System YW under the low initial wind speed is interconnected with System X is shown in col.7. The IUCR shown in col. 7 is less than the IUCR shown in col. 6. The UCR of System YW for the load levels in col.3 are shown in col.8 for high initial wind speed and the IUCR are shown in col.9. A comparison of the IUCR shown in col.5,7 and 9 indicates that the IUCR decreases due to System Y having wind power.

Case 2: System XW Interconnected with System Y

The two conditions discussed earlier in which System XW does not consider and when System XW does consider the available wind power to have capacity value are investigated in this case. The UCR and IUCR under the different conditions are shown in Table 7.11. When System XW does not consider wind as a power source, it commits 2761 MW of conventional generation to meet the load of 2359 MW. When System XW considers its wind of capacity value, the scheduled capacity in System X will be 2561MW, 2661 MW, 2661 MW and 2761 MW for lead times of 1,2,3 and 4 hours respectively for the high wind speed as shown in col.8. The scheduled capacity and the risk remains at 2761 MW whether System XW considers or does not consider wind as a capacity provider in the low wind speed case, as shown in col.5 and 7. The low initial wind speed is not sufficient to create any changes in the scheduled capacity. The UCR in Table 7.11 shown in col. 8 varies according to the scheduled capacity. If the scheduled capacity is low then the risk will generally be higher despite the higher initial wind speed.

Table 7.10: Risk in Systems Y and YW due to interconnection with System X

		Isol. Syst. Y (SC 2861 MW) Conventional units only		Inter.Syst. Y Conventi-onal units only	Isol Syst. YW. (LIWS)	Syst. YW Inter. with Syst. X (LIWS)	Isol Syst. YW. (HIWS)	Syst. YW Inter.with Syst. X (HIWS)
Lead time (col.1)	UCRC (col.2)	PLCC in MW (col.3)	UCR (col.4)	IUCR (col.5)	UCR (col.6)	IUCR (col.7)	UCR (col.8)	IUCR (col.9)
1 hour	0.001	2460.9	3.240708 E-05	1.325568 E-07	2.651679 E-05	1.041592 E-07	2.494644 E-06	7.632139 E-09
	0.0001	2460.9	3.240708 E-05	1.325568 E-07	2.651679 E-05	1.041592 E-07	2.494644 E-06	7.632139 E-09
	0.00001	2305.9	8.218693 E-06	2.352049 E-08	2.522632 E-06	7.812292 E-09	4.630729 E-08	8.055378 E-11
2 hours	0.001	2460.9	1.293092 E-04	1.067554 E-06	7.792343 E-05	6.115783 E-07	1.827009 E-05	1.196223 E-07
	0.0001	2360.9	8.791692 E-05	7.213992 E-07	3.654940 E-05	2.539662 E-07	5.058982 E-06	3.130414 E-08
	0.00001	2158.9	9.991001 E-06	5.016910 E-08	4.065576 E-06	1.959184 E-08	1.735431 E-07	8.859816 E-10
3 hours	0.001	2460.9	2.902228 E-04	3.626070 E-06	1.891581 E-04	2.211100 E-06	7.063695 E-05	7.509106 E-07
	0.0001	2305.9	7.527576 E-05	6.703409 E-07	3.638690 E-05	3.272318 E-07	1.179082 E-05	1.015964 E-07
	0.00001	2110.9	8.760410 E-06	4.988390 E-08	3.082176 E-06	1.905737 E-08	3.613562 E-07	2.674230 E-09
4 hours	0.001	2460.9	5.146582 E-04	8.647768 E-06	2.892892 E-04	4.583851 E-06	1.360254 E-04	2.007124 E-06
	0.0001	2263.9	4.731283 E-05	6.538775 E-07	2.936398 E-05	3.627296 E-07	1.394016 E-05	1.635656 E-07
	0.00001	2060.9	1.707466 E-06	2.155466 E-08	8.731423 E-07	1.048038 E-08	3.628170 E-07	4.084508 E-09

The assistance model available to System Y depends on the scheduled capacities shown in Table 7.11. The IUCR of System Y when System XW does not and does consider its wind to have capacity value are shown in col. 6, 7 and 8, 9 respectively in Table 7.12. The IUCR depends on the scheduled capacity in System XW, which is influenced by the condition that the System XW considers its wind power to have a capacity value or not. The IUCR values are lower when the initial wind speed is high under the condition that System XW does not consider the wind to have a capacity value as the scheduled capacity remains the same for both the initial wind speed conditions.

Table 7.11: Risk in isolated System X for no wind, low wind and high wind conditions

				System X does not consider its wind power of any capacity value (Scheduled capacity 2761 MW)		System X considers its wind power of capacity value	
			Isol. Syst. X (SC 2761 MW) Conventional units only	Isol. Syst.XW (LIWS)	Isol. Syst. XW (HIWS)	Isol. Syst. XW (SC 2761 MW) (LIWS)	Isol. Syst. XW (HIWS)
Lead time (col.1)	UCRC (col.2)	Load level in MW (col.3)	UCR (col.4)	UCR (col.5)	UCR (col.6)	UCR (col.7)	UCR (col.8)
1 hour	0.001	2359	3.018251E-05	2.501694E-05	2.483862E-06	2.501694E-05	2.250086E-05 Scheduled 2561 MW
2 hours	0.001	2359	1.204437E-04	7.381986E-05	1.810608E-05	7.381986E-05	1.149390E-04 Scheduled 2661 MW
3 hours	0.001	2359	2.703499E-04	1.750934E-04	6.895747E-05	1.750934E-04	7.374882E-04 Scheduled 2661 MW
4 hours	0.001	2359	4.794618E-04	2.743104E-04	1.311057E-04	2.743104E-04	1.311057E-04 Scheduled 2761 MW

System XW schedules 2761 MW at the low initial wind speed and 2561 MW at the high initial wind speed for a lead time of 1 hour when it considers the wind power to have a capacity value. The IUCR in col.8 (with low initial wind speed) in Table 7.12 for a lead time of 1 hour is lower that in col. 9 (with high initial wind speed) due to the higher assistance available to System Y. The scheduled capacity at the low initial wind speed is also higher (2761 MW) than at the high initial wind speed (2661 MW) for a lead time of 2 hours. The IUCR values in col. 8 of Table 7.12 are now higher than those in col. 9 due to the different CWPD at the low initial wind

speed and high initial wind speed conditions. A high initial wind speed generally results in a CWPD with higher probabilities of having high wind power than a low initial wind speed condition. The IUCR values in col.8 for a lead time of 3 hours are generally lower than those in col.9 which is the opposite of what was observed for the lead time of 2 hours with the scheduled capacity and load level unchanged. This indicates that not only does the conventional scheduled capacity have a major role to play in the IUCR value in the assisted system but the CWPD available at different lead times has a significant influence in determining the IUCR value.

Table 7.12: Risk in System Y risk when System XW is interconnected with System Y

		Both systems have conventional units only			System XW does not consider its wind power of any capacity value		System XW considers its wind power of capacity value	
		Isol. Syst.Y (SC 2861 MW) Conventional units only		Inter. Syst.Y Convent-ional units only	Syst. Y inter. with syst. XW (LIWS)	Syst. Y inter. with syst. XW (HIWS)	Syst. Y Inter. with Syst. XW (LIWS)	Syst. Y inter. with syst. XW (HIWS)
Lead time *(col.1)*	UCRC *(col.2)*	PLCC in MW *(col.3)*	UCR *(col.4)*	IUCR *(col.5)*	IUCR *(col. 6)*	IUCR *(col.7)*	IUCR *(col.8)*	IUCR *(col.9)*
1 hour	0.001	2460.9	3.240708 E-05	1.325568 E-07	1.111590 E-07	1.264446 E-08	1.111590 E-07	1.203676 E-07
	0.0001	2460.9	3.240708 E-05	1.325568 E-07	1.111590 E-07	1.264446 E-08	1.111590 E-07	1.203676 E-07
	0.00001	2305.9	8.218693 E-06	2.352049 E-08	8.662210 E-09	1.125042 E-09	8.662210 E-09	1.003977 E-08
2 hours	0.001	2460.9	1.293092 E-04	1.067554 E-06	8.303746 E-07	1.413770 E-07	8.303746 E-07	7.144452 E-07
	0.0001	2360.9	8.791692 E-05	7.213992 E-07	2.240609 E-07	3.183308 E-08	2.240609 E-07	1.666000 E-07
	0.00001	2158.9	9.991001 E-06	5.016910 E-08	1.599525 E-08	1.264161 E-09	1.599525 E-08	9.987070 E-09
3 hours	0.001	2460.9	2.902228 E-04	3.626070 E-06	3.423813 E-06	8.879164 E-07	3.423813 E-06	4.024110 E-06
	0.0001	2305.9	7.527576 E-05	6.703409 E-07	3.889990 E-07	1.213949 E-07	3.889990 E-07	4.017145 E-07
	0.00001	2110.9	8.760410 E-06	4.988390 E-08	2.453434 E-08	5.763138 E-09	2.453434 E-08	2.402814 E-08
4 hours	0.001	2460.9	5.146582 E-04	8.647768 E-06	4.992110 E-06	2.224627 E-06	4.992110 E-06	2.225641 E-06
	0.0001	2263.9	4.731283 E-05	6.538775 E-07	3.662358 E-07	1.710926 E-07	3.662358 E-07	1.709841 E-07
	0.00001	2060.9	1.707466 E-06	2.155466E-08	1.185181E-08	4.516696E-09	1.185181E-08	4.515989 E-09

Case 3: System XW Interconnected with System YW

The UCR of System XW when both systems have 666 MW of wind capacity is examined. The scheduled capacities in System X are the same as those shown in Table 7.11. The assistance models for the scheduled capacities in Table 7.11 were used to obtain the risk values in Table 7.13. Col.6 and 7 show the IUCR when system XW does not consider wind power to have capacity value and col.8 and 9 when system XW does.

Table 7.13: Risk in System YW when System XW and YW are interconnected

		Both systems have conventional units only			System XW does not consider its wind power of any capacity value		System XW considers its wind power of capacity value	
		Isol. Syst.Y (SC 2861 MW) Conventional units only		Inter. Syst. Y Conventi-onal units only	Syst. YW inter. with syst. XW (LIWS)	Syst. YW inter. with syst. XW (HIWS)	Syst. YW Inter. with syst. XW (LIWS)	Syst. YW inter. with syst. XW (HIWS)
Lead time *(col.1)*	UCRC *(col.2)*	PLCC in MW *(col.3)*	UCR *(col.4)*	IUCR *(col.5)*	IUCR *(col. 6)*	IUCR *(col.7)*	IUCR *(col.8)*	IUCR *(col.9)*
1 hour	0.001	2460.9	3.240708 E-05	1.325568 E-07	3.390319 E-08	3.862016 E-10	3.390319 E-08	6.233723E-10
	0.0001	2460.9	3.240708 E-05	1.325568 E-07	3.390319 E-08	3.862016 E-10	3.390319 E-08	6.233723E-10
	0.00001	2305.9	8.218693 E-06	2.352049 E-08	6.452892 E-09	6.641990 E-12	6.452892 E-09	6.206403E-11
2 hours	0.001	2460.9	1.293092 E-04	1.067554 E-06	3.127158 E-07	8.440446 E-09	3.127158 E-07	2.663433E-08
	0.0001	2360.9	8.791692 E-05	7.213992 E-07	8.613867 E-08	1.987407 E-09	8.613867 E-08	6.349989E-09
	0.00001	2158.9	9.991001 E-06	5.016910 E-08	5.919627 E-09	3.579578 E-11	5.919627 E-09	1.702346E-10
3 hours	0.001	2460.9	2.902228 E-04	3.626070 E-06	1.228543 E-06	1.192734 E-07	1.228543 E-06	3.445588E-07
	0.0001	2305.9	7.527576 E-05	6.703409 E-07	1.639122 E-07	1.517165 E-08	1.639122 E-07	3.985182E-08
	0.00001	2110.9	8.760410 E-06	4.988390 E-08	8.079489 E-09	3.521473 E-10	8.079489 E-09	1.109552E-09
4 hours	0.001	2460.9	5.146582 E-04	8.647768 E-06	2.048529 E-06	3.746582 E-07	2.048529 E-06	3.746582E-07
	0.0001	2263.9	4.731283 E-05	6.538775 E-07	1.617691 E-07	2.484488 E-08	1.617691 E-07	2.484488E-08
	0.00001	2060.9	1.707466 E-06	2.155466 E-08	4.228927 E-09	6.003787 E-10	4.228927 E-09	6.003787E-10

The IUCR are higher when System XW considers its wind power to have capacity value than when it does not consider it to have capacity value due to the lower assistance from System XW. The IUCR are lower when the initial wind speed increases to the high value in both cases. The IUCR shown in Table 7.13 are lower than those in Table 7.12 as both systems now have wind power. This case is the most likely scenario for most interconnected power systems as wind power penetration increases in the future.

7.5 Conclusion

This chapter examines the isolated and interconnected system UCR for two interconnected power systems with wind power. A probabilistic technique based on the CWSD and CWPD introduced in Chapters 3 and 4 is utilized in this chapter to evaluate the isolated and interconnected system risk in the assisted system. Wind data from the Swift Current site for the month of January at hours 4-7 have been applied. The RBTS and IEEE-RTS are used for the analysis under two different initial wind speed conditions. The assistance model contains large number of derated states for a large test system such as the IEEE-RTS, and therefore the number of derated states needs to be reduced to smaller number. The table rounding approach is utilized to reduce the number of derated states in the assistance model to reduce the computation times for evaluating the risk indices.

The assistance model depends on the scheduled capacity and the load level in the assisting system. The potential assistance decreases as the load in the assisting system increases. The load level in the assisting system plays a significant role in the IUCR of the assisted system. The IUCR changes when one or both systems have wind power. Electric power utilities may or may not consider its wind power to have any capacity value. This situation significantly affects the IUCR calculation. When the assisting system considers wind power to have capacity value then it may decrease its scheduled capacity and hence the capacity assistance to the assisted system decreases. This can result in a higher IUCR in the assisted system. The CWPD at different lead times under different initial wind speed conditions also play an important role in the assisted system IUCR. The IUCR values are also affected by whether WTG are in the

assisting or the assisted system and in that situation whether the system treats the wind as a power source. The estimated IUCR are generally greater as the lead time increases in both conventional and wind integrated power systems.

The studies shown in this chapter illustrate that the concepts developed in the earlier chapters can be applied to study the effects of wind power in interconnected systems.

8. SUMMARY AND CONCLUSIONS

The focus of the research described in this thesis and the research objectives are presented in Chapter 1 together with a brief introduction to the research area. The procedure used to evaluate the Unit Commitment Risk (UCR) in a power system is described in Chapter 2. Two test systems (the RBTS and the IEEE-RTS) are used to illustrate the determination of the scheduled capacity, number of scheduled generating units and the spinning reserve required to maintain a specified Unit Commitment Risk Criterion (UCRC).

The UCR at a given load level and a specified number of scheduled units increases with lead time as the failure probability of the operating units increase with time. A small decrease in the UCR occurs if the system is able to sustain the outage of a relatively small unit but a relatively larger UCR decrease occurs at certain load points irrespective of the lead time. In both test systems, significant risk decreases occur when the difference between the total committed generation and the load level are integer multiples of the largest operating unit in the system.

If the scheduled generating capacity is insufficient to carry the system peak load and maintain the reliability criterion (UCRC) then assistance is required from other sources. The analyses carried out illustrate that the required lead time has a significant impact on the system operating conditions. At short lead times the operating conditions for various UCRC may not change due to the relatively small outage replacement rates. The operating conditions, however, will be generally different for higher lead times. Each power system is different in size, unit types, unit capacities and failure rates. Each system therefore has its own unique operating reserve requirements, including the system lead time, even for the same UCRC. The operating reserve requirements should, therefore, be evaluated for each individual system.

The operating reserve in a power system at a given load level is determined by the specified UCRC. If a low value of UCRC is selected, the spinning reserve required to maintain the reliability criterion will be generally high. The operating reserve requirement for a given UCRC generally increases with increased system lead times.

Chapter 2 illustrates the concept of UCR and its response to a number of basic elements in the calculation process by application to the RBTS and the IEEE-RTS. The following chapters in this thesis illustrate the research conducted to integrate wind power in the assessment of operating risk and to determine the contribution that wind power can add under a constant risk criterion.

The approach developed to forecast short term future wind speeds is presented in Chapter 3. The technique is based on the ARMA model and depends on the historical value of the wind at a particular site. The approach does not try to bring the uncertainty associated with the stochastic nature of the wind into a certainty domain. It recognizes that the uncertainty in the future wind speed can be directly applied in UCR analysis of wind integrated power system operation. The developed model is unique, as it is based on the local wind conditions and predicts the future wind speed in the form of a Conditional Wind Speed Distribution (CWSD). The model also recognizes the dependence of short term future wind speeds on the present wind speed.

A persistence model is a very simple model of wind speed forecasting that assumes that the future wind speed will be the same as the wind speed at the present time. The model has shown to be more accurate for short forecast horizons than highly sophisticated models. Highly advanced techniques such as Numerical Weather Predication (NWP) models require input data on the state of the present atmosphere. It takes a considerably long time for weather services to generate the weather map of the atmosphere and by the time the local weather conditions are predicted the state of the atmosphere could have already changed, which results in new set of forecasts. Highly sophisticated models are not suitable for short term wind speed forecasting and are usually suitable only for long time horizons. Short term wind power output could be obtained directly from the initial wind speed and the power curve using only the Persistence model. This, however, does not recognize the residual uncertainty in the future wind power. The studies

shown in this chapter illustrate that there is considerable uncertainty in the wind power output in the next hour given the wind speed at the initial point in time. The proposed model acknowledges the strength of the Persistence approach and extends this concept using an uncertainty forecast in the form of a probability distribution that essentially captures the possible wind speeds in the next few hours.

The use of a probabilistic method to examine the benefits of adding wind power to a conventional power system is illustrated in Chapter 4. The initial system state conditions are assumed to be known in a power system security study and therefore a specific initial wind speed is used in all the study cases to compare the operating capacity benefits in different scenarios. Short term wind speed probability distributions based on the initial known wind speeds are generated to produce Conditional Wind Power Distributions (CWPD). The CWPD are then used to create derated state models that can be combined with the conventional generating capacity models to determine the UCR associated with different loading conditions and lead times. The novel contribution in this thesis is the recognition that wind power output during a specified lead time can be modeled in the form of a multi-state generating unit and added to quickly create a total generating unit Capacity Outage Probability Table (COPT) that can be updated on an hourly or period basis. The process is not stationary and therefore regular updating of the COPT on a period basis is essential to accommodate the new wind condition as time moves on. This situation is typical in power system operation where the system has to be continuously monitored and updated as the system state involving load changes or some form of contingency such as generation outages, line outages, transmission line congestions etc. occurs. This procedure provides a consistent approach to calculating the operating risk in a wind integrated generating system.

The approach presented in Chapter 4 uses auto-regressive moving average time series models and regression analysis to create the short term probability distributions of future wind speeds at a given wind site. Each model is unique to the site and the local wind conditions. The focus is on the inherent variability associated with the wind power output rather than on an exact future wind speed forecast. The system operating performance is examined in terms of the Load Carrying Capability (LCC), Peak Load Carrying Capability (PLCC) and the Increase in Peak

Load Carrying Capability (IPLCC) associated with wind power generation. The concepts and the implications of using different UCRC and lead times are examined and illustrated using a small test system and a relatively large test system in the form of the RBTS and the IEEE-RTS respectively.

The effect of incorporating derated states in a Unit Commitment Risk and Peak Load Carrying Capability analysis of a wind integrated power system is examined using the IEEE-RTS. The PLCC of the system is highly dependent on the UCRC and influenced by recognizing the possible generating unit derated states. The application of derated state generating unit models can show higher or lower PLCC values than those obtained using two state models but produces smoother and more representative UCR-load profiles compared to those for two state models, which create large discrete steps in the UCR levels. Detailed multi-state models provide a more accurate representation of the performance of a generating unit and therefore a more accurate assessment of the UCR. They also require considerable generating unit performance data collected over a suitable period of time under consistent and carefully prepared protocols.

In a general sense, the addition of wind power to a conventional generating system is always beneficial in terms of decreasing the UCR or increasing the PLCC. The load carrying capability benefit is a complex phenomenon and depends on the initial wind speed, the time of the day and year, the site wind regime, the wind capacity and the size and types of the conventional units etc. Each power system has unique characteristics in terms of its unit sizes, lead-times and failure rates, and has different operating strategies. A general conclusion regarding wind power benefits is hard to achieve and each system should be evaluated individually in order to quantify the actual benefits.

The most important factors in assessing the operating benefits associated with a specific wind site are the initial wind speed and the site wind regime. The initial wind speed can be continuously monitored and updated to produce revised risk assessments for the required lead time. The IPLCC attributable to the wind generating capacity will therefore vary with time. In systems with high wind power penetration this may result in requiring frequent unit commitment decisions in order to maintain an acceptable Unit Commitment Risk.

The studies show that wind capacity can make a recognizable contribution to the system operating reserve and that this contribution can be quantified. This is an important conclusion in view of the increasing additions of wind generating capacity to electric power systems throughout the world

The effect of the daily variation in mean wind speed parameter trends on the PLCC of a wind integrated power system is illustrated in Chapter 5. Two typical sets of hourly wind speeds, one in January and another in August are analyzed. The wind speed parameter trends in January are similar although they are at different times of the same day. The results indicate that the IPLCC are very similar. It can therefore be concluded that if the hourly mean wind speed parameter trend at different times of the day are similar, they will produce similar results for the same initial wind speed and therefore it may not be necessary to develop CWSD for each individual hour in the day. Similar analyses were carried out for the month of August where the mean wind speed trends are quite different. One set of hours has a historically increasing mean wind speed trend and the other set has a decreasing mean wind speed trend. The PLCC benefits are higher for the hours which show an increasing trend and result in an increased IPLCC. The historical mean wind speed trend is an important indicator and should be considered in the IPLCC evaluation. This can be of practical significance at some wind sites where for a certain period of time the wind shows an increasing mean wind speed trend while at other times it is either decreasing or relatively constant.

The effects of seasonality and wind site variations on the PLCC of a wind integrated power system are demonstrated in this chapter. Wind speed data for two sites located at Regina and Swift Current in Saskatchewan, Canada for the month of January and August are used in the described studies. Two cases were investigated for the two sites, one with different historical means but similar standard deviations and the other with similar historical means but different standard deviations. The study results show that the IPLCC is significantly influenced by the changes in the season rather than the change in wind site locations. The benefits are highly dependent on the initial wind speed and the historical wind speed profile.

Chapter 5 also illustrates operating capacity credits associated with adding independent and dependent wind farms to a system composed of conventional generating units. The concepts are presented using the IEEE-RTS. The numerical results are a function of the test system and the input data used in the studies. Similar studies can be conducted for other systems. The studies described show a number of conditions and trends that are applicable to a wide range of systems.

The capacity credits attributable to wind power are evaluated using the concept of increased peak load carrying capability at the criterion risk level. The Operating Capacity Credit (OCC) is a function of the initial wind speed and the lead time associated with the additional available system capacity.

The studies presented clearly illustrate the considerable difference in operating capacity credits attributable to wind power additions associated with dependent and independent wind regimes. The dependent and independent conditions provide boundary values that clearly indicate the effects of site wind speed correlation. This is an important factor in all wind integrated power systems and will become increasingly important in the future as wind power penetration levels increase.

An Approximate method for evaluating the well-being state probabilities is presented in Chapter 6 and the results are compared with those from an established method. It is observed that the Approximate method provides reasonably accurate results in significantly less time. The method is applied in the system studies described in this chapter.

The Unit Commitment Risk as suggested in the PJM method is a single value risk index and does not directly indicate the system spinning reserve margin. It also does not directly consider the generally adopted deterministic criterion used in system operation, which assumes that a system should have at least enough spinning reserve to cope with the loss of the largest operating unit. Well-being analysis incorporates this deterministic criterion in a probabilistic domain and can be used to evaluate the system operating state risks. Well-being analysis of wind integrated RBTS and IEEE-RTS are presented in this chapter. The PLCC and IPLCC are

determined and illustrated for two different initial wind speed conditions. The analyses were conducted using two different risk criteria designated as single risk and dual risk criteria. The UCRC and Healthy State Probability Criterion (HSPC) are applied individually as a single criterion and combined to form a dual risk criterion. A single risk criterion in a general sense can indicate higher PLCC than the application of a similar dual criterion. The dual criterion approach, however, takes full advantage of the ability to incorporate an accepted deterministic criterion such as N-1 in the PLCC and IPLCC evaluation process.

The studies presented clearly illustrate the effects of having higher initial wind speeds on the PLCC and IPLCC of wind integrated power systems. The studies also show that having additional wind capacity by increasing the number of WTG does not create a significant increase in the IPLCC due to the added wind power at low initial wind speed using a dual risk criterion. The PLCC and the IPLCC due to added generating capacity are very dependent on the magnitude of the acceptable UCR and Healthy State Probability (HSP). This is illustrated in the studies shown in this chapter using single risk and dual risk criteria.

A sensitivity study of the HSP arising from different UCRC values was conducted for the RBTS, IEEE-RTS and the modified IEEE-RTS. The studies show that in all of these test systems, the HSP does not improve significantly when the UCRC is decreased from 0.0001 to 0.00001 and the decrease in PLCC is relatively high. The increase in the HSP when the UCRC is decreased from 0.001 to 0.0001 is considerable, especially when the lead times are short. It is therefore suggested that a UCR value should be used that provides the maximum benefit in terms of the system HSP without severely compromising the PLCC. This is a general comment based on the studies conducted on the three test systems and should be investigated by further work in this area using the concepts introduced in this research. The actual selection of acceptable numerical risk indices is, however, in the end a management decision.

The isolated and interconnected system UCR designated as the UCR and IUCR respectively for two interconnected power systems with wind power are illustrated in Chapter 7. The probabilistic technique based on the CWSD and CWPD introduced in Chapters 3 and 4 is utilized in this chapter to evaluate the isolated and interconnected system risk in the assisted

system. The RBTS and IEEE-RTS are used for the analysis under two different initial wind speed conditions. The developed assistance model contains a large number of derated states for a large system such as the IEEE-RTS, and therefore the number of derated states needs to be reduced to a smaller number. The table rounding approach is utilized to reduce the number of derated states in the assistance model to reduce the computation time required to evaluate the risk indices.

The assistance model depends on the scheduled capacity and the load level in the assisting system. The potential assistance decreases as the load in the assisting system increases. The load level in the assisting system plays a significant role in the IUCR of the assisted system. The IUCR changes when one or both systems have wind power. Electric power utilities may or may not consider their wind power to have capacity value. This situation significantly affects the IUCR calculation. When the assisting system considers wind power to have capacity value it may decrease its scheduled capacity and hence the capacity assistance to the assisted system decreases. This can result in a higher IUCR in the assisted system. The CWPD at different lead times under different initial wind speed conditions also plays an important role in the assisted system IUCR. The IUCR values are also affected by whether WTG are in the assisting or the assisted system and in that situation whether the system treats the wind as a power source. The estimated IUCR are generally greater as the lead time increases in both conventional and wind integrated power systems.

The studies shown in Chapter 7 illustrate that the concepts developed in the earlier chapters can be applied to study the effects of wind power in interconnected systems. The research described in this thesis clearly illustrates that the operating capacity benefits associated with wind power can be quantified and used in making generating capacity scheduling decisions in a wind integrated power system.

REFERENCES

[1] R. Billinton and R. N. Allan, *Reliability Evaluation of Power Systems.* ,2nd ed.New York: Plenum Press, 1996, pp. 514.

[2] R. Billinton and W. Li, *Reliability Assessment of Electrical Power Systems using Monte Carlo Methods.* New York: Plenum Press, 1994, pp. 351.

[3] R. Billinton and J. S. Tatla, "Hierarchical indices in system adequacy assessment " vol. 22, Canadian Electrical Assoc, Engineering & Operating Div, Montr, Engineering and Operating Division. 1983.

[4] R. Billinton and R. N. Allan, "Power system reliability in perspective," *Electronics and Power. Journal of the Institution of Electrical Engineers,* Vol. 30, No.3, March 1984, pp. 231-236.

[5] P. Kundur, J. Paserba, V. Ajjarapu, G. Andersson, A. Bose, C. Canizares, N. Hatziargyriou, D. Hill, A. Stankovic, C. Taylor, T. Van Cutsem and V. Vittal, "Definition and classification of power system stability IEEE/CIGRE joint task force on stability terms and definitions," *IEEE Trans. Power Syst.,* Vol. 19, No. 3, Sept. 2004, pp. 1387-1401.

[6] P. Kundur, N. J. Balu and M. G. Lauby, *Power System Stability and Control.* McGraw-Hill Professional, 1994.

[7] R. Billinton, "Criteria used by Canadian utilities in the planning and operation of generating capacity," IEEE *Trans. Power Syst.,* Vol. 3, No. 4, Nov. 1988, pp. 1488-1493.

[8] M. E. Khan and R. Billinton, "Generating unit commitment in composite generation and transmission systems," *IEE Proceedings, Part C: Generation, Transmission and Distribution*, Vol. 140, No. 5, 1993, pp. 404-410.

[9] R. Billinton, "Bibliography on the application of probability methods in power system reliability evaluation," *IEEE Transactions on Power Apparatus and Systems*, Vol. PAS-91, No. 2, Mar. 1972, pp. 649-660.

[10] IEEE-PES APM Subcommittee, "Bibliography on the application of probability methods in power system reliability evaluation 1971-1977," *IEEE Transactions on Power Apparatus and Systems*, Vol. PAS-97, No.6, Nov. 1978, pp. 2235-2242.

[11] R. N. Allan, R. Billinton and S. H. Lee, "Bibliography on the application of probability methods in power system reliability evaluation," *IEEE Transactions on Power Apparatus and Systems*, Vol. PAS-103, No. 2, 1984, pp. 275-282.

[12] R. N. Allan, R. Billinton, S. M. Shahidehpour and C. Singh, "Bibliography on the application of probability methods in power system reliability evaluation: 1982-1987," *IEEE Trans. Power Syst.*, Vol. 3, No. 4, 1988, pp. 1555-1564.

[13] L. T. Anstine, R. E. Burke, J. E. Casey, R. Holgate, R. S. John and H. G. Stewart, "Application of probability methods to the determination of spinning reserve requirements for the Pennsylvania-New Jersey-Maryland interconnection," *IEEE Transactions on Power Apparatus and Systems*, Vol. PAS-82, No. 68, Oct. 1963, pp. 726-735.

[14] R. Billinton and M. P. Musick, "Spinning reserve criteria in a hydro thermal system by the application of probability mathematics," *Eng. J.*, Vol. 48, No. 10, Oct. 1965, pp. 40-45.

[15] R. Billinton and A. V. Jain, "The effect of rapid start and hot reserve units in spinning reserve studies," *IEEE Transactions on Power Apparatus and Systems,* Vol. PAS-91, No. 2, Mar. 1972, pp. 511-516.

[16] R. Billinton and A. V. Jain, "Interconnected system spinning reserve requirements," *IEEE Transactions on Power Apparatus and Systems,* Vol. PAS-91, No.2, Mar. 1972, pp. 517-525.

[17] R. Billinton and A. V. Jain, "Power system spinning reserve determination in a multisystem configuration," *IEEE Transactions on Power Apparatus and Systems,* Vol. PAS-92, No. 2, 03. 1973, pp. 433-441.

[18] M. Fotuhi-Firuzabad, R. Billinton and M. E. Khan, "Extending unit commitment health analysis to include transmission considerations," *Electr. Power Syst. Res.,* Vol. 50, No. 1, Mar. 1999, pp. 35-42.

[19] M. E. Khan, "Bulk load points reliability evaluation using a security based model," *IEEE Trans. Power Syst.,* Vol. 13, No. 2, 1998, pp. 456-461.

[20] M. E. Khan and R. Billinton, "Composite system spinning reserve assessment in interconnected systems," *IEE Proceedings: Generation, Transmission and Distribution,* Vol. 142, No. 3, 1995, pp. 305-309.

[21] R. Billinton and M. E. Khan, "Security considerations in composite power system reliability evaluation " in *Third International Conference on Probabilistic Methods Applied to Electric Power Systems,* 1991, pp. 58-63.

[22] R. Billinton and A. V. Jain, "Unit derating levels in spinning reserve studies," *IEEE Transactions on Power Apparatus and Systems,* Vol. PAS-90, No. 4, pp. 1677-87, July. 1971.

[23] R. Billinton and M. Fotuhi-Firuzabad, "A methodology to determine interruptible load carrying capability in a generation system," in *35th Universities Power Engineering Conference, September 6, 2000 - September 8,* 2000, pp. 132.

[24] M. Fotuhi-Firuzabad and R. Billinton, "Impact of load management on composite system reliability evaluation short-term operating benefits," *IEEE Trans. Power Syst.*, Vol. 15, No. 2, May 2000, pp. 858-64.

[25] M. Fotuhi-Firuzabad, "Interruptible load considerations in well-being analysis of interconnected systems," *Qual. Reliab. Eng. Int.*, Vol. 14, No.3, 1998, pp. 137-144.

[26] A. V. Jain and R. Billinton, "Reliable loading of generating units for system operation," in *8th Power Industry Computer Application Conference,* 1973, pp. 221-229.

[27] F. Aminifar, M. Fotuhi-Firuzabad and M. Shahidehpour, "Unit commitment with probabilistic spinning reserve and interruptible load considerations," *IEEE Trans. Power Syst.*, Vol. 24, No. 1, Feb. 2009, pp. 388-97.

[28] R. Billinton and M. Fotuhi-Firuzabad, "Generating system operating health analysis considering stand-by units, interruptible load and postponable outages," *IEEE Trans. Power Syst.*, Vol. 9, No.3, 1994, pp. 1618-1625.

[29] R. Billinton and M. Fotuhi-Firuzabad, "A reliability framework for generating unit commitment," *Electr. Power Syst. Res.*, Vol. 56, No.1, May 2000, pp. 81-8.

[30] A. D. Patton, "A probability method for bulk power system security assessment. I. Basic concepts," *IEEE Transactions on Power Apparatus and Systems*, Vol. PAS-91, No.1, Jan. 1972, pp. 54-61.

[31] A. D. Patton, "Probability method for bulk power system security assessment -II. Development of probability models for normally operating components," IEEE *Transactions on Power Apparatus and Systems*, Vol. PAS-91, No.6, 1972, pp. 2480-2485.

[32] A. D. Patton, "A probability method for bulk power system security assessment. III. Models for stand-by generators and field data collection and analysis," *IEEE Transactions on Power Apparatus and Systems*, Vol. PAS-91, No.6, Nov. 1972, pp. 2486-93.

[33] R. Billinton, M. Fotuhi-Firuzabad and S. Aboreshaid, "Unit commitment health analysis for interconnected systems," *IEEE Trans. Power Syst.*, Vol. 12, No.3, 1997, pp. 1194-1201.

[34] M. Fotuhi-Firuzabad, R. Billinton and S. Aboreshaid, "Spinning reserve allocation using response health analysis," *IEE Proceedings-Generation, Transmission and Distribution*, Vol. 143, No.4, July 1996, pp. 337-343.

[35] M. Fotuhi-Firuzabad, R. Billinton and S. Aboreshaid, "Response health constraints in economic load dispatch considering standby units, interruptible loads and postponable outages," *IEE Proceedings-Generation, Transmission and Distribution*, Vol. 143, No.6, 11. 1996, pp. 599-607.

[36] R. Billinton and M. Fotuhi-Firuzabad, "A probabilistic technique for operating reserve assessment using system operating states " in *The IEEE Western Canada Conference and Exhibition, WESCANEX 95* 1995, pp. 169-174.

[37] R. Billinton, M. Fotuhi-Firuzabad and S. Aboreshaid, "An approach to evaluating system well-being in engineering reliability applications," *Reliab. Eng. Syst. Saf.*, Vol. 50, No.1, 1995, pp. 1-5.

[38] R. Billinton and M. Fotuhi-Firuzabad, "A basic framework for generating system operating health analysis," *IEEE Trans. Power Syst.*, Vol. 9, No.3, Aug. 1994, pp. 1610-1617.

[39] M. E. Khan and R. Billinton, "A hybrid model for quantifying different operating states of composite power systems," *IEEE Trans. Power Syst.*, Vol. 7, No.1, 1992, pp. 187-193.

[40] Global wind energy council, "http://www.gwec.net/"

[41] American Wind Energy Association, "http://www.awea.org/policy/rpsbrief.html"

[42] Canadian Wind Energy Association, "http://www.canwea.ca"

[43] Danish wind industry association, "http://www.windpower.org/EN/core.htm"

[44] T. Ackermann, *Wind Power in Power Systems*. John Wiley, 2005

[45] Spanish wind energy association, "http://www.aeeolica.es/en/"

[46] Yahoo groups- wind power integration, "http://ca.groups.yahoo.com/"

[47] Google alert- wind energy, "http://www.google.com/alerts"

[48] Australian wind energy association, "http://www.auswind.org/main.php"

[49] European wind energy association, "http://www.ewea.org/"

[50] New Zealand wind energy association, "http://www.windenergy.org.nz/"

[51] P. Giorsetto and K. F. Utsurogi, "Development of a new procedure for reliability modeling of wind turbine generators," *IEEE Transactions on Power Apparatus and Systems*, Vol. PAS-102, No. 1, Jan. 1983, pp. 134-143.

[52] R. Billinton, S. Kumar, N. Chowdhury, K. Chu, K. Debnath, L. Goel, E. Khan, P. Kos, G. Nourbakhsh and J. Oteng-Adjei, "A reliability test system for educational purposes-basic data," *IEEE Trans. Power Syst.*, Vol. 4, No.3, Aug. 1989, pp. 1238-1244.

[53] C. Grigg, P. Wong, P. Albrecht, R. Allan, M. Bhavaraju, R. Billinton, Q. Chen, C. Fong, S. Haddad, S. Kuruganty, W. Li, R. Mukerji, D. Patton, N. Rau, D. Reppen, A. Schneider, M. Shahidehpour and C. Singh, "The IEEE Reliability Test System-1996. A report prepared by the Reliability Test System Task Force of the Application of Probability Methods Subcommittee," *IEEE Trans. Power Syst.*, Vol. 14, No. 3, Aug. 1999, pp. 1010-1020.

[54] R. Billinton, H. Chen and R. Ghajar, "Time-series models for reliability evaluation of power systems including wind energy," *Microelectron. Reliab.*, Vol. 36, No. 9, 1996, pp. 1253-1261.

[55] R. Billinton and R. Karki, "Capacity reserve assessment using system well-being analysis," *IEEE Trans. Power Syst.*, Vol. 14, No. 2, 1999, pp. 433-438.

[56] R. Billinton, Bagen and Y. Cui, "Reliability evaluation of small stand-alone wind energy conversion systems using a time series simulation model," *IEE Proceedings-Generation, Transmission and Distribution*, Vol. 150, No. 1, Jan. 2003, pp. 96-100.

[57] R. Karki and R. Billinton, "Cost-effective wind energy utilization for reliable power supply," *IEEE Trans. Energy Convers.*, Vol. 19, No. 2, 2004, pp. 435-440.

[58] B. Bagen and R. Billinton, "Reliability cost/worth associated with wind energy and energy storage utilization in electric power systems," in *10th International Conference on Probablistic Methods Applied to Power Systems (PMAPS 2008),* 2008, pp. 7.

[59] R. Billinton and B. Bagen, "A sequential simulation method for the generating capacity adequacy evaluation of small stand-alone wind energy conversion systems " in *Canadian Conference on Electrical and Computer Engineering, CCECE2002,* pp. 72-77.

[60] W. Wangdee and R. Billinton, "Reliability assessment of bulk electric systems containing large wind farms," *International Journal of Electrical Power and Energy Systems,* Vol. 29, No.10, 2007, pp. 759-766.

[61] R. Billinton and W. Wangdee, "Reliability-based transmission reinforcement planning associated with large-scale wind farms," *IEEE Trans. Power Syst.,* Vol. 22, No.1, Feb. 2007, pp. 34-41.

[62] D. Huang and R. Billinton, "Effects of wind power on bulk system adequacy evaluation using the well-being analysis framework," *IEEE Trans. Power Syst.,* Vol. 24, No.3, 2009, pp. 1232-1240.

[63] Y. Gao and R. Billinton, "Adequacy assessment of generating systems containing wind power considering wind speed correlation," *IET Renewable Power Generation,* Vol. 3, No.2, June. 2009, pp. 217-226.

[64] R. Billinton and Y. Gao, "Multistate wind energy conversion system models for adequacy assessment of generating systems incorporating wind energy," *IEEE Trans. Energy Convers.,* Vol. 23, No.1, 03. 2008, pp. 163-170.

[65] X. Wang, Hui-Zhu Dai and R. J. Thomas, " Reliability modeling of large wind farms and associated electric utility interface systems," *IEEE Transactions on Power Apparatus and Systems,* Vol. PAS-103, No.3, 1984, pp. 569-575.

[66] R. P. Schulte, K. D. Le, R. H. Vierra, G. D. Nagel and R. T. Jenkins, "Problems associated with unit commitment in uncertainty," *IEEE Transactions on Power Apparatus and Systems*, Vol. PAS-104, No.8, Aug. 1985, pp. 2072-8.

[67] N. Chowdhury and R. Billinton, "Interruptible load carrying capability of a generation system," *IEEE Trans. Power Syst.*, Vol. 4, No.1, Feb. 1989, pp. 115-121.

[68] N. Chowdhury and R. Billinton, "Interruptible load considerations in spinning reserve assessment of isolated and interconnected generating systems," *IEE Proceedings C: Generation Transmission and Distribution*, Vol. 137, No.2, 1990, pp. 159-167.

[69] N. Chowdhury and R. Billinton, "Unit commitment in interconnected generating systems using a probabilistic technique," *IEEE Trans. Power Syst.*, Vol. 5, No.4, 11. 1990, pp. 1231-1238.

[70] Y. -. Hsu, Y. -. Lee, J. -. Jien, C. C. Liang, K. -. Chen, T. -. Lai and T. -. Lee, "Operating reserve and reliability analysis of the Taiwan power system," *IEE Proceedings C: Generation, Transmission and Distribution*, Vol. 137, No.5, 1990, pp. 349-357.

[71] C. L. Chen and S. L. Chen, "Short-term unit commitment with simplified economic dispatch," *Electr. Power Syst. Res.*, Vol. 21, No.2, June. 1991, pp. 115-120.

[72] F. N. Lee and Q. Feng, "Multi-area unit commitment," *IEEE Trans. Power Syst.*, Vol. 7, No.2, May 1992, pp. 591-599.

[73] R. Billinton and G. Lian, "Generating unit operating reserve assessment in a composite generation and transmission system," in *11th Power Systems Computation Conference*, 1993, pp. 63-69.

[74] G. Lian and R. Billinton, "Operating reserve risk assessment in composite power systems," *IEEE Trans. Power Syst.,* Vol. 9, No. 3, Aug. 1994, pp. 1270-1276.

[75] J. J. Shaw, "A direct method for security-constrained unit commitment," *IEEE Trans. Power Syst.,* Vol. 10, No.3, Aug. 1995, pp. 1329-1342.

[76] W. L. Peterson and S. R. Brammer, "A capacity based Lagrangian relaxation unit commitment with ramp rate constraints," *IEEE Trans. Power Syst.,* Vol. 10, No. 2, May 1995, pp. 1077-1084.

[77] C. Li, E. Hsu, A. J. Svoboda, C. Tseng and R. B. Johnson, "Hydro unit commitment in hydro-thermal optimization," *IEEE Trans. Power Syst.,* Vol. 12, No.2, 1997, pp. 764-769.

[78] R. Billinton and M. Fotuhi-Firuzabad, "Composite systems operating reserve assessment using a reliability framework," *in Canadian Conference on Electrical and Computer Engineering, CCECE 2001,* 2001, pp. 725-30.

[79] R. Chhetri, B. Venkatesh and E. F. Hill, "Security constraints unit commitment for a multi-regional electricity market," *in Large Engineering System Conference on Power Systems,* 2006, pp. 47-52.

[80] J. P. S. Catalao, S. J. P. Mariano, V. M. F. Mendes and L. A. F. Ferreira, "Short-term scheduling of thermal units: emission constraints and trade-off curves," European *Transactions on Electrical Power,* Vol. 18, No.1, 01. 2008, pp. 1-14.

[81] I. J. Raglend and N. P. Padhy, "Comparison of practical unit commitment problem solutions," *Electric Power Components and Systems,* Vol. 36, No.8, 2008, pp. 844-863.

[82] L. Wu, M. Shahidehpour and T. Li, "Cost of reliability analysis based on stochastic unit commitment," *IEEE Trans. Power Syst.,* Vol. 23, No.3, 2008, pp. 1364-1374.

[83] R. H. Kerr, J. L. Scheidt, J. Fontana A.J. and J. K. Wiley, "Unit commitment," *IEEE Transactions on Power Apparatus and Systems*, Vol. PAS-85, No.5, 1966, pp. 417-421.

[84] P. G. Lowery, "Generating unit commitment by dynamic programming," *IEEE Transactions on Power Apparatus and Systems*, Vol. PAS-85, No.5, 05. 1966, pp. 422-426.

[85] H. H. Happ, R. C. Johnson and W. J. Wright, "Large scale hydro-thermal unit commitment-method and results," *IEEE Transactions on Power Apparatus and Systems*, Vol. PAS-90, No.3, 05. 1971, pp. 1373-1384.

[86] A. V. Jain and R. Billinton, "Unit commitment in Hydro-Thermal systems," Canadian Electrical Association, Eng and Oper. Div, Trans, Part 3, 1973.

[87] R. R. Shoults, K. C. Show, S. Helmick and W. M. Grady, "A practical approach to unit commitment, economic dispatch and savings allocation for multiple area pool operation with import/export constraints," *IEEE Transactions on Power Apparatus and Systems*, Vol. PAS-99, No.2, 03. 1980, pp. 625-635.

[88] R. Billinton and M. Fotuhi-Firuzabad, "A reliability test system for educational purposes operating reserve assessment," in *Proceedings of Thirty-Fourth Universities Power Engineering Conference (UPEC'99)*, 1999, pp. 189-192.

[89] U. Focken, M. Lange, K. Mo̲nnich, H. -. Waldl Hans-Peter, H. G. Beyer and A. Luig, "Short-term prediction of the aggregated power output of wind farms - A statistical analysis of the reduction of the prediction error by spatial smoothing effects," *J. Wind Eng. Ind. Aerodyn.*, Vol. 90, No.3, 2002, pp. 231-246.

[90] L. Landberg, "Short-term prediction of the power production from wind farms," *J. Wind Eng. Ind. Aerodyn.*, Vol. 80, No.1, 1999, pp. 207-220.

[91] L. Landberg and S. J. Watson, "Short-term prediction of local wind conditions," *Bound. -Layer Meteorol.*, Vol. 70, No.1, 1994, pp. 171-195.

[92] U. F. Matthias Lange, *Physical Approach to Short-Term Wind Power Prediction.* Springer, 2005

[93] World Meteorological Organization, "http://www.wmo.int/pages/index_en.html"

[94] R. A. Pielke, *Mesoscale Meteorological Modeling.* London, UK: Academic Press, 1984, pp. 612.

[95] J. Eichhorn, K. Cui, M. Flender, T. Kandlbinder, W. -. Panhans, R. Ries, J. Siebert, T. Trautmann, N. Wedi and W. G. Zdunkowski, "A three-dimensional viscous topography mesoscale model," *Contributions to Atmospheric Physics*, Vol. 70, No.4, 11. 1997, pp. 301-317.

[96] H. Kapitza and D. P. Eppel, "The non-hydrostatic mesoscale model GESIMA. I. Dynamical equations and tests," *Contributions to Atmospheric Physics*, Vol. 65, No.2, 05. 1992, pp. 129-146.

[97] H. -. Mengelkamp, H. Kapitza and U. Pfluger, "Statistical-dynamical downscaling of wind climatologies," *J. Wind Eng. Ind. Aerodyn.*, Vol. 67-68, 1997, pp. 449-457.

[98] Pielke R.A. Sr and M. E. Nicholls, "Use of meteorological models in computational wind engineering," *J. Wind Eng. Ind. Aerodyn.*, Vol. 67-68, 1997, pp. 363-372.

[99] B. H. Sass, N. W. Nielsen, J. U. Jørgensen, B. Amstrup, M. Kmit and K. S. Mogensen, *The Operational DMI-HIRLAM System 2002-Version* Danish Meteorological Institute, Ministry of Transport, Available at: http://www.dmi.dk/dmi/en/print/tr02-05.pdf,

[100] ENFOR- Wind Power Prediction Tool, "http://www.enfor.eu/wind_power_prediction_tool_wppt.php"

[101] G. Giebel, L. Landberg, J. Badger, K. Sattler, H. Feddersen, T. S. Nielsen, H. A. Nielsen and H. Madsen, "Using ensemble forecasting for wind power," in *CD-Proceedings of the 2003 European Wind Energy Association Conference, EWEC'03, Madrid, Spain,* June-16-20, 2003.

[102] G. Giebel, L. Landberg, G. Kariniotakis and R. Brownsword, "State-of-the-art on methods and software tools for short-term prediction of wind energy production," in *Proc. of the 2003 European Wind Energy Association Conference,* 2003, pp. 16-19.

[103] I. Martí, G. Kariniotakis, P. Pinson, I. Sanchez, T. Nielsen, H. Madsen, G. Giebel, J. Usaola, A. Palomares and R. Brownsword, "Evaluation of advanced wind power forecasting Models–Results of the anemos project," in *Proceedings of the 2006 European Wind Energy Conference, February,* 2006, pp. 1-9.

[104] H. Bludszuweit, J. Dominguez-Navarro and A. Llombart, "Statistical analysis of wind power forecast error," *IEEE Trans. Power Syst.,* Vol. 23, No.3, 2008, pp. 983-991.

[105] N. B. Negra, O. Holmstrm, B. Bak-Jensen and P. Srensen, "Model of a synthetic wind speed time series generator," *Wind Energy,* Vol. 11, No.2, 2008, pp. 193-209.

[106] G. Sideratos and N. D. Hatziargyriou, "An advanced statistical method for wind power forecasting," *IEEE Trans. Power Syst.,* Vol. 22, No.1, Feb. 2007, pp. 258-265.

[107] M. Gibescu, B. Ummels and W. Kling, "Statistical wind speed interpolation for simulating aggregated wind energy production under system studies," in *Probabilistic Methods Applied to Power Systems, PMAPS 2006,* pp. 1-7.

[108] S. Kennedy and P. Rogers, "A probabilistic model for simulating long-term wind-power output," Wind *Eng*, Vol. 27, No.4, 2003, pp. 167-81.

[109] M. Milligan, M. Schwartz and Y. Wan, "Statistical Wind Power Forecasting Models: Results for US Wind Farms," *National Renewable Energy Laboratory, Golden, CO*, NREL/CP-500-33956, May 2003.

[110] Yih-huei Wan and D. Bucaneg Jr., "Short-term power fluctuations of large wind power plants," *Transactions of the ASME. Journal of Solar Energy Engineering,* Vol. 124, No.4, Nov. 2002, pp. 427-431.

[111] E. A. Bossanyi, "Short-term wind prediction using Kalman filters," *Wind Eng,* Vol. 9, No.1, 1985, pp. 1-8.

[112] T. Nielsen, H. Madsen, H. A. Nielsen, P. Pinson, G. Kariniotakis, N. Siebert, I. Marti, M. Lange, U. Focken and L. von Bremen, "Short-term wind power forecasting using advanced statistical methods," in *Proceedings of the European Wind Energy Conference,* 2006.

[113] P. Pinson, L. Christensen, H. Madsen, P. E. Sørensen, M. Donovan and L. Jensen, "Fluctuations of offshore wind generation-statistical modelling," in *European Wind Energy Conference and Exhibition,* 2007, pp. 87-92.

[114] G. Turbelin, P. Ngae and M. Grignon, "Wavelet cross-correlation analysis of wind speed series generated by ANN based models," *Renewable Energy,* Vol. 34, No.4, Apr. 2009, pp. 1024-1032.

[115] B. Ernst, B. Oakleaf, M. L. Ahlstrom, M. Lange, C. Moehrlen, B. Lange, U. Focken and K. Rohrig, "Predicting the wind," *IEEE Power & Energy Magazine,* Vol. 5, No.6, Nov. 2007, pp. 78-89.

[116] X. Wang, G. Sideratos, N. Hatziargyriou and L. H. Tsoukalas, "Wind speed forecasting for power system operational planning," in *International Conference on Probabilistic Methods Applied to Power Systems*, 2004, pp. 470-474.

[117] M. C. Alexiadis, P. S. Dokopoulos and H. S. Sahsamanoglou, "Wind speed and power forecasting based on spatial correlation models," *IEEE Trans. Energy Convers.*, Vol. 14, No.3, 1999, pp. 836-42.

[118] L. Wang and C. Singh, "Population-based intelligent search in reliability evaluation of generation systems with wind power penetration," *IEEE Trans. Power Syst.*, Vol. 23, No.3, 2008, pp. 1336-1345.

[119] C. W. Potter and M. Negnevitsky, "Very short-term wind forecasting for Tasmanian power generation," *IEEE Trans. Power Syst.*, Vol. 21, No.2, May 2006, pp. 965-72.

[120] G. N. Kariniotakis, G. S. Stavrakakis and E. F. Nogaret, "Wind power forecasting using advanced neural networks models," *IEEE Trans. Energy Convers.*, Vol. 11, No.4, 1996, pp. 762-767.

[121] K. Methaprayoon, C. Yingvivatanapong, Wei-Jen Lee and J. R. Liao, "An integration of ANN wind power estimation into unit commitment considering the forecasting uncertainty," *IEEE Trans. Ind. Appl.*, Vol. 43, No.6, 11. 2007, pp. 1441-1448.

[122] I. G. Damousis, M. C. Alexiadis, J. B. Theocharis and P. S. Dokopoulos, "A fuzzy model for wind speed prediction and power generation in wind parks using spatial correlation," *IEEE Trans. Energy Convers.*, Vol. 19, No.2, 2004, pp. 352-361.

[123] IWES- Institute for Wind Energy and Energy System Technology, "http://www.iset.uni-kassel.de/pls/w3isetdad/www_iset_new.main_page?p_name=7261001&p_lang=eng "

[124] G. Giebel, R. Brownsword and G. Kariniotakis, "The state-of-the-art in short-term prediction of wind Power–A literature overview," Tech. Rep. Project Anemos, Contract No.ENK5-CT-2002-00665, 2003.

[125] L. Landberg, "Short-term prediction of local wind conditions," *J. Wind Eng. Ind. Aerodyn.*, Vol. 89, No.3, 2001, pp. 235-245.

[126] Andrew Boone, "Simulation of Short-term Wind Speed Forecast Errors using a Multi-variate ARMA(1,1) Time-series Model," M.Sc Thesis, Royal Institute of Technology, Sweden, 2005.

[127] V. Monbet, P. Ailliot and M. Prevosto, "Survey of stochastic models for wind and sea state time series," *Prob. Eng. Mech.*, Vol. 22, No.2, 2007, pp. 113-126.

[128] T. H. M. El-Fouly, E. F. El-Saadany and M. M. A. Salama, "One day ahead prediction of wind speed and direction," *IEEE Trans. Energy Convers.*, Vol. 23, No.1, Mar. 2008, pp. 191-201.

[129] R. Billinton, B. Karki, R. Karki, R. Gokaraju, "Unit Commitment Risk Analysis of Wind Integrated Power Systems," *IEEE Trans.Power Syst.*, Vol. 24, No.2, May 2009, pp.930-939.

[130] W. Wangdee and R. Billinton, "Considering load-carrying capability and wind speed correlation of WECS in generation adequacy assessment," *IEEE Trans. Energy Convers.*, Vol. 21, No.3, 2006, pp. 734-41.

[131] E. L. Petersen, N. G. Mortensen, L. Landberg, J. Højstrup and H. P. Frank, "Wind power meteorology," *Wind Energy*, Vol. 1, 1998, pp. 2-22.

[132] NERC Planning Standards (1997, Sept.), "http://www.nerc.com/"

[133] C. Ensslin, M. Milligan, H. Holttinen, M. O'Malley and A. Keane, "Current methods to calculate capacity credit of wind power, IEA collaboration," in *2008 IEEE Power & Energy Society General Meeting,* 2008.

[134] M. Ni, J. D. McCalley, V. Vittal and T. Tayyib, "Online risk-based security assessment," *IEEE Trans. Power Syst.,* Vol. 18, No.1, 02. 2003, pp. 258-265.

[135] G. B. Sheble and G. N. Fahd, "Unit commitment literature synopsis," *Power Systems, IEEE Transactions on,* Vol. 9, No.1, 1994, pp. 128-135.

[136] N. P. Padhy, "Unit commitment-a bibliographical survey," *Power Systems, IEEE Transactions on,* Vol. 19, No.2, 2004, pp. 1196-1205.

[137] Chun-Lung Chen, "Optimal wind-thermal generating unit commitment," *IEEE Trans. Energy Convers.,* Vol. 23, No.1, Mar. 2008, pp. 273-280.

[138] Tsung-Ying Lee, "Optimal spinning reserve for a wind-thermal power system using EIPSO," *IEEE Trans. Power Syst.,* Vol. 22, No.4, Nov. 2007, pp. 1612-21.

[139] J. Wang, M. Shahidehpour and Z. Li, "Security-constrained unit commitment with volatile wind power generation," *IEEE Trans. Power Syst.,* Vol. 23, No.3, Aug. 2008, pp. 1319-1327.

[140] R. Billinton, B. Karki, R. Karki and R. Gokaraju, "Operating reserve assessment of wind integrated power systems," in *CIGRÉ Canada Conference on Power Systems, Winnipeg,* Oct. 19-21,2008.

[141] Kamal Debnath, Reliability Modeling of Power System Components using the CEA-ERIS data base , Ph.D. thesis, University of Saskatchewan, 1988.

[142] B. Karki, R. Billinton, R. Karki and R. Gokaraju, "Load carrying capability of wind integrated power systems," in *North American Power Symposium,Calgary,* 28-30 Sept.,2008.

[143] R. Billinton and G. Bai, "Generating capacity adequacy associated with wind energy," *IEEE Transaction on Energy Conversion,* Vol. 19, No.3, 2004, pp. 641-646.

[144] B.Karki and R. Billinton, "Utilization of Multi-State Generating Unit Models in Unit Commitment Risk Analysis of Wind Integrated Power Systems," *Electric Power Components and Systems,* Vol. 37, No.10, 2009.

[145] R. Billinton and B. Karki, " Effect of hourly wind trends on the peak load-carrying capability of wind-integrated power systems. *Proc. IMechE, Part O: J. Risk and Reliability,* 2009, **223** (4), 279-287. DOI 10.1243/1748006XJRR249.

[146] B.Karki and R. Bilinton, "Effects of seasonality and locality on the operating capacity benefit of wind power," in *Electric Power and Energy Conference (EPEC), Montreal, QC, Canada,* 22-23 October,2009.

[147] L. L. Garver, "Effective load carrying capability of generating units," *IEEE Transactions on Power Apparatus and Systems,* Vol. PAS-85, No. 8, Aug. 1966, pp. 910-919.

[148] V. M. Cook, C. D. Galloway, M. J. Steinberg and A. J. Wood, "Determination of reserve requirements of two interconnected systems," *IEEE Transactions on Power Apparatus and Systems,* Vol. 82 , No. 65, Apr. 1963, pp. 18-33.

[149] R. Billinton and C. Singh, "Generating capacity reliability evaluation in interconnected systems using a frequency and duration approach. I. Mathematical analysis," *IEEE Transactions on Power Apparatus and Systems,* Vol. PAS-90, No.4, Jul. 1971, pp. 1646-1654.

[150] F. N. Lee, "Multi-area reliability-a new approach," *IEEE Trans. Power Syst.*, vol. PWRS-2, No.4, Nov. 1987, pp. 848-855.

[151] C. Singh, A. D. Patton, A. Lago-Gonzalez, A. R. Vojdani, G. Gross, F. F. Wu and N. J. Balu, "Operating considerations in reliability modeling of interconnected systems - an analytical approach," *IEEE Trans. Power Syst.*, Vol. 3, No. 3, 1988, pp. 1119-1126.

APPENDIX A1: RBTS PRIORITY LOADING ORDER

The RBTS consists of 11 generating units with a total installed capacity of 240 MW. It has different types of generating units with different failure rates as shown in Table A1. There are four thermal units and seven hydro units of different sizes.

Table A1: RBTS priority loading order

Priority loading order	Unit size (MW)	Type	Failure rate (failure per year)
1	40	Hydro	3
2–3	20	Hydro	2.4
4–5	40	Thermal	6
6	20	Thermal	5
7	10	Thermal	4
8–9	20	Hydro	2.4
10–11	5	Hydro	2

APPENDIX A2: IEEE-RTS PRIORITY LOADING ORDER

The IEEE-RTS consists of 32 generating units with a total generating capacity of 3405 MW. It has different types of generating units with different sizes and failure rates. This is a relatively large test system and approximately equals the capacity size of the SaskPower, a crown utility corporation in Saskatchewan, Canada. The IEEE-RTS priority loading order is shown in Table A2.

Table A2. IEEE-RTS basic unit data

Priority loading order	Unit size (MW)	Type	Failure Rate (failure per year)
1-4	50	Hydro	4.4676
5-6	400	Nuclear	7.9716
7	350	Coal/Steam	7.6212
8-10	197	Oil/Steam	9.198
11-14	155	Coal/Steam	9.1104
15-17	100	Oil/ Steam	7.2708
18-21	76	Coal/Steam	4.4676
22-26	12	Oil/ Steam	2.9784
27-30	20	Oil/CT	19.4472
31-32	50	Hydro	4.4676

APPENDIX A3: DEFINITION OF POWER SYSTEM OPERATING STATES

The definition of the normal state is:

In the normal state, the generation is adequate to supply the existing total load demand. In this state, there is sufficient margin such that the loss of any generating units, specified by some criterion, will not result in load curtailment. The particular criterion, such as the loss of any single generating unit will depend on the planning and operating philosophy of the particular utility.

The definition of the Marginal state is:

If a system enters a condition where the loss of generating capacity covered by the operating criteria will result in load curtailment then the system is in the Marginal state. The Marginal state is similar to the normal state in that the constraint is satisfied, but there is no longer sufficient margin to withstand some outages. The system can enter the Marginal state by the outage of generation units(s), or by growth in the system load.

The definition of the emergency state is:

If a contingency occurs or the load changes before a corrective action can be (or is) taken, the system will enter the emergency state. There is no reserve margin and no load is curtailed in the emergency state.

The definition of the extreme emergency state is:

In this state, the system constraint is violated and some portion of the system load is curtailed.

APPENDIX 4: COMPARISON OF THE APPROXIMATE METHOD AND THE CONTINGENCY ENUMERATION APPROACH

This section provides comparisons of the Contingency Enumeration approach and the Approximate method under various conditions. The units are scheduled from the RBTS merit order shown in Table A1.

Case 1: Load 50 MW and Generation 120 MW

Four generating units are scheduled from the RBTS merit order and the load is 50 MW. System lead time is 4 hours.

Table A4.1: Contingency Enumeration for a load of 50 MW and generation of 120 MW at a lead time of 4 hours

Unit no. Out	Capacity In (CIn) (MW)	Reserve = CIn-Load (MW)	CLOU (MW)	System Operating State	Probability
0	120	70	40	H	0.99371265
1	80	30	40	M	0.00136312
2	100	50	40	H	0.00109019
3	100	50	40	H	0.00109019
4	80	30	40	M	0.00272998
1,2	60	10	40	M	0.00000150
1,3	60	10	40	M	0.00000150
1,4	40	-10	20	R	0.00000374
2,3	80	30	40	M	0.00000120
2,4	60	10	40	M	0.00000300
3,4	60	10	40	M	0.00000300
1,2,3	40	-10	40	R	1.64E-09
1,2,4	20	-30	20	R	4.11E-09
1,3,4	20	-30	20	R	4.11E-09
2,3,4	40	-10	40	R	3.29E-09
1,2,3,4	0	-50	0	R	4.51E-12

where CLOU = Capacity of the largest operating unit

$$P(h) = \left[P(0) + P(2) + P(3)\right] \quad \text{A(4.1)}$$

where P(x) is the probability of having unit x out of service

$$\text{Or, } P(h) = \sum P(120) + P(100) \text{ MW In} \quad \text{A(4.2)}$$

$$P(m) = \left[P(1) + P(4) + P(1,2) + P(1,3) + P(2,3) + P(2,4) + P(3,4)\right] \quad \text{A(4.3)}$$

$$\text{Or, } P(m) = \sum P(80) + P(60) \text{ MW In} \quad \text{A (4.4)}$$

$$P(r) = \left[P(1,4) + P(1,2,3) + P(1,2,4) + P(1,3,4) + P(2,3,4) + P(1,2,3,4)\right] \quad \text{A(4.5)}$$

$$\text{Or, } P(r) = \sum P(40) + P(20) + P(0) \text{ MW In} \quad \text{A(4.6)}$$

P (h) = 0.99589303

P(r) = 0.00000375

P (m) = 0.00410330

Marginal state can be obtained by P (m) = 1-P(h)-P(r) =0.00410322

The Approximate method:

Table A4.2 presents the Approximate method table for the four scheduled units in the RBTS merit order.

Table A4.2: Approximate method table for a scheduled capacity of 120 MW at a lead time of 4 hours

Capacity In (CIn) (MW)	CIn–CLOU (MW) (Healthy loads)	Individual Probability (IP)	Cumulative probability (CP)
120	80	9.937126E-01	1
100	60	2.180390E-03	6.287422E-03
80	40	4.094293E-03	4.107032E-03
60	20	8.981014E-06	1.273899E-05
40	0	3.749755E-06	3.757976E-06
20	-20	8.216847E-09	8.221354E-09
0	-40	4.507322E-12	4.507322E-12

CLOU = Capacity of the largest operating Unit i.e. 40 MW

The load is 50 MW and therefore,

P (h) = $\sum P(120) + P(100)$ MW In A(4.7)

Or, P (h) = 0.99589299

Equation A (4.2) of the Contingency Enumeration and A (4.7) of Approximate method are the same.

P(r) = 3.757976E-06 (obtained directly from col. 4 of Table 2)

=0.00000375

P(m)= 1-P(h)-P(r) = 0.00410325

Case 2: Load 120 MW and Generation 160 MW

Table A4.3: Contingency Enumeration for a load of 120 MW and generation 160 MW at a lead time of 4 hours

Unit no. Out	Capacity In (CIn) (MW)	Reserve = CIn-Load (MW)	CLOU (MW)	System Operating State	Probability
0	160	40	40	H	0.99099017
1	120	0	40	R	0.00135938
2	140	20	40	M	0.00108721
3	140	20	40	M	0.00108721
4	120	0	40	R	0.00272250
5	120	0	40	R	0.00272250
1,2	100	-20	40	R	0.00000149
1,3	100	-20	40	R	0.00000149
1,4	80	-40	40	R	0.00000373
1,5	80	-40	40	R	0.00000373
2,3	120	0	40	R	0.00000119
2,4	100	-20	40	R	0.00000299
2,5	100	-20	40	R	0.00000299
3,4	100	-20	40	R	0.00000299
3,5	100	-20	40	R	0.00000299
4,5	80	-40	40	R	0.00000748
1,2,3	80	-40	40	R	1.64E-09
1,2,4	60	-60	40	R	4.10E-09
1,2,5	60	-60	40	R	4.10E-09
1,3,4	60	-60	40	R	4.10E-09
1,3,5	60	-60	40	R	4.10E-09
1,4,5	40	-80	20	R	1.03E-08
2,3,4	80	-40	40	R	3.28E-09
2,3,5	80	-40	40	R	3.28E-09
2,4,5	60	-60	40	R	8.21E-09
3,4,5	60	-60	40	R	8.21E-09
1,2,3,4	40	-80	40	R	4.49E-12
1,2,3,5	40	-80	40	R	4.49E-12
1,2,4,5	20	-100	20	R	1.13E-11
1,3,4,5	20	-100	20	R	1.13E-11
2,3,4,5	40	-80	40	R	9.00E-12
1,2,3,4,5	0	-120	0	R	1.23E-14

P (h) = P (0) A(4.8)

Or, P (h) = P (160) MW In A(4.9)

Or, P(h) = 0.99099017

P (m) = [p (2) +p (3)] A(4.10)

Or, P (m) = P (140) MW In A(4.11)

Or, P (m) = 0.00217442

P(r)

=

$$\left[\begin{array}{l} P(4)+P(5)+P(1,2)+P(1,3)+P(1,4)+P(1,5)+P(2,3)+P(2,4)+P(2,5)+P(3,4) \\ +P(3,5)+P(4,5)+P(1,2,3)+P(1,2,4)+P(1,2,5)+P(1,3,4)+P(1,3,5)+P(1,4,5)+P(2,3,4)+P(2,3,5) \\ +P(2,4,5)+P(3,4,5)+P(1,2,3,4)+P(1,2,3,5)+P(1,2,4,5)+P(1,3,4,5)+P(2,3,4,5)+P(1,2,3,4,5)\ \end{array}\right]$$

A (4.12)

Or, P(r) = $\sum P(120)+P(100)+P(80)+P(60)+P(40)+P(20)+P(0)$ MW In A(4.13)

P(r) = 0.00683550

Approximate method:

Table A4.4: Approximate method table for a scheduled capacity of 160 MW at a lead time of 4 hours

Capacity In (CIn) (MW)	CIn–CLOU (MW) (Healthy loads)	Individual Probability (IP)	Cumulative probability (CP)
160	120	9.909901E-01	1
140	100	2.174416E-03	9.009922E-03
120	80	6.805576E-03	6.835506E-03
100	60	1.493008E-05	2.992990E-05
80	40	1.495672E-05	1.499982E-05
60	20	3.279985E-08	4.310018E-08
40	0	1.027780E-08	1.030032E-08
20	-20	2.251191E-11	2.252426E-11
0	-40	1.234883E-14	1.234883E-14

The load is 120 MW and therefore,

$$P(h) = \left[P(160)\right] \text{ MW In} \qquad \text{A(4.14)}$$

Equation A (4.9) of the Contingency Enumeration and A (4.14) of Approximate method are the same.

Or, P (h) = 9.909901E-01=0.9909901

P(r) = 6.805576E-03=0.006805576

P(m)=1-P(h)-P(m)= 0.00220432

The Contingency Enumeration requires considerable space to show all the contingency states and therefore the results of both the methods are presented in Case 3, 4, 5, 6 and 7 without explicitly showing the Tables.

Case 3: Load 100 MW and Generation 160 MW

Using the Contingency Enumeration approach:

$$P(h) = \left[P(0) + P(2) + P(3)\right] \qquad \text{A(4.15)}$$

$$\text{Or, } P(h) = \sum P(160) + P(140) \text{ MW In} \qquad \text{A(4.16)}$$

Or, P (h) = 0.99316459

$$P(m) = \sum P(1) + P(4) + P(5) + P(2,3) \text{ unit no. out} \qquad \text{A(4.17)}$$

$$\text{Or, } P(m) = \sum P(120) \text{ MW In} \qquad \text{A (4.18)}$$

= 0.00680557

P(r)

=

$$\left[\begin{array}{l} P(1,2) + P(1,3) + P(1,4) + P(1,5) + P(2,4) + P(2,5) + P(3,4) \\ + P(3,5) + P(4,5) + P(1,2,3) + P(1,2,4) + P(1,2,5) + P(1,3,4) + P(1,3,5) + P(1,4,5) + P(2,3,4) + P(2,3,5) \\ + P(2,4,5) + P(3,4,5) + P(1,2,3,4) + P(1,2,3,5) + P(1,2,4,5) + P(1,3,4,5) + P(2,3,4,5) + P(1,2,3,4,5) \end{array}\right]$$

A(4.19)

$$\text{Or, } P(r) = \sum P(100) + P(80) + P(60) + P(40) + P(20) + P(0) \text{ MW In} \qquad \text{A (4.20)}$$

P(r) = 0.00002993

Using the Approximate method:

Since the scheduled capacity and the lead times are the same as is described in Table A4.4. Table A4.4 therefore, can be used to deduce the risk indices in the Approximate method.

The load is 100 MW and therefore,

$$P(h) = \sum P(160) + P(140) \text{ MW In} \qquad \text{A (4.21)}$$

Or, P(h) = 0.99316452

Equation A (4.16) of the Contingency Enumeration and A (4.21) of Approximate method are the same.

P (m) = 1-P (h)-P(r)

= 0.00680555

Case 4: Load 120 MW and Generation 180 MW

Using the Contingency Enumeration approach:

$$P(h) = \left[P(0) + P(2) + P(3) + P(6)\right] \text{ unit no. out} \qquad \text{A (4.22)}$$

$$\text{Or, } P(h) = \sum P(180) + P(160) \text{ MW In} \qquad \text{A (4.23)}$$

Or, P (h) = 0.99315963

Using the Approximate method:

$$P(h) = \sum P(180) + P(160) \text{ MW In} \qquad \text{A (4.24)}$$

Or, P(h) = 0.99995459

Equation A (4.23) of the Contingency Enumeration and A (4.24) of Approximate method are the same

Case 5: Load is 100 MW and Generation 180 MW

Using the Contingency Enumeration approach:

$$P(h) = \begin{bmatrix} P(0) + P(1) + P(2) + P(3) + P(4) \\ + P(5) + P(6) + P(2,3) + P(2,6) + P(3,6) \end{bmatrix} \text{ Unit no. out} \qquad \text{A (4.25)}$$

$$\text{Or, } P(h) = \sum P(180) + P(160) + P(140) \text{ MW In} \qquad \text{A (4.26)}$$

Or, P (h) = 0.99995462

Using the Approximate method:

P (h) = $\sum P(180) + P(160) + P(140)$ MW In A (4.27)

Or, P(h)= 0.99995459

Equation A (4.26) and A (4.27) are exactly the same.

Case 6: Load 190 MW and Generation 240 MW

Using the Contingency Enumeration Approach:

P (h) = $\left[P(0) + P(7) + P(10) + P(11) + P(10,11)\right]$ unit no. out A(4.28)

P (h) = $\sum P(240) + P(235) + P(230)$ MW In A(4.29)

Or, P(h)= 9.865585E-01

Using the Approximate method:

The load is 190 MW and therefore,

P (h) = $\sum P(240) + P(235) + P(230)$ MW In A(4.30)

Or, P (h) = 9.865584E-01

Equation A (4.29) and A (4.30) are exactly the same.

Case 7: Load 60 MW and Generation 100 MW

In this case, the 4th generating unit in the priority loading order is replaced by a 20 MW generating unit with the same failure rate.

Using the Contingency Enumeration approach:

P(h)= $\left[P(0)\right]$ unit no. out A(4.31)

Or, P(h)= $\sum P(100)$ MW In A(4.32)

Or, P(h)= 0.99371265

Using the Approximate method:

P(h)= $P(100)$ MW In A(4.33)

Equation A(4.32) of the Contingency Enumeration and A(4.33) of Approximate method are the same.

Or, P(h)= 0.9937126

APPENDIX 5: LIMITATION OF THE APPROXIMATE METHOD

In this case, the 4th generating unit in the priority loading order is replaced by a 20 MW generating unit with the same failure rate. The Contingency Enumeration table and the Approximate method table are presented in Table A5.1 and A5.2 respectively.

Table A5.1 Contingency Enumeration for a load of 40 MW and generation 100 MW at a lead time of 4 hours

Unit no. Out	Capacity In (CIn) (MW)	Reserve = CIn-Load (MW)	CLOU (MW)	System Operating State	Probability
0	100	60	40	H	0.99371265
1	60	20	20	H	0.00136312
2	80	40	40	H	0.00109019
3	80	40	40	H	0.00109019
4	80	40	40	H	0.00272998
1,2	40	0	40	R	0.00000150
1,3	40	0	40	R	0.00000150
1,4	40	0	20	R	0.00000374
2,3	60	20	40	M	0.00000120
2,4	60	20	40	M	0.00000300
3,4	60	20	40	M	0.00000300
1,2,3	20	-20	40	R	1.64E-09
1,2,4	20	-20	20	R	4.11E-09
1,3,4	20	-20	20	R	4.11E-09
2,3,4	40	0	40	R	3.29E-09
1,2,3,4	0	-40	0	R	4.51E-12

P(h)= $\left[P(0)+P(1)+P(2)+P(3)+P(4)\right]$ unit no. out A(5.1)

Or, P(h)= $\sum P(100) + P(80) + P(1out)$ MW In A(5.2)

Or, P(h)= 0.99998613

P(m)= $\left[P(2,3) + P(2,4) + P(3,4)\right]$ unit no. out A(5.3)

Or, P(m)= $\sum P(60) - P(1out)$

Or, P(m)= 0.00000720

P(r) = $\begin{bmatrix} P(1,2) + P(1,3) + P(1,4) + P(1,2,3) + P(1,2,4) \\ + P(1,3,4) + P(2,3,4) + P(1,2,3,4) \end{bmatrix}$ unit no. out A(5.4)

Or, P(r) = $\sum P(40) + P(20) + P(0)$ MW In

Or, P(r) = 0.00000675

Approximate method:

Table A5.2: Approximate method table for a scheduled capacity of 100 MW at a lead time of 4 hours

Capacity In (CIn) (MW)	CIn–CLOU (MW) (Healthy loads)	Individual Probability (IP)	Cumulative probability (CP)
100	60	9.937126E-01	1
80	40	4.910369E-03	6.287422E-03
60	20	1.370304E-03	1.377053E-03
40	0	6.739047E-06	6.748909E-06
20	-20	9.857512E-09	9.862020E-09
0	-40	4.507322E-12	4.507322E-12

The load is 40 MW and therefore,

P(h)= $\sum P(100) + P(80)$ MW In A(5.6)

Equation A(5.2) of the Contingency Enumeration and A(5.6) of Approximate method are NOT the same.

Or, P(h)= 9.986230E-01=0.99862297

P(r) = 6.748909E-06 = 0.00000675

P(m)= 1-P(h)-P(m) = 0.00137028

The Healthy state and MSP obtained by the two methods are different. The Approximate method fails to recognize that the failure of the largest unit (contingency number 1) can still lead to a Healthy state in this particular case. The approximation method recognizes the Healthy state of contingency number 1 (Table 5.1) as a Marginal state and therefore, the MSP calculated from

the Approximate method is slightly higher and HSP is slightly lower than the Contingency Enumeration approach.

The Approximate method gives a pessimistic appraisal of the HSP and places the operator on the safe side when it comes to integrating wind power in power systems. This situation is similar to the case where the load is equal to the largest operating unit and the largest operating unit fails. It is, however, important to note that the results obtained for P(h) in both methods are very close. The HSP is not as sensitive to load changes as the At risk state.

The probability of system load being so low that it is equal to the largest operating unit in a practical power system is very low and that the probability of the largest unit failing at that instant makes this event extremely rare. The Approximate method, therefore, provides a reasonable estimate of the system operating state probabilities and can be applied in making operating decisions.